UNIVERSITY OF CALIFORNIA,
IRVINE

Supramolecular Antibiotics Inspired by Teixobactin and Leveraging Undergraduate Learning Assistants When Implementing New Laboratory Curricula

DISSERTATION

submitted in partial satisfaction of the requirements
for the degree of

DOCTOR OF PHILOSOPHY

in Chemistry

by

James Harrison Griffin

Dissertation Committee:
Distinguished Professor James S. Nowick, Chair
Professor Jennifer A. Prescher
Assistant Professor Elizabeth N. Bess

2024

DEDICATION

To each of my students, for making the journey more meaningful than the destination.

TABLE OF CONTENTS

Page

LIST OF FIGURES vi

LIST OF SCHEMES ix

LIST OF TABLES x

ACKNOWLEDGEMENTS xii

VITA xiv

ABSTRACT OF THE DISSERTATION xv

CHAPTER I: Cyclodepsipeptide Natural Products Containing 13-Membered Macrolactone Rings 1

- Abstract 1
- Introduction 1
- D-L-L-L: Hypeptin/Teixobactin/Clovibactin, Nobilamides, and Putisolvins 3
  - Hypeptin/Teixobactin/Clovibactin 3
  - Nobilamides 6
  - Putisolvins 9
- D-L-D-L: Lystabactin B and Pseudobactin 7SR1 11
  - Pseudobactin 7SR1 11
  - Lystabactin B 12
- L-L-D-L: Kurstakins, Brevicidines, and Cyanogripeptides 13
  - Kurstakins 13
  - Brevicidines 17
  - Cyanogripeptides 19
- L-D-L-L: Lydiamycins, Malleipeptins, Endopyrroles, Bolagladins, and Cycloacetamides 21
  - Lydiamycins 21
  - Malleipeptins 24
  - Endopyrroles 26
  - Bolagladins 28
  - Cycloacetamides 29
- Conclusion 31
- References for Chapter I 33

CHAPTER II: PEGylated Teixobactin Analogues 49

- Abstract 49
- Introduction 49
- Results and Discussion 51
  - Design and Synthesis of PEGylated Teixobactin Analogues 51
  - Study of PEGylated Teixobactin Analogues 56
- Conclusion 61

Supporting Information for Chapter II 63
Materials and Methods 65
Synthesis of PEGylated Teixobactin Analogues 65
Minimum Inhibitory Concentration (MIC) Assays 69
Solubility Assay of PEGylated Teixobactin Analogues in PBS Buffer 70
Characterization Data 75
References for Chapter II 86

CHAPTER III: Supramolecular Antibiotics Inspired by Teixobactin 89
Abstract 89
Introduction 90
Results and Discussion 92
Teixobactin "Swapmers" 92
"Chimeric" Teixobactin Analogues 97
Conclusion 101
Supporting Information for Chapter III 103
General Information. 103
Peptide Synthesis of Teixobactin Analogues. 103
Minimum Inhibitory Concentration (MIC) Assays. 108
Peptide Characterization Data 110
References for Chapter III 135

CHAPTER IV: Structure-Activity Relationship Studies of the Peptide Antibiotic Clovibactin 139
Abstract 139
Introduction 139
Results and Discussion 140
Structure-Activity Relationship Studies 141
X-ray Crystallography 146
Further Study of D-Thr_5-clovibactin and Analogues 153
Conclusion 161
Supporting Information for Chapter IV 162
Supplementary Tables 162
Materials and Methods 165
Synthesis of Peptides 166
MIC Assays 170
X-ray Crystallography 171
Characterization Data 176
References for Chapter IV 223

CHAPTER V: Leveraging Undergraduate Learning Assistants When Implementing New Laboratory Curricula 229
Abstract 229
Introduction 230
Pedagogical Frameworks 231
Vertical Learning Communities with Near-Peer Instructors 231
Affective Domain in Laboratory Instruction 232
Learning Environment 232

Results 234
Methods 234
Survey Results 238
Discussion 248
Comparison to Previous Results 248
Tandem LA Training/Experiment Testing 248
Student and LA Perspectives of Laboratory LA Benefits 249
Limitations 252
Conclusion 253
Supplementary Material for Chapter V 255
IRB Statement 255
Sample Learning Assistant Application Form 255
Student Response Anonymization 258
Open-Ended Response Analysis 258
Learning Assistant Application Rubric 259
Student Survey Results 261
Learning Assistant Survey Results 269
References for Chapter V 277

LIST OF FIGURES

Page

Figure 1.1. Hypeptin, teixobactin, and clovibactin. 4

Figure 1.2. A-3302-A, TL-119 / A-3302-B / ASP-1, and nobilamides D–I. 8

Figure 1.3. Proposed structures of putisolvins I / III, II / IV, and V. 10

Figure 1.4. Pseudobactin 7SR1. 12

Figure 1.5. Lystabactin B. 13

Figure 1.6. Kurstakins A–D. 15

Figure 1.7. Brevicidine and brevicidine B. 17

Figure 1.8. Cyanogripeptides A–C. 21

Figure 1.9. Lydiamycins A–H. 23

Figure 1.10. Malleipeptins A and B. 25

Figure 1.11. Endopyrroles A and C. 27

Figure 1.12. Bolagladins A and B. 29

Figure 1.13. Cycloacetamides A–F. 30

Figure 2.1. Teixobactin. 50

Figure 2.2. PEGylated analogues of teixobactin. 53

Figure 2.3. Qualitative gel assay of PEGylated teixobactin analogues. 61

Figure S2.1. Crystal structure of a teixobactin analogue depicting a β-sheet dimer that binds sulfate anions. 63

Figure S2.2. Analytical HPLC comparison of teixobactin and PEGylated teixobactin diastereomeric separation. 64

Figure S2.4. Gels formed by teixobactin and PEGylated analogues. 74

Figure 3.1. Teixobactin structure and X-ray crystallographic structure of a teixobactin analogue (N-Me-D-Phe$^{I}_{1}$,N-Me-D-Gln$_{4}$,Lys$_{10}$-teixobactin, PDB 6E002). 91

Figure 3.2. Cartoon representations of (A) an L-amino acid β-strand and (B) a teixobactin β-strand. 91

Figure 3.3. Amyloid-like properties of teixobactin..... 92

Figure 3.4. Chemical structures of teixobactin analogues prepared and studied..... 95

Figure 3.5. Cartoon representation of a supramolecular teixobactin assembly bound to lipid II molecules. 98

Figure 3.6. Design of MAX1-teixobactin "chimeras." 99

Figure 3.7. MAX1-teixobactin "chimeras" prepared in this study. 100

Figure 4.1. Clovibactin and representative analogues for SAR studies..... 142

Figure 4.2. Crystallographically based molecular model of clovibactin and X-ray crystallographic structures of *N*-methylated and stapled clovibactin analogues. 148

Figure 4.3. D-Thr$_5$-clovibactin analogues. 149

Figure 4.4. X-ray crystallographic structures of *N*-Me-D-Leu$_2$,D-Thr$_5$-clovibactin..... 151

Figure 4.5. Comparison of the backbone conformation of three clovibactin analogue crystal structures, aligned by their macrolactone rings. 152

Figure 4.6. Additional D-Thr$_5$-clovibactin analogues. 154

Figure 4.7. Hypeptin and prepared hypeptin analogues..... 159

Figure 4.8. SDS-PAGE studies of D-Thr$_5$-clovibactin and *N*-Me-D-Leu$_2$,D-Thr$_5$-clovibactin at various concentrations (10, 100, and 1000 μM). 160

Figure 5.1. Timeline of curricula development, curricula testing, LA training, LA implementation, and survey collection. 234

Figure 5.2. Student and LA responses to survey questions about the appropriateness and observation of LA duties..... 240

Figure 5.3. Student responses to the question "Please indicate the order in which you would approach the following people (GTA, LA, peer) to ask the following types of questions." 242

Figure 5.4. Student responses to the question "Please rate the degree to which you agree with the following statement: 'I felt [adjective] performing in-person laboratory experiments this quarter.'" 245

Figure S5.1. Student learning from LAs only..... 261

Figure S5.2. Student learning from LAs and GTAs. 262

Figure S5.3. Student priorities in the laboratory..... 262

Figure S5.4. Student learning from GTAs only. 263

Figure S5.5. Student satisfaction with GTA and LA answers to questions. 264

Figure S5.6. Student perception of timeliness of answers to questions. 265

Figure S5.7. Student perception of time management during experiments. 266

Figure S5.8. Student perception of time spent waiting for questions to be answered (overall). 267

Figure S5.9. Student perception of time spent waiting for questions to be answered (by term). 268

Figure S5.10. LA self-assessment of skills and abilities..... 271

Figure S5.11. How LAs prepared for laboratory meetings. 273

Figure S5.12. LA self-assessment of student interactions. 273

Figure S5.13. Frequency of questions received by LAs. 274

Figure S5.14. LA self-assessment of the value of the LA program. 276

LIST OF SCHEMES

Page

Scheme 1.1. Generic form of the 13-membered macrolactone ring in the cyclodepsipeptides discussed. 2

Scheme 2.1. Representative synthesis of Lys$(PEG_n)_{10}$-teixobactin. 55

Scheme 4.1. Synthesis of clovibactin. 143

Scheme 4.2. Synthesis of aza-D-Thr_5-clovibactin. 155

LIST OF TABLES

Page

Table 1.1. Amino acid sequences of hypeptin, teixobactin, and clovibactin. 4

Table 1.2. Amino acid sequences of A-3302-A, A-3302 B / TL-119 / ASP-1, and nobilamides D–I. 8

Table 1.3. Amino acid sequences of putisolvins I / III, II / IV, and V. 10

Table 1.4. Amino acid sequence of pseudobactin 7SR1. 12

Table 1.5. Amino acid sequence of lystabactin B. 13

Table 1.6. Amino acid sequences of kurstakins A–D. 16

Table 1.7. Amino acid sequences of brevicidine and brevicidine B. 17

Table 1.8. Amino acid sequence of cyanogripeptides A–C. 21

Table 1.9. Amino acid sequences of lydiamycins A–H. 23

Table 1.10. Amino acid sequences of malleipeptins A and B. 25

Table 1.11. Amino acid sequences of endopyrroles A and C. 27

Table 1.12. Amino acid sequences of bolagladins A and B. 29

Table 1.13. Amino acid sequences of cycloacetamides A–F. 31

Table 2.1. MIC values for PEGylated teixobactin analogues and controls in μg/mL. 57

Table S2.1. Chemical yields of purified peptides. 69

Table 3.1. MIC values of teixobactin, isobactin, and "swapmer" analogues in μg/mL. 96

Table 3.2. MIC values of MAX1-teixobactin "chimeras" in μg/mL. 101

Table 4.1. MIC values of clovibactin and SAR analogues of clovibactin in μg/mL. 143

Table 4.2. MIC values of additional D-Thr_5-clovibactin analogues and hypeptin analogues in μg/mL. 156

Table S4.1. Dihedral angles of *epi*-clovibactin (PDB 8CUG), *N*-Me-D-Leu_2,D-Thr_5-clovibactin, and stapled D-Thr_5-clovibactin. 162

Table S4.2. Crystallographic properties, crystallization conditions, and data collection and model refinement statistics for stapled D-Thr_5-clovibactin (CCDC 2358085). 163

Table S4.3. Crystallographic properties, crystallization conditions, and data collection and model refinement statistics for *N*-Me-D-Leu$_2$,D-Thr$_5$-clovibactin (PDB ID 9BIC). 164

Table 5.1. Representative examples of common responses to open-ended survey questions. .. 245

Table S5.1. LA characteristics. 269

Table S5.2. Perceived benefits of LA training. 269

Table S5.3. LA comments on professional development..... 270

ACKNOWLEDGEMENTS

Financial support was provided by the University of California, Irvine and NIH-NIAID grants R21AI156565 and R21AI168966.

Portions of Chapter III have been submitted to an academic journal for publication. A full attribution is included on the first page of the chapter.

Portions of Chapter IV have been submitted to and are under review by *The Journal of Organic Chemistry*. A full attribution is included on the first page of the chapter.

Chapter V is reprinted with permission from *Front. Educ.* **2024**, 9:1367087. The co-authors of this manuscript are Jordan Thompson, Pía López, and Prof. Renée Link.

Thank you to "The Mech(wo)men": Alex, Alissa, Anneka, Aoon, Barry, Brooke, Bryant, Catherine, Cynthia, Dora, Madi, Joe, Maj, Mariana, Michael, Nick, Paul, Robby, and Sarah. Our time together was sweet!

Thank you to my first-year instructors: Professors Bess, Dong, Pronin, Rychnovsky, Van Vranken, and Vanderwal. Honorable mention to Prof. Nowick for my second, third, and fourth times taking Spec — I think I've almost got the hang of it now!

Thank you to the Pedagogical Fellows, TA Mentors, and 51L teaching team in my first year: Kate, Kellen, Mike, Renée, and Simon. You recognized the need for pedagogical excellence in our department and built the foundation for each TA who came after you.

Thank you to Dave, Ramesh, and Susan for giving me additional teaching opportunities outside of 51L, and thank you to Amanda and Steve for continuing to promote this department's teaching mission.

Thank you to former Nowick lab members: Drs. Krumberger, Ferracane (Honorary Member^{TM}), Morris, Parrocha, Wierzbicki, and Zhang; and former undergraduate researchers Ana, Andrews (both of them), Denise, Emily, Katelyn, Mike, and Sepehr.

Thank you to current Nowick lab members: James, thank you for all of the teaching and writing opportunities you encouraged me to pursue. Adam, Jason, Jackson, Sophie, Jovanna, Grant, and Jeramiah: Best of luck in your continued research! Fingers crossed for more of that NIH funding!

Ana, I was always nervous about taking on the responsibility of a research mentee, which is why you were such a perfect fit. You were the most self-driven and focused undergraduate I have ever met, and I feel privileged to have shared even a small fraction of experience and preparation with you. I hope that grad school treats you well, and I am sure that you will be writing one of these soon. Your new lab is lucky to have you.

Being accepted to the Pedagogical Fellowship program was the first time I felt like I belonged at UCI. Alex, Ashley, and Danny, thank you so much for organizing and advocating for us PFFs. Alessandra and Josh, thank you for keeping CLAP going and growing strong. It's because of you

that our undergraduate students have the opportunity to realize their potential for effective teaching. Anneka and Deanna, thank you for being my PFFs! TAPDP was not easy, but it was important. I literally could not have done it without you. Thank you all for allowing me to feel that I left this campus just a little bit better than I found it.

Teaching has been the most fulfilling part of my professional life for the past six years, and that opportunity would not have come without people willing to invest in me. Renée, few people truly recognize what you do not just for this campus, but for our field. I am grateful to have been a part of that. Thank you for continuing to mentor me; I hope you agree that the person I am now is a more effective instructor than I would have been without the opportunities and guidance you gave me. Pía, without you, our dream of the 51L LA program would not have been possible — you share every bit as much praise for how many people have been positively impacted by it. Jordan, you are exactly the type of person every team needs to function. I think that, even now, you don't fully realize the scope of how many people have been supported by your behind-the-scenes work. Regardless of where life takes you, I know people will value your talent for, and contributions to, making things *happen*.

Thank you to Misa and Phong for your guidance and mentorship. I wouldn't be here today without your help.

Thank you to the D&D and Magic crews: Barry, even though you were far away, you helped keep us *together*. Thank you. Bryant and Paul, I wish we could just play Magic forever! I'm confident that the three of us will find success, even if we're apart. Alissa, I'm so proud that you've found a place you feel you belong. Please continue to positively impact others the way you did for our cohort; I know that you'll be an indispensable mentor to so many. Jordan, Alex, Jess, and Eric, you were my lab-away-from-lab. You might not realize how important it was for me to have that "home," so thank you. Please continue to take good care of your cats and/or Magic cards, as applicable.

Thank you to the Marangoni lab: Francesco, Alex, Rachel, and Claire. You were, and will continue to be, my lab-away-from-lab-away-from-lab.

Mom, Dad, Jessica, Andrew, Travis, Eric, Rachel, Caitlin, Sophie, Emma, and Bailey, thank you for letting me be a part of your family. I didn't know what it meant to have siblings, but now I can't imagine living without them.

Mom and Dad, thank you for preparing me to make the world better in whatever way I could. I'm not going to be a lawyer or an engineer, and I'm not going to cure cancer (Shannon's working on it) — but I'm a doctor now, and I think I've finally found what I was put here to do. I couldn't have gotten to this point without you both. Thank you.

Shannon and Finn, I love you more than anything. Thank you for being my everything.

VITA

James H. Griffin

EDUCATION

2018–2024 PhD Chemistry
University of California, Irvine

2014–2018 BS Chemical Biology
University of California, Berkeley

RESEARCH EXPERIENCE

2018–2024 Graduate Student Researcher
Advisor: Prof. James S. Nowick
Department of Chemistry, University of California, Irvine

2016–2018 Undergraduate Research Assistant
Advisor: Prof. Felix R. Fisher
Department of Chemistry, University of California, Berkeley

PUBLICATIONS

Griffin, J. H.; Mendoza, A.; Nowick, J. S. Teixobactin "Swapmers" with L Tail Stereochemistry Retain Antibiotic Activity. **2024** [Manuscript submitted for publication].

Brunicardi, J. E. H.*; Griffin, J. H.*; Ferracane, M. J.; Kreutzer, A. G.; Small, J.; Mendoza, A; Ziller, J. W.; Nowick, J. S. Structure-Activity Relationship Studies of the Peptide Antibiotic Clovibactin. *J. Org. Chem.* **2024** [Manuscript in revision].

Thompson, J. C.; Griffin, J. H.; Link, R. Evaluating Student Engagement With Quick Reference (QR) Videos for Common Organic Chemistry Laboratory Techniques. *J. Chem. Ed.* **2024** [Manuscript in revision].

Griffin, J. H.; Thompson, J. C.; López, P.; Link, R. Leveraging Undergraduate Learning Assistants When Implementing New Laboratory Curricula. *Front. Educ.* **2024**, 9:1367087.

von Kugelgen, S.; Piskun, I.; Griffin, J. H.; Eckdahl, C. T.; Jarenwattananon, N. N.; Fischer, F. R. Templated Synthesis of End-Functionalized Graphene Nanoribbons through Living Ring-Opening Alkyne Metathesis Polymerization. *J. Am. Chem. Soc.* **2019**, *141* (28), 11050−11058.

ABSTRACT OF THE DISSERTATION

Supramolecular Antibiotics Inspired by Teixobactin and
Leveraging Undergraduate Learning Assistants When Implementing New Laboratory Curricula

by

James Harrison Griffin

Doctor of Philosophy in Chemistry

University of California, Irvine, 2024

Professor James S. Nowick, Chair

Chapter I is a literature review of cyclodepsipeptide natural products containing 13-membered macrolactone rings. “Depsipeptide” refers to any polypeptide containing an ester linkage, and “cyclodespsipeptide” refers to any depsipeptide containing a macrocycle. Cyclodepsipeptide natural products are commonly non-ribosomally synthesized peptides derived from bacteria. For the purposes of this review, I focus on cyclodepsipeptide natural products containing macrolactone rings. The 13-membered macrolactone ring motif in specific is noteworthy due to its biosynthetic origin, in which the β-hydroxyl of the amino acid at the n-3 position forms a macrocyclic ester with the *C*-terminus. This review provides context for the studies of teixobactin and teixobactin-like peptides in later chapters of the dissertation.

Chapter II describes PEGylated teixobactin analogues. At the time of its discovery, teixobactin showed poor solubility in aqueous conditions. I proposed PEGylation, or polyethyleneglycol (PEG) functionalization, of teixobactin as a way to improve its solubility. The syntheses of teixobactin and PEGylated teixobactin analogues, antibacterial efficacy assays, and solubility assays are described. Unexpectedly, PEGylated teixobactins simultaneously show

no improvement in solubility and a decrease in antibiotic efficacy. These results lead directly into Chapter III.

Chapter III describes "supramolecular antibiotics," or teixobactin-like antibiotic peptides designed to assemble in a fashion similar to wild type teixobactin. Following the discovery that supramolecular assembly of teixobactin, while imparting poor solubility, is a necessary component of its mechanism of action, I sought to design *de novo* antibiotics using our structural understanding of wild type teixobactin. These include "chimeras" of teixobactin and an assembly-prone peptide sequence, as well as "swapmers," which are teixobactin analogues designed with modified tail stereochemistry in order to promote antiparallel β sheet formation. Design, syntheses, and antibacterial efficacy assays of these peptides are described.

Chapter IV describes an alanine scan and additional SAR studies of clovibactin, a related antibiotic peptide to teixobactin. Clovibactin contains the unnatural β-hydroxylated amino acid (2*R*,3*R*)-3-hydroxyasparagine at the depsicycle position 5. A successful synthesis of Fmoc-protected (2*R*,3*R*)-3-hydroxyasparagine by other members of the group enabled an alanine scan, as well as other SAR analogues, of clovibactin. Design, syntheses, antibacterial efficacy assays, and X-ray crystallography of these peptides are described.

Chapter V describes a chemistry education research project designed and conducted with Dr. Renée Link, Professor of Teaching. Beginning in 2020, in-person undergraduate general and organic chemistry laboratory courses at UC Irvine were converted to remote delivery in response to the COVID-19 pandemic. When in-person organic chemistry laboratories resumed in 2021, the incoming cohort of students did not have typical hands-on laboratory experience, as they took the prerequisite general chemistry laboratories online. To alleviate this transition from online to in-person labs, we simultaneously (1) developed new, remedial laboratory curricula for

the organic laboratory series and (2) introduced a Learning Assistant program for in-person organic chemistry laboratories for non-chemistry majors for the first time at UC Irvine. The initial cohort of Learning Assistants also lacked in-person laboratory experience, so they were trained while beta testing the remedial laboratory curricula. We use coded survey responses to categorize the benefits perceived by students and Learning Assistants in response to the creation of this new program.

CHAPTER I: Cyclodepsipeptide Natural Products Containing 13-Membered Macrolactone Rings

Abstract

Teixobactin and clovibactin are non-ribosomally synthesized cyclic depsipeptide antibiotics, both isolated from recently-reported strains of soil bacteria. Because of their structural similarity and conserved mechanism of action, our group has pioneered the structure-activity relationship studies of these two promising drug candidates. In the course of reviewing relevant literature concerning teixobactin, clovibactin, and the closely related compound hypeptin, I have identified several classes of nonribosomal peptides (NRPs) containing the same 13-membered macrolactone ring — albeit with distinct ring stereochemistries. In this chapter, I collect the structures and peptide sequences of each cyclodepsipeptide natural product containing a 13-membered macrolactone ring. I envision that, in the course of rediscovery, stereochemical reassignment, and total synthesis, one or more of these compounds may be found to have a similar mechanism of action to that of teixobactin and clovibactin.

Introduction

Many bacterial and fungal natural products are nonribosomal peptides (NRPs) produced by non-ribosomal peptide synthetases (NRPSs).[1,2,3] This broad class of compounds is differentiated from ribosomal peptide natural products by their biosynthesis, which can incorporate non-proteinogenic amino acids and produce cyclized and other nonlinear structures.[4] NRPs are frequently bioactive, especially towards other bacteria or fungi, offering the producing organism a way to compete within its ecological niche.[5,6] A recurring motif among NRPs is that of the depsipeptide, a natural product which contains both amide and ester bonds;[7] a "cyclodepsipeptide" arises when the depsipeptide NRP forms a macrocycle.[8]

This chapter collects all known literature reports of cyclodepsipeptide NRP natural products containing 13-membered macrolactone rings. This ring motif arises when the *C*-terminus of an NRP is esterified onto the β-hydroxy group of an amino acid three positions away from the *C*-terminus (AA_{n-3}), such as serine, threonine, or amino acids β-hydroxylated by unique NRPS domains (Scheme 1.1).[9] Specifically, the thioesterase domain responsible for hydrolytic release of the NRP from the NRPS catalyzes this ester ring formation.[7] By definition, these peptides are therefore tetrapeptide rings with an *N*-terminal peptidic tail. Other depsicycle sizes are produced by NRPSs, in units of 3 atoms (i.e., 10, 16, 19, etc.). Larger and more flexible depsicycle rings appear to be much more prevalent in nature, and many of the 13-membered ring-containing compounds collected in this chapter are produced by organisms which also produce compounds with larger ring sizes. In the case of teixobactin and clovibactin, the 13-membered ring is uniquely constrained to adopt an anion-binding conformation which chelates its bacterial target, and ring expansion reduces antibiotic activity.[10] I have chosen the 13-membered macrolactones (1) because there is no single published collection of these related compounds, (2) because the 13-membered ring is rare among the depsicycles, and (3) because these molecules resemble the subjects of my dissertation research, teixobactin and clovibactin.

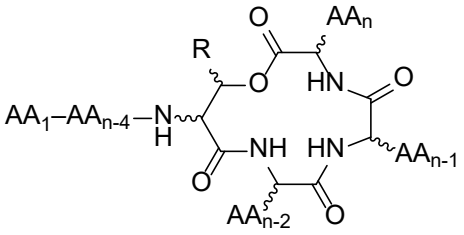

Scheme 1.1. Generic form of the 13-membered macrolactone ring in the cyclodepsipeptides discussed.

I will review the initial report, producing organism, structural assignment (including stereochemistry), and reported bioactivity for each known cyclodepsipeptide natural products

containing a 13-membered macrolactone ring. The compounds are organized by their ring stereochemistries, specifically the L- or D-configuration of each amino acid in the tetracycle. These are:

(1) D-AA_{n-3},L-AA_{n-2},L-AA_{n-1},L-AA_n (D-L-L-L): Hypeptin/Teixobactin/Clovibactin, Nobilamides, and Putisolvins

(2) D-L-D-L: Lystabactin B and Pseudobactin 7SR1

(3) L-L-D-L: Kurstakins, Brevicidines, and Cyanogripeptides

(4) L-D-L-L: Lydiamycins, Malleipeptins, Endopyrroles, Bolagladins, and Cycloacetamides

D-L-L-L: Hypeptin/Teixobactin/Clovibactin, Nobilamides, and Putisolvins

Each of the depsipeptide and depsipeptide classes in this section follow D-L-L-L stereochemistry about the macrolactone ring. Note that the β-position stereochemistry of AA_{n-3} is identical for hypeptin, teixobactin, and clovibactin (Cahn–Ingold–Prelog priority assigns hypeptin and clovibactin as *R* and teixobactin as *S*), while for the nobilamides this position is in the opposite configuration. The putisolvins are achiral at the β-position of AA_{n-3}.

Hypeptin/Teixobactin/Clovibactin

For the purposes of this chapter, hypeptin, teixobactin, and clovibactin will be grouped as the same depsipeptide "class," as the same research teams have conducted the majority of the research pertaining to these compounds and they are derived from organisms sharing significant sequence homology.

Hypeptin

Shoji et al. reported hypeptin in 1989.[11] Hypeptin was isolated from Gram-negative *Pseudomonas* strain PB-6269 and exhibited antibiotic activity against predominantly Gram-

positive bacteria, with some activity against Gram-negative anaerobes (e.g., MIC *S. aureus* = 0.78 μg/mL). It is an octapeptide with a free *N*-terminus and a 13-membered macrolactone depsicycle formed by esterification of the *C*-terminal L-Ile$_8$ to the side-chain hydroxyl group of D-(3*R*)-3-hydroxyasparagine (Figure 1.1, Table 1.1). Hypeptin contains four unusual β-hydroxylated residues, three of which are in the macrocycle.

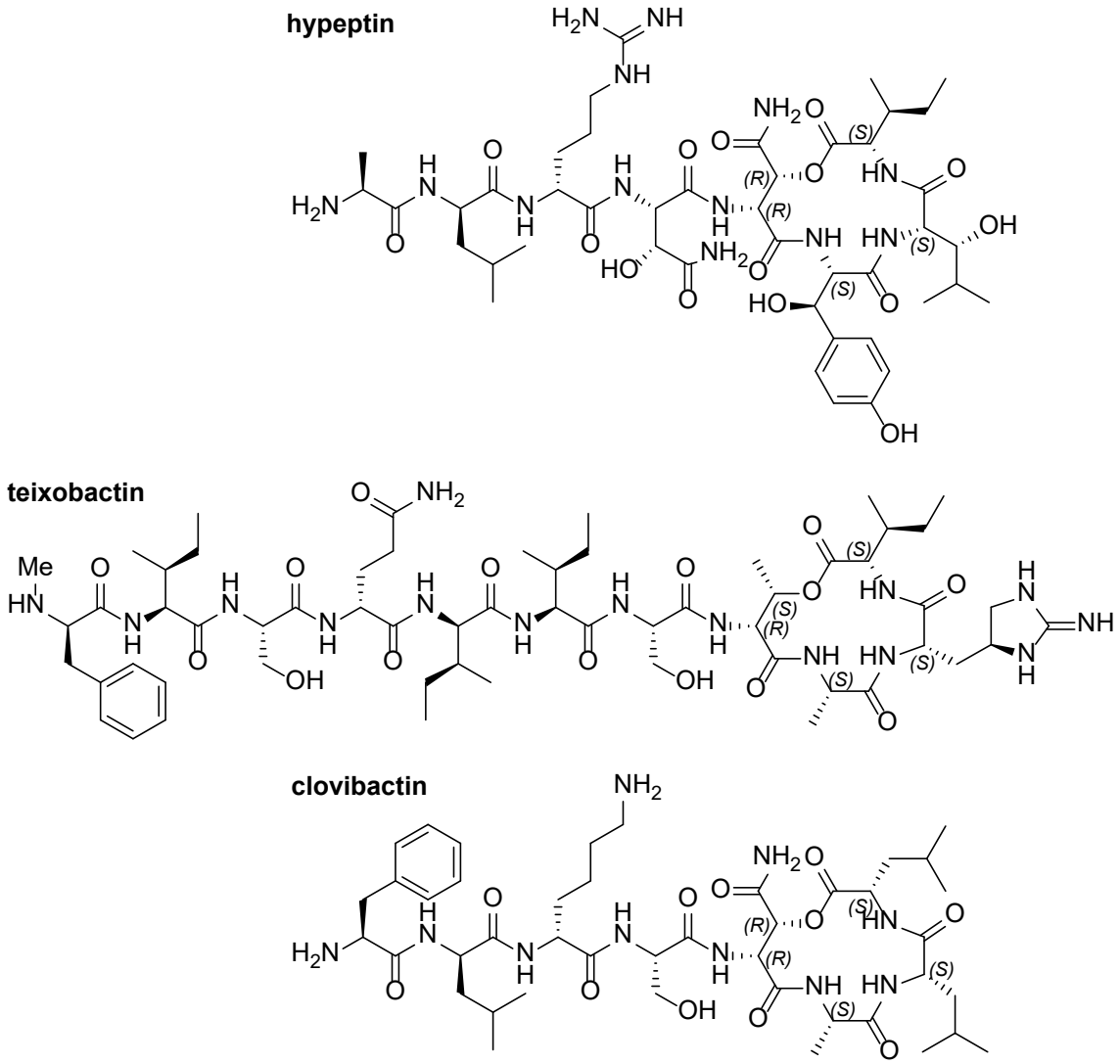

Figure 1.1. Hypeptin, teixobactin, and clovibactin.

Table 1.1. Amino acid sequences of hypeptin, teixobactin, and clovibactin.

Amino acid	Hypeptin (n = 7)	Teixobactin (n = 11)	Clovibactin (n = 7)
AA$_{n-10}$		D-*N*-Me-Phe	
AA$_{n-9}$		L-Ile	

AA_{n-8}		L-Ser	
AA_{n-7}	L-Ala	D-Gln	L-Phe
AA_{n-6}	D-Leu	D-*allo*-Ile	D-Leu
AA_{n-5}	D-Arg	L-Ile	D-Lys
AA_{n-4}	L-(3*R*)-3-OH-Asn	L-Ser	L-Ser
AA_{n-3}	D-(3*R*)-3-OH-Asn	D-Thr	D-(3*R*)-3-OH-Asn[a]
AA_{n-2}	L-(3*S*)-3-OH-Tyr	L-Ala	L-Ala
AA_{n-1}	L-(3*R*)-3-OH-Ile	L-*allo*-End[a]	L-Leu
AA_n	L-Ile	L-Ile	L-Leu

[a] End is enduracididine.

Hypeptin was rediscovered in 2021 by Wirtz et al., in partnership with teams led by Schneider and coworkers at the University of Bonn, Ling and coworkers at NovoBiotic Pharmaceuticals, and Lewis at Northeastern University.[12] In this report, hypeptin was isolated from Gram-negative *Lysobacter* strain K5869 using "iChip" technology, which was developed by Lewis and coworkers to culture previously unculturable soil bacteria for the purpose of finding new bacteria-derived antibiotics (also used to discover teixobactin and clovibactin, see below). Wirtz et al. comprehensively prove the structure of hypeptin, characterize the biosynthetic gene cluster responsible for its production (including the domains responsible for β-hydroxylation of four amino acids), and assign its antibiotic mechanism of action. Hypeptin binds to the pyrophosphate group of lipid II and related bacterial cell wall precursor molecules, preventing their incorporation into the peptidoglycan cell wall of Gram-positive bacteria and therefore blocking cell wall biosynthesis.

Teixobactin

Teixobactin, one of two primary subjects of this dissertation, was reported by Ling et al. in 2015, also in partnership with teams led by Schneider and coworkers at the University of Bonn, Hughes and coworkers at NovoBiotic Pharmaceuticals, and Lewis and coworkers at Northeastern University.[13] This report was a landmark publication in the field of peptide antibiotics for two primary reasons: (1) Teixobactin belonged to a new structural class of

bacteria-derived antibiotic peptides, and (2) teixobactin appeared to kill important drug-resistant bacterial pathogens with very high efficacy and no detectable resistance (e.g., MIC *S. aureus* = 0.25 μg/mL). Teixobactin was immediately the subject of many structure-activity relationship studies, owing to its interesting structure, excellent activity, and compelling lack of resistance. Multiple reviews have already discussed teixobactin in great detail, which I will not repeat here.[14–22]

Our group has pioneered the solid-phase synthesis and structure-activity relationship studies of teixobactin, specifically focusing on its unique mechanism of supramolecular assembly by obtaining X-ray crystallographic structures of analogues.[23–35] Weingarth and coworkers at Utrecht University have driven understanding of teixobactin's supramolecular structure and mechanism of action through solid-state NMR models.[32,36] Teixobactin is discussed further in Chapters II and III.

Clovibactin

Clovibactin, the second primary subject of this dissertation, was reported by Shukla et al., also in partnership with teams led by Schneider and coworkers at the University of Bonn, Hughes and coworkers at NovoBiotic Pharmaceuticals, and Lewis and coworkers at Northeastern University, as well as Weingarth and coworkers at Utrecht University.[37] Clovibactin, including our group's contribution to structure-activity relationship studies of the peptide, is discussed further in Chapter IV.

Nobilamides

Shoji et al. first reported a compound they called TL-119 in 1975.[38] TL-119 was isolated from a Gram-positive *Bacillus* strain (believed to be similar to *B. subtilis*) and exhibited antibiotic activity against other Gram-positive bacteria resistance (e.g., MIC *S. aureus* = 1.56

μg/mL). Later that year, the same research team further clarified the structure of TL-119 to be a hexapeptide acylated at the *N*-terminus and containing a 13-membered macrolactone depsicycle (Figure 1.2, Table 1.2).[39] In 1977, Ogawa et al. reported two new compounds from a *Bacillus subtilis* strain, A-3302-A and A-3302-B; the latter was proposed to be identical to TL-119, and the former differed from A-3302-B only by an additional methylene on the *N*-terminal lipid.[40] Kitajima et al. then revised the structure of TL-119 / A-3302-B by chemical synthesis and spectrometric comparison to assign the depsicycle threonine as D-*allo*-threonine.[41] In 2018, Chalasani et al. reported ASP-1 from *Bacillus subtilis* strain URID 12.1, with an identical mass and amino acid sequence to TL-119 / A-3302-B.[42] ASP-1 exhibited antibiotic activity against methicillin-resistant *Staphylococcus aureus* with no hemolytic activity or cytotoxicity. Finally, Sureram et al. clarified by spectrometric comparison in 2022 that TL-119, A-3302-B, and ASP-1 were, in fact, the same compound. Interestingly, the compound used in the authors' study was isolated from the marine bacterium *Micromonospora* species MAG 9-7 rather than a *Bacillus* species.

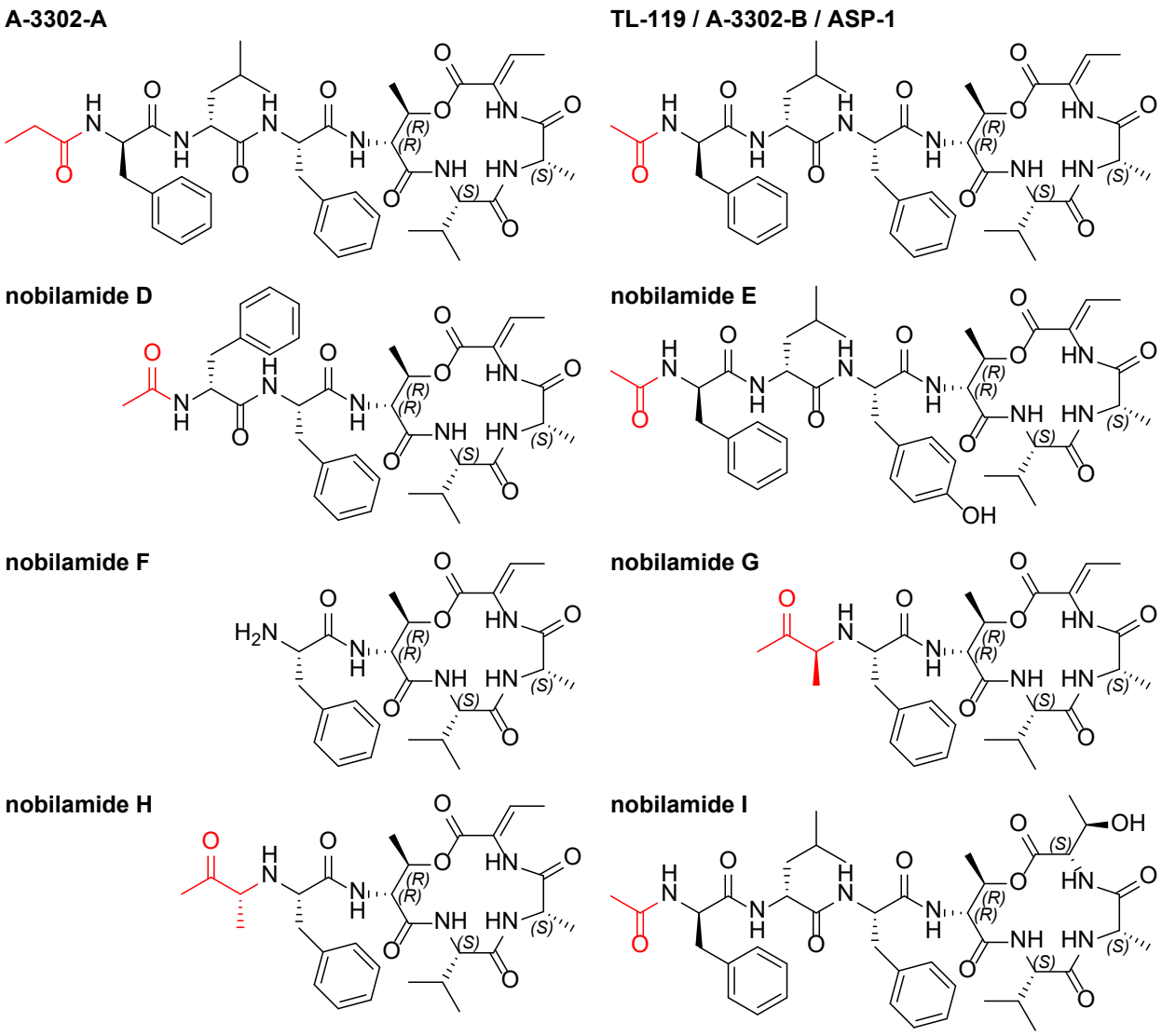

Figure 1.2. A-3302-A, TL-119 / A-3302-B / ASP-1, and nobilamides D–I. The *N*-terminal modifications are highlighted in red.

Table 1.2. Amino acid sequences of A-3302-A, A-3302 B / TL-119 / ASP-1, and nobilamides D–I.

Amino acid	A-3302-A, TL-119 / A-3302-B / ASP-1	Nobilamide			
		D (n = 6)	E (n = 7)	F–H (n = 5)	I (n = 7)
AA_{n-6}	D-Phe		D-Phe		D-Phe
AA_{n-5}	D-Leu	D-Phe	D-Leu		D-Leu
AA_{n-4}	L-Phe	L-Phe	L-Tyr	L-Phe	L-Phe
AA_{n-3}	D-*allo*-Thr	D-*allo*-Thr	D-*allo*-Thr	D-*allo*-Thr	D-*allo*-Thr
AA_{n-2}	L-Val	L-Val	L-Val	L-Val	L-Val
AA_{n-1}	L-Ala	L-Ala	L-Ala	L-Ala	L-Ala
AA_n	(*Z*)-Dhb[a]	(*Z*)-Dhb[a]	(*Z*)-Dhb[a]	(*Z*)-Dhb[a]	L-Thr

[a] Dhb is dehydrobutyrine.

In 2010, Lin et al. coined and added to the family of "nobilamides" to include A-3302-A, TL-119 / A-3302-B / ASP-1, and new compounds nobilamides A–H.[43] Nobilamides A–C are linear, but share similar or truncated amino acid sequences to D–H. Each of the compounds was isolated from mollusk-associated Gram-positive *Streptomyces* strains. Because A-3302-A and nobilamide B acted as antagonists of mouse and human TRPV1 channels, the authors proposed further development of related analogues as therapeutics for pain treatment. Yamashita et al. performed a total synthesis of nobilamide D in 2014.[44] Le et al. then contributed nobilamide I in 2022, also isolated from a marine bacterium (Gram-positive *Saccharomonospora* strain CNQ-490) and with antimetastatic activity by suppressing epithelial−mesenchymal transition.[45] Nobilamide I is the only nobilamide to feature a chiral residue at AA_n (L-Thr) rather than the achiral (*Z*)-dehydrobutyrine.

Putisolvins

Kuiper et al. reported putisolvins I and II from Gram-negative *Pseudomonas putida* strain PCL1445 in 2004.[46] The compounds are biosurfactants (acting as detergents, not antimicrobials) which inhibit biofilm formation and break down existing biofilms of other *Pseudomonas* strains. Collectively, the putisolvins took an interesting path towards structural and stererochemical determination: In the initial 2004 report, only the amino acid sequence and *N*-terminal hexanoic lipid were determined (with no amino acid configurations claimed). Furthermore, some ambiguity existed with respect to the leucine vs. isoleucine assignments of certain residues. In 2020, Oni et al. reported putisolvins III–V, in which two residues (4 and 8) originally reported by Kuiper et al. to be isoleucines were instead leucine.[47] Finally, Muangkaew et al. in 2024 performed comparative spectroscopic analysis of linearized putisolvin natural products with synthetic analogues.[48] Interestingly, the authors found that the NMR spectra reported by Oni et

al. for putisolvins III and IV precisely matched their own spectral data for isolated putisolvins I and II, respectively. This prompted the authors to propose a structural revision of putisolvins I to III and II to IV, reducing the number of unique putisolvins to only three (Figure 1.3, Table 1.3). Muangkaew et al. confidently assigned the absolute configuration of each residue in putisolvin I / III by total synthesis of a linear analogue, and this stereochemistry is expected to match the other two compounds.

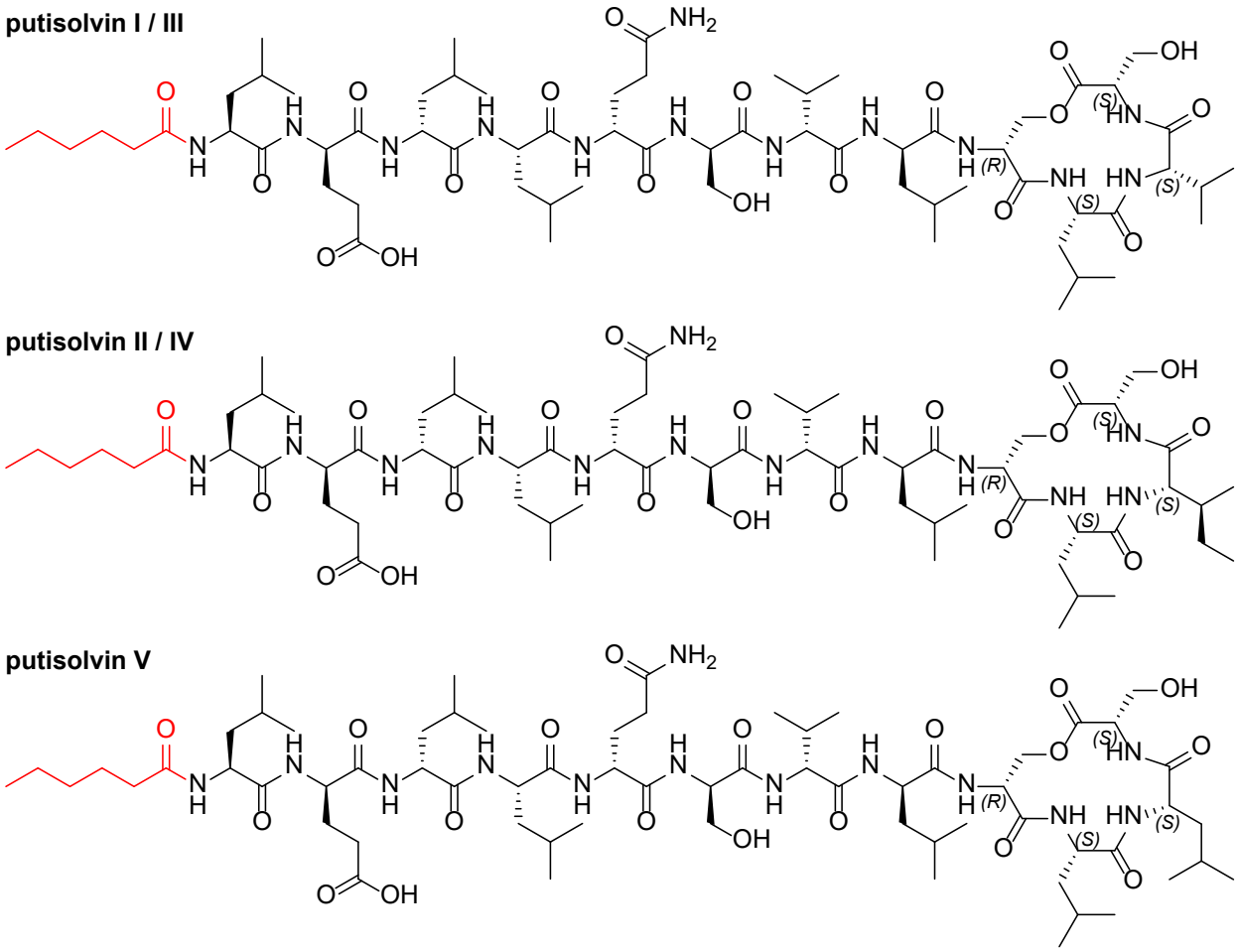

Figure 1.3. Proposed structures of putisolvins I / III, II / IV, and V. The *N*-terminal modifications are highlighted in red.

Table 1.3. Amino acid sequences of putisolvins I / III, II / IV, and V.

Amino acid (n = 12)	**Putisolvin**		
	I / III	**II / IV[a]**	**V[a]**
AA_{n-11}	L-Leu	L-Leu	L-Leu

AA_{n-10}	D-Glu	D-Glu	D-Glu
AA_{n-9}	D-Leu	D-Leu	D-Leu
AA_{n-8}	L-Leu	L-Leu	L-Leu
AA_{n-7}	D-Gln	D-Gln	D-Gln
AA_{n-6}	D-Ser	D-Ser	D-Ser
AA_{n-5}	D-Val	D-Val	D-Val
AA_{n-4}	D-Leu	D-Leu	D-Leu
AA_{n-3}	D-Ser	D-Ser	D-Ser
AA_{n-2}	L-Leu	L-Leu	L-Leu
AA_{n-1}	L-Val	L-Ile	L-Leu
AA_{n}	L-Ser	L-Ser	L-Ser

[a] The amino acid configurations of putisolvins II / IV and V have not been spectrometrically compared to synthetic compounds. These configurations are proposed based on biosynthetic gene cluster analysis and anticipated similarity to putisolvin I / III.

Dunbern et al. have investigated the biosynthetic factors that control putisolvin production in *P. putida.* In 2005, the authors showed that putisolvin appears to be regulated by heat shock genes and that production is favored at low temperatures.[49] In 2006, the authors described a quorum-sensing system composed of three genes (*ppuI-rsaL-ppuR*) which, when mutated, can either disrupt or promote putisolvin production.[50] *P. putida* is an obligate aerobe; the authors reported that growth at 1% oxygen and/or at increased salt concentration (1 M KCl or NaCl) increased putisolvin production.[51] Finally, in 2008 the authors performed a comprehensive analysis of the biosynthetic gene cluster responsible for putisolvin production.[52] The authors report that non-ribosomal peptide synthetases encoded by the same genes (*psoA*, *psoB*, and *psoC*) make all putisolvins, and the position 11 module is promiscuous for each of valine, leucine, and isoleucine, but prioritized valine.

D-L-D-L: Lystabactin B and Pseudobactin 7SR1

Both of the depsipeptides in this section follows D-L-D-L stereochemistry about the macrolactone ring.

Pseudobactin 7SR1

Yang and Leong reported pseudobactin 7SR1 in 1984.[53] As a fluorescent siderophore produced by a *Pseudomonas* species, the compound belongs to the wider family of pyoverdines. The authors initially assigned pseudobactin 7SR1 to be a cyclized by the *C*-terminus onto the amine group of D-Ser$_1$, but the structure was revised in 2000 by Voßen et al. to be a 13-membered macrolactone ring esterified between the *C*-terminus and the side-chain hydroxy group of D-Ser$_5$. (Figure 1.4, Table 1.4))[54] Position 2 is a δ*N*-acetylated, δ*N*-hydroxylated ornithine, and the chromophore — (*S*)-5-(4-amino-*N*-methyl-4-oxobutanamido)-8,9-dihydroxy-2,3-dihydro-1H-pyrimido[1,2-*a*]quinoline-1-carboxylic acid — is amidated to the *N*-terminus.

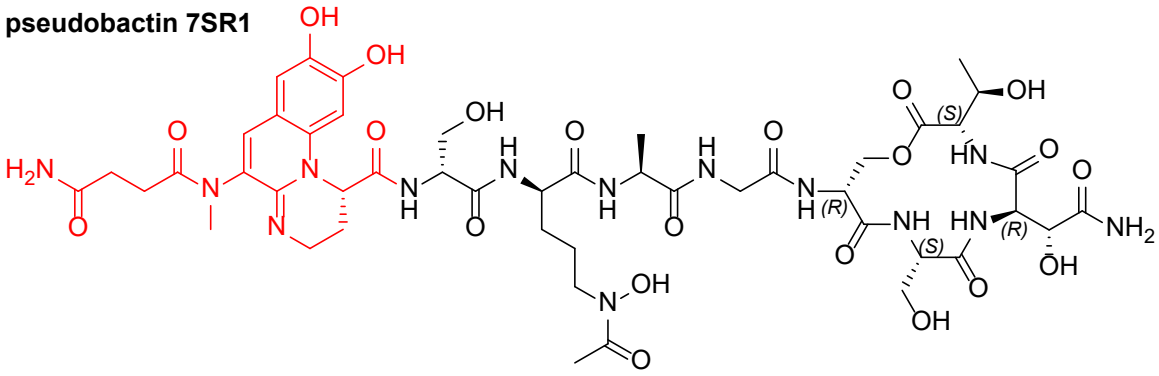

Figure 1.4. Pseudobactin 7SR1. The *N*-terminal modification is highlighted in red.

Table 1.4. Amino acid sequence of pseudobactin 7SR1.

Amino acid (n = 8)	Pseudobactin 7SR1
AA$_{n-7}$	D-Ser
AA$_{n-6}$	L-δ*N*-acetyl-δ*N*-hydroxyornithine
AA$_{n-5}$	L-Ala
AA$_{n-4}$	Gly
AA$_{n-3}$	D-Ser
AA$_{n-2}$	L-Ser
AA$_{n-1}$	D-(3*R*)-3-OH-Asn
AA$_n$	L-Thr

Lystabactin B

Kane and Butler reported lystabactins A–C in 2013, and there are no further reports of these compounds.[55] Of the only four α-amino acids which comprise the lystabactin B (and

therefore the entire macrolactone), two are ornithines which have been both formylated and hydroxylated (Figure 1.5, Table 1.5). The *N*-terminus of the lystabactins consists of the rare γ-amino acid 4,8-diamino-3-hydroxyoctanoic acid amidated at the C8 amine by 2,3-dihydroxybenzoic acid. Lystabactins A and C have similar amino acid sequences to B, but are linear. The lystabactins are produced by the marine Gram-negative bacterium *Pseudoalteromonas* species S2B and act as siderophores.

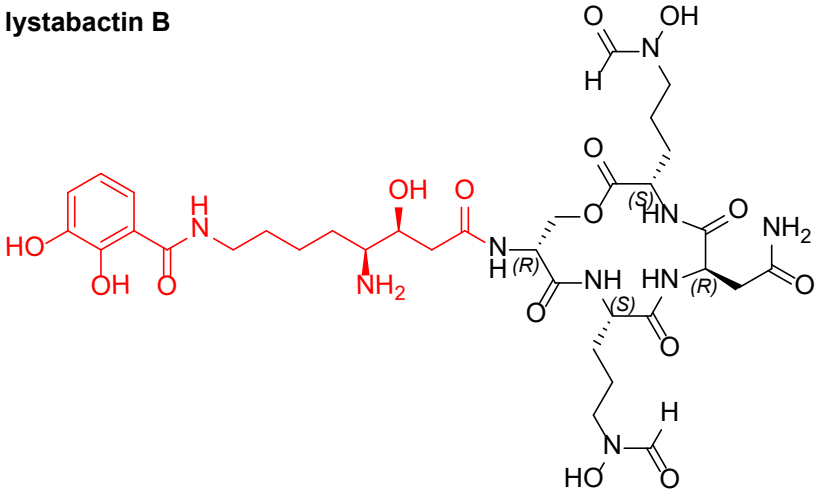

Figure 1.5. Lystabactin B. The *N*-terminal modification is highlighted in red.

Table 1.5. Amino acid sequence of lystabactin B.

Amino acid (n = 4)	Lystabactin B
AA$_{n-3}$	D-Ser
AA$_{n-2}$	L-δ*N*-formyl-δ*N*-hydroxyornithine
AA$_{n-1}$	D-Asn
AA$_n$	L-δ*N*-formyl-δ*N*-hydroxyornithine

L-L-D-L: Kurstakins, Brevicidines, and Cyanogripeptides

Each of the depsipeptide classes in this section follows L-L-D-L stereochemistry about the macrolactone ring.

Kurstakins

Hathout et al. first reported kurstakins A–D in 2000, isolated from the Gram-positive *Bacillus thuringiensis* subspecies *kurstaki* HD-1.[56] Each of the four kurstakins has the same

amino acid sequence, but different fatty acids at the *N*-terminus (Figure 1.6, Table 1.6). Hathout et al. observed the kurstakins to have antifungal activity against *Stachybotrus charatum* comparable to that of polymyxin B.

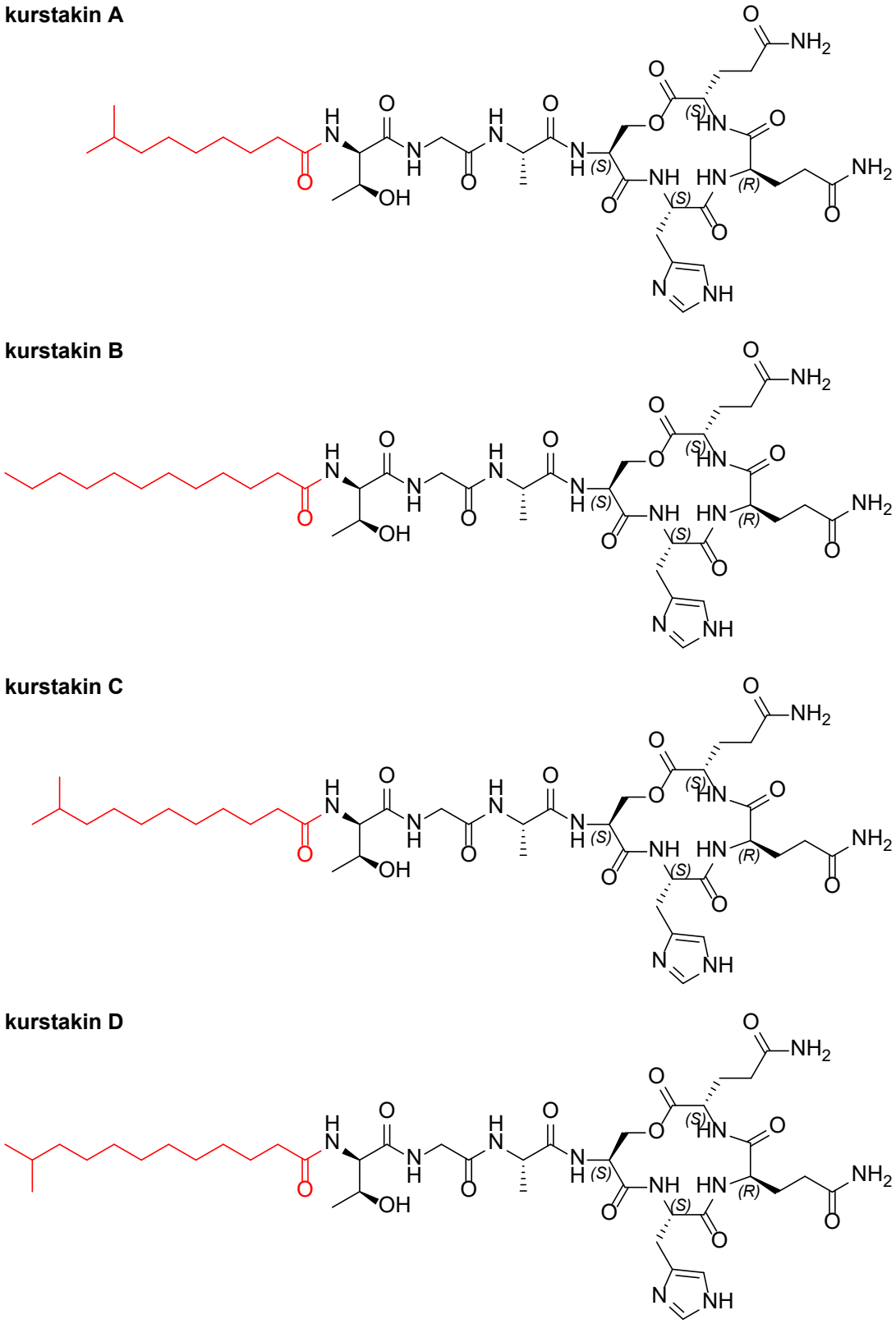

Figure 1.6. Kurstakins A–D. The *N*-terminal modifications are highlighted in red.

Table 1.6. Amino acid sequences of kurstakins A–D.

Amino acid (n = 7)	Kurstakins A–D[a]
$\mathbf{AA_{n-6}}$	D-Thr
$\mathbf{AA_{n-5}}$	Gly
$\mathbf{AA_{n-4}}$	L-Ala
$\mathbf{AA_{n-3}}$	L-Ser
$\mathbf{AA_{n-2}}$	L-His
$\mathbf{AA_{n-1}}$	D-Gln
$\mathbf{AA_{n}}$	L-Gln

[a] The absolute configurations of the kurstakins are not reported, but are proposed by analysis of non-ribosomal peptide synthetase gene clusters.

In 2012, Béchet et al. published a mini review of the kurstakins that addressed publications since the initial report, three of which are expounded upon herein.[57] Price et al. observed kurstakins in 20 of 54 additional *Bacillus* strains analyzed.[58] The authors of the latter report noted that kurstakins were predominantly found in bacterial colonies rather than liquid culture, which implies that the natural product is retained by cells rather than secreted. Bumpus et al. identified natural products related to the kurstakins, also from *Bacillus* species, which are hydrolylated β to the fatty acid.[59] Of these homologues, three are cyclic; the cyclic homologues with β-hydroxylation are proposed to have 3-hydroxyundecanoic, 3-hydroxytridecanoic, and 3-hydroxytetradecanoic acid isomers at the *N*-termini. Finally, Abderrahmani et al. characterized an orphan biosynthetic gene cluster that was found to produce kurstakins. [60] By genome analysis of related species for this new biosynthetic gene cluster, kurstakin production was found in six new strains.

Since the review by Béchet et al., kurstakins have been the subject of many genome analysis studies, but no synthetic efforts. Because kurstakins are addressed frequently with related lipopeptides, such as surfactins, I will only address the most notable reports. *Bacillus cereus* strain AR156 colonizes rice plants; Yu et al. found that kurstakins are associated with antagonism towards plant-pathogenic fungi.[61] Mandal et al. identified kurstakin isoforms

containing up to C15 acid tails.[62] Gélis-Jeanvoine et al. further investigated the *krs* gene cluster and identified genetic factors that regulate transcription and subsequent kurstakin synthesis; the authors also showed that the *krs* locus is necessary for *B. cereus* to form biofilms.[63]

Brevicidines

Li et al. reported brevicidine in 2018, along with laterocidine (a depsipeptide containing a 16-membered macrolactone ring).[64] Brevicidine was isolated from Gram-positive *Bacillus laterosporus* strain DSM 25 and showed selective antibiotic activity against Gram-negative bacteria, including antibiotic-resistant pathogens such as *Pseudomonas aeruginosa* and *Escherichia coli* (e.g., MIC *E. coli* = 2 μg/mL); furthermore, *E. coli* did not develop resistance to brevicidine. Five of the twelve amino acids are D-configured, and the *N*-terminus is amidated by 4-methyl-hexanoic acid of undetermined stereochemistry (Figure 1.7, Table 1.7).

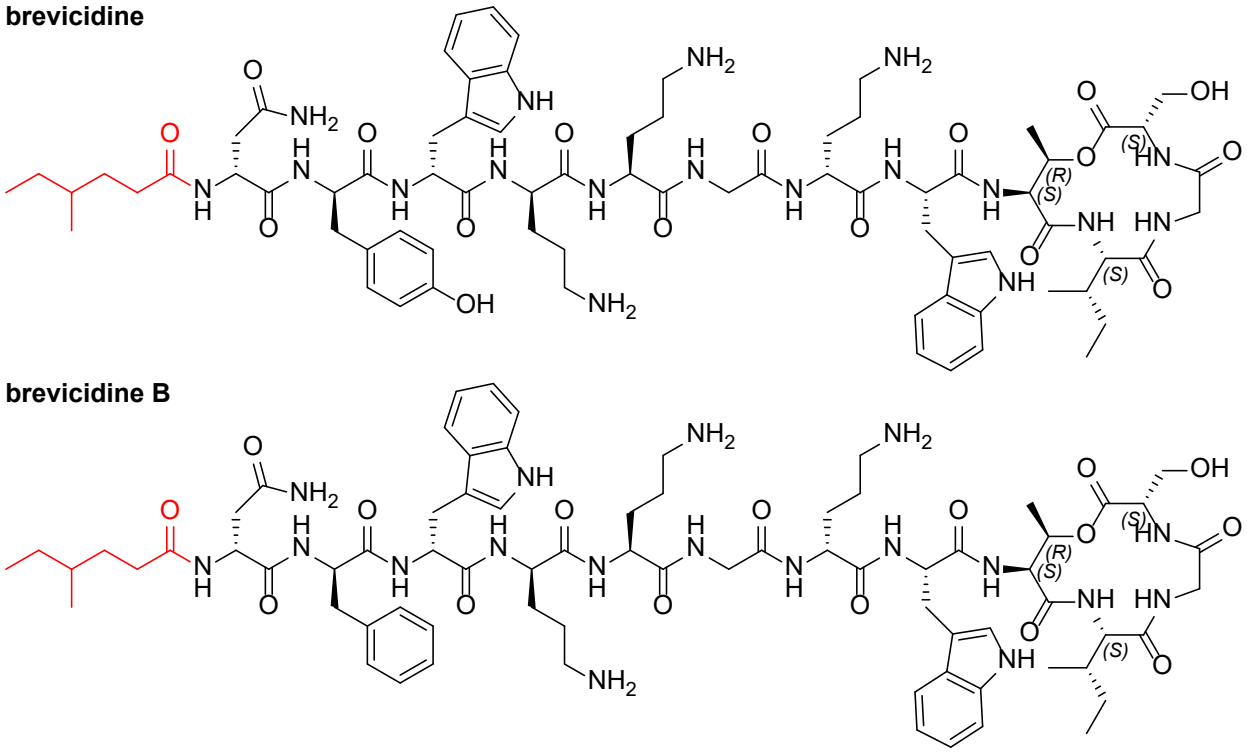

Figure 1.7. Brevicidine and brevicidine B. The *N*-terminal modifications are highlighted in red.

Table 1.7. Amino acid sequences of brevicidine and brevicidine B.

Amino acid (n = 12)	Brevicidine	Brevicidine B
AA_{n-11}	D-Asn	D-Asn
AA_{n-10}	D-Tyr	D-Phe
AA_{n-9}	D-Trp	D-Trp
AA_{n-8}	D-Orn[a]	D-Orn[a]
AA_{n-7}	L-Orn[a]	L-Orn[a]
AA_{n-6}	Gly	Gly
AA_{n-5}	D-Orn[a]	D-Orn[a]
AA_{n-4}	L-Trp	L-Trp
AA_{n-3}	L-Thr	L-Thr
AA_{n-2}	L-Ile	L-Ile
AA_{n-1}	Gly	Gly
AA_n	L-Ser	L-Ser

[a] Orn is ornithine.

Zhao et al. subsequently investigated brevicidine. While brevicidine is a non-ribosomally-synthesized peptide, the authors leveraged ribosomally synthesized and post-translationally modified peptide (RiPP) biosynthesis machinery — including the thioether cyclase LanC — to prepare a macro-thioether analogue of brevicidine that retained antibiotic activity.[65] In 2021, the same authors reported brevicidine B, a natural product from the same *Bacillus* strain as brevicidine, differing only by a single atom resulting from the amino acid mutation of D-Tyr_2 to D-Phe_2.[66] Brevicidine B showed similar antibiotic activity against Gram-negative bacteria, but additionally showed antibiotic efficacy against Gram-positive pathogens. The authors determined that brevicidine B acts through membrane disruption, and that the hydrophobic mutation at position 2 was responsible for the increased membrane disruption potential towards Gram-positive bacteria. Both brevicidine and brevicidine B are non-hemolytic and non-cytotoxic. In 2023, Zhao et al. reported that brevicidine targets lipopolysaccharide in the Gram-negative outer membrane and phosphatidylglycerol and cardiolpin in the inner membrane, disrupting proton motive force and leading to cell death.[67] The authors also showed the effectiveness of brevicidine in treating a mouse sepsis model.

Brevicidine has been the subject of synthetic efforts and structure-activity relationship studies. Hermant et al. reported the first synthesis of brevicidine in 2021 using a hybrid solid-phase linear synthesis and solution-phase macrocyclization strategy.[68] Palapl-latoc et al. (the same research group as Hermant et al.) reported the first total synthesis of brevicidine B 2024, following same hybrid strategy.[69] However, they found that synthetic brevicidine B did not have match the previously reported activity against Gram-positive bacteria and suggested that the structure of brevicidine B should be revisited. They also found that brevicidines are nephrotoxic. In 2022, Ayed et al. reported an additional solid-phase synthesis, which allowed for some SAR with amino acid substitutions.[70] One of these SAR analogues was a macrolactam analogue, which had improved hydrolytic stability in serum but reduced antibiotic activity. Ballantine et al. reported two brevicidine studies: in 2022, an SAR studies with varied, achiral *N*-terminal lipids,[71] and in 2023 the preparation of linearized brevicidine analogues which retain antibiotic activity.[72] The authors also performed an alanine scan of the linearized analogues and determined that the aromatic and cationic residues are most critical for activity.

Recently, further mechanistic studies of brevicidines have been performed. Zhong et al. found that brevicidine has a synergistic effect with antibiotics such as erythromycin, azithromycin, and rifampicin against *Acinetobacter baumannii* by permeabilizing the cell membrane.[73] The dual-drug strategy was also successful at treating a mouse sepsis model. Kim et al. identified brevicidine production from *Brevibacillus laterosporus* strain TSA31-5, and confirmed the previously proposed mode membrane permeabilization.[74] Finally, Buchholz et al. observed accumulation of brevicidine in outer membrane vesicles, supporting the proposed mechanism of action.[75]

Cyanogripeptides

Zhang et al. reported cyanogripeptides A–C from the Gram-positive *Actinoalloteichus cyanogriseus* strain LHW52806 in 2023, and there are no additional reports of these compounds.[76] Each of the cyanogripeptides has an identical amino acid sequence, differing only in the fatty acid amidated to the *N*-terminus (Figure 1.8, Table 1.8). Of note in the amino acid sequence are two instances of L-(3*R*)-3-methyl-leucine, an amino acid found only in three other classes of peptide natural products. The authors assigned the absolute configuration of these residues by stereoselective biosynthesis followed by Marfey's method. Cyanogripeptide C only exhibited weak antibacterial activity against *Heliobacter pylori* and *Mycolicibacterium smegmatis*.

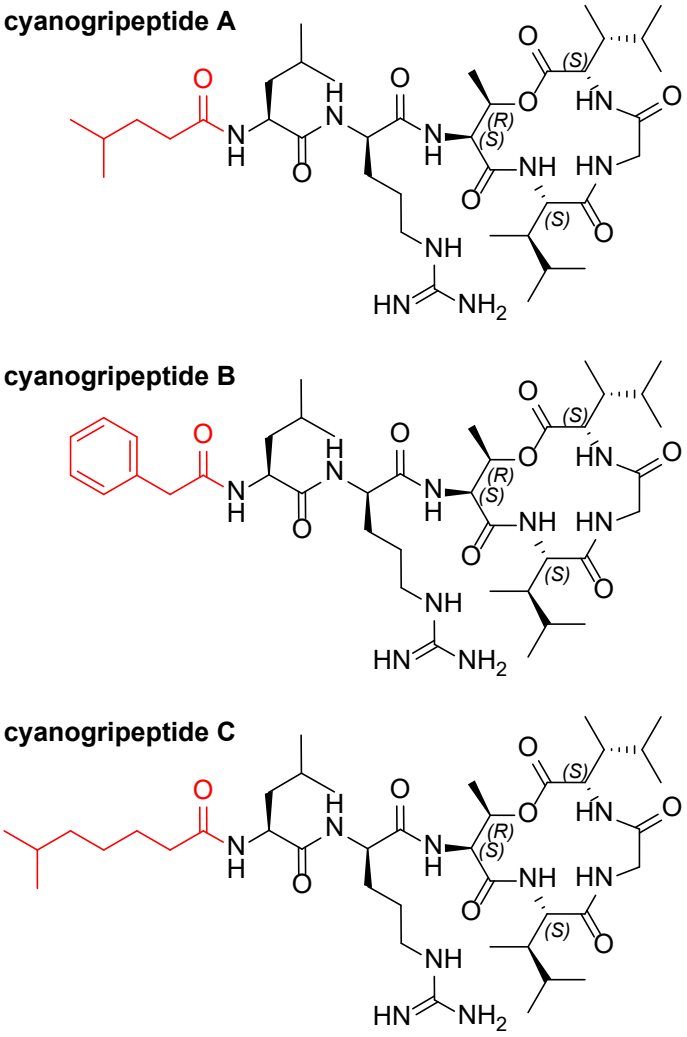

Figure 1.8. Cyanogripeptides A–C. The *N*-terminal modifications are highlighted in red.

Table 1.8. Amino acid sequence of cyanogripeptides A–C.

Amino acid (n = 6)	Cyanogripeptides A–C
$\mathbf{AA_{n-5}}$	L-Leu
$\mathbf{AA_{n-4}}$	D-Arg
$\mathbf{AA_{n-3}}$	L-Thr
$\mathbf{AA_{n-2}}$	L-(3*R*)-3-Me-Leu
$\mathbf{AA_{n-1}}$	Gly
$\mathbf{AA_{n}}$	L-(3*R*)-3-Me-Leu

L-D-L-L: Lydiamycins, Malleipeptins, Endopyrroles, Bolagladins, and Cycloacetamides

Each of the depsipeptide classes in this section follows L-D-L-L stereochemistry about the macrolactone ring.

Lydiamycins

Huang et al. first reported lydiamycins A–D in 2006,[77] and Wang et al. reported lydiamycins E–H in 2023.[78] In both cases, the natural products were obtained from Gram-positive *Streptomyces* species — *S. lydicus* for A–D, and strain HBQ95 (an endophyte associated with the Chinese cinnamon tree, *Cinnamomum cassia*) for E–H. For lydiamycin A, the authors reported selective activity against *Mycobacterium* species with no human cell cytotoxicity; for F–H, the authors reported antimetastatic activity against human pancreatic cancer cells, also without off-target cytotoxicity. In 2022, Libis et al. identified a biosynthetic gene cluster that produces lydiamycin A; this cluster was associated with either *S. albus* or *S. lividans*.[79]

The initial report of lydiamycins A–D by Huang et al. in 2006 incorrectly reported the absolute configurations of, at minimum, lydiamycins A and B. In 2009, Chen et al.[80] and Li et al.[81] independently prepared four synthetic diastereomers each of lydiamycin A and B, respectively. In both cases, the NMR spectra of the synthetic products did not match the natural

products, indicating that the piperazic acid located in the macrolactone ring was likely incorrectly assigned by Huang et al.

In 2020, Hwang et al. published two separate reports concerning lydiamycin A. In the first report, the authors identified lydiamycin A production in *Streptomyces* strain GG23.[82] In the second report, the authors proposed a structural revision of lydiamycin A based in part on chemical derivatization of the natural products by reduction, which allowed for use of Marfey's method to more accurately assign the absolute configurations of each piperazic acid (Figure 1.9, Table 1.9).[83] The authors also reevaluated the antituberculosis activity of lydiamycin A and found it to be more modest than originally reported.

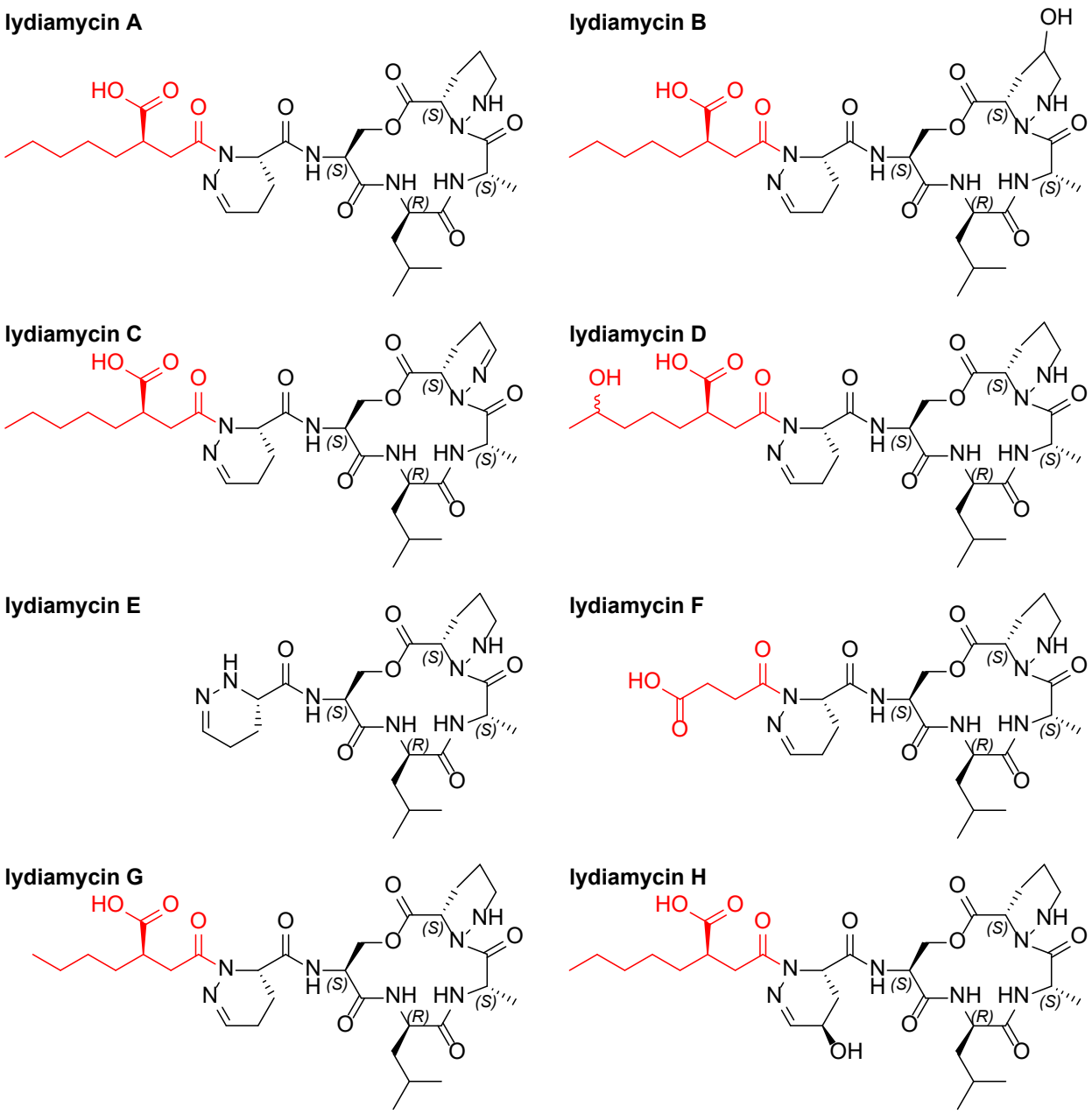

Figure 1.9. Lydiamycins A–H. The *N*-terminal modifications are highlighted in red.

Table 1.9. Amino acid sequences of lydiamycins A–H.

Amino acid (n = 5)	Lydiamycin			
	A, D–G	B	C	H
AA_{n-4}	L-Dpz[a]	L-Dpz[a]	L-Dpz[a]	L-Dpz[a]
AA_{n-3}	L-Ser	L-Ser	L-Ser	L-Ser
AA_{n-2}	D-Leu	D-Leu	D-Leu	D-Leu
AA_{n-1}	L-Ala	L-Ala	L-Ala	L-Ala
AA_n	L-Piz[b]	L-5-OH-Piz[b,c]	L-Dpz[a]	L-(5*R*)-5-OH-Dpz[a]

[a] Dpz is dehydropiperazic acid.

[b] Piz is piperazic acid.
[c] The initially proposed absolute configuration of D-(5*R*)-5-OH-Piz in Lydiamycin B was disproven following a total synthesis and spectroscopic characterization, and the stereochemistry of the 5-hydroxy group is therefore indeterminate.

Each of the lydiamycins contains the unusual L-dehydropiperazic acid, and all except C also contain the reduced form, L-piperazic acid. In B, the ring piperazic acid is hydroxylated, and in H, the tail dehydropiperazic acid is hydroxylated. All lydiamycins except E are capped on the α-amine of dehydropiperazic acid by a succinic acid derivative.

Because of the presence of piperazic acid, the lydiamycins have been addressed in several reviews. In 2011, Oelke et al. reviewed all piperazic acid-containing natural products, focusing on total syntheses. [84] In 2018, Morgan et al. also reviewed piperazic acid-containing natural products, but chose to focus on their biosynthetic origins. [85] Both of these reviews were written prior to the structural revision of lydiamycin A or the reports of E–H. In 2023, the lydiamycins were addressed by Zotchev in a mini review[86] and Shin et al. in their method development for the discovery of new piperazic acid-bearing natural products by genomic and spectroscopic comparison with known compounds, such as lydiamycin A. [87]

Malleipeptins

Biggins et al. reported malleipeptins A and B from the Gram-negative bacteria *Burkholderia pseudomallei* — the etiological agent of melioidosis, or Whitmore's disease — in 2014.[88] Esmaeel et al. independently reported malleipeptin A as "burkhomycin" in 2016.[89] The malleipeptins were addressed in a review of novel antimicrobial lipopeptides by Clements-Decker et al. in 2022.[90] Also in 2022, Borlee et al. showed that deletion of the biosynthetic gene clusters responsible for malleipeptin synthesis contribute to *B. pseudomallei* biofilm formation.[91]

Because *B. pseudomallei* is classified by the NIH and CDC as a Select Agent, owing to its high antibiotic resistance, Biggins et al. began their study with the genetically related species

B. mallei and *B. thailandensis*. Malleipeptins A and B were then identified from NRP and polyketide synthetases unique to a strain of *B. pseudomallei* rendered incapable of growing outside the laboratory. Malleipeptins A and B each contain the unnatural amino acids (*E*)-dehydrobutyrine and D-4-hydroxyglutamine; the 4-position stereochemistry was not assigned by Biggins et al. for the latter (Figure 1.10, Table 1.10). The *N*-terminus of each peptide is capped by (*E*)-2-decenoic acid.

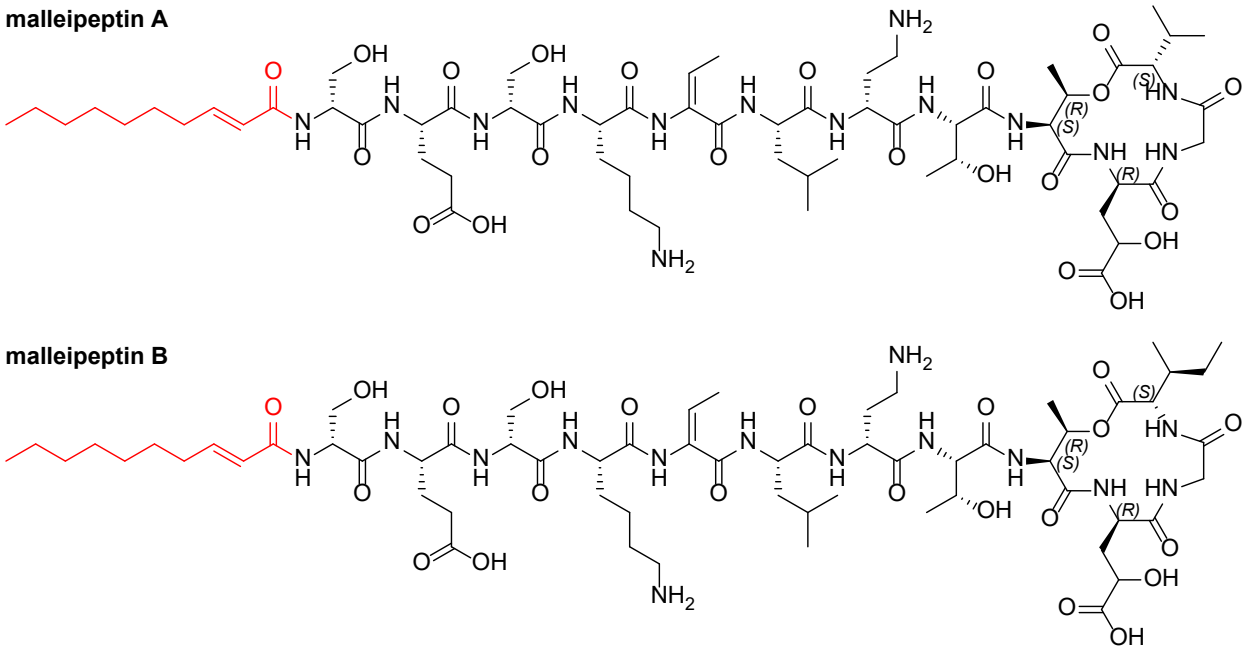

Figure 1.10. Malleipeptins A and B. The *N*-terminal modifications are highlighted in red.

Table 1.10. Amino acid sequences of malleipeptins A and B.

Amino acid (n = 12)	Malleipeptin	
	A	B
AA_{n-11}	D-Ser	D-Ser
AA_{n-10}	L-Glu	L-Glu
AA_{n-9}	D-Ser	D-Ser
AA_{n-8}	L-Lys	L-Lys
AA_{n-7}	(*E*)-Dhb[a]	(*E*)-Dhb[a]
AA_{n-6}	L-Leu	L-Leu
AA_{n-5}	D-Dab[b]	D-Dab[b]
AA_{n-4}	L-Thr	L-Thr
AA_{n-3}	L-Thr	L-Thr
AA_{n-2}	D-4-OH-Glu[c]	D-4-OH-Glu[c]

AA_{n-1}	Gly	Gly
AA_n	L-Val	L-Ile

[a] Dhb is dehydrobutyrine.
[b] Dab is 2,4-diaminobutyric acid.
[c] The absolute configuration of the 4-hydroxy group was not determined.

In bioactivity assays, malleipeptins A and B showed no significant bactericidal activity or human cell cytotoxicity. Biggins et al. then performed a "toluene emulsion assay" to compare extracts from a control *B. pseudomallei* strain and a *B. pseudomallei* strain with an inducible biosynthetic gene cluster to produce the malleipeptins. In this assay, bacterial extracts from various *B. pseudomallei* strains were mixed with a toluene-media interface, and the occurrence of emulsions (indicating surfactant activity) was observed. Only the extracts of *B. pseudomallei* stains actively producing malleipeptins acted as surfactants. Because malleipeptin production is necessary for *B. pseudomallei* virulence, the authors therefore concluded that the malleipeptins confer critical biosurfactant activity during bacterial infections.

Endopyrroles

Niehs et al. reported endopyrroles A–C in 2019, and there are no additional reports of these compounds.[92] Endopyrroles A and C contain 13-membered depsicycles, while endopyrrole B is linear (Figure 1.11). Endopyrrole B lacks the *C*-terminal L-tyrosine residue, which in A and B forms the macrolactone by esterification to L-Thr_5 (AA_{n-3}) (Table 1.11). Each of the endopyrroles is capped at the *N*-terminus by a pyrrole group, which the authors show originates from dehydrogenation of proline.

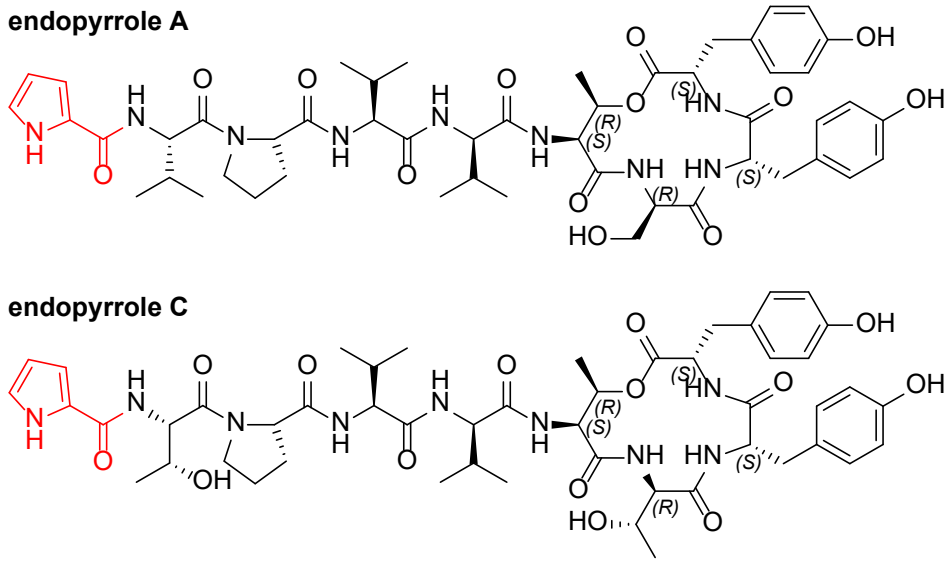

Figure 1.11. Endopyrroles A and C. The *N*-terminal modifications are highlighted in red.

Table 1.11. Amino acid sequences of endopyrroles A and C.

Amino acid (n = 8)	Endopyrrole	
	A	C
AA_{n-7}	L-Val	L-Thr
AA_{n-6}	L-Pro	L-Pro
AA_{n-5}	L-Val	L-Val
AA_{n-4}	D-Val	D-Val
AA_{n-3}	L-Thr	L-Thr
AA_{n-2}	D-Ser	D-Thr
AA_{n-1}	L-Tyr	L-Tyr
AA_{n}	L-Tyr	L-Tyr

The endopyrroles are produced by *Burkholderia rhizoxinica*, which is a Gram-negative bacteria endosymbiotic with the fungus *Rhizopus microsporus*. *Burkholderia* species are known to produce other cyclic and depsipeptide NRPs. However, many of these "cryptic" biosynthetic gene clusters are only expressed under unique, non-laboratory growth conditions. Niehs et al. began their study by investigating the genome of *B. rhizoxinica* for NRPSs and polyketide synthases that were unassociated with known natural products. This led the authors to discover that the endopyrroles are only produced by *B. rhizoxinica* when in endosymbiosis with *R. microsporus*. No noteworthy bioactivity of the endopyrroles was observed.

Bolagladins

Bolagladins A and B were independently reported in the same issue of *Angew. Chem. Int. Ed.* in 2020 by Dashti et al.[93] and by Dose et al.[94] The former report obtained clinical isolates of *Burkholderia gladioli* from cystic fibrosis patients and identified a NRP/polyketide synthetase gene cluster responsible for producing bolagladins A and B. No antimicrobial activity against the ESKAPE pathogens, *Mycobacterium bovis*, or *Candida albicans* was observed. Both bolagladins bound ferric iron, and in a growth assay, addition of ferric iron suppressed bolagladin production. The authors determined that the biosynthetic gene cluster responsible for bolagladin production was located adjacent to a gene encoding an outer-membrane ferric-siderophore receptor, leading to the hypothesis that the bolagladins were themselves siderophores.

The latter report also identified the bolagladins from NRPSs in *B. gladioli*. Specifically, genome mining revealed five NRPS gene clusters, including an orphan gene cluster (*bol*) with no known relatives. The authors identified both the citrate synthase responsible for producing the unprecedented tricarboxylic fatty acid tail and a novel desaturase for enamide formation of the unusual dehydro-β-alanine residue.

Structurally, the bolagladins comprise the 13-membered macrolactone, which is linked by the free L-serine amine to (*E*)-dehydro-β-alanine (Dhb) (Figure 1.12, Table 1.12). This β-amino acid, in turn, is linked by the free β-amine to a unique tricarboxylic fatty acid. Because the free acids and polar macrolactone are bridged by a hydrophobic hydrocarbon, the bolagladins are considered bolaamphiphiles.

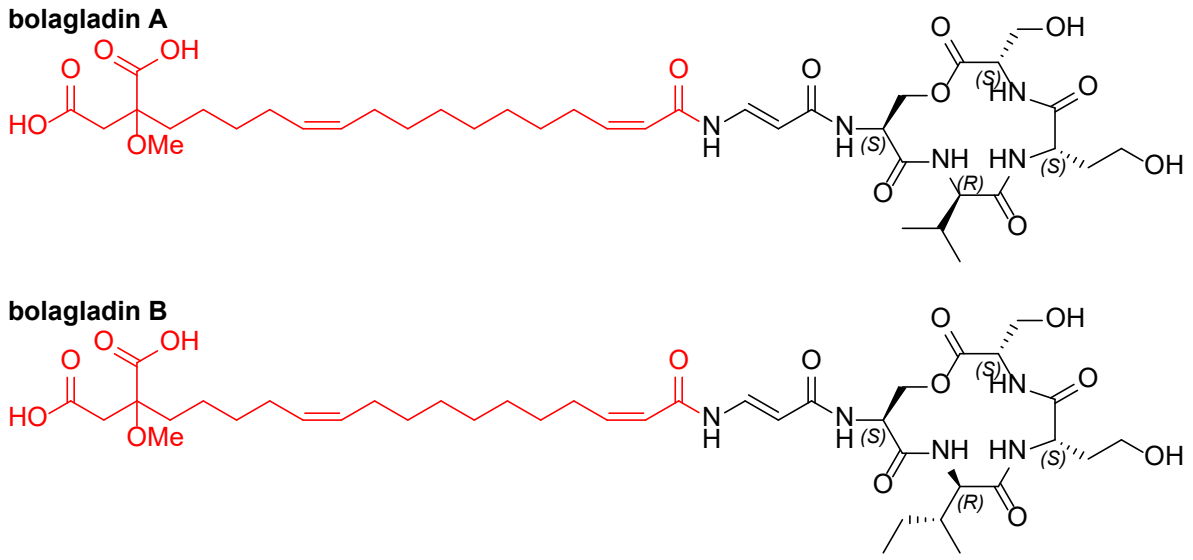

Figure 1.12. Bolagladins A and B. The *N*-terminal modifications are highlighted in red.

Table 1.12. Amino acid sequences of bolagladins A and B.

Amino acid (n = 5)	Bolagladin	
	A	**B**
AA_{n-4}	(*E*)-Dba[a]	(*E*)-Dba[a]
AA_{n-3}	L-Ser	L-Ser
AA_{n-2}	D-Val	D-Ile
AA_{n-1}	L-Hse[b]	L-Hse[b]
AA_{n}	L-Ser	L-Ser

[a] Dba is dehydro-β-alanine.
[b] Hse is homoserine.

Cycloacetamides

Rassback et al. reported cycloacetamides A–F in 2023, and there are no additional reports of these compounds (Figure 1.13).[95] Unlike the other cyclodepsipeptides collected in this chapter, the cycloacetamides were isolated from a soil fungus, *Mortierella alpina*. *M. alpina* produces the cycloacetamides via bacterial-like NRPSs (i.e., multiple enzyme domains whose expression is controlled by a shared operon, rather than a single NRPS[96]). Because *Mortierella* species can host endobacteria capable of non-ribosomal peptide synthesis, the authors performed (1) PCR analysis of *M. alpina* for endobacterial DNA and (2) growth of *M. alpina* with antibiotic treatment to confirm that the fungus was responsible for synthesizing the natural product.

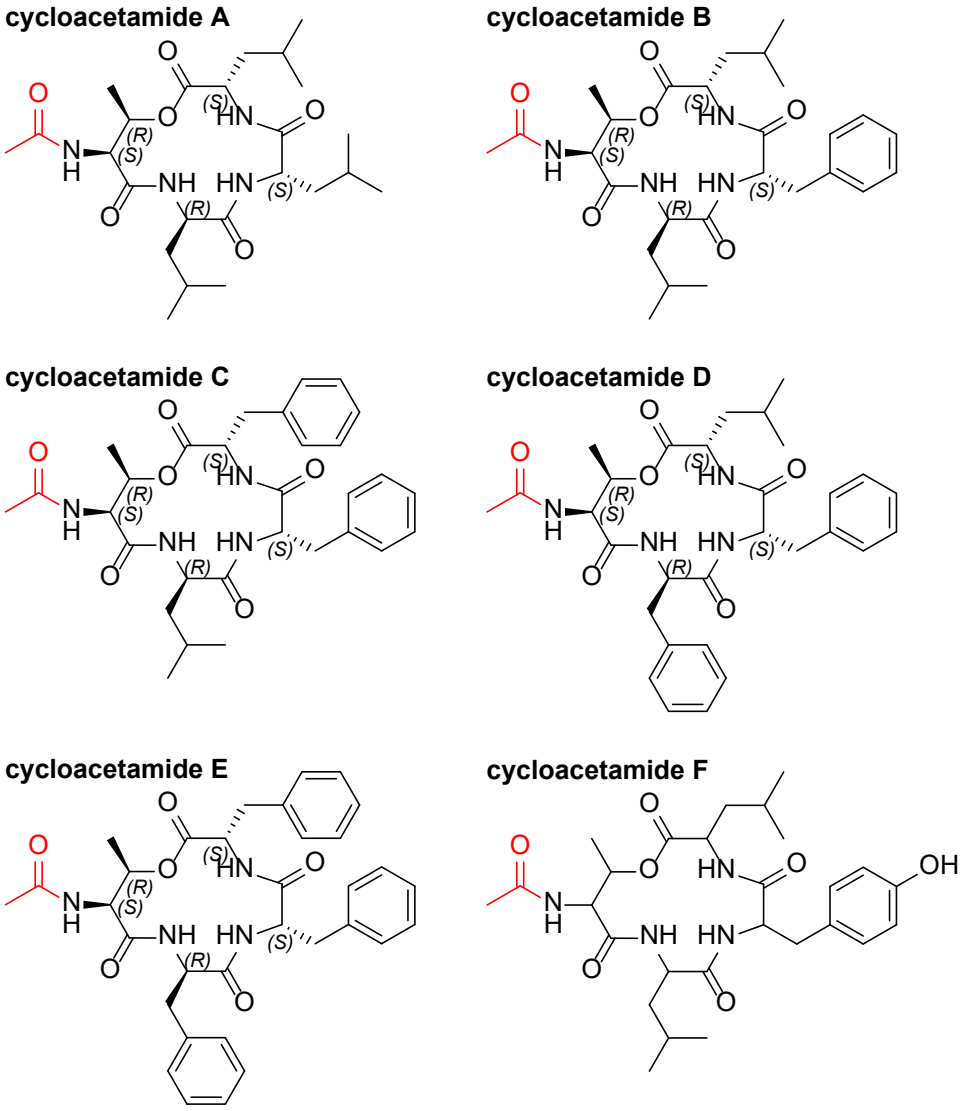

Figure 1.13. Cycloacetamides A–F. The *N*-terminal modifications are highlighted in red.

Each of the cycloacetamides is a tetrapeptide, with a depsicycle formed by esterification of L-threonine. The amino acid sequences of cycloacetamides A–F were determined by NMR and MS/MS analyses (Table 1.13). For each of the cycloacetamides, the *N*-terminus is capped by an acyl group. The absolute configurations of the amino acids in cycloacetamides A–E were determined via Marfey's analysis, and a total synthesis of cycloacetamide B was performed to assign the configurations of Leu_2 (AA_{n-2}) and Leu_4 (AA_n). The absolute configuration of

cycloacetamide F was not determined due to low yields of the isolated natural product, though it is expected to follow the amino acid configurations of A–E.

Table 1.13. Amino acid sequences of cycloacetamides A–F.

Amino acid (n = 4)	Cycloacetamide					
	A	**B**	**C**	**D**	**E**	**F**[a]
AA_{n-3}	L-Thr	L-Thr	L-Thr	L-Thr	L-Thr	Thr
AA_{n-2}	D-Leu	D-Leu	D-Leu	D-Phe	D-Phe	Leu
AA_{n-1}	L-Leu	L-Phe	L-Phe	L-Phe	L-Phe	Tyr
AA_n	L-Leu	L-Leu	L-Phe	L-Leu	L-Phe	Leu

[a] The absolute configuration of cycloacetamide F is not reported.

In bioactivity assays, cycloacetamides A and B showed no antibacterial or antifungal activity, human cytotoxicity, antiproliferative or immunomodulating effects, or protease inhibition. The authors noted that *M. alpina* was previously shown to be toxic to waxmoth and housefly larvae, but that a specific toxic agent was never identified. Following this hypothesis, cycloacetamides A and B exhibited dose-dependent toxicity to *Drosophila melanogaster* larvae. The authors hypothesized that the cycloacetamides therefore protect *M. alpina* from predation by mycophagous insect larvae.

Conclusion

Of the natural products discussed in this chapter, the mechanistic role of the 13-membered macrolactone ring is only described for teixobactin and clovibactin. In fact, linear analogues of the nobilamides, lystabactins, and endopyrroles are produced by the same organisms that produce the cyclic analogues, and linear brevicidine analogues retain bioactivity. The majority of the compounds are antimicrobial and act against bacterial cell membranes, but there is no consistent selectivity for Gram-positive and/or Gram-negative targets. Similarly, the compounds are isolated from both Gram-positive and Gram-negative bacteria with no observable trend, and the cycloacetamides are derived from fungi. Many of the natural products are reported to act as amphiphilic biosurfactants through nonspecific interactions. It appears that more

targeted mechanistic research is needed to establish whether the conserved 13-membered depsicycle is a useful biosynthetic motif and an example of convergent evolution, or a coincidence of non-ribosomal biosynthesis.

References for Chapter I

[1] Schwarzer, D.; Finking, R.; Marahiel, M. A. Nonribosomal Peptides: From Genes to Products. *Nat. Prod. Rep.* **2003**, *20* (3), 275. DOI: 10.1039/b111145k

[2] Felnagle, E. A.; Jackson, E. E.; Chan, Y. A.; Podevels, A. M.; Berti, A. D.; McMahon, M. D.; Thomas, M. G. Nonribosomal Peptide Synthetases Involved in the Production of Medically Relevant Natural Products. *Mol. Pharmaceutics* **2008**, *5* (2), 191–211. DOI: 10.1021/mp700137g

[3] Fisch, K. M. Biosynthesis of Natural Products by Microbial Iterative Hybrid PKS–NRPS. *RSC Adv.* **2013**, *3* (40), 18228. DOI: 10.1039/c3ra42661k

[4] Duban, M.; Cociancich, S.; Leclère, V. Nonribosomal Peptide Synthesis Definitely Working Out of the Rules. *Microorganisms* **2022**, *10* (3), 577. DOI: 10.3390/microorganisms10030577

[5] Oide, S.; Turgeon, B. G. Natural Roles of Nonribosomal Peptide Metabolites in Fungi. *Mycoscience* **2020**, *61* (3), 101–110. DOI: 10.1016/j.myc.2020.03.001

[6] Maglangit, F.; Yu, Y.; Deng, H. Bacterial Pathogens: Threat or Treat (a Review on Bioactive Natural Products from Bacterial Pathogens). *Nat. Prod. Rep.* **2021**, *38* (4), 782–821. DOI: 10.1039/D0NP00061B

[7] Alonzo, D. A.; Schmeing, T. M. Biosynthesis of Depsipeptides, or Depsi: The Peptides with Varied Generations. *Prot. Sci.* **2020**, *29* (12), 2316–2347. DOI: 10.1002/pro.3979

[8] Farah, H. I.; Supratman, U.; Hidayat, A. T.; Maharani, R. An Overview of the Synthesis of Biologically Active Cyclodepsipeptides. *ChemistrySelect* **2022**, *7* (1), e202103470. DOI: 10.1002/slct.202103470

[9] Jaremko, M. J.; Davis, T. D.; Corpuz, J. C.; Burkart, M. D. Type II Non-Ribosomal Peptide Synthetase Proteins: Structure, Mechanism, and Protein–Protein Interactions. *Nat. Prod. Rep.* **2020**, *37* (3), 355–379. DOI: 10.1039/C9NP00047J

[10] Yang, H.; Pishenko, A. V.; Li, X.; Nowick, J. S. Design, Synthesis, and Study of Lactam and Ring-Expanded Analogues of Teixobactin. *J. Org. Chem.* **2020**, *85* (3), 1331–1339. DOI: 10.1021/acs.joc.9b02631

[11] Shoji, J.; Hinoo, H.; Hattori, T.; Hirooka, K.; Kimura, Y.; Yoshida, T. Isolation and Characterization of Hypeptin from Pseudomonas *Sp. J. Antibiot.* **1989**, *42* (10), 1460–1464. DOI: 10.7164/antibiotics.42.1460

[12] Wirtz, D. A.; Ludwig, K. C.; Arts, M.; Marx, C. E.; Krannich, S.; Barac, P.; Kehraus, S.; Josten, M.; Henrichfreise, B.; Müller, A.; König, G. M.; Peoples, A. J.; Nitti, A.; Spoering, A. L.; Ling, L. L.; Lewis, K.; Crüsemann, M.; Schneider, T. Biosynthesis and Mechanism of Action of the Cell Wall Targeting Antibiotic Hypeptin. *Angew. Chem. Int. Ed.* **2021**, *60* (24), 13579–13586. DOI: 10.1002/anie.202102224

[13] Ling, L. L.; Schneider, T.; Peoples, A. J.; Spoering, A. L.; Engels, I.; Conlon, B. P.; Mueller, A.; Schäberle, T. F.; Hughes, D. E.; Epstein, S.; Jones, M.; Lazarides, L.; Steadman, V. A.; Cohen, D. R.; Felix, C. R.; Fetterman, K. A.; Millett, W. P.; Nitti, A. G.; Zullo, A. M.; Chen, C.; Lewis, K. A New Antibiotic Kills Pathogens without Detectable Resistance. *Nature* **2015**, *517* (7535), 455–459. DOI: 10.1038/nature14098

[14] Piddock, L. J. V. Teixobactin, the First of a New Class of Antibiotics Discovered by iChip Technology? *J. Antimicrob. Chemother.* **2015**, *70* (10), 2679–2680. DOI: 10.1093/jac/dkv175

[15] Fiers, W. D.; Craighead, M.; Singh, I. Teixobactin and Its Analogues: A New Hope in Antibiotic Discovery. *ACS Infect. Dis.* **2017**, *3* (10), 688–690. DOI: 10.1021/acsinfecdis.7b00108

[16] Guo, C.; Mandalapu, D.; Ji, X.; Gao, J.; Zhang, Q. Chemistry and Biology of Teixobactin. *Chem. Eur. J.* **2018**, *24* (21), 5406–5422. DOI: 10.1002/chem.201704167

[17] McCarthy, M. W. Teixobactin: A Novel Anti-Infective Agent. *Expert Rev. Anti-infect. Ther.* **2019**, *17* (1), 1–3. DOI: 10.1080/14787210.2019.1550357

[18] Matheson, E.; Jin, K.; Li, X. Establishing the Structure-Activity Relationship of Teixobactin. *Chin. Chem. Lett.* **2019**, *30* (8), 1468–1480. DOI: 10.1016/j.cclet.2019.07.004

[19] Iyer, A.; Madder, A.; Singh, I. Teixobactins: A New Class of 21st Century Antibiotics to Combat Multidrug-Resistant Bacterial Pathogens. *Future Microbiol.* **2019**, *14* (6), 457–460. DOI: 10.2217/fmb-2019-0056

[20] Karas, J. A.; Chen, F.; Schneider-Futschik, E. K.; Kang, Z.; Hussein, M.; Swarbrick, J.; Hoyer, D.; Giltrap, A. M.; Payne, R. J.; Li, J.; Velkov, T. Synthesis and Structure−activity Relationships of Teixobactin. *Ann. N. Y. Acad. Sci.* **2020**, *1459* (1), 86–105. DOI: 10.1111/nyas.14282

[21] Gunjal, V. B.; Thakare, R.; Chopra, S.; Reddy, D. S. Teixobactin: A Paving Stone toward a New Class of Antibiotics? *J. Med. Chem.* **2020**, *63* (21), 12171–12195. DOI: 10.1021/acs.jmedchem.0c00173

[22] Qi, Y.; Tang, X.; Wei, N.; Pang, C.; Du, S.; Wang, K. Discovery, Synthesis, and Optimization of Teixobactin, a Novel Antibiotic without Detectable Bacterial Resistance. *J. Pept. Sci.* **2022**, *28* (11), e3428. DOI: doi.org/10.1002/psc.3428

[23] Yang, H.; Chen, K. H.; Nowick, J. S. Elucidation of the Teixobactin Pharmacophore. *ACS Chem. Biol.* **2016**, *11* (7), 1823–1826. DOI: 10.1021/acschembio.6b00295

[24] Yang, H.; Du Bois, D. R.; Ziller, J. W.; Nowick, J. S. X-Ray Crystallographic Structure of a Teixobactin Analogue Reveals Key Interactions of the Teixobactin Pharmacophore. *Chem. Commun.* **2017**, *53* (18), 2772–2775. DOI: 10.1039/C7CC00783C

[25] Chen, K. H.; Le, S. P.; Han, X.; Frias, J. M.; Nowick, J. S. Alanine Scan Reveals Modifiable Residues in Teixobactin. *Chem. Commun.* **2017**, *53* (82), 11357–11359. DOI: 10.1039/C7CC03415F

[26] Yang, H.; Wierzbicki, M.; Du Bois, D. R.; Nowick, J. S. X-Ray Crystallographic Structure of a Teixobactin Derivative Reveals Amyloid-like Assembly. *J. Am. Chem. Soc.* **2018**, *140* (43), 14028–14032. DOI: 10.1021/jacs.8b07709

[27] Yang, H.; Pishenko, A. V.; Li, X.; Nowick, J. S. Design, Synthesis, and Study of Lactam and Ring-Expanded Analogues of Teixobactin. *J. Org. Chem.* **2020**, *85* (3), 1331–1339. DOI: 10.1021/acs.joc.9b02631

[28] Morris, M. A.; Malek, M.; Hashemian, M. H.; Nguyen, B. T.; Manuse, S.; Lewis, K.; Nowick, J. S. A Fluorescent Teixobactin Analogue. *ACS Chem. Biol.* **2020**, *15* (5), 1222–1231. DOI: 10.1021/acschembio.9b00908

[29] Hurst, P. J.; Morris, M. A.; Graham, A. A.; Nowick, J. S.; Patterson, J. P. Visualizing Teixobactin Supramolecular Assemblies and Cell Wall Damage in *B. subtilis* Using CryoEM. *ACS Omega* **2021**, *6* (41), 27412–27417. DOI: 10.1021/acsomega.1c04331

[30] Morris, M. A.; Jones, C. R.; Nowick, J. S. Synthesis and Application of Fluorescent Teixobactin Analogs. In *Methods in Enzymology*; Elsevier, **2022**; Vol. 665, pp 233–258. DOI: 10.1016/bs.mie.2021.12.006

[31] Morris, M. A.; Vallmitjana, A.; Grein, F.; Schneider, T.; Arts, M.; Jones, C. R.; Nguyen, B. T.; Hashemian, M. H.; Malek, M.; Gratton, E.; Nowick, J. S. Visualizing the Mode of Action and Supramolecular Assembly of Teixobactin Analogues in *Bacillus subtilis*. *Chem. Sci.* **2022**, *13* (26), 7747–7754. DOI: 10.1039/D2SC01388F

[32] Shukla, R.; Lavore, F.; Maity, S.; Derks, M. G. N.; Jones, C. R.; Vermeulen, B. J. A.; Melcrová, A.; Morris, M. A.; Becker, L. M.; Wang, X.; Kumar, R.; Medeiros-Silva, J.; Van Beekveld, R. A. M.; Bonvin, A. M. J. J.; Lorent, J. H.; Lelli, M.; Nowick, J. S.; MacGillavry, H. D.; Peoples, A. J.; Spoering, A. L.; Ling, L. L.; Hughes, D. E.; Roos, W. H.; Breukink, E.; Lewis, K.; Weingarth, M. Teixobactin Kills Bacteria by a Two-Pronged Attack on the Cell Envelope. *Nature* **2022**, *608* (7922), 390–396. DOI: 10.1038/s41586-022-05019-y

[33] Jones, C. R.; Guaglianone, G.; Lai, G. H.; Nowick, J. S. Isobactins: O -Acyl Isopeptide Prodrugs of Teixobactin and Teixobactin Derivatives. *Chem. Sci.* **2022**, *13* (44), 13110–13116. DOI: 10.1039/D2SC02670H

[34] Yang, H.; Kreutzer, A. G.; Nowick, J. S. Supramolecular Interactions of Teixobactin Analogues in the Crystal State. *J. Org. Chem.* **2024**, *89* (7), 5104–5108. DOI: 10.1021/acs.joc.3c02617

[35] Jones, C. R.; Lai, G. H.; Padilla, M. S. T. L.; Nowick, J. S. Investigation of Isobactin Analogues of Teixobactin. *ACS Med. Chem. Lett.* **2024**, *15* (7), 1136–1142. DOI: 10.1021/acsmedchemlett.4c00215

[36] Shukla, R.; Medeiros-Silva, J.; Parmar, A.; Vermeulen, B. J. A.; Das, S.; Paioni, A. L.; Jekhmane, S.; Lorent, J.; Bonvin, A. M. J. J.; Baldus, M.; Lelli, M.; Veldhuizen, E. J. A.; Breukink, E.; Singh, I.; Weingarth, M. Mode of Action of Teixobactins in Cellular Membranes. *Nat. Commun.* **2020**, *11* (1), 2848. DOI: 10.1038/s41467-020-16600-2

[37] Shukla, R.; Peoples, A. J.; Ludwig, K. C.; Maity, S.; Derks, M. G. N.; De Benedetti, S.; Krueger, A. M.; Vermeulen, B. J. A.; Harbig, T.; Lavore, F.; Kumar, R.; Honorato, R. V.; Grein, F.; Nieselt, K.; Liu, Y.; Bonvin, A. M. J. J.; Baldus, M.; Kubitscheck, U.; Breukink, E.; Achorn, C.; Nitti, A.; Schwalen, C. J.; Spoering, A. L.; Ling, L. L.; Hughes, D.; Lelli, M.; Roos, W. H.; Lewis, K.; Schneider, T.; Weingarth, M. An Antibiotic from an Uncultured Bacterium Binds to an Immutable Target. *Cell* **2023**, *186* (19), 4059-4073.e27. DOI: 10.1016/j.cell.2023.07.038

[38] Shoji, J.; Hinoo, H.; Wakisaka, Y.; Koizumi, K.; Mayama, M. Studies on Antibiotics from the Genus *Bacillus*. IV. Isolation of a New Peptide Antibiotic TL-119. *J. Antibiot.* **1975**, *28* (2), 126–128. DOI: 10.7164/antibiotics.28.126

[39] Nakagawa, Y.; Nakazawa, T.; Shoj, J. On the Structure of a New Antibiotic TL-119. Studies on Antibiotics from the Genus *Bacillus*. VI. *J. Antibiot.* **1975**, *28* (12), 1004–1005. DOI: 10.7164/antibiotics.28.1004

[40] Ogawa, Y.; Mori, H.; Ichihashi, M.; Ueno, T.; Nakashima, T.; Fukami, H.; Kakajima, R.; Ida, H. Structure elucidation of the antibiotics A-3302-A and-B produced by a new strain of *Bacillus subtilis*. *Peptide Chem.* **1977**, 123-6.

[41] Kitajima, Y.; Waki, M.; Shoji, J.; Ueno, T.; Izumiya, N. Revised Structure of the Peptide Lactone Antibiotic, TL-119 and/or A-3302-B. *FEBS Lett.* **1990**, *270* (1–2), 139–142. DOI: 10.1016/0014-5793(90)81253-K

[42] Chalasani, A. G.; Roy, U.; Nema, S. Purification and Characterisation of a Novel Antistaphylococcal Peptide (ASP-1) from *Bacillus* Sp. URID 12.1. *Int. J. Antimicrob. Agents* **2018**, *51* (1), 89–97. DOI: 10.1016/j.ijantimicag.2017.08.030

[43] Lin, Z.; Reilly, C. A.; Antemano, R.; Hughen, R. W.; Marett, L.; Concepcion, G. P.; Haygood, M. G.; Olivera, B. M.; Light, A.; Schmidt, E. W. Nobilamides A–H, Long-Acting Transient Receptor Potential Vanilloid-1 (TRPV1) Antagonists from Mollusk-Associated Bacteria. *J. Med. Chem.* **2011**, *54* (11), 3746–3755. DOI: 10.1021/jm101621u

[44] Yamashita, T.; Matoba, H.; Kuranaga, T.; Inoue, M. Total Syntheses of Nobilamides B and D: Application of Traceless Staudinger Ligation. *Tetrahedron* **2014**, *70* (42), 7746–7752. DOI: 10.1016/j.tet.2014.05.091

[45] Le, T. C.; Pulat, S.; Lee, J.; Kim, G. J.; Kim, H.; Lee, E.-Y.; Hillman, P. F.; Choi, H.; Yang, I.; Oh, D.-C.; Kim, H.; Nam, S.-J.; Fenical, W. Marine Depsipeptide Nobilamide I Inhibits Cancer Cell Motility and Tumorigenicity via Suppressing Epithelial–Mesenchymal Transition and MMP2/9 Expression. *ACS Omega* **2022**, *7* (2), 1722–1732. DOI: 10.1021/acsomega.1c04520

[46] Kuiper, I.; Lagendijk, E. L.; Pickford, R.; Derrick, J. P.; Lamers, G. E. M.; Thomas-Oates, J. E.; Lugtenberg, B. J. J.; Bloemberg, G. V. Characterization of Two *Pseudomonas putida* Lipopeptide Biosurfactants, Putisolvin I and II, Which Inhibit Biofilm Formation and Break

down Existing Biofilms. *Molecular Microbiology* **2004**, *51* (1), 97–113. DOI: 10.1046/j.1365-2958.2003.03751.x

[47] Oni, F. E.; Geudens, N.; Onyeka, J. T.; Olorunleke, O. F.; Salami, A. E.; Omoboye, O. O.; Arias, A. A.; Adiobo, A.; De Neve, S.; Ongena, M.; Martins, J. C.; Höfte, M. Cyclic Lipopeptide-producing *Pseudomonas koreensis* Group Strains Dominate the Cocoyam Rhizosphere of a Pythium Root Rot Suppressive Soil Contrasting with *P. putida* Prominence in Conducive Soils. Environmental Microbiology 2020, 22 (12), 5137–5155. https://doi.org/10.1111/1462-2920.15127.

[48] Muangkaew, P.; Prasad, D.; De Roo, V.; Verleysen, Y.; Zhou, L.; De Mot, R.; Höfte, M.; Madder, A.; Geudens, N.; Martins, J. C. Breaking Cycles: Saponification-Enhanced NMR Fingerprint Matching for the Identification and Stereochemical Evaluation of Cyclic Lipodepsipeptides from Natural Sources. *Chem. Eur. J.* **2024**, e202400667. DOI: 10.1002/chem.202400667

[49] Dubern, J.-F.; Lagendijk, E. L.; Lugtenberg, B. J. J.; Bloemberg, G. V. The Heat Shock Genes *dnaK* , *dnaJ* , and *grpE* Are Involved in Regulation of Putisolvin Biosynthesis in *Pseudomonas putida* PCL1445. *J. Bacteriol.* **2005**, *187* (17), 5967–5976. DOI: 10.1128/JB.187.17.5967-5976.2005

[50] Dubern, J.-F.; Lugtenberg, B. J. J.; Bloemberg, G. V. The *ppuI-rsaL-ppuR* Quorum-Sensing System Regulates Biofilm Formation of *Pseudomonas putida* PCL1445 by Controlling Biosynthesis of the Cyclic Lipopeptides Putisolvins I and II. *J. Bacteriol.* **2006**, *188* (8), 2898–2906. DOI: 10.1128/JB.188.8.2898-2906.2006

[51] Dubern, J.-F.; Bloemberg, G. V. Influence of Environmental Conditions on Putisolvins I and II Production in *Pseudomonas putida* Strain PCL1445. *FEMS Microbiol. Lett.* **2006**, *263* (2), 169–175. DOI: 10.1111/j.1574-6968.2006.00406.x.

[52] Dubern, J.-F.; Coppoolse, E. R.; Stiekema, W. J.; Bloemberg, G. V. Genetic and Functional Characterization of the Gene Cluster Directing the Biosynthesis of Putisolvin I and II in *Pseudomonas putida* Strain PCL1445. *Microbiology* **2008**, *154* (7), 2070–2083. DOI: 10.1099/mic.0.2008/016444-0

[53] Yang, C. C.; Leong, J. Structure of Pseudobactin 7SR1, a Siderophore from a Plant-Deleterious Pseudomonas. *Biochemistry* **1984**, *23* (15), 3534–3540. DOI: 10.1021/bi00310a023

[54] Voßen, W.; Fuchs, R.; Taraz, K.; Budzikiewicz, H. Can the Peptide Chain of a Pyoverdin Be Bound by an Ester Bond to the Chromophore? - The Old Problem of Pseudobactin 7SR1. *Zeitschrift für Naturforschung C* **2000**, *55* (3–4), 153–164. DOI: 10.1515/znc-2000-3-405.

[55] Zane, H. K.; Butler, A. Isolation, Structure Elucidation, and Iron-Binding Properties of Lystabactins, Siderophores Isolated from a Marine *Pseudoalteromonas* Sp . *J. Nat. Prod.* **2013**, *76* (4), 648–654. DOI: 10.1021/np3008655

[56] Hathout, Y.; Ho, Y.-P.; Ryzhov, V.; Demirev, P.; Fenselau, C. Kurstakins: A New Class of Lipopeptides Isolated from *Bacillus thuringiensis*. *J. Nat. Prod.* **2000**, *63* (11), 1492–1496. DOI: 10.1021/np000169q

[57] Béchet, M.; Caradec, T.; Hussein, W.; Abderrahmani, A.; Chollet, M.; Leclère, V.; Dubois, T.; Lereclus, D.; Pupin, M.; Jacques, P. Structure, Biosynthesis, and Properties of Kurstakins,

Nonribosomal Lipopeptides from *Bacillus* Spp. *Appl. Microbiol. Biotechnol.* **2012**, *95* (3), 593–600. DOI: 10.1007/s00253-012-4181-2

[58] Price, N. P. J.; Rooney, A. P.; Swezey, J. L.; Perry, E.; Cohan, F. M. Mass Spectrometric Analysis of Lipopeptides from *Bacillus* Strains Isolated from Diverse Geographical Locations: MALDI-TOF MS Analysis of *Bacillus* Sp. Biomarkers. *FEMS Microbiology Letters* **2007**, *271* (1), 83–89. DOI: 10.1111/j.1574-6968.2007.00702.x

[59] Bumpus, S. B.; Evans, B. S.; Thomas, P. M.; Ntai, I.; Kelleher, N. L. A Proteomics Approach to Discovering Natural Products and Their Biosynthetic Pathways. *Nat. Biotechnol.* **2009**, *27* (10), 951–956. DOI: 10.1038/nbt.1565

[60] Abderrahmani, A.; Tapi, A.; Nateche, F.; Chollet, M.; Leclère, V.; Wathelet, B.; Hacene, H.; Jacques, P. Bioinformatics and Molecular Approaches to Detect NRPS Genes Involved in the Biosynthesis of Kurstakin from *Bacillus thuringiensis*. *Appl. Microbiol. Biotechnol.* **2011**, *92* (3), 571–581. DOI: 10.1007/s00253-011-3453-6

[61] Yu, Y.-Y.; Zhang, Y.-Y.; Wang, T.; Huang, T.-X.; Tang, S.-Y.; Jin, Y.; Mi, D.-D.; Zheng, Y.; Niu, D.-D.; Guo, J.-H.; Jiang, C.-H. Kurstakin Triggers Multicellular Behaviors in *Bacillus cereus* AR156 and Enhances Disease Control Efficacy Against Rice Sheath Blight. *Plant Disease* **2023**, *107* (5), 1463–1470. DOI: 10.1094/PDIS-01-22-0078-RE

[62] Mandal, S. M.; Sharma, S.; Pinnaka, A. K.; Kumari, A.; Korpole, S. Isolation and Characterization of Diverse Antimicrobial Lipopeptides Produced by *Citrobacter* and *Enterobacter*. *BMC Microbiol.* **2013**, *13* (1), 152. DOI: 10.1186/1471-2180-13-152

[63] Gélis-Jeanvoine, S.; Canette, A.; Gohar, M.; Caradec, T.; Lemy, C.; Gominet, M.; Jacques, P.; Lereclus, D.; Slamti, L. Genetic and Functional Analyses of Krs, a Locus Encoding

Kurstakin, a Lipopeptide Produced by *Bacillus thuringiensis*. *Research in Microbiology* **2017**, *168* (4), 356–368. DOI: 10.1016/j.resmic.2016.06.002

[64] Li, Y.-X.; Zhong, Z.; Zhang, W.-P.; Qian, P.-Y. Discovery of Cationic Nonribosomal Peptides as Gram-Negative Antibiotics through Global Genome Mining. *Nat. Commun.* **2018**, *9* (1), 3273. DOI: 10.1038/s41467-018-05781-6

[65] Zhao, X.; Li, Z.; Kuipers, O. P. Mimicry of a Non-Ribosomally Produced Antimicrobial, Brevicidine, by Ribosomal Synthesis and Post-Translational Modification. *Cell Chemical Biology* **2020**, *27* (10), 1262-1271.e4. DOI: 10.1016/j.chembiol.2020.07.005

[66] Zhao, X.; Kuipers, O. P. BrevicidineB, a New Member of the Brevicidine Family, Displays an Extended Target Specificity. *Front. Microbiol.* **2021**, *12*, 693117. DOI: 10.3389/fmicb.2021.693117

[67] Zhao, X.; Zhong, X.; Yang, S.; Deng, K.; Liu, L.; Song, X.; Zou, Y.; Li, L.; Zhou, X.; Jia, R.; Lin, J.; Tang, H.; Ye, G.; Yang, J.; Zhao, S.; Lang, Y.; Wan, H.; Yin, Z.; Kuipers, O. P. Elucidating the Mechanism of Action of the Gram-Negative-Pathogen-Selective Cyclic Antimicrobial Lipopeptide Brevicidine. *Antimicrob. Agents Chemother.* **2023**, *67* (5), e00010-23. DOI: 10.1128/aac.00010-23

[68] Hermant, Y.; Palpal-latoc, D.; Kovalenko, N.; Cameron, A. J.; Brimble, M. A.; Harris, P. W. R. The Total Chemical Synthesis and Biological Evaluation of the Cationic Antimicrobial Peptides, Laterocidine and Brevicidine. *J. Nat. Prod.* **2021**, *84* (8), 2165–2174. DOI: 10.1021/acs.jnatprod.1c00222

[69] Palpal-latoc, D.; Horsfall, A. J.; Cameron, A. J.; Campbell, G.; Ferguson, S. A.; Cook, G. M.; Sander, V.; Davidson, A. J.; Harris, P. W. R.; Brimble, M. A. Synthesis, Structure–Activity

Relationship Study, Bioactivity, and Nephrotoxicity Evaluation of the Proposed Structure of the Cyclic Lipodepsipeptide Brevicidine B. *J. Nat. Prod.* **2024**, *87* (4), 764–773. DOI: 10.1021/acs.jnatprod.3c00876

[70] Al Ayed, K.; Ballantine, R. D.; Hoekstra, M.; Bann, S. J.; Wesseling, C. M. J.; Bakker, A. T.; Zhong, Z.; Li, Y.-X.; Brüchle, N. C.; Van Der Stelt, M.; Cochrane, S. A.; Martin, N. I. Synthetic Studies with the Brevicidine and Laterocidine Lipopeptide Antibiotics Including Analogues with Enhanced Properties and in Vivo Efficacy. *Chem. Sci.* **2022**, *13* (12), 3563–3570. DOI: 10.1039/D2SC00143H

[71] Ballantine, R. D.; Al Ayed, K.; Bann, S. J.; Hoekstra, M.; Martin, N. I.; Cochrane, S. A. Synthesis and Structure–Activity Relationship Studies of N-Terminal Analogues of the Lipopeptide Antibiotics Brevicidine and Laterocidine. *RSC Med. Chem.* **2022**, *13* (12), 1640–1643. DOI: 10.1039/D2MD00281G

[72] Ballantine, R. D.; Al Ayed, K.; Bann, S. J.; Hoekstra, M.; Martin, N. I.; Cochrane, S. A. Linearization of the Brevicidine and Laterocidine Lipopeptides Yields Analogues That Retain Full Antibacterial Activity. *J. Med. Chem.* **2023**, *66* (8), 6002–6009. DOI: 10.1021/acs.jmedchem.3c00308

[73] Zhong, X.; Deng, K.; Yang, X.; Song, X.; Zou, Y.; Zhou, X.; Tang, H.; Li, L.; Fu, Y.; Yin, Z.; Wan, H.; Zhao, X. Brevicidine Acts as an Effective Sensitizer of Outer Membrane-Impermeable Conventional Antibiotics for Acinetobacter Baumannii Treatment. *Front. Microbiol.* **2023**, *14*, 1304198. DOI: 10.3389/fmicb.2023.1304198

[74] Kim, J.; Kim, J.; Yun, H.; Ganbaatar, B.; Tahmasebi, A.; Seo, S. I.; Kim, P. I.; Lee, C. W. New Strain *Brevibacillus laterosporus* TSA31-5 Produces Both Brevicidine and

Brevibacillin, Exhibiting Distinct Antibacterial Modes of Action against Gram-Negative and Gram-Positive Bacteria. *PLoS ONE* **2024**, *19* (4), e0294474. DOI: 10.1371/journal.pone.0294474

[75] Buchholz, K. R.; Reichelt, M.; Johnson, M. C.; Robinson, S. J.; Smith, P. A.; Rutherford, S. T.; Quinn, J. G. Potent Activity of Polymyxin B Is Associated with Long-Lived Super-Stoichiometric Accumulation Mediated by Weak-Affinity Binding to Lipid A. *Nat. Commun.* **2024**, *15* (1), 4733. DOI: 10.1038/s41467-024-49200-5

[76] Zhang, S.-S.; Li, L.; Wu, Y.; Wu, Z.-M.; Kong, C.; Hong, L.-L.; Zhang, S.; Lin, X.-L.; Lin, H.-W.; Wang, S.-P. LC-MS-Guided Isolation of Cyanogripeptides A–C, Cyclolipopeptides with β-Methyl-Leucine Residues, from an *Actinoalloteichus cyanogriseus* LHW52806. *J. Nat. Prod.* **2023**, *86* (7), 1708–1714. DOI: 10.1021/acs.jnatprod.3c00127

[77] Huang, X.; Roemer, E.; Sattler, I.; Moellmann, U.; Christner, A.; Grabley, S. Lydiamycins A–D: Cyclodepsipetides with Antimycobacterial Properties. *Angew. Chem. Int. Ed.* **2006**, *45* (19), 3067–3072. DOI: 10.1002/anie.200503381

[78] Wang, W.; Kim, S.; Vu, T. H. N.; Quach, N. T.; Oh, E.; Park, K.-H.; Park, C.; Cho, Y.; Jang, H.; Roh, E.; Lee, J.; Kang, E.; Han, S.; Phi, Q.-T.; Kang, H. Bioactive Piperazic Acid-Bearing Cyclodepsipeptides, Lydiamycins E–H, from an Endophytic *Streptomyces* Sp. Associated with Cinnamomum Cassia. *J. Nat. Prod.* **2023**, *86* (4), 751–758. DOI: 10.1021/acs.jnatprod.2c00902

[79] Libis, V.; MacIntyre, L. W.; Mehmood, R.; Guerrero, L.; Ternei, M. A.; Antonovsky, N.; Burian, J.; Wang, Z.; Brady, S. F. Multiplexed Mobilization and Expression of Biosynthetic Gene Clusters. *Nat. Commun.* **2022**, *13* (1), 5256. DOI: 10.1038/s41467-022-32858-0

[80] Chen, B.; Dai, L.; Zhang, H.; Tan, W.; Xu, Z.; Ye, T. Towards the Stereochemical Assignment of Natural Lydiamycin A. *Chem. Commun.* **2010**, *46* (4), 574–576. DOI: 10.1039/B922544G

[81] Li, W.; Gan, J.; Ma, D. A Concise Route to the Proposed Structure of Lydiamycin B, an Antimycobacterial Depsipeptide. *Org. Lett.* **2009**, *11* (24), 5694–5697. DOI: 10.1021/ol9024474

[82] Hwang, S.; Le, L. T. H. L.; Jo, S.-I.; Shin, J.; Lee, M. J.; Oh, D.-C. Pentaminomycins C–E: Cyclic Pentapeptides as Autophagy Inducers from a Mealworm Beetle Gut Bacterium. *Microorganisms* **2020**, *8* (9), 1390. DOI: 10.3390/microorganisms8091390

[83] Hwang, S.; Shin, D.; Kim, T. H.; An, J. S.; Jo, S.-I.; Jang, J.; Hong, S.; Shin, J.; Oh, D.-C. Structural Revision of Lydiamycin A by Reinvestigation of the Stereochemistry. *Org. Lett.* **2020**, *22* (10), 3855–3859. DOI: 10.1021/acs.orglett.0c01110

[84] Oelke, A. J.; France, D. J.; Hofmann, T.; Wuitschik, G.; Ley, S. V. Piperazic Acid-Containing Natural Products: Isolation, Biological Relevance and Total Synthesis. *Nat. Prod. Rep.* **2011**, *28* (8), 1445. DOI: 10.1039/c1np00041a.

[85] Morgan, K. D.; Andersen, R. J.; Ryan, K. S. Piperazic Acid-Containing Natural Products: Structures and Biosynthesis. *Nat. Prod. Rep.* **2019**, *36* (12), 1628–1653. DOI: 10.1039/C8NP00076J

[86] Zotchev, S. B. Unlocking the Potential of Bacterial Endophytes from Medicinal Plants for Drug Discovery. *Microbial Biotechnology* **2024**, *17* (2), e14382. DOI: doi.org/10.1111/1751-7915.14382

[87] Shin, D.; Byun, W. S.; Kang, S.; Kang, I.; Bae, E. S.; An, J. S.; Im, J. H.; Park, J.; Kim, E.; Ko, K.; Hwang, S.; Lee, H.; Kwon, Y.; Ko, Y.-J.; Hong, S.; Nam, S.-J.; Kim, S. B.; Fenical, W.; Yoon, Y. J.; Cho, J.-C.; Lee, S. K.; Oh, D.-C. Targeted and Logical Discovery of Piperazic Acid-Bearing Natural Products Based on Genomic and Spectroscopic Signatures. *J. Am. Chem. Soc.* **2023**, *145* (36), 19676–19690. DOI: 10.1021/jacs.3c04699

[88] Biggins, J. B.; Kang, H.-S.; Ternei, M. A.; DeShazer, D.; Brady, S. F. The Chemical Arsenal of *Burkholderia pseudomallei* Is Essential for Pathogenicity. *J. Am. Chem. Soc.* **2014**, *136* (26), 9484–9490. DOI: doi.org/10.1021/ja504617n

[89] Esmaeel, Q.; Pupin, M.; Kieu, N. P.; Chataigné, G.; Béchet, M.; Deravel, J.; Krier, F.; Höfte, M.; Jacques, P.; Leclère, V. Burkholderia Genome Mining for Nonribosomal Peptide Synthetases Reveals a Great Potential for Novel Siderophores and Lipopeptides Synthesis. *MicrobiologyOpen* **2016**, *5* (3), 512–526. DOI: doi.org/10.1002/mbo3.347

[90] Clements-Decker, T.; Kode, M.; Khan, S.; Khan, W. Underexplored Bacteria as Reservoirs of Novel Antimicrobial Lipopeptides. *Front. Chem.* **2022**, *10*, 1025979. DOI: doi.org/10.3389/fchem.2022.1025979

[91] Borlee, G. I.; Mangalea, M. R.; Martin, K. H.; Plumley, B. A.; Golon, S. J.; Borlee, B. R. Disruption of C-Di-GMP Signaling Networks Unlocks Cryptic Expression of Secondary Metabolites during Biofilm Growth in *Burkholderia pseudomallei*. *Appl. Environ. Microbiol.* **2022**, *88* (8), e02431-21. DOI: 10.1128/aem.02431-21

[92] Niehs, S. P.; Dose, B.; Scherlach, K.; Pidot, S. J.; Stinear, T. P.; Hertweck, C. Genome Mining Reveals Endopyrroles from a Nonribosomal Peptide Assembly Line Triggered in

Fungal–Bacterial Symbiosis. *ACS Chem. Biol.* **2019**, *14* (8), 1811–1818. DOI: 10.1021/acschembio.9b00406

[93] Dashti, Y.; Nakou, I. T.; Mullins, A. J.; Webster, G.; Jian, X.; Mahenthiralingam, E.; Challis, G. L. Discovery and Biosynthesis of Bolagladins: Unusual Lipodepsipeptides from *Burkholderia gladioli* Clinical Isolates. *Angew. Chem. Int. Ed.* **2020**, *59* (48), 21553–21561. DOI: 10.1002/anie.202009110

[94] Dose, B.; Ross, C.; Niehs, S. P.; Scherlach, K.; Bauer, J. P.; Hertweck, C. Food-Poisoning Bacteria Employ a Citrate Synthase and a Type II NRPS To Synthesize Bolaamphiphilic Lipopeptide Antibiotics. *Angew. Chem. Int. Ed.* **2020**, *59* (48), 21535–21540. DOI: 10.1002/anie.202009107

[95] Rassbach, J.; Merseburger, P.; Wurlitzer, J. M.; Binnemann, N.; Voigt, K.; Rohlfs, M.; Gressler, M. Insecticidal Cyclodepsitetrapeptides from Mortierella Alpina. *J. Nat. Prod.* **2023**, *86* (7), 1715–1722. DOI: 10.1021/acs.jnatprod.3c00146

[96] Schwarzer, D.; Finking, R.; Marahiel, M. A. Nonribosomal Peptides: From Genes to Products. *Nat. Prod. Rep.* **2003**, *20* (3), 275. DOI: 10.1039/b111145k

CHAPTER II: PEGylated Teixobactin Analogues

Abstract

Bacterial infections by new antibiotic-resistant pathogens are a growing threat to public health. Teixobactin, a peptide antibiotic with excellent activity against Gram-positive bacteria, is a potential therapeutic against emerging antibiotic-resistant bacterial strains, as its mechanism of action appears to preclude the development of bacterial resistance. However, teixobactin may be limited in clinical applications due to insolubility, and preliminary data suggests that teixobactin is nephrotoxic in mice. In order to overcome these two limitations of teixobactin, I hypothesized that functionalization with poly(ethylene glycol) (PEG) chains would increase the solubility of teixobactin analogues. I prepared five PEGylated analogues of teixobactin and evaluated their antibiotic activities against two Gram-positive bacterial strains. All PEGylated analogues formed insoluble gels in aqueous buffer, and in all cases PEGylation decreased antibiotic efficacy by at least two-fold compared to non-PEGylated controls. Based on this evidence, PEGylation is not an effective strategy for improving the clinical viability of teixobactin.

Introduction

Teixobactin is a promising candidate to address the public health challenge of antibiotic resistance. First reported in 2015 by Lewis and coworkers, teixobactin is a macrocyclic peptide with remarkable antibiotic activity against pathogenic Gram-positive bacteria (Figure 3.1).[1] Teixobactin inhibits Gram-positive bacterial growth by binding to the pyrophosphate groups of lipid II precursor molecules, preventing their incorporation into the bacterial cell wall.[2] Due to the relative immutability of lipid II and its high genomic conservation among Gram-positive bacteria, resistance to teixobactin occurs slowly and is costly to bacteria.[3,4,5]

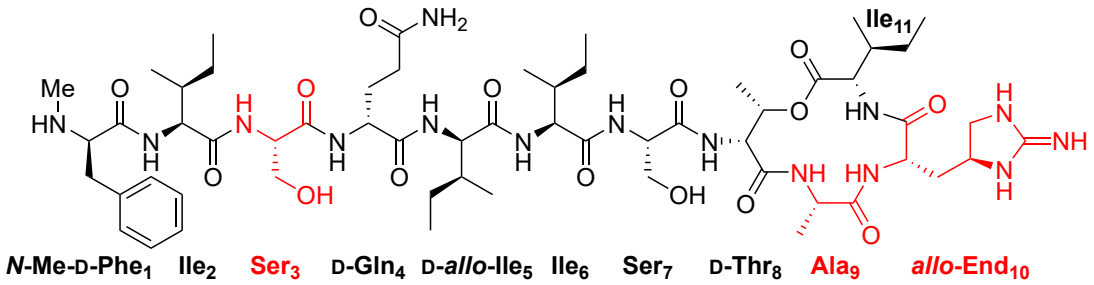

Figure 2.1. Teixobactin. Residues chosen for PEG incorporation are highlighted red.

Teixobactin is a cyclodepsipeptide, with a macrolactone ring formed by esterification of the *C*-terminus onto the side chain hydroxy group of D-Thr$_8$. The linear tail of teixobactin features a unique pattern of D- and L-amino acids which gives the peptide distinct hydrophobic and hydrophilic faces. Structure-activity relationship studies of teixobactin have shown that the non-proteinogenic amino acid *allo*-enduracididine at position 10 (*allo*-End$_{10}$) can be substituted with arginine or lysine while retaining antibiotic activity.[6,7,8,9] As *allo*-enduracididine is not commercially available, Arg$_{10}$- and Lys$_{10}$-teixobactin are commonly used as controls when assessing the antibiotic activity of teixobactin analogues.

Teixobactin and antimicrobially active analogues of teixobactin form insoluble gels in aqueous buffer at physiological pH, and this gelation may contribute to nephrotoxicity.[6] In 2018, our group reported the X-ray crystallographic structure of a supramolecular assembly of teixobactin analogues, which resembles a double helix of antiparallel β-sheets.[9] This same teixobactin analogue formed amyloid-like fibrils observed by transmission electron microscopy. Collectively, these studies informed our hypothesis for the molecular basis of teixobactin gel formation: Teixobactin forms amphiphilic β-strands which in turn form antiparallel β-sheets. These β-sheet assemblies form insoluble fibril bundles which manifest as macroscopic gels.

I hypothesized that functionalizing teixobactin with poly(ethylene glycol) (PEG) chains would increase the solubility of teixobactin while preserving its excellent antibiotic activity.

PEGylation has been shown to improve the solubility of protein and small-molecule drugs.[10,11] Antibiotics functionalized with PEG retain antibiotic activity and have increased bioavailability and reduced off-target toxicity.[12,13,14] PEGylation may prevent the supramolecular fibrilization that leads to teixobactin gelation.[15]

Results and Discussion

Design and Synthesis of PEGylated Teixobactin Analogues

Design of PEGylated Teixobactin Analogues

I strategically incorporated PEG based on previous structure-activity relationship studies of teixobactin. The crystal structure of a teixobactin analogue shows that it forms an antiparallel β-sheet dimer (Figure S2.1).[9] This β -sheet dimer is now understood to be the active pyrophosphate-binding species of teixobactin.[16,17] In the dimeric assembly, the amino acid side chains Ala_9 and *allo*-End_{10} face away from the active pyrophosphate-binding amide NH groups in the macrolactone ring. I hypothesized that PEGylation at positions 9 and 10 would minimize disruption of the formation of β-sheet teixobactin dimers, thus preserving the assembly, binding, and activity of teixobactin.

In alanine and lysine scans of teixobactin analogues, mutation of Ser_3 and other polar residues resulted in the smallest decreases in antibiotic activity. Similarly to Ala_9 and *allo*-End_{10}, Ser_3 also faces away from the hydrophobic interactions in the dimer unit.[6,9] I therefore tested PEG incorporation at position 3.

Two lengths of PEG were chosen for the study: short (n = 3) and long (n = 10). I first incorporated the short PEG as a proof-of-concept that on-resin PEG coupling was feasible. The long PEG allowed for direct comparison of the effect of PEG length on antibiotic activity and solubility.

In order to preserve the overall charge state of the prepared analogues, Ala_9 was mutated to Arg in two cases. Furthermore, in analogues where PEGylation occurred at positions other than 10, commercially available Arg was used in place of *allo*-End. PEGylated analogues of teixobactin prepared in this study are shown in Figure 2.2.

n = 3: Arg_9,$Lys(PEG3)_{10}$-teixobactin (**1**)

n = 10: Arg_9,$Lys(PEG10)_{10}$-teixobactin (**3**)

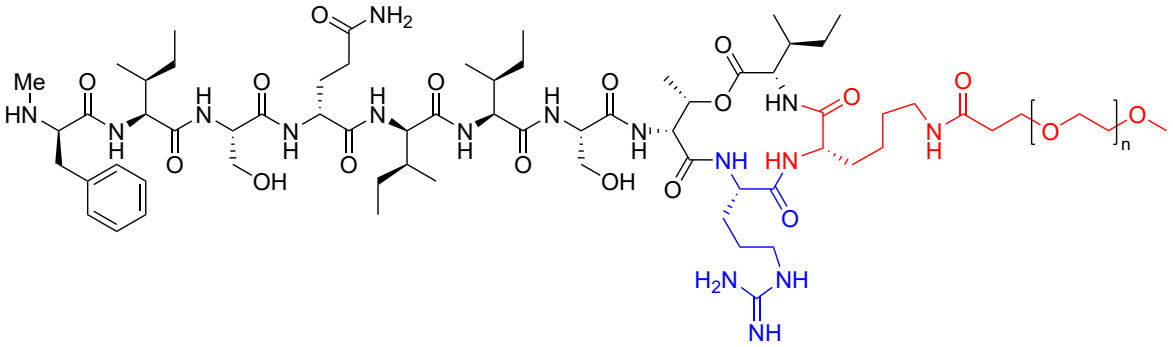

$Lys(PEG3)_9$,Arg_{10}-teixobactin (**2**)

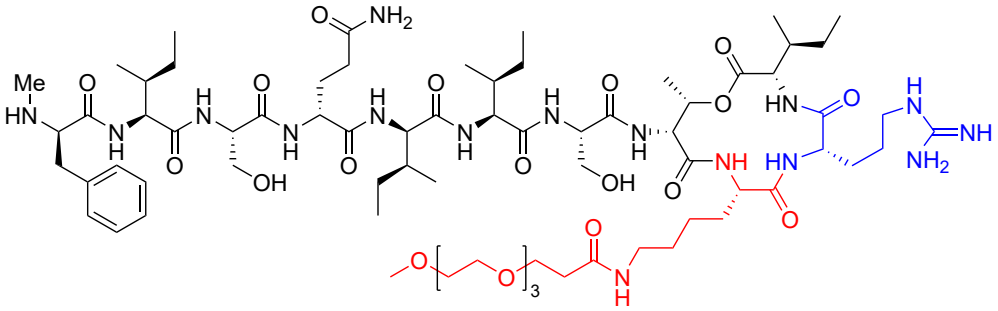

n = 3: $Lys(PEG3)_{10}$-teixobactin (**4**)

n = 10: $Lys(PEG10)_{10}$-teixobactin

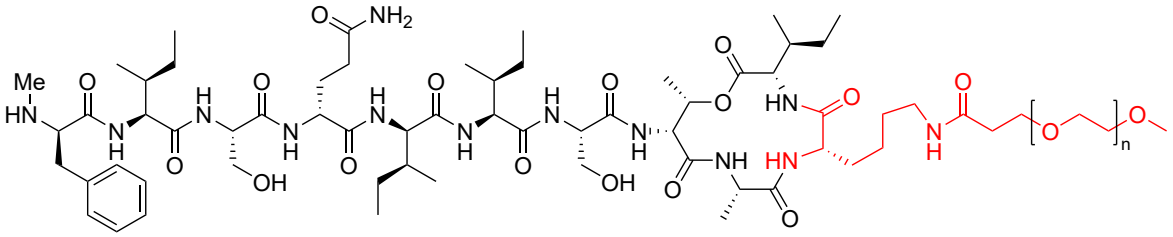

$Lys(PEG10)_3$,Arg_{10}-teixobactin (**5**)

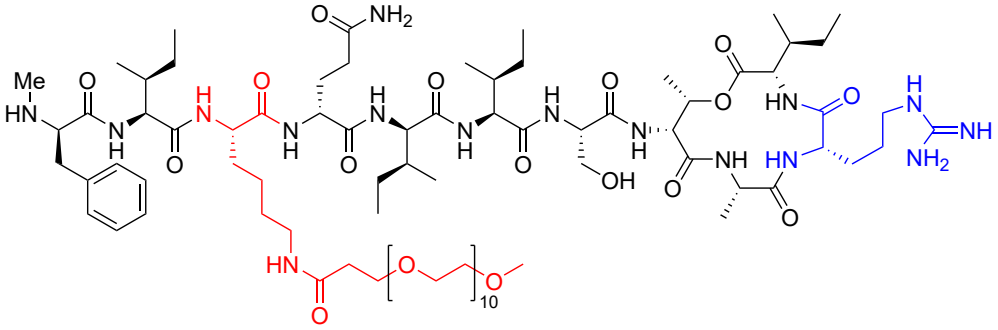

Figure 2.2. PEGylated analogues of teixobactin. PEGylated residues are shown in red. Residues in which Arg is used to preserve the overall charge state of the molecule or in place of commercially unavailable *allo*-End at position 10 are shown in blue.

Synthesis of PEGylated Teixobactin Analogues

The synthesis of PEGylated teixobactin analogues was adapted from a solid-phase strategy previously developed by our group (Scheme 1).[6,8,9] The linear sequence of residues 10–1 was prepared on 2-chlorotrityl chloride resin using standard Fmoc-based solid-phase peptide synthesis chemistry. Isoleucine was installed at position 11 by acylation onto the side-chain hydroxyl group of D-Thr$_8$. After cleaving the linear peptide from resin, solution-phase macrolactonization followed by global deprotection of side-chain protecting groups gives the crude peptide.

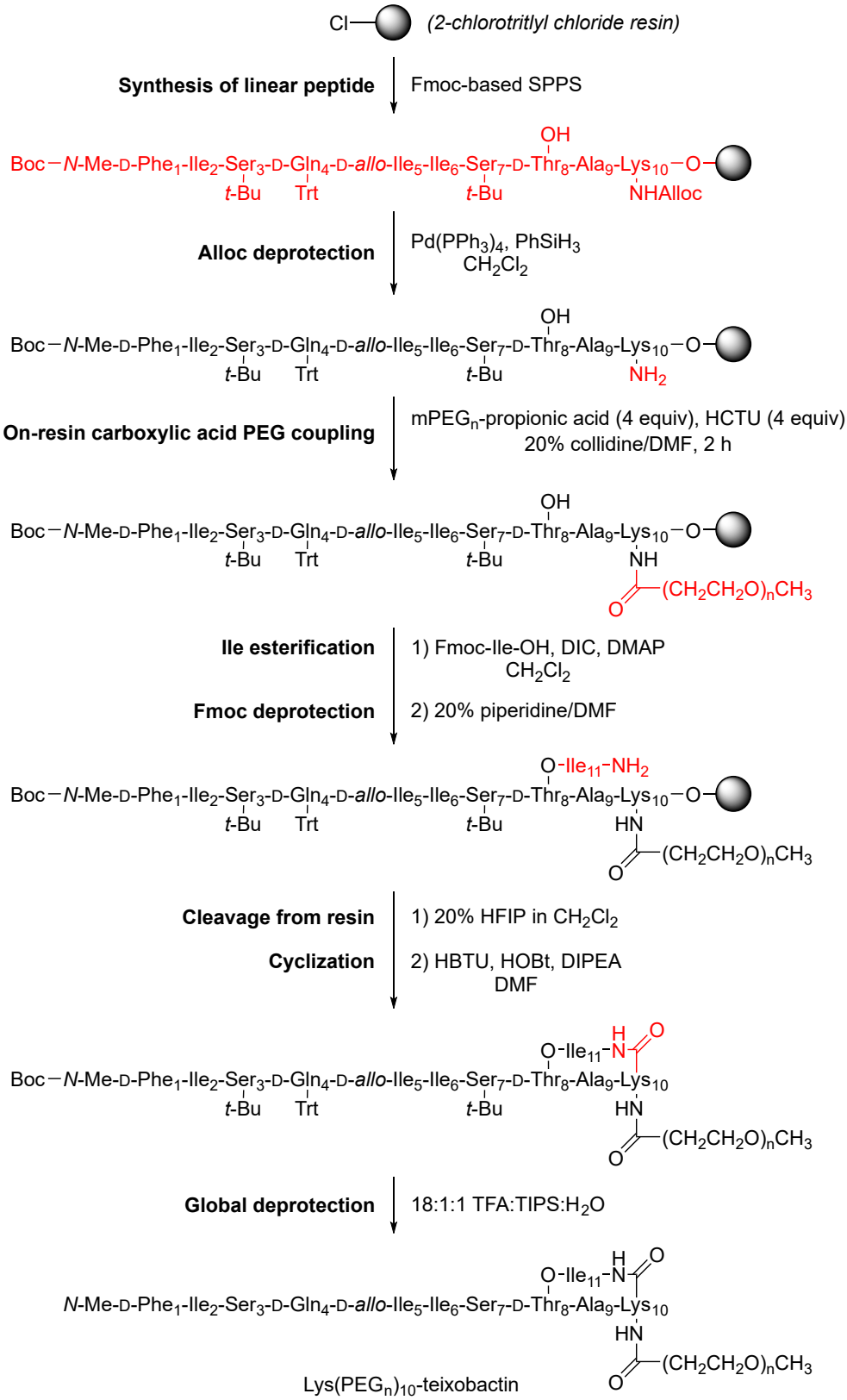

Scheme 2.1. Representative synthesis of Lys(PEG$_n$)$_{10}$-teixobactin.

To allow for regioselective PEG incorporation, allyloxycarbonyl-protected lysine (Lys(Alloc)) was coupled in place of the native residue at the position being modified (3, 9, or 10).[18] Following synthesis of the linear peptide, Lys(Alloc) was orthogonally deprotected on-resin with tetrakis(triphenylphosphine)palladium(0) and phenylsilane to give the free amine, which was then condensed with the appropriate length of propionic acid PEG by HCTU activation to give an amide linkage. When position 10 was not used for PEG incorporation, arginine was used in place of *allo*-enduracididine.

The ester linkage between Ile_{11} and D-Thr_8 was formed by Steglich esterification: acylation of the carboxylic acid of isoleucine to the unprotected β-hydroxy group of D-threnonine using *N*,*N*'-diisopropylcarbodiimide and 4-dimethylaminopyridine. In these conditions, the α-proton of the activated ester intermediate can be deprotonated to give a planar species. The resulting epimerization of the Ile_{11} stereocenter typically gives Ile and D-*allo*-Ile in a 2:1 mixture of epimers.[6] In non-PEGylated analogues of teixobactin, the diastereomer resulting from d-*allo*-Ile incorporation is separable from the desired peptide by reversed-phase HPLC purification. However, I have observed that the chromatographic retention times of PEGylated teixobactin diastereomers to be much closer to one another than for non-PEGylated analogues (Figure S2.2). I hypothesize that this contraction in retention times is caused by the shared PEG group between the diastereomers. For this reason, I was not able to obtain diastereomerically pure PEGylated teixobactin analogues.

Study of PEGylated Teixobactin Analogues

*Arg_9,$Lys(PEG3)_{10}$-teixobactin (**1**) and $Lys(PEG3)_9$,Arg_{10}-teixobactin (**2**)*

The first two peptides studied were PEGylated at positions 9 and 10 on the macrolactone ring: Arg_9,$Lys(PEG3)_{10}$-teixobactin (peptide **1**) and $Lys(PEG3)_9$,Arg_{10}-teixobactin (peptide **2**).

Peptides 1 and 2 were characterized by matrix-assisted laser desorption/ionization-time of flight (MALDI-TOF) mass spectrometry. The diastereomeric ratios of these peptides were quantified by integration of the analytical HPLC trace; peptides 1 and 2 were obtained in greater than 9:1 ratio of the desired diastereomer.

Our group has previously observed a positive correlation between antibiotic activity and propensity to form insoluble gels in teixobactin analogues.[8] I first identified PEGylated analogues of teixobactin that retained antibiotic activity before characterizing their solubility. To determine antibiotic activity, I performed minimum inhibitory concentration (MIC) assays against two Gram-positive bacterial strains, *Bacillis subtilis* and *Staphylococcus epidermidis*, as well as the Gram-negative *Escherichia coli* as a negative control. MIC assays were performed by two-fold serial dilution of broth medium containing teixobactin analogues of interest in a 96-well microtiter plate. The minimum concentration of a teixobactin analogue necessary to prevent the growth of bacteria was determined over a range of 0.03125–16 μg/mL. The MIC values of natural teixobactin, as well as Arg_{10}- and Lys_{10}-teixobactin, were used as benchmarks by which to compare the activities of PEGylated analogues (Table 2.1).

Table 2.1. MIC values for PEGylated teixobactin analogues and controls in μg/mL. Experiments were performed with 0.002% polysorbate 80.

	Bacillus subtilis ATCC 6051	*Staphylococcus epidermidis* ATCC 14990	*Escherichia coli* ATCC 10798
teixobactin	<0.3125	0.0625	>16
Arg_{10}-teixobactin	<0.3125	2	>16
Lys_{10}-teixobactin	<0.3125	1	>16
Arg_9,$Lys(PEG3)_{10}$-teixobactin **1**	2–4	2–4	>16
$Lys(PEG3)_9$,Arg_{10}-teixobactin **2**	>16	>16	>16
Arg_9,$Lys(PEG10)_{10}$-teixobactin **3**	8–16	8	>16
$Lys(PEG3)_{10}$-teixobactin **4***	16	>16	>16
$Lys(PEG10)_3$,Arg_{10}-teixobactin **5**	4–8	>16	>16

***** Peptide **4** was studied as an impure mixture.

Peptide **1** has an MIC of 2–4 μg/mL against both Gram-positive strains. For teixobactin and teixobactin analogues with tolerated mutations at position 10, we commonly observe very low MIC values against *B. subtilis*. While peptide **1** does not meet this exceptional activity against *B. subtilis*, it has comparable activity to the Arg_{10}- and Lys_{10}-teixobactin controls. Peptide **2**, by contrast, was inactive against all bacteria in the concentration range tested. Collectively, these results indicate that PEGylation at position 9 abrogates antibiotic activity, while PEGylation at position 10 is tolerated with loss of activity only against *B. subtilis*.

Arg_{9},Lys(PEG10)$_{10}$-teixobactin (3)

I next increased the length of the PEG chain to determine the effect of PEG length on activity of PEGylated teixobactin analogues. Residue 10 was chosen over 9 for PEGylation as peptide **1** retained antibiotic activity, while peptide **2** did not. Synthesis and purification of Arg_9,Lys(PEG10)$_{10}$-teixobactin **3** proceeded normally until two peaks in a 54:46 ratio separated by 0.1 min retention time were observed in the analytical HPLC trace. As each peak was identical by mass spectrometric analysis, I suspected that the peaks reflected Ile_{11} diastereomers of peptide **3**, as previously mentioned. An additional purification allowed for each of these peaks to be isolated in greater than 9:1 diastereomeric ratio each. As diastereomers of teixobactin with non-native stereochemistry at positions along the macrolactone ring have previously been shown to have reduced antibiotic activity, I used a MIC assay to functionally differentiate peptide **3** from its diastereomer.[6] Peptide **3** has an MIC value of 8–16 μg/mL against both Gram-positive bacteria, and the D-*allo*-Ile_{11} diastereomer is inactive. In comparing this analogue to the previously discussed **1**, increasing the length of the PEG chain appears to reduce activity four-fold. Therefore, PEGylation disrupts the antibiotic activity of teixobactin analogues, and this disruption is proportional to PEG length.

Lys(PEG3)$_{10}$-teixobactin (4) and Lys(PEG10)$_{10}$-teixobactin

I next investigated whether an analogue more closely resembling natural teixobactin would retain superior antibiotic activity. I prepared Lys(PEG3)$_{10}$-teixobactin **4**, restoring the native alanine at position 9. Peptide **4** therefore has a reduced overall charge at physiological pH (+2 → +1), but structurally differs from teixobactin only at the mutable residue 10. Peptide **4** formed an insoluble gel in a solution of 20% acetonitrile (MeCN)/H2O containing 0.1% trifluoroacetic acid (TFA), which are the standard conditions for preparative HPLC purification. This indicated that removal of charge at position 10 greatly increased the propensity of peptide **4** to aggregate in aqueous solution relative to peptides **1**-**3**. Increasing the proportion of organic solvent in the solution to 40% MeCN/H_2O was sufficient to solubilize peptide **4**. Despite repeated synthesis attempts and rounds of purification, I was not able to separate peptide **4** from co-eluting impurities, one of which is likely the D-*allo*-Ile$_{11}$ diastereomer. In the impure mixture used for further experiments, the major peak comprised 45% of the total area by analytical HPLC UV-vis quantification. In an MIC assay, the mixture of compounds containing peptide **4** showed antibiotic activity at 16 μg/mL against B. subtilis and no activity against S. epidermidis. A possible explanation for this result is that peptide **4** retains some antibiotic activity, but inactive impurities reduce the overall activity of the mixture.

Lys(PEG10)$_{10}$-teixobactin, with a PEG chain of length n = 10, followed the same trend as peptide **4** and immediately began to form a cloudy aggregate upon dissolving the crude peptide. Interestingly, following filtration of this cloudy solution, the initially clear and homogenous filtrate again showed evidence of aggregation within minutes. Addition of 10% DMSO to the filtered solution completely disaggregated the peptide, but prevented purification in that mass ions corresponding to Lys(PEG10)$_{10}$-teixobactin were not observed by mass spectrometry in any

collected fractions. I concluded that analogues with a +1 overall charge were infeasible to purify due to their substantial gel formation.

*Lys(PEG3)$_3$,Arg$_{10}$-teixobactin (**5**)*

As PEGylation on the macrolactone ring appeared to reduce the antibiotic activity of teixobactin, I prepared Lys(PEG10)$_3$,Arg$_{10}$-teixobactin **5**, in which position 10 is mutated to arginine and Ser$_3$ is mutated to a PEGylated lysine. Despite repeated rounds of purification, I was unable to obtain peptide **5** in greater than a 74:26 diastereomeric ratio. Analogue **5** has an MIC of 4–8 μg/mL against *B. subtilis*, but is inactive against *S. epidermidis*. This result indicates that position 3 tolerates PEGylation to a lesser degree than position 10.

Gelation of PEGylated Teixobactin Analogues in Aqueous Buffer

Each crude PEGylated analogue aggregated under the aqueous conditions of preparative HPLC purification, which qualitatively indicated that PEGylation was not increasing the solubility of these teixobactin analouges. In order to determine whether PEGylation had improved the solubility of any analogues, I performed an assay to visualize teixobactin gelation in aqueous buffer. An aliquot of peptide in DMSO was added to phosphate-buffered saline (PBS) containing a small amount of crystal violet for visual contrast. Upon addition to buffer, all PEGylated analogues formed a gel that persisted after mechanical stirring with a micropipette tip (Figure 2.3). I previously hypothesized that PEGylation would increase the solubility of teixobactin monomers and prevent the supramolecular fibrilization that leads to gel formation while preserving antiparallel β-sheet formation of the lipid II-binding dimer. The observed gel formation provides evidence that PEGylation does not sufficiently disrupt macroscopic aggregation. Based on the reduced activity of the analogues, PEGylation may instead be preventing teixobactin from binding lipid II or localizing to the bacterial cell wall.

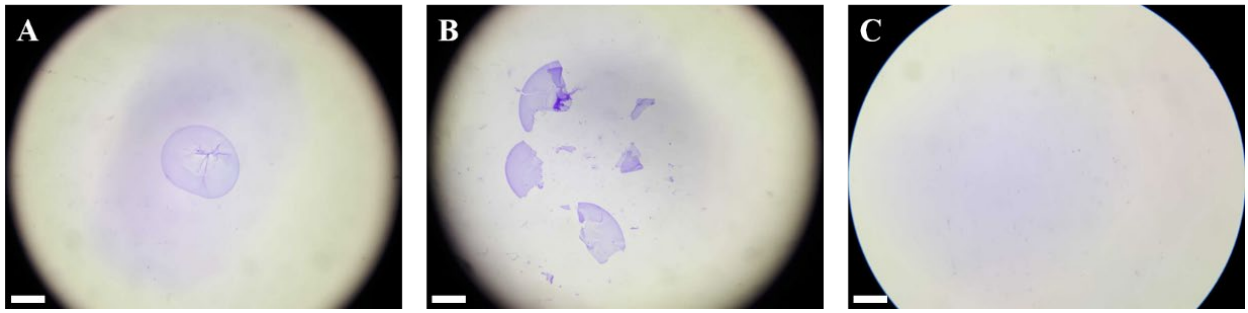

Figure 2.3. Qualitative gel assay of PEGylated teixobactin analogues. A gel formed by peptide 1 in PBS buffer (A) before and (B) after stirring with a pipette tip. Natural teixobactin and all PEGylated analogues formed similar gels that persisted through stirring. (C) No gel formation is observed for DMSO vehicle control in PBS buffer. Scale bar is 1 mm.

Conclusion

In this study, I demonstrated that on-resin PEGylation of synthetic teixobactin analogues is possible, but that PEGylated diastereomers formed as a result of Ile_{11} esterification are prohibitively difficult to separate due to their increased overlap in chromatographic retention times. Contrary to the initial hypothesis, PEGylation of teixobactin hinders its antibiotic activity, as all PEGylated analogues prepared were less active than the corresponding control peptides. Position 10 can be PEGylated with greater retention of antibiotic activity than position 9, and position 3 on the N-terminal tail can be PEGylated with some retention of activity. This may be explained by the fact that modification of positions 3 and 10 with large PEG chains do not prevent teixobactin from forming an active lipid II-binding dimer, as the side chains of these residues do not impact β-sheet formation. Among the five analogues subjected to MIC assays, only Arg_9,$Lys(PEG3)_{10}$-teixobactin **1**, with a short (n = 3) PEG chain on the macrolactone ring and +2 overall charge, has an MIC value against *S. epidermidis* comparable to Arg_{10}- or Lys_{10}-teixobactin.

PEGylation does not increase the solubility of teixobactin or inhibit its propensity to aggregate. All analogues tested formed gels in aqueous buffer that persisted after stirring.

Reducing the overall charge state of teixobactin through PEGylation at position 10 dramatically reduces its solubility in the conditions required for preparative HPLC purification, further complicating purification of the peptide. Improving the preclinical viability of teixobactin does not appear to be achievable by PEGylation.

Contrary to both initial hypotheses, PEGylated teixobactin analogues have reduced (not unchanged) antibiotic activity and unaffected or increased (not reduced) propensity to form insoluble gels in aqueous buffer. Collectively, these results suggested that supramolecular assembly of teixobactin into amyloid-like fibrils is directly responsible for its exceptional antibiotic activity. This new hypothesis was later supported by further studies into the mechanism of action of teixobactin,[16,17] and my improved understanding of the relationship between teixobactin assembly and activity directly lays the foundation for the studies presented in Chapter III.

Supporting Information for Chapter II

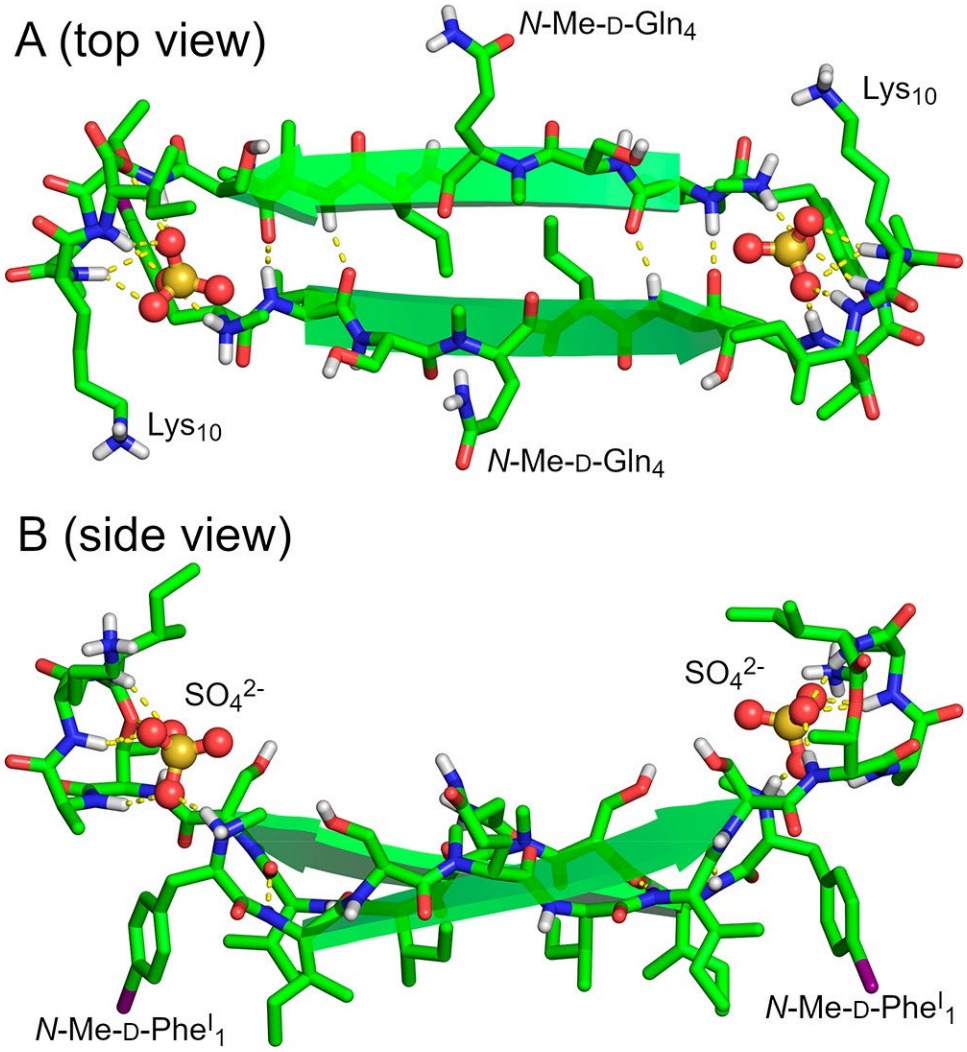

Figure S2.1. Crystal structure of a teixobactin analogue depicting a β-sheet dimer that binds sulfate anions. Residues Ser_3, Ala_9, and Arg_{10} face away from the sulfate anion that is bound by the macrolactone ring. Figure reproduced with permission from Yang et al. *J. Am. Chem. Soc.* **2018**, *140* (43), 14028–14032.[9]

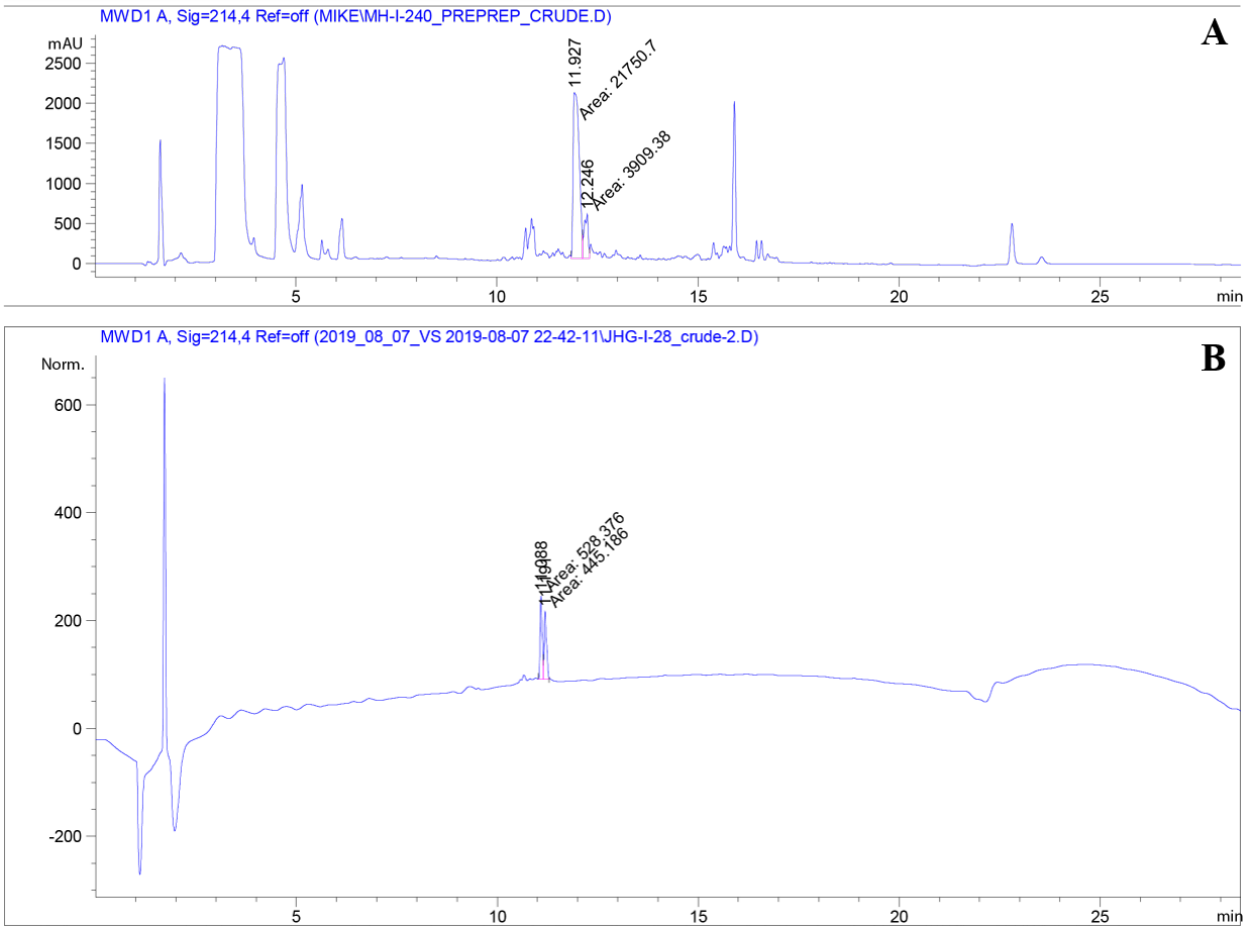

Figure S2.2. Analytical HPLC comparison of teixobactin and PEGylated teixobactin diastereomeric separation. Analytical reverse-phase HPLC traces of (A) crude Arg_{10}-teixobactin and (B) peptide **3**. The diastereomers of teixobactin resulting from Ile epimerization are indicated by their retention times and peak integrals. The difference in retention times for the non-PEGylated Arg_{10}-teixobactin is 0.3 min. The difference in retention times for the PEGylated peptide **3** is 0.1 min.

Materials and Methods

General Information

Reagent-grade solvents, chemicals, amino acids, and resin were used as received, with two exceptions: (1) Methylene chloride (CH_2Cl_2) was passed through alumina under argon prior to use. (2) Amine-free *N,N*-dimethylformamide (DMF) was purchased from Alfa Aesar and dried through alumina and an amine scavenger resin column under argon prior to use. Solid-phase peptide synthesis was carried out manually in a solid-phase reaction vessel. Preparative reverse-phase HPLC was performed on a Rainin Dynamax instrument equipped with a ZORBAX SB-C18 column (Agilent). Analytical reverse-phase HPLC was performed on an Agilent 1200 instrument equipped with an Aeris PEPTIDE 2.6u XB-C18 column (Phenomonex). UV detection (214 nm) was used for both preparative and analytical HPLC. HPLC grade acetonitrile (CH_3CN) and deionized water (18 MΩ), each containing 0.1% trifluoroacetic acid (TFA), were used as solvents for both preparative and analytical reverse-phase HPLC. Deionized water (18 MΩ) was obtained from a Barnstead NANOpure Diamond water purification system. All teixobactin analogues were prepared and studied as the trifluoroacetate salts.

Synthesis of PEGylated Teixobactin Analogues

Teixobactin analogues were synthesized as the trifluoroacetate salts following procedures previously reported by our group.[6,8,9] In each analogue, the residue to be functionalized with poly(ethylene glycol) (PEG) propionic acid was exchanged from the natural amino acid for that position to Fmoc-Lys(Alloc)-OH.

Resin loading. 2-Chlorotrityl chloride resin (300 mg, 1.46 mmol/g) was added to a 10-mL Bio-Rad Poly-Prep chromatography column. The resin was suspended in dry CH_2Cl_2 (10 mL) and allowed to swell for 30 min. The resin was loaded with a solution of Fmoc-Arg(Pbf)-OH (117 mg,

0.180 mmol, 0.500 equiv) and 2,4,6-collidine (300 μL) in dry CH_2Cl_2 (5 mL). The suspension was gently rocked for 4 h. The solution was drained from the column, and the resin was washed with dry CH_2Cl_2 (3 x 5 mL). A mixture of CH_2Cl_2/MeOH/DIPEA (17:2:1, 8 mL) was added to the resin and gently rocked for 1 h to cap any unreacted resin sites. The solution was drained from the column, and the resin was washed with CH_2Cl_2 (3×5 mL).

Quantifying resin loading. After draining the solution from the column, 1.0 mg of loaded resin was weighed out and transferred to a scintillation vial containing 20% (v/v) piperidine in dry DMF (3 mL). The reaction mixture was shaken at 80 RPM for 10 min. The solution was filtered through glass wool to remove resin beads, and absorbance of the filtered solution at 290 nm was measured. The resin loading was determined to be 0.15 mmol (0.49 mmol/g, 33% loading) using the following formula:

$$\%\ loading = \frac{A_{290} \times V \times 10^3}{\varepsilon \times m_{resin} \times l} \times 100\%$$

where:

A_{290} = absorbance measured at 290 nm

V = volume of piperidine in DMF in mL (3.0 mL)

ε = molar absorptivity of piperidine adduct (6,089 L mol^{-1} cm^{-1})

m_{resin} = mass of resin in mg (1.0 mg)

l = cell pathlength in cm (1.0 cm)

Linear peptide synthesis. The loaded resin was suspended in dry DMF and transferred to a solid-phase peptide synthesis reaction vessel for manual peptide synthesis using Fmoc-Ala-OH, Fmoc-D-Thr-OH (free alcohol OH), Fmoc-Ser(*t*-Bu)-OH, Fmoc-Ile-OH, Fmoc-D-*allo*-Ile-OH, Fmoc-D-Gln(Trt)-OH, Fmoc-Ser(*t*-Bu)-OH, Fmoc-Ile-OH, and Boc-*N*-Me-D-Phe-OH. The linear peptide was synthesized through the following cycles: *i.* Fmoc deprotection with 20% (v/v)

piperidine in dry DMF (5 mL) for 10 min, *ii.* resin washing with dry DMF (3 x 5 mL), *iii.* coupling of amino acid (0.60 mmol, 4.0 equiv) with HCTU (237 mg, 0.600 mmol, 4.00 equiv) in 20% (v/v) 2,4,6-collidine in dry DMF (5 mL) with agitation by bubbling of nitrogen gas for 20 min, and *iv.* resin washing with dry DMF (3×5 mL). For D-to-L and L-to-D amino acid couplings, the reaction time in step *iii.* was increased to 1 h.

On-resin Alloc deprotection. $Pd(PPh_3)_4$ (19 mg, 0.020 mmol, 0.10 equiv) and $PhSiH_3$ (185 µL, 1.50 mmol, 10.0 equiv) were dissolved in dry CH_2Cl_2 (5 mL). The solution was added to the resin in the solid-phase peptide synthesis reaction vessel and allowed to react with the resin with agitation by bubbling of nitrogen gas. After 30 min, the solution was drained, and the resin was washed with dry CH_2Cl_2 (3×5 mL). The deprotection reaction was repeated one additional time using the same procedure, and the solution was drained.

On-resin coupling of m-PEG$_n$-propionic acid. m-PEG3-propionic acid (142 µL, 0.600 mmol, 4.00 equiv) or m-PEG10-propionic acid (327 µL, 0.600 mmol, 4.00 equiv) and HCTU (237 mg, 0.600 mmol, 4.00 equiv) were dissolved in 20% (v/v) 2,4,6-collidine in dry DMF (5 mL). The solution was added to the resin in the solid-phase peptide synthesis reaction vessel and allowed to react with the resin with agitation by bubbling of nitrogen gas. After 2 h, the solution was drained, and the resin was washed with dry DMF (3×5 mL).

Esterification. The resin was transferred to a 10-mL Bio-Rad Poly-Prep chromatography column and washed with dry CH_2Cl_2 (3×5 mL). In a test tube, Fmoc-Ile-OH (505 mg, 1.50 mmol, 10.0 equiv) and diisopropylcarbodiimide (233 µL, 1.50 mmol, 10.0 equiv) were dissolved in dry CH_2Cl_2 (5 mL). The resulting solution was filtered through a 0.20-µm nylon filter, and 4-dimethylaminopyridine (18.0 mg, 0.150 mmol, 1.00 equiv) was added to the filtrate. The resulting

solution was transferred to the resin and gently rocked for 1 h. The solution was drained, and the resin was washed with dry CH_2Cl_2 (3×5 mL) and dry DMF (3×5 mL).

Fmoc deprotection and cleavage of linear peptide from resin. To remove the Fmoc protecting group on Ile_{11}, the resin was treated with 20% (v/v) piperidine in dry DMF (5 mL) and gently rocked for 30 min. The solution was drained, and the resin was washed with dry DMF (3×5 mL) and dry CH_2Cl_2 (3×5 mL). To cleave the peptide, the resin was treated with 20% (v/v) 1,1,1,3,3,3-hexafluoroisopropanol (HFIP) in dry CH_2Cl_2 (8 mL) and gently rocked for 1 h. The filtrate was collected in a round-bottomed flask. The resin was washed with a second aliquot of 20% (v/v) HFIP in dry CH_2Cl_2 (8 mL) and dry CH_2Cl_2 (3 x 5 mL). The filtrates were combined and concentrated under reduced pressure to afford a clear oil. The oil was placed under vacuum (≤10 mTorr) to remove any residual solvents.

Cyclization. The oil was dissolved in dry DMF (100 mL). HBTU (325 mg, 0.900 mmol, 6.00 equiv) and HOBt (117 mg, 0.900 mmol, 6.00 equiv) were added to the solution. The reaction mixture was stirred under nitrogen for 30 min. DIPEA (157 μL, 0.900 mmol, 6.00 equiv) was added dropwise to the solution, and the reaction mixture was stirred under nitrogen for 12 h. The mixture was concentrated under reduced pressure to afford the cyclized peptide as a yellow solid. The solid was placed under vacuum (≤10 mTorr) to remove any residual solvents.

Global deprotection, ether precipitation, and purification. The crude protected peptide was dissolved in a mixture of trifluoroacetic acid (TFA)/triisopropylsilane/H_2O (18:1:1, 10 mL), and the solution was stirred under nitrogen for 1 h. The deprotection mixture was then evenly aliquoted between two 40-mL portions of ice-cold diethyl ether in 50-mL conical tubes. The 50-mL conical tubes were centrifuged (500×*g*) for 15 min to precipitate the crude peptide. The diethyl ether supernatant was discarded, and the precipitated pellets were dried under flow of nitrogen. The

pellets were dissolved in 20% (v/v) CH_3CN in H_2O (8 mL) and centrifuged (1380×*g*) for 5 min, and the solution was filtered through a 0.20-μm nylon filter. The peptide was purified by reverse-phase HPLC (gradient elution of 20–40% CH_3CN w/ 0.1% TFA over 120 min). Pure fractions analyzed by analytical HPLC and matrix-assisted laser desorption/ionization time of flight-time of flight (MALDI TOF-TOF) mass spectrometry were combined and lyophilized. The trifluoroacetic acid (TFA) salt Arg_9,$Lys(PEG3)_{10}$-teixobactin was isolated as a white powder (41.4 mg, 15.7% yield as the TFA salt based on resin loading).

The other teixobactin analogues were prepared using similar procedures. Analogues **1**, **2**, and **3** were estimated to be of at least 90% purity based on analytical HPLC analysis.

Table S2.1. Chemical yields of purified peptides.

analogue	yield (mg)	% yield	calcd. MW as TFA salt
Arg_9,$Lys(PEG3)_{10}$-teixobactin **1**	41.4 mg	15.7%	1746.89 (· 2 TFA)
$Lys(PEG3)_9$,Arg_{10}-teixobactin **2**	2.1 mg	0.6%	1746.89 (· 2 TFA)
Arg_9,$Lys(PEG10)_{10}$-teixobactin **3**	7.52 mg	2.4%	2055.07 (· 2 TFA)
$Lys(PEG3)_3$,Arg_{10}-teixobactin **5**	6.43 mg	2.9%	2039.08 (· 2 TFA)

Preparation of DMSO Stock Solutions

All DMSO stock solutions were stored in a −20 °C freezer until needed for experiments.

DMSO stocks for MIC assays. A 1 mg/mL DMSO stock solution of each peptide was prepared by dissolving 1.0 mg of the lyophilized peptide in 1.0 mL of sterile DMSO in an autoclaved Eppendorf tube.

DMSO stocks for solubility assays. A 20 mg/mL DMSO stock solution of each peptide was prepared by dissolving 2.0 mg of the lyophilized peptide in 100 μL of DMSO in an Eppendorf tube.

Minimum Inhibitory Concentration (MIC) Assays

MIC assays were conducted following procedures previously reported by our group.[6,18] In all cases except for the initial overnight culture, Mueller-Hinton culture media contained 0.002% polysorbate 80 to prevent teixobactin from adhering to the 96-well microtiter plate.

Bacillus subtilis (ATCC 6051), *Staphylococcus epidermidis* (ATCC 14990), and *Escherichia coli* (ATCC 10798) were cultured from glycerol stocks in Mueller-Hinton media overnight in a shaking incubator at 37 °C. After incubation, the OD_{600} of each overnight bacterial culture was measured as 200 µL of culture in a single well in a 96-well plate. Based on previously reported colony-forming units (CFU)/mL for each bacterial strain, each overnight culture was diluted to 1×10^6 CFU/mL with Mueller-Hinton media.

An aliquot of 1 mg/mL peptide stock solution in DMSO was diluted with Mueller-Hinton media to 64 µg/mL of peptide in culture media. A 200 µL aliquot of the 64 µg/mL peptide stock solution was transferred to a single well of a 96-well microtiter plate. Two-fold serial dilutions were made with Muller-Hinton media across 11 wells of the 96-well plate to achieve a final volume of 100 µL with the following concentrations of peptide: 32, 16, 8, 4, 2, 1, 0.5, 0.25, 0.125, 0.0625, and 0.03125 µg/mL.

A 100 µL aliquot of the previously prepared 1×10^6 CFU/mL bacterial solution was added to each of the 11 wells, resulting in a final bacterial concentration of 5×10^5 CFU/mL and the following final concentrations of peptide: 16, 8, 4, 2, 1, 0.5, 0.25, 0.125, 0.0625, 0.03125, and 0.015625 µg/mL. The plate was covered with a lid and incubated at 37 °C for 16 h. The OD_{600} of each well was measured using a 96-well UV/Vis plate reader (MultiSkan GO, Thermo Scientific). The MIC values were taken as the lowest concentration of peptide that had no bacterial growth. Each MIC assay was run in triplicate.

Solubility Assay of PEGylated Teixobactin Analogues in PBS Buffer

Solubility assays were conducted following procedures previously reported by our group.[8] DMSO containing no peptide was used as a vehicle control.

A small amount of crystal violet was added to PBS buffer at pH 7.4. The resulting solution was diluted further with PBS buffer until individual crystals of crystal violet were no longer visible when viewed under a low magnification stereoscopic microscope. The addition of crystal violet to the PBS buffer provides color contrast that aids in identifying insoluble, gelatinous mass.

A 20 μL aliquot of the PBS buffer containing crystal violet was placed onto a glass depression well microscope slide. A 1 μL aliquot of 20 mg/mL peptide stock solution in DMSO was placed directly onto the center of the PBS buffer droplet. A low magnification stereoscopic microscope was used to visually observe the droplet. Natural teixobactin and all PEGylated analogues of teixobactin formed a gelatinous mass upon addition of the peptide stock solution in DMSO onto the PBS buffer. Upon stirring with a micropipette tip, the masses were sheared into fragments, but did not form a homogenous solution (Figure S2.4).

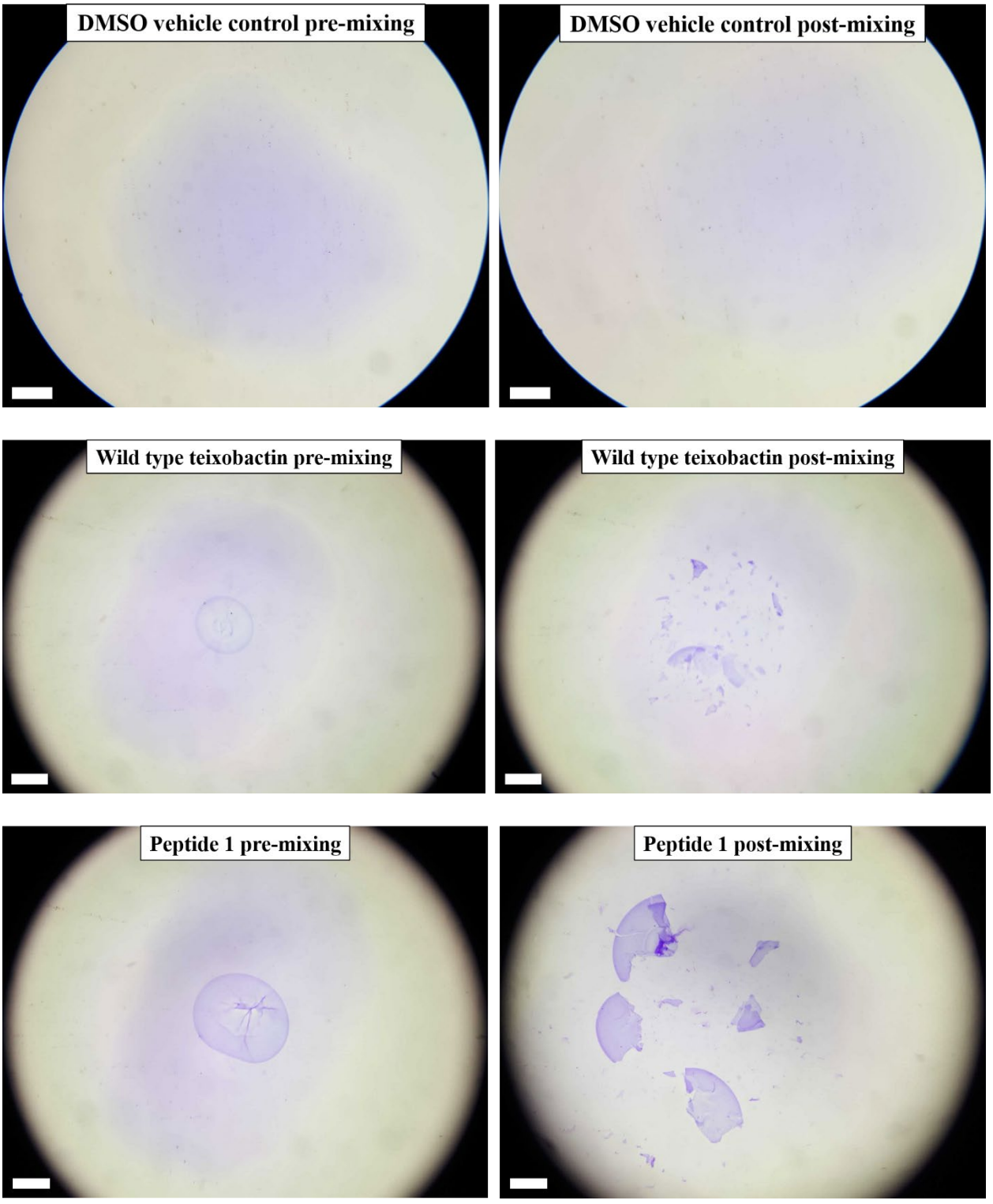
DMSO vehicle control pre-mixing
DMSO vehicle control post-mixing
Wild type teixobactin pre-mixing
Wild type teixobactin post-mixing
Peptide 1 pre-mixing
Peptide 1 post-mixing

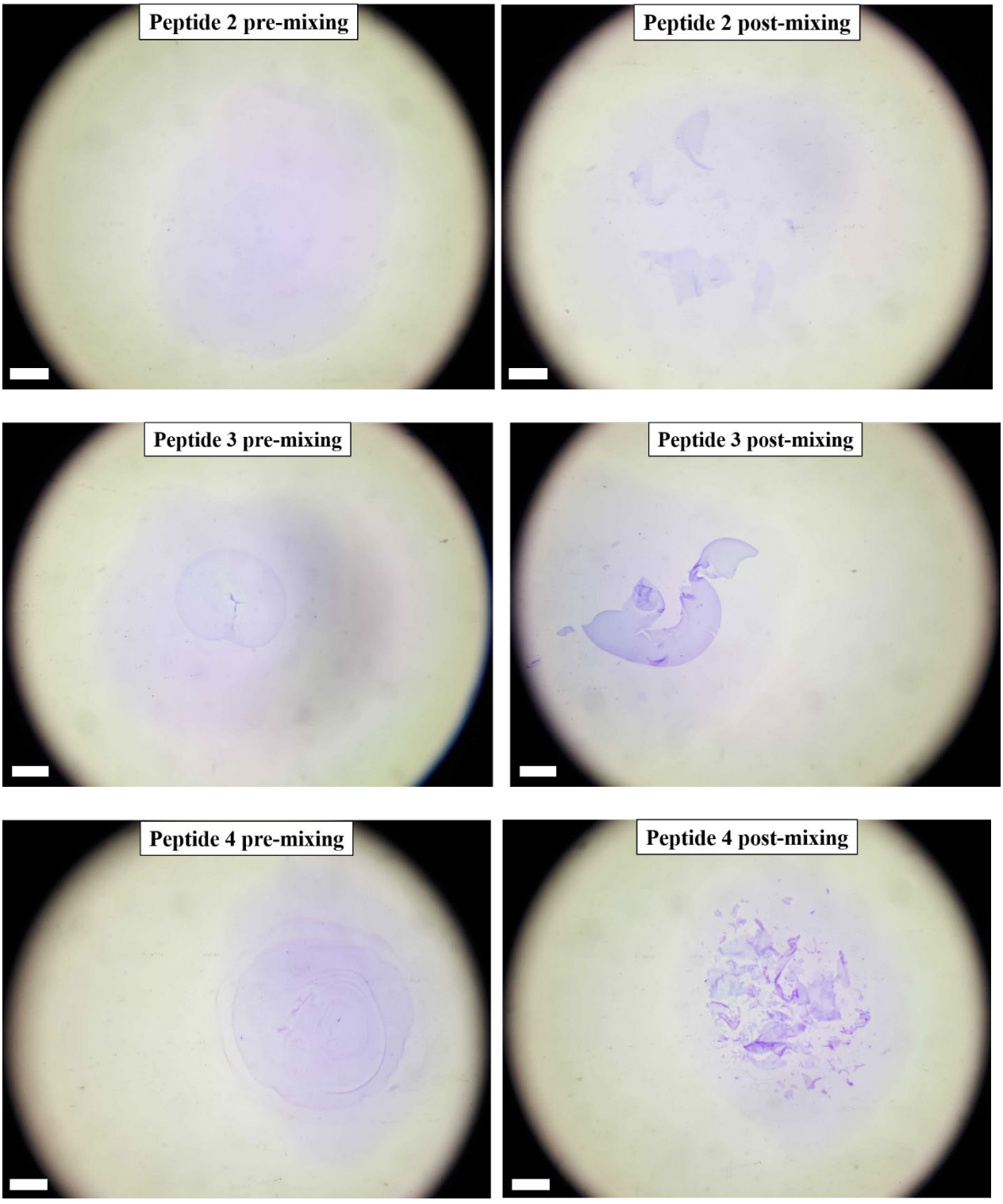
Peptide 2 pre-mixing
Peptide 2 post-mixing
Peptide 3 pre-mixing
Peptide 3 post-mixing
Peptide 4 pre-mixing
Peptide 4 post-mixing

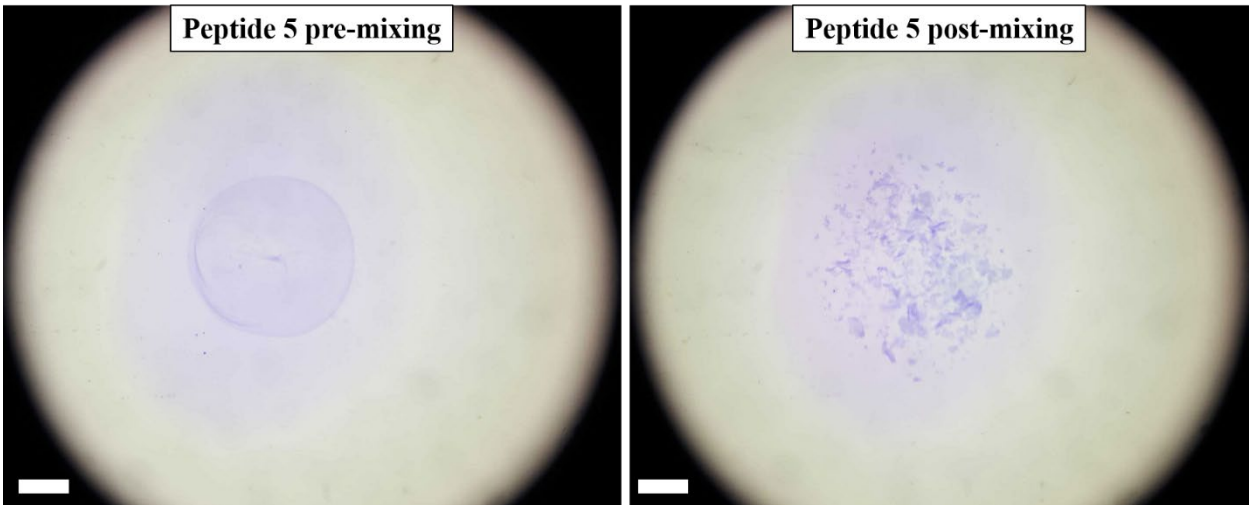

Figure S2.4. Gels formed by teixobactin and PEGylated analogues. A small amount of crystal violet added to PBS buffer allows for visualization of the gels formed. Scale bar is 1 mm.

Characterization Data

*Characterization of peptide **1***

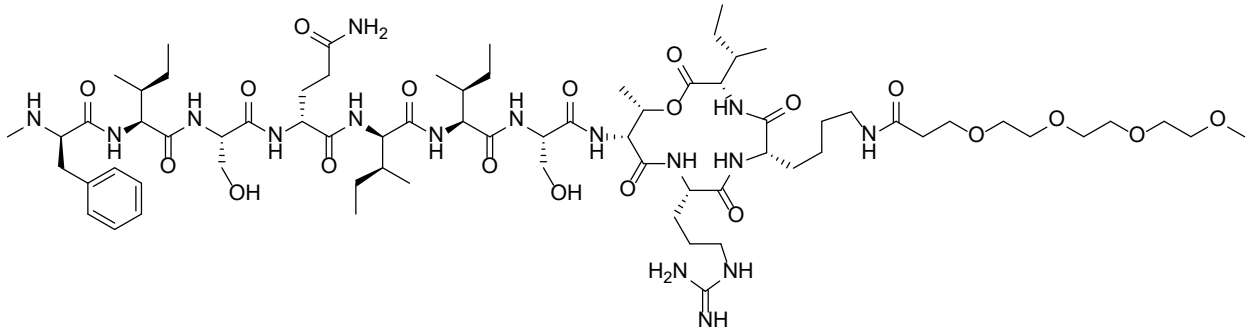

Exact Mass: 1518.9021

Arg_{9},Lys(PEG3)$_{10}$-teixobactin (**1**)

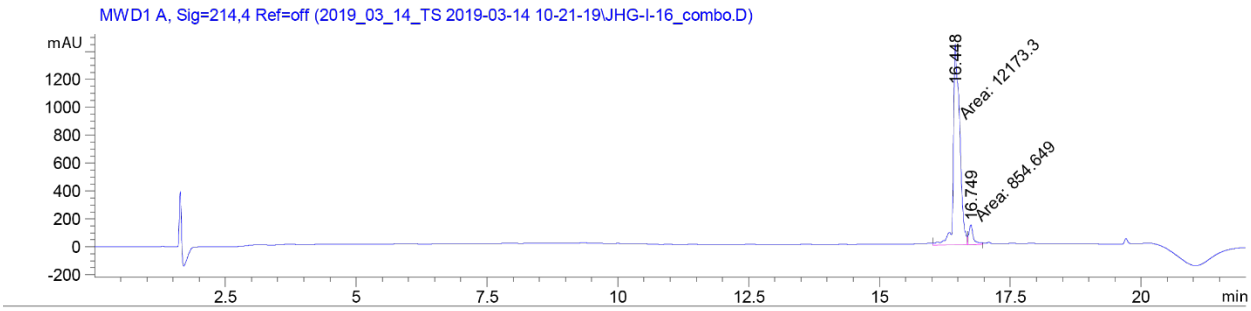

Peak #	RetTime [min]	Type	Width [min]	Area [mAU*s]	Height [mAU]	Area %
1	16.448	MF	0.1412	1.21733e4	1436.85413	93.4399
2	16.749	FM	0.1018	854.64917	139.94237	6.5601

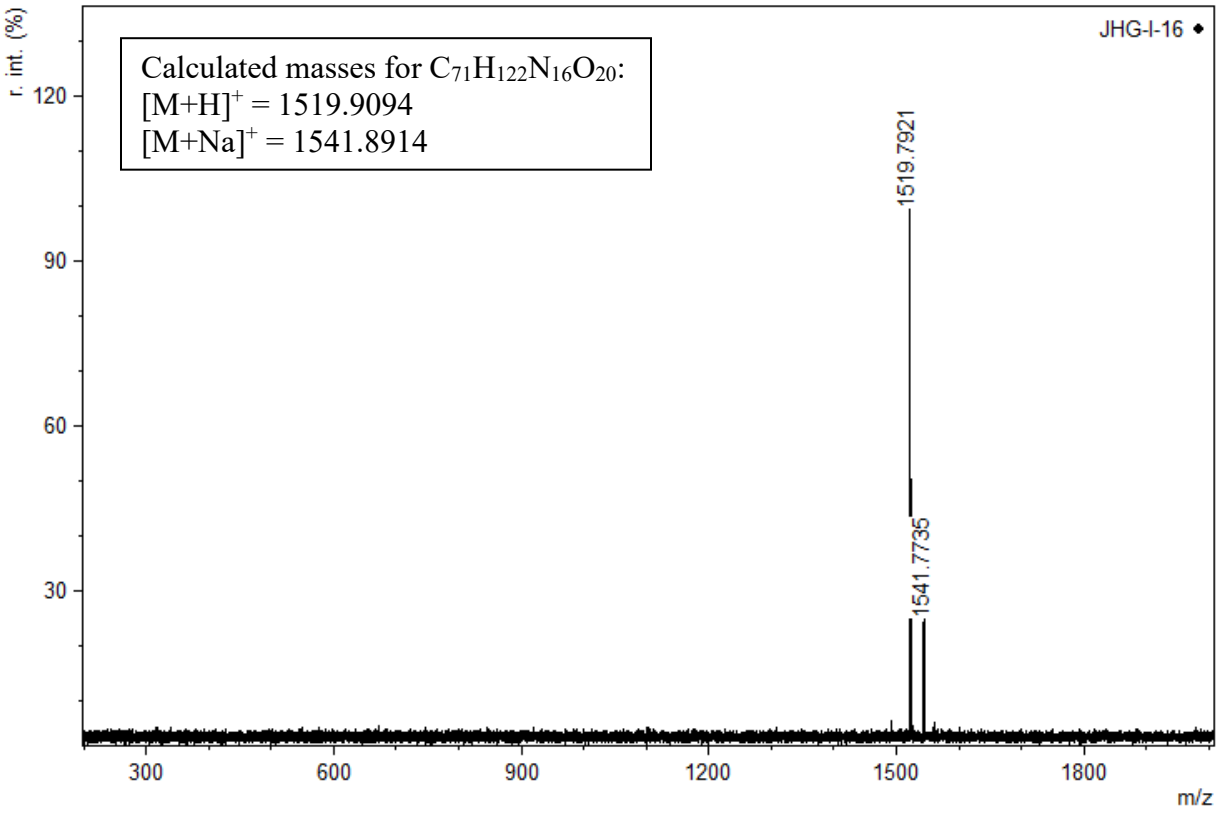
JHG-I-16
Calculated masses for C71H122N16O20:
[M+H]+ = 1519.9094
[M+Na]+ = 1541.8914
r. int. (%)
120
90
60
30
1519.7921
1541.7735
300
600
900
1200
1500
1800
m/z

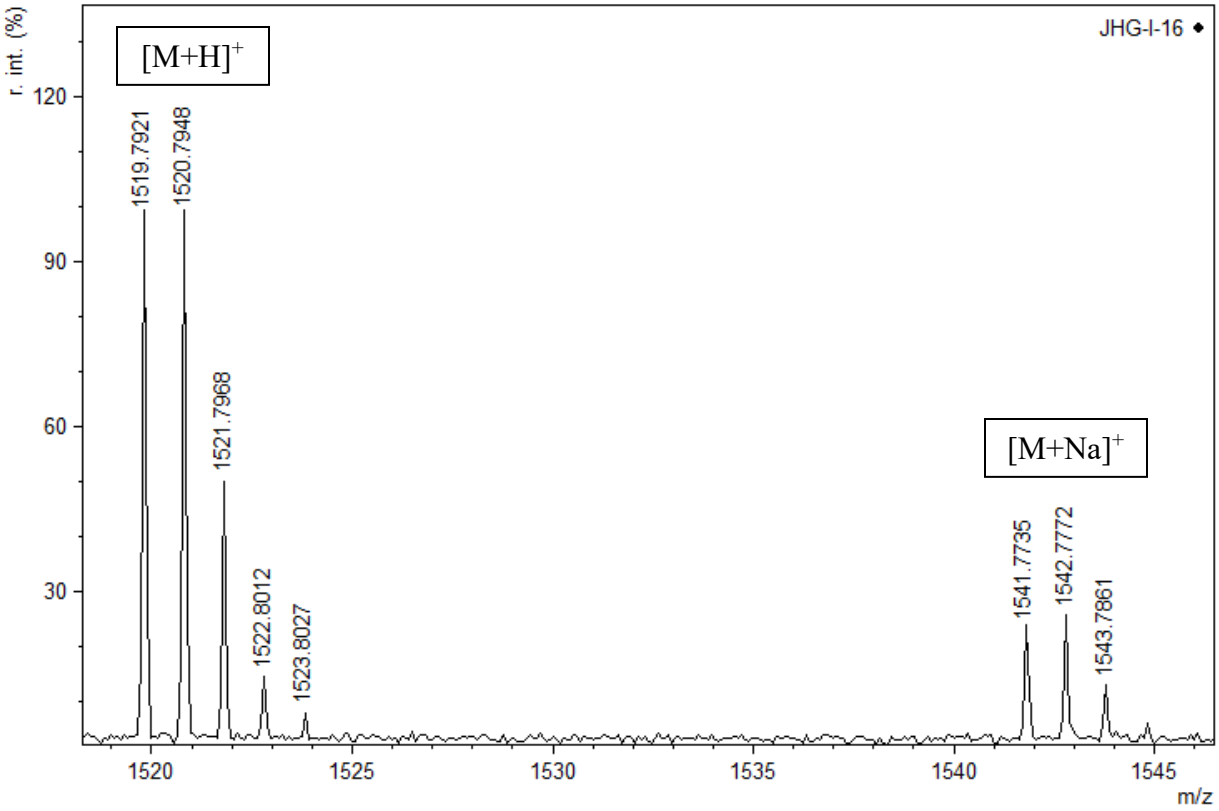
JHG-I-16
[M+H]+
[M+Na]+
r. int. (%)
120
90
60
30
1519.7921
1520.7948
1521.7968
1522.8012
1523.8027
1541.7735
1542.7772
1543.7861
1520
1525
1530
1535
1540
1545
m/z

Characterization of peptide ***2***

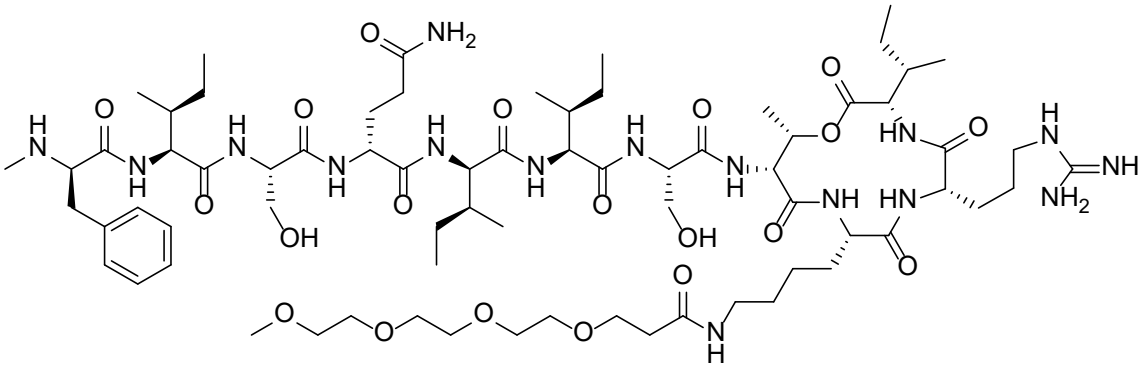

Exact Mass: 1518.9021

Lys(PEG3)$_9$,Arg$_{10}$-teixobactin (**2**)

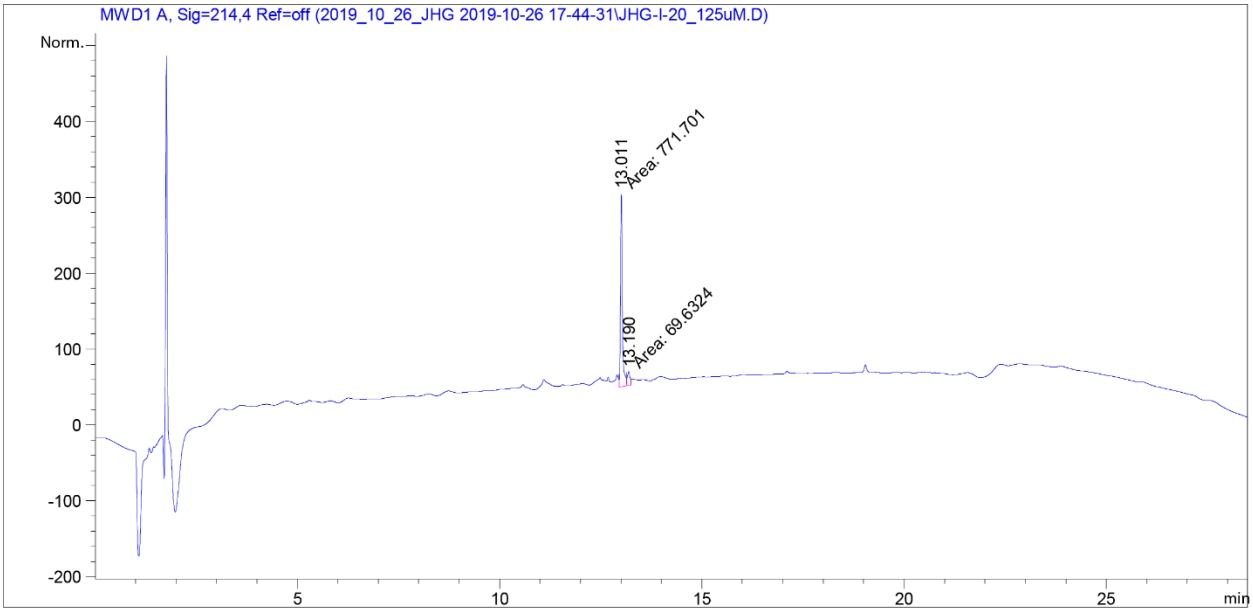

Peak #	RetTime [min]	Type	Width [min]	Area [mAU*s]	Height [mAU]	Area %
1	13.011	MF	0.0557	771.70074	231.00136	91.7236
2	13.190	FM	0.0698	69.63244	16.61714	8.2764

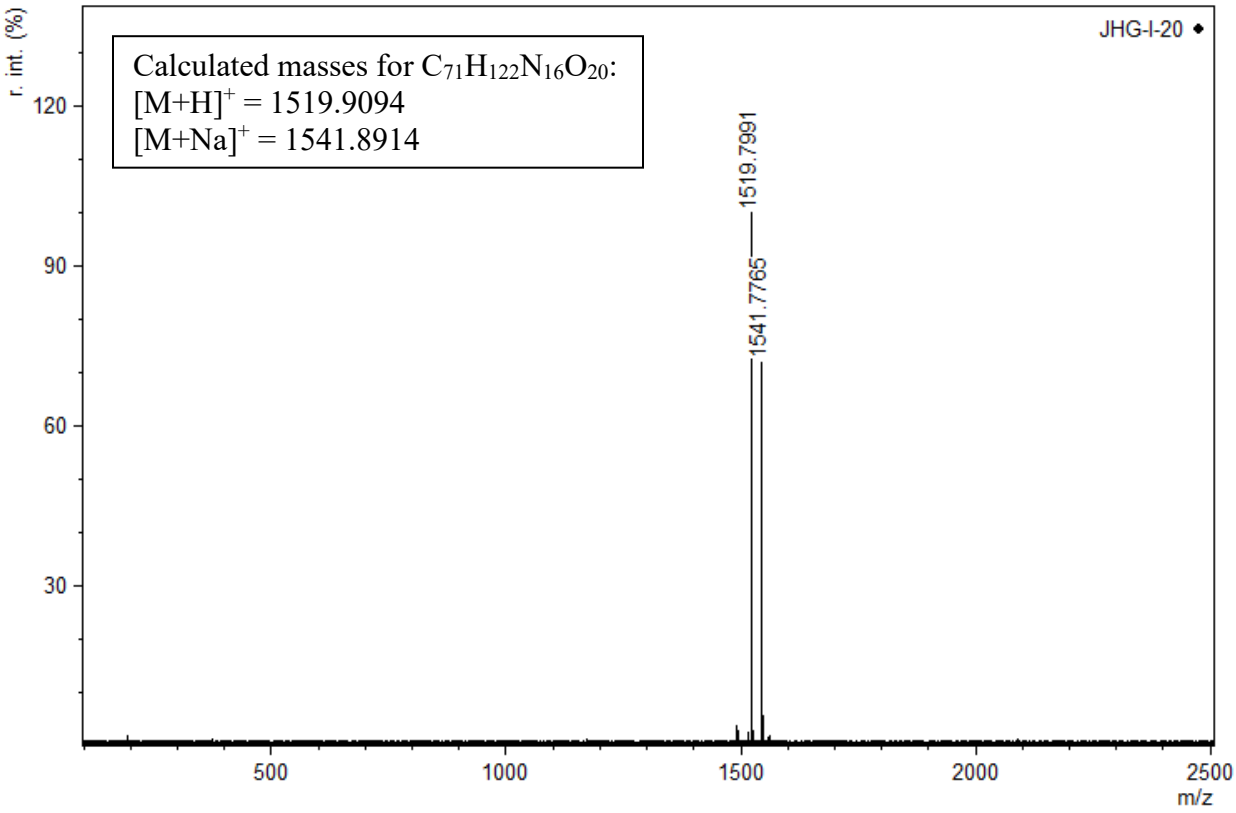
JHG-I-20
r. int. (%)
Calculated masses for $C_{71}H_{122}N_{16}O_{20}$:
$[M+H]^+$ = 1519.9094
$[M+Na]^+$ = 1541.8914
1519.7991
1541.7765
120
90
60
30
500
1000
1500
2000
2500
m/z

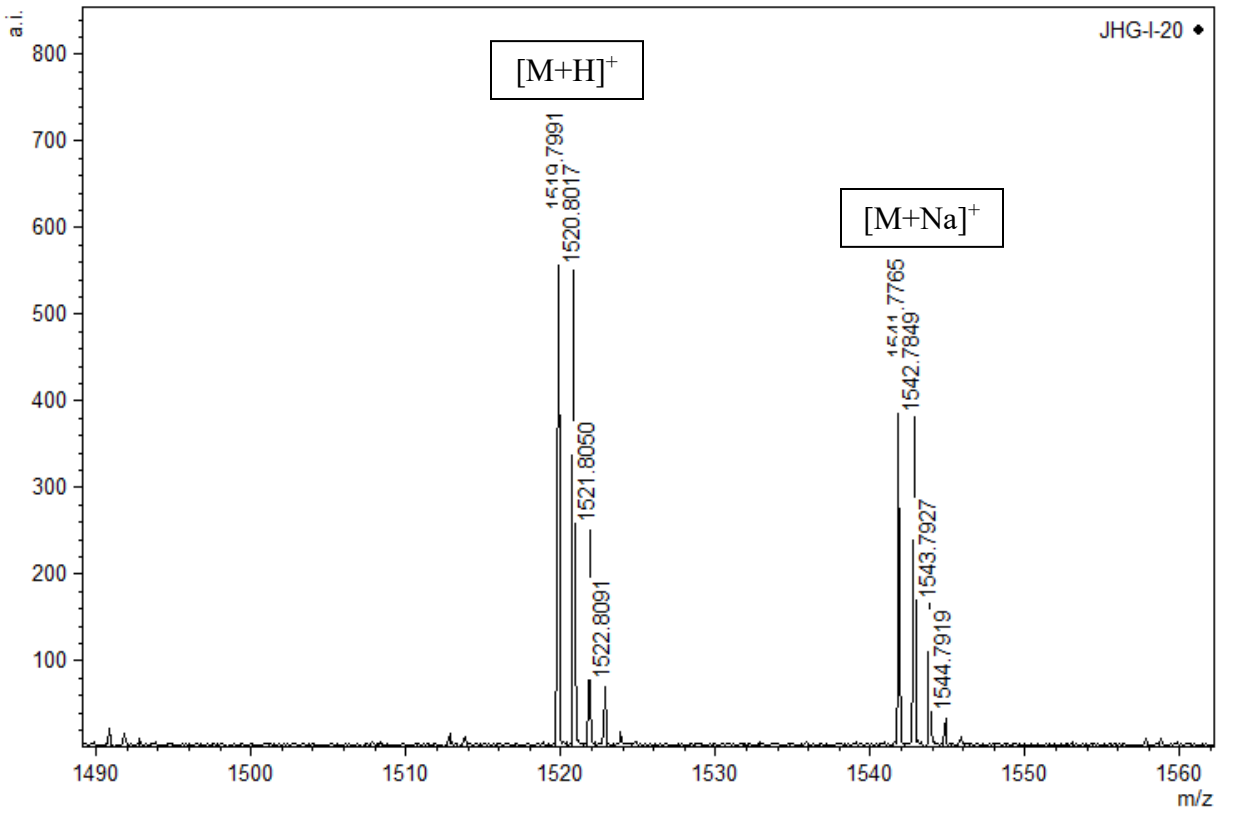
JHG-I-20
a.i.
$[M+H]^+$
$[M+Na]^+$
1519.7991
1520.8017
1521.8050
1522.8091
1541.7765
1542.7849
1543.7927
1544.7919
800
700
600
500
400
300
200
100
1490
1500
1510
1520
1530
1540
1550
1560
m/z

*Characterization of peptide **3***

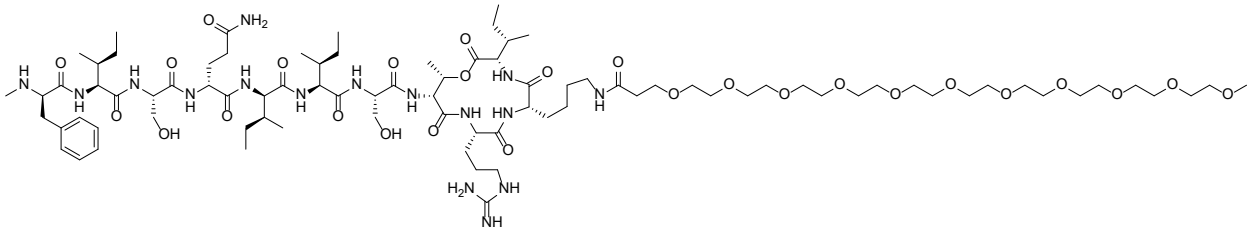

Exact Mass: 1827.0856

Arg_{9},$Lys(PEG10)_{10}$-teixobactin (**3**)

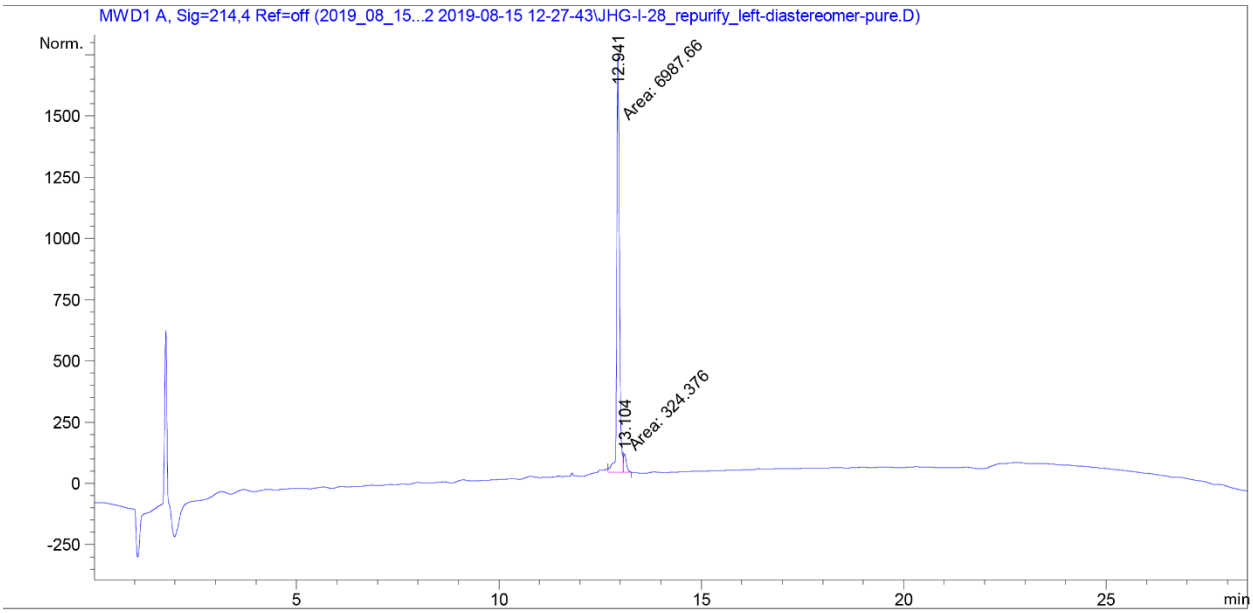

Peak #	RetTime [min]	Type	Width [min]	Area [mAU*s]	Height [mAU]	Area %
1	12.941	MF T	0.0757	6987.65771	1538.60950	95.5638
2	13.104	FM T	0.0807	324.37613	66.95826	4.4362

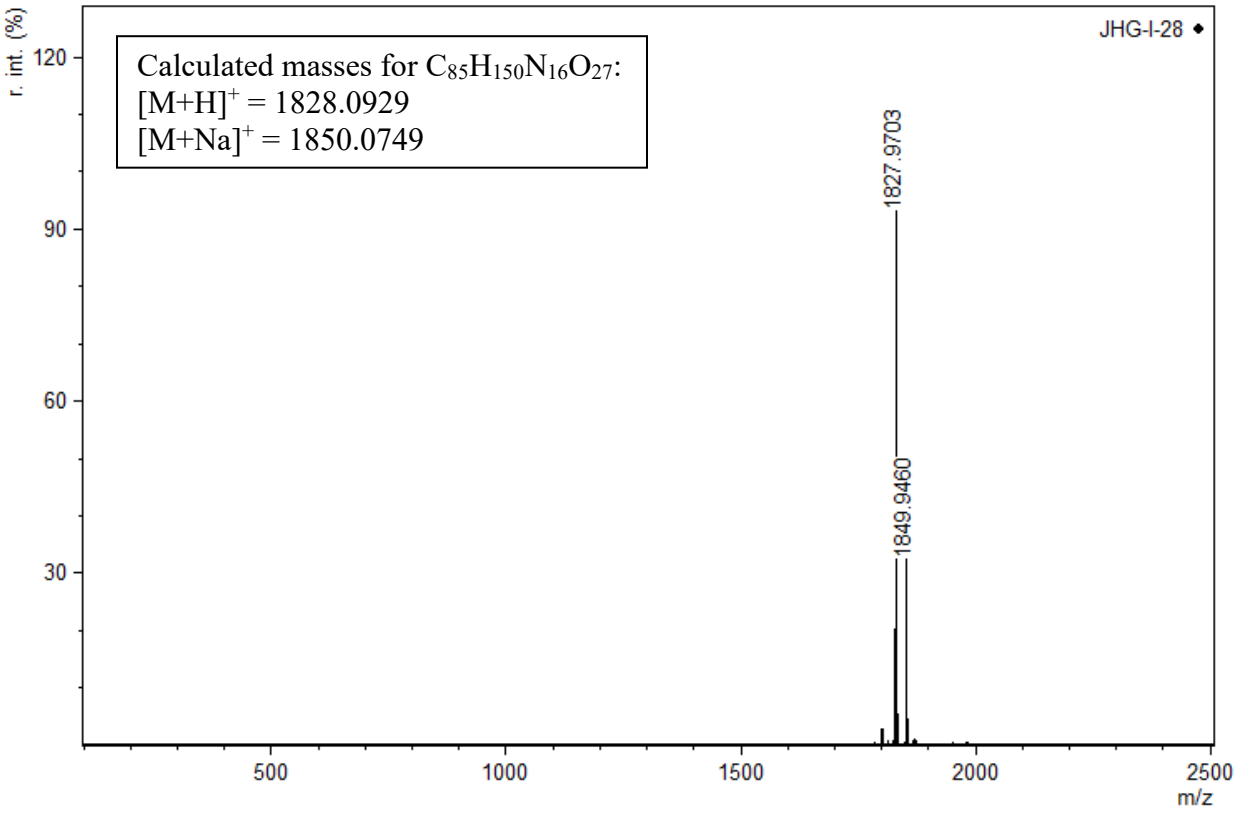
JHG-I-28
Calculated masses for $C_{85}H_{150}N_{16}O_{27}$:
$[M+H]^+$ = 1828.0929
$[M+Na]^+$ = 1850.0749
r. int. (%)
120
90
60
30
1827.9703
1849.9460
500
1000
1500
2000
2500
m/z

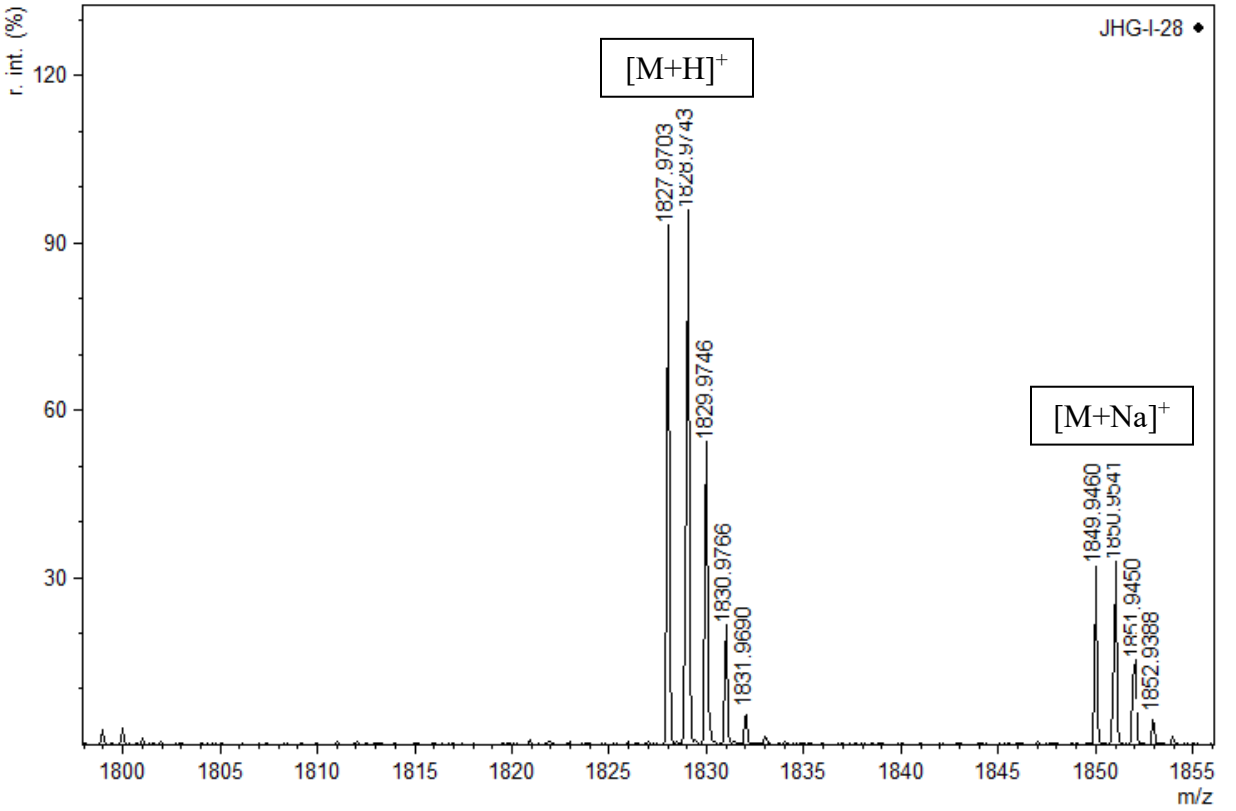
JHG-I-28
$[M+H]^+$
$[M+Na]^+$
r. int. (%)
120
90
60
30
1827.9703
1829.9746
1830.9766
1831.9690
1849.9460
1851.9450
1852.9388
1800
1805
1810
1815
1820
1825
1830
1835
1840
1845
1850
1855
m/z

*Characterization of peptide **4***

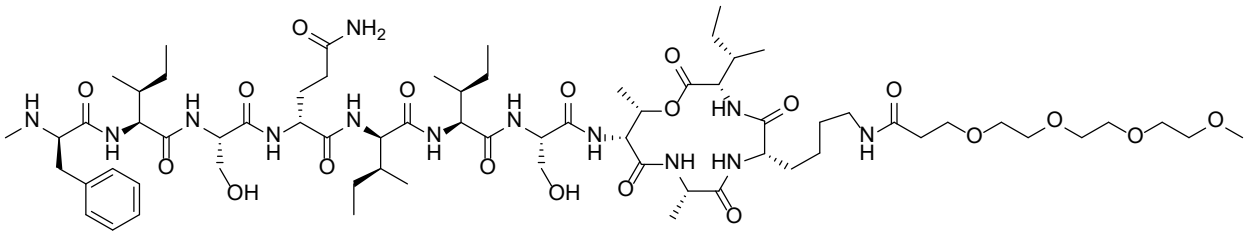

Exact Mass: 1433.8381

Lys(PEG3)$_{10}$-teixobactin (**4**)

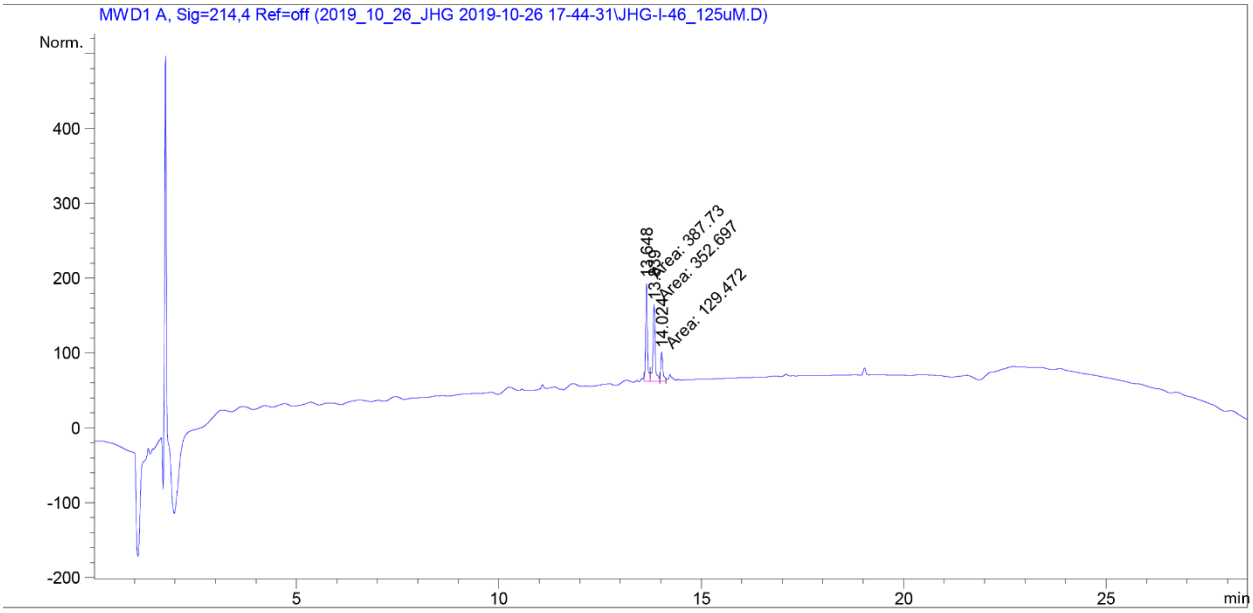

Peak #	RetTime [min]	Type	Width [min]	Area [mAU*s]	Height [mAU]	Area %
1	13.648	MF T	0.0541	387.73010	119.35897	44.5719
2	13.839	FM T	0.0635	352.69684	92.61067	40.5446
3	14.024	FM T	0.0614	129.47180	35.14640	14.8835

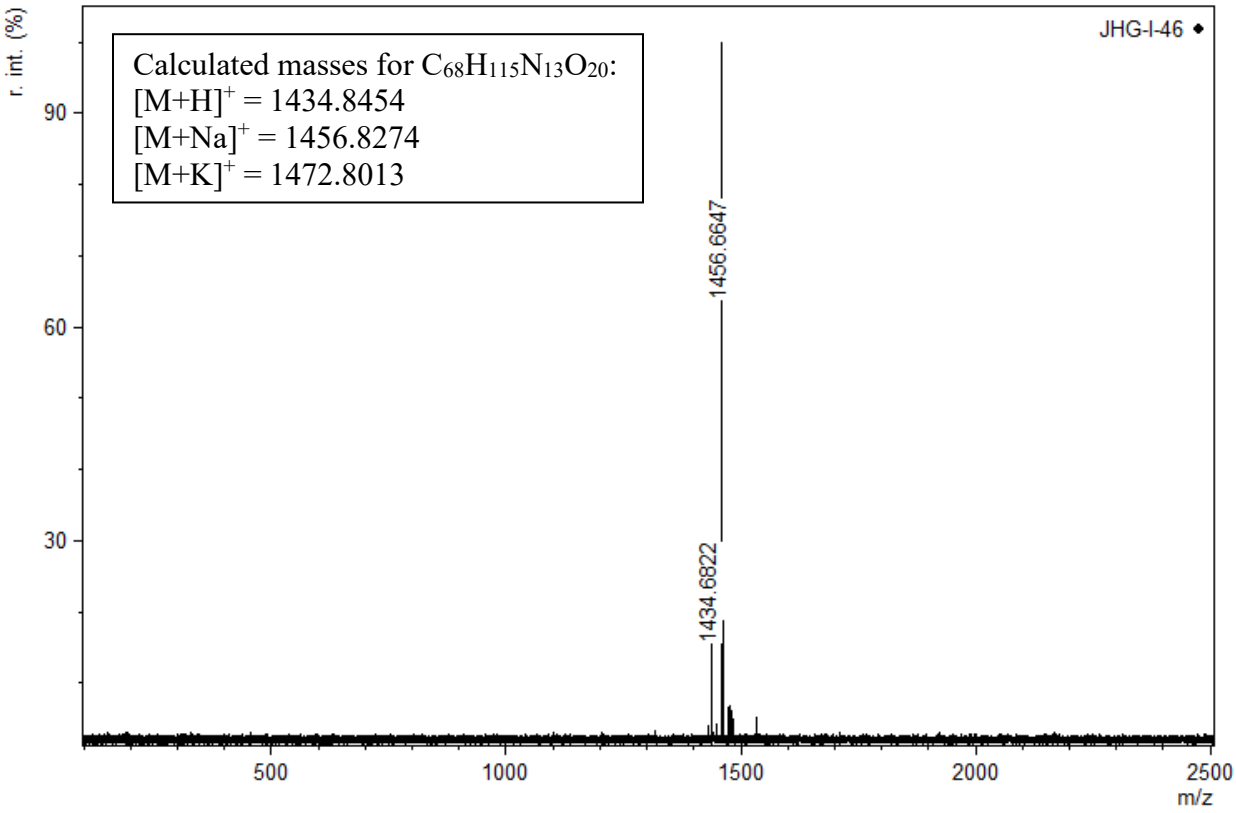
JHG-I-46
r. int. (%)
Calculated masses for $C_{68}H_{115}N_{13}O_{20}$:
$[M+H]^+$ = 1434.8454
$[M+Na]^+$ = 1456.8274
$[M+K]^+$ = 1472.8013
1456.6647
1434.6822
90
60
30
500
1000
1500
2000
2500
m/z

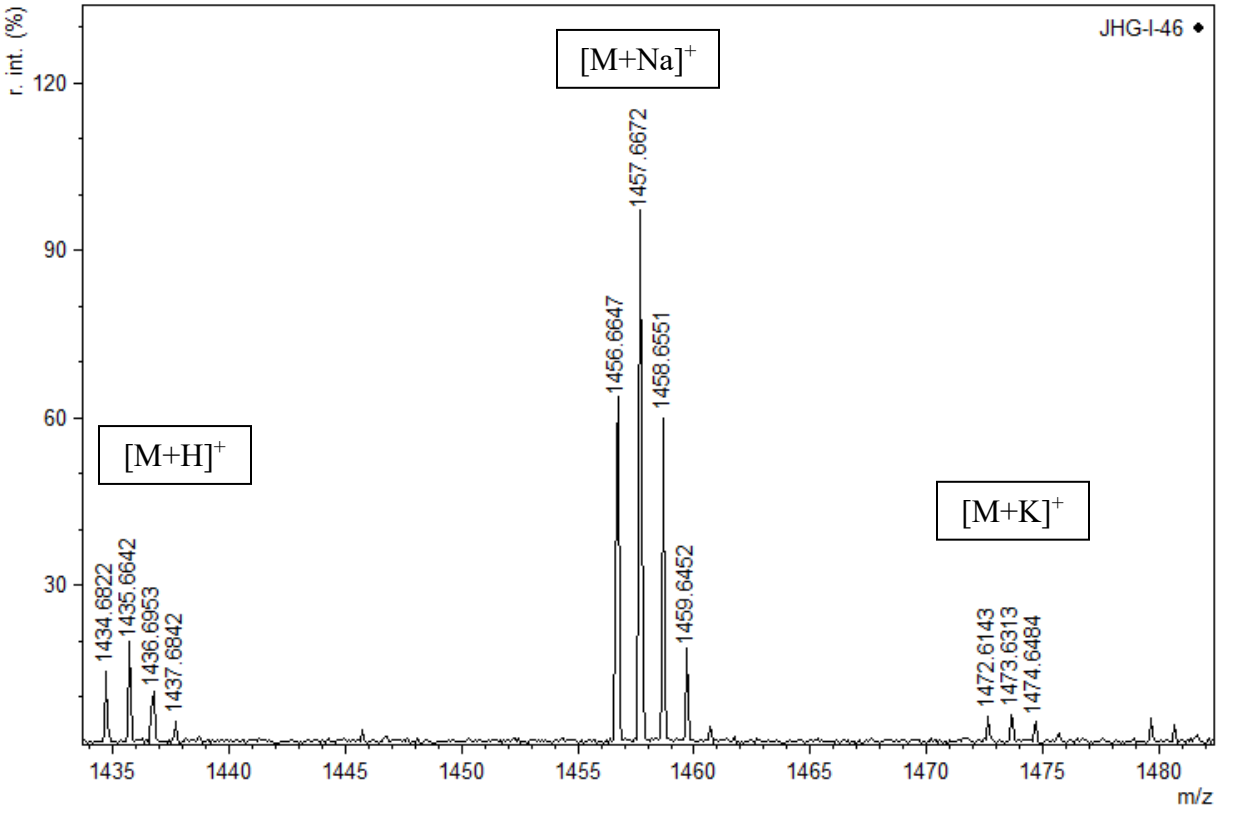
JHG-I-46
r. int. (%)
$[M+Na]^+$
$[M+H]^+$
$[M+K]^+$
1457.6672
1456.6647
1458.6551
1459.6452
1434.6822
1435.6642
1436.6953
1437.6842
1472.6143
1473.6313
1474.6484
120
90
60
30
1435
1440
1445
1450
1455
1460
1465
1470
1475
1480
m/z

Characterization of peptide ***5***

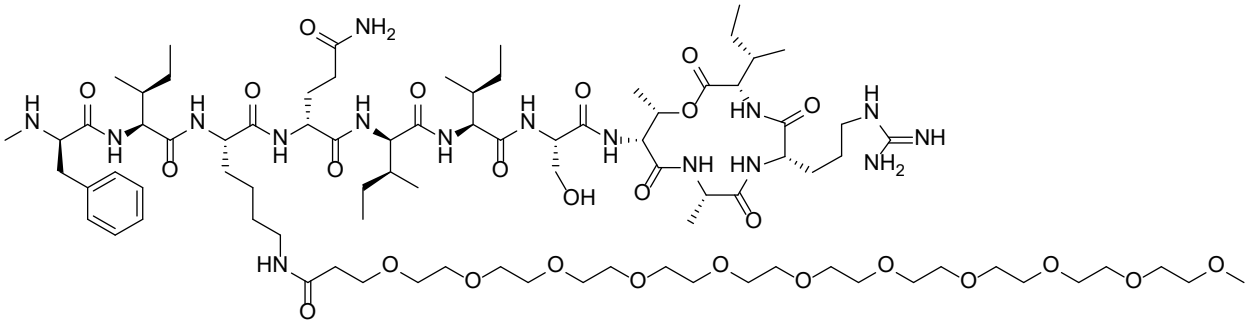

Exact Mass: 1811.0907

Lys(PEG10)$_3$,Arg$_{10}$-teixobactin (**5**)

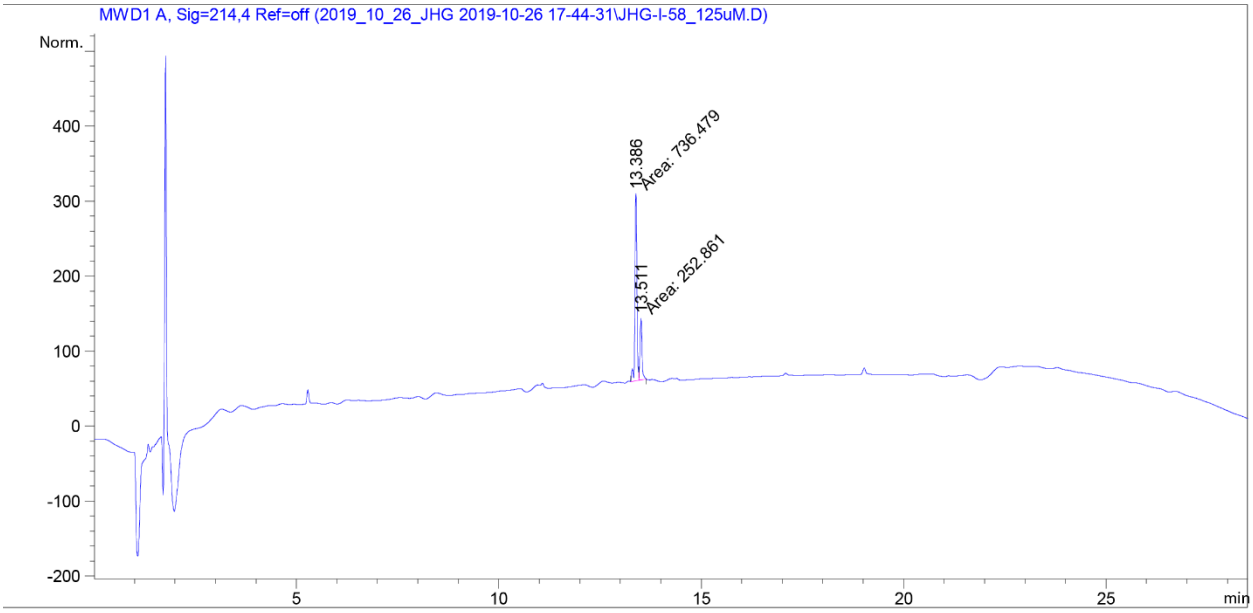

Peak #	RetTime [min]	Type	Width [min]	Area [mAU*s]	Height [mAU]	Area %
1	13.386	MF T	0.0545	736.47900	225.33408	74.4414
2	13.511	FM T	0.0562	252.86124	75.03718	25.5586

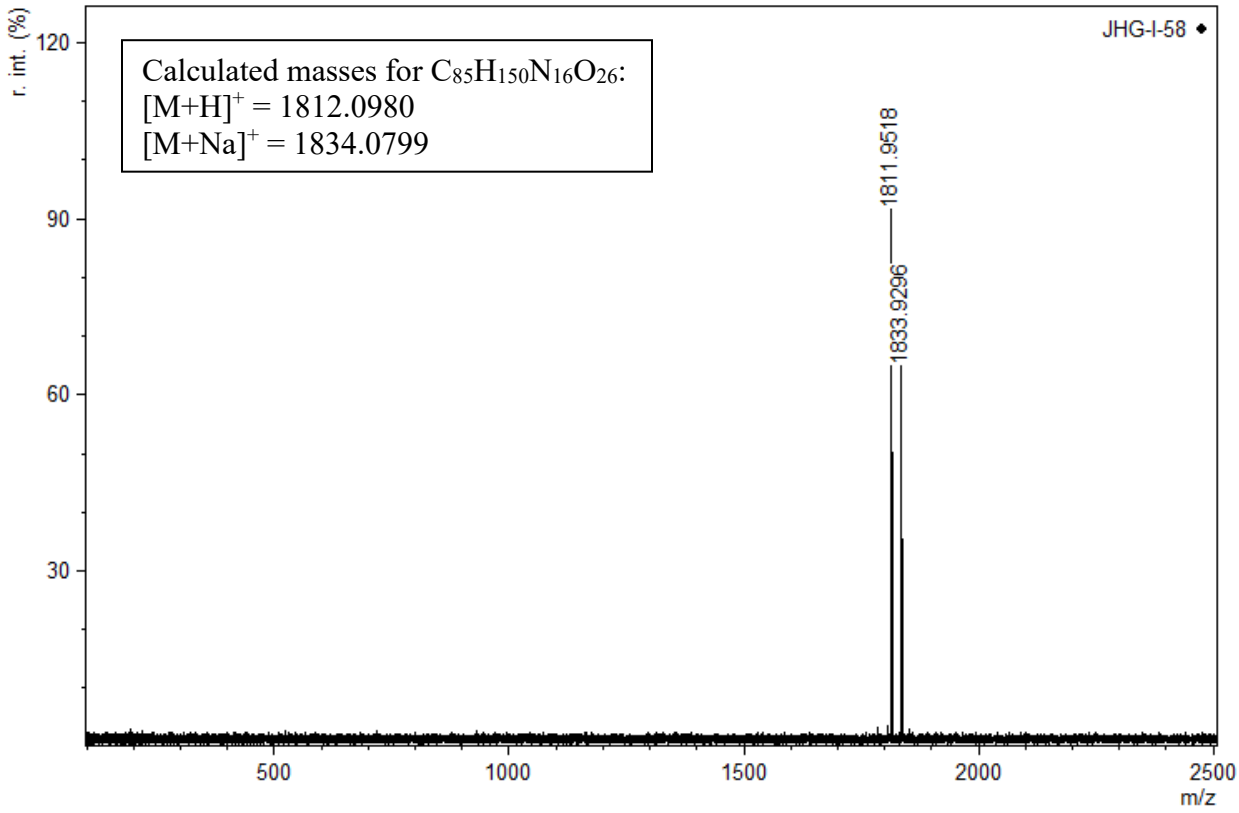
JHG-I-58
Calculated masses for C85H150N16O26:
[M+H]+ = 1812.0980
[M+Na]+ = 1834.0799
r. int. (%)
120
90
60
30
1811.9518
1833.9296
500
1000
1500
2000
2500
m/z

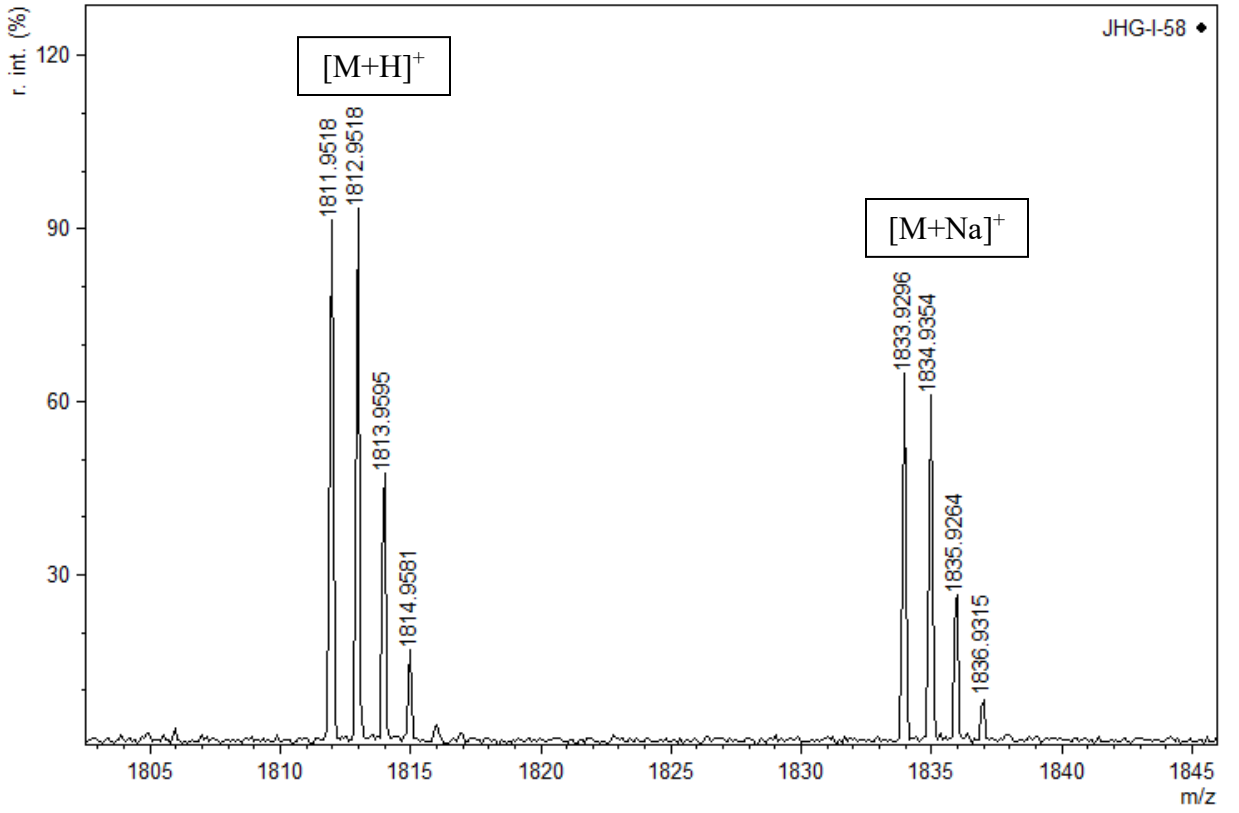
JHG-I-58
[M+H]+
[M+Na]+
r. int. (%)
120
90
60
30
1811.9518
1812.9518
1813.9595
1814.9581
1833.9296
1834.9354
1835.9264
1836.9315
1805
1810
1815
1820
1825
1830
1835
1840
1845
m/z

References for Chapter II

[1] Ling, L. L.; Schneider, T.; Peoples, A. J.; Spoering, A. L.; Engels, I.; Conlon, B. P.; Mueller, A.; Schäberle, T. F.; Hughes, D. E.; Epstein, S.; et al. A New Antibiotic Kills Pathogens without Detectable Resistance. *Nature* **2015**, *517* (7535), 455–459.

[2] Homma, T.; Nuxoll, A.; Gandt, A. B.; Ebner, P.; Engels, I.; Schneider, T.; Götz, F.; Lewis, K.; Conlon, B. P. Dual Targeting of Cell Wall Precursors by Teixobactin Leads to Cell Lysis. *Antimicrob. Agents Chemother.* **2016**, *60* (11), 6510–6517.

[3] Breukink, E.; de Kruijff, B. Lipid II as a Target for Antibiotics. *Nat. Rev. Drug Discov.* **2006**, *5*, 321–323.

[4] de Kruijff, B.; van Dam, V.; Breukink, E. Lipid II: A Central Component in Bacterial Cell Wall Synthesis and a Target for Antibiotics. *Prostaglandins Leukot. Essent. Fat. Acids* **2008**, *79* (3–5), 117–121.

[5] Lloyd, D. G.; Schofield, B. J.; Goddard, M. R.; Taylor, E. J. De Novo Resistance to Arg 10 - Teixobactin Occurs Slowly and Is Costly. *Antimicrob Agents Chemother* **2020**, 65 (1), e01152-20. DOI: 10.1128/AAC.01152-20

[6] Yang, H.; Chen, K. H.; Nowick, J. S. Elucidation of the Teixobactin Pharmacophore. *ACS Chem. Biol.* **2016**, *11* (7), 1823–1826.

[7] Abdel Monaim, S. A. H.; Jad, Y. E.; Ramchuran, E. J.; El-Faham, A.; Govender, T.; Kruger, H. G.; de la Torre, B. G.; Albericio, F. Lysine Scanning of Arg_{10}-Teixobactin: Deciphering the Role of Hydrophobic and Hydrophilic Residues. *ACS Omega* **2016**, *1* (6), 1262–1265.

[8] Chen, K. H.; Le, S. P.; Han, X.; Frias, J. M.; Nowick, J. S. Alanine Scan Reveals Modifiable Residues in Teixobactin. *Chem. Commun.* **2017**, *53* (82), 11357–11359.

[9] Yang, H.; Wierzbicki, M.; Du Bois, D. R.; Nowick, J. S. X-Ray Crystallographic Structure of a Teixobactin Derivative Reveals Amyloid-like Assembly. *J. Am. Chem. Soc.* **2018**, *140* (43), 14028–14032.

[10] Li, W.; Zhan, P.; De Clercq, E.; Lou, H.; Liu, X. Current Drug Research on PEGylation with Small Molecular Agents. *Prog. Polym. Sci.* **2013**, *3–4*, 421–444.

[11] Hamidi, M.; Azadi, A.; Rafiei, P. Pharmacokinetic Consequences of Pegylation. *Drug Deliv.* **2006**, *13* (6), 399–409.

[12] Brunetti, J.; Falciani, C.; Roscia, G.; Pollini, S.; Bindi, S.; Scali, S.; Arrieta, U. C.; Gomez-Vallejo, V.; Quercini, L.; Ibba, E.; et al. In Vitro and in Vivo Efficacy, Toxicity, Bio-Distribution and Resistance Selection of a Novel Antibacterial Drug Candidate. *Sci. Rep.* **2016**, *6*, 26077.

[13] Benincasa, M.; Zahariev, S.; Pelillo, C.; Milan, A.; Gennaro, R.; Scocchi, M. PEGylation of the Peptide Bac7(1-35) Reduces Renal Clearance While Retaining Antibacterial Activity and Bacterial Cell Penetration Capacity. *Eur. J. Med. Chem.* **2015**, *95*, 210–219.

[14] Morris, C. J.; Beck, K.; Fox, M. A.; Ulaeto, D.; Clark, G. C.; Gumbleton, M. Pegylation of Antimicrobial Peptides Maintains the Active Peptide Conformation, Model Membrane Interactions, and Antimicrobial Activity While Improving Lung Tissue Biocompatibility Following Airway Delivery. *Antimicrob. Agents Chemother.* **2012**, *56* (6), 3298–3308.

[15] Burkoth, T. S.; Benzinger, T. L. S.; Jones, D. N. M.; Hallenga, K.; Meredith, S. C.; Lynn, D. G. C-Terminal PEG Blocks the Irreversible Step in β-Amyloid(10-35) Fibrillogenesis. *J. Am. Chem. Soc.* **1998**, *120* (30), 7655–7656.

[16] Shukla, R.; Medeiros-Silva, J.; Parmar, A.; Vermeulen, B. J. A.; Das, S.; Paioni, A. L.; Jekhmane, S.; Lorent, J.; Bonvin, A. M. J. J.; Baldus, M.; Lelli, M.; Veldhuizen, E. J. A.; Breukink, E.; Singh, I.; Weingarth, M. Mode of Action of Teixobactins in Cellular Membranes. *Nat Commun* **2020**, *11* (1), 2848. DOI: 10.1038/s41467-020-16600-2

[17] Shukla, R.; Lavore, F.; Maity, S.; Derks, M. G. N.; Jones, C. R.; Vermeulen, B. J. A.; Melcrová, A.; Morris, M. A.; Becker, L. M.; Wang, X.; Kumar, R.; Medeiros-Silva, J.; Van Beekveld, R. A. M.; Bonvin, A. M. J. J.; Lorent, J. H.; Lelli, M.; Nowick, J. S.; MacGillavry, H. D.; Peoples, A. J.; Spoering, A. L.; Ling, L. L.; Hughes, D. E.; Roos, W. H.; Breukink, E.; Lewis, K.; Weingarth, M. Teixobactin Kills Bacteria by a Two-Pronged Attack on the Cell Envelope. *Nature* **2022**, *608* (7922), 390–396. DOI: 10.1038/s41586-022-05019-y

[18] Morris, M. A.; Malek, M.; Hashemian, M. H.; Nguyen, B. T.; Manuse, S.; Lewis, K.; Nowick, J. S. A Fluorescent Teixobactin Analogue. *ACS Chem. Biol.* **2020**, *15* (5), 1222–1231. DOI: 10.1021/acschembio.9b00908

CHAPTER III: Supramolecular Antibiotics Inspired by Teixobactin*

Abstract

The unusual D-L-L-D-D-L-L pattern of stereochemistry in residues 1–7 of the peptide antibiotic teixobactin is critical to its extraordinary antibiotic activity, creating an unusual amphiphilic β-sheetlike structure that is essential to its mechanism of action. Following the conclusions made in Chapter II, I sought to engineer new antibiotics that take advantage of this unique mechanism of action rather than create analogues with reduced propensity to aggregate. I approached this goal through two routes, which I term "bottom-up" and "top-down" design. Using "bottom-up" design, I sought to replace the three D-amino acids with L-amino acids while maintaining amphiphilicity. I find that swapping residues D-Gln_4 and D-*allo*-Ile_5 permits introduction of L-stereochemistry with retention of antibiotic activity. Nevertheless, modifying the *N*-terminal stereochemistry results in loss of antibiotic activity. Using "top-down" design, I sought to replace residues 1–7 with archetypal, amyloid-forming, all-L, antiparallel β-sheet forming sequences, such as that found in the Aβ peptide. The synthesis and purification of these analogues was similarly difficult to the previously described PEGylated analogues, and while a small number of these "chimeric" teixobactin peptides have antibiotic activity, this activity is modest compared to both teixobactin and the teixobactin swapmers.

* Portions of this chapter have been submitted to an academic journal for publication as of 2024-08-02. The section pertaining to teixobactin "swapmers" is adapted or taken verbatim from the submitted manuscript. Ana-Teresa Mendoza contributed to the peptide synthesis of swapmer analogues. Prof. James Nowick participated in writing and editing the submitted manuscript.

Introduction

In the current study, I divide my approaches to preparing supramolecular antibiotics inspired by, but structurally dissimilar to, teixobactin into two categories: "bottom-up" design and "top-down" design. By "bottom-up" design, I mean a strategy in which I design peptides that emulate the supramolecular assembly of teixobactin through only small and directed changes to the linear peptide tail. This design resulted in teixobactin "swapmers." By "top-down" design, I mean a strategy in which I apply only the macrolactone ring of teixobactin to non-teixobactin linear tails which are observed to natively form antiparallel β-sheets, such as the Aβ peptide. This design resulted in "chimeric" teixobactin analogues.

Teixobactin achieves its remarkable activity through the unique pattern of D-L-L-D-D-L-L stereochemistry in amino acid residues 1–7. [1,2,3] Teixobactin comprises a macrolactone ring (residues 8–11) and a linear tail (residues 1–7); the ring binds the pyrophosphate anion of lipid II and related bacterial cell wall precursor molecules, and the tail forms an amphiphilic β-strand which induces β-sheet assembly (Figure 3.1). The pattern of hydrophobic and hydrophilic amino acid side chains works in concert with the alternating D and L backbone stereochemistry to give rise to the amphiphilic β-strand, and the avidity conferred by this supramolecular assembly contributes to high antibiotic activity.

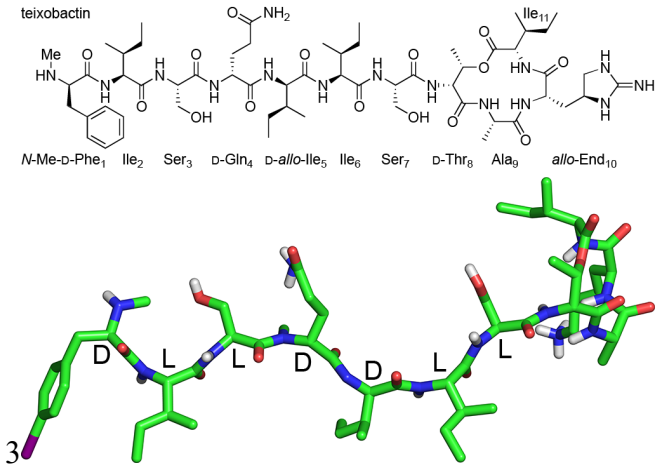

Figure 3.1. Teixobactin structure and X-ray crystallographic structure of a teixobactin analogue (N-Me-D-Phe$^{I}_{1}$,N-Me-D-Gln$_4$,Lys$_{10}$-teixobactin, PDB 6E002). The stereochemistry in each amino acid residue 1–7 is indicated.

Previous structure-activity relationship studies have shown that teixobactin does not tolerate stereochemical modifications to the linear tail. Mutating *N*-Me-D-Phe$_1$, D-Gln$_4$, or D-*allo*-Ile$_5$ to their respective L-amino acids results in loss of antibiotic activity.[4,5,6,7] The stereochemistry of these residues is critical, because they enable the tail to adopt an unusual β-strandlike conformation. In a β-strand with all-L stereochemistry, the side chains are arranged down-up-down-up-down-up-down (Figure 3.2A). In teixobactin, the stereochemical pattern is instead down-down-up-up-down-down-up (Figure 3.2B). This pattern, coupled with the arrangement of hydrophobic and hydrophilic amino acids, gives rise to the amphiphilicity of the teixobactin tail.

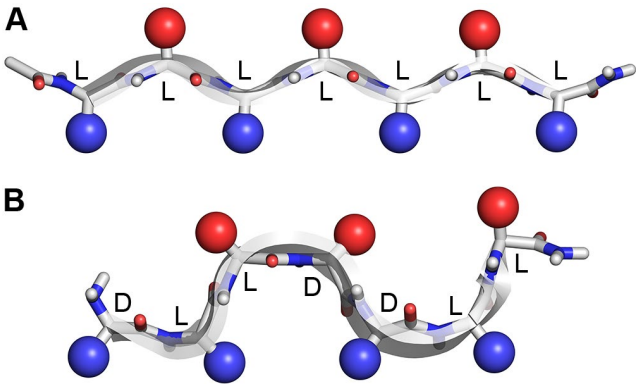

Figure 3.2. Cartoon representations of (A) an L-amino acid β-strand and (B) a teixobactin β-strand. Polar and nonpolar residues are shown as red and blue spheres, respectively. The cartoon representation in A is an idealized β-strand, and the cartoon representation in B is adapted from PDB 6PSL.[8]

In carrying out SAR studies of teixobactin, our group observed that teixobactin and analogues with good antibiotic activity form gels in aqueous buffer and culture media, while analogues with poor activity do not.[9] Upon further study, our group discovered that gel-forming analogues behave like amyloidogenic peptides, exhibiting a lag time followed by the onset of fluorescence in a thioflavin T (ThT) fluorescence assay (Figure 3.3A).[2] The gels are composed of

fibrils that can be observed by transmission electron microscopy (TEM) (Figure 3.3B). Through X-ray crystallography, our group elucidated the structure of a teixobactin analogue and observed the formation of an amyloid-like assembly, consisting of a double helix of β-sheet fibrils bound to sulfate anions (Figure 3.3C). These observations suggest that amyloid-like assembly of teixobactin is directly related to its antibiotic activity, making teixobactin an "supramolecular antibiotic."

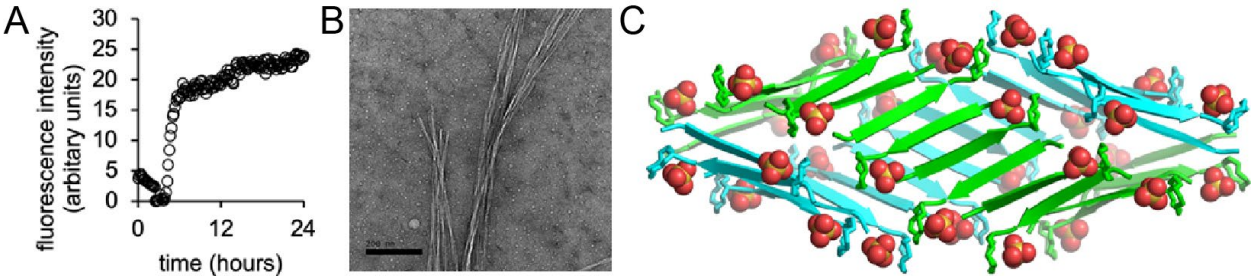

Figure 3.3. Amyloid-like properties of teixobactin. (A) TEM image of teixobactin fibrils, ca. 8–10 nm in diameter. (B) ThT fluorescence assay of teixobactin. (C) X-ray crystallographic structure of a double helix of β-sheet fibrils formed by a teixobactin analogue (PDB 6E00). Each figure reproduced with permission from Yang et al. *J. Am. Chem. Soc.* **2018**, *140* (43), 14028–14032.[2]

Results and Discussion

Teixobactin "Swapmers"

In the current study, I ask whether I can alter the backbone stereochemistry of teixobactin while retaining antibiotic activity by concurrently altering both the stereochemistry and the pattern of hydrophobic and hydrophilic residues of its linear tail. Of the three D-amino acids in the tail, D-Gln$_4$ and D-*allo*-Ile$_5$ are adjacent to one another and have opposite philicity. I hypothesized that pairwise swapping of D-Gln$_4$ and D-*allo*-Ile$_5$ to L-Ile$_4$ and L-Gln$_5$ would preserve the amphiphilicity of the resulting β-strand. The resulting "swapmer" has L stereochemistry in each tail residue except the *N*-terminal *N*-Me-D-Phe$_1$. I tested this hypothesis with analogues of teixobactin containing lysine or arginine at position 10, because the native L-*allo*-enduracidine (L-*allo*-End) amino acid is not commercially available.

Although our group has synthesized more than 200 teixobactin derivatives, I was unable to synthesize the swapmer Ile_4,Gln_5,Lys_{10}-teixobactin. In monitoring the solid-phase coupling reactions by LC-MS and analytical HPLC, I observed poor coupling efficiencies, which is a hallmark of aggregation-prone peptides. To address this problem, I employed a strategy that our group has previously used for aggregation-prone peptides: the incorporation of an *O*-acyl linkage to serine.[10,11] This "isoacyl dipeptide" strategy was first introduced by Kiso and coworkers to facilitate the preparation of aggregation-prone peptides.[12] The resulting isopeptides then convert cleanly and rapidly at neutral pH to the corresponding peptides. Our group has previously used this strategy to create prodrugs of teixobactin analogues, which convert to the corresponding teixobactin analogues during the conditions of minimum inhibitory concentration (MIC) assays.[10,11] These prodrugs exhibit comparable or better antibiotic activity in MIC assays. I used this prodrug strategy to prepare, purify, and study Ile_4,Gln_5,[Ile_6-O-Ser_7],Lys_{10}-teixobactin and Ile_4,Gln_5,[Ile_6-O-Ser_7],Arg_{10}-teixobactin. I refer to these compounds as Lys_{10}-swapmer prodrug **3** and Arg_{10}-swapmer prodrug **8**, respectively (Figure 3.3).

Lys$_{10}$-teixobactin **1**

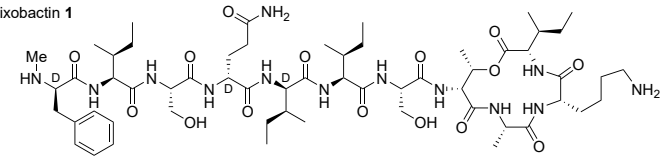

[Ile$_6$-O-Ser$_7$],Lys$_{10}$-teixobactin (Lys$_{10}$-teixobactin prodrug **2**)

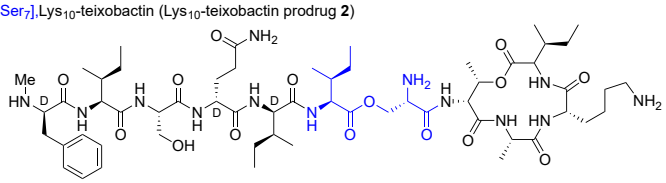

Ile$_4$,Gln$_5$,[Ile$_6$-O-Ser$_7$],Lys$_{10}$-teixobactin (Lys$_{10}$-swapmer prodrug **3**)

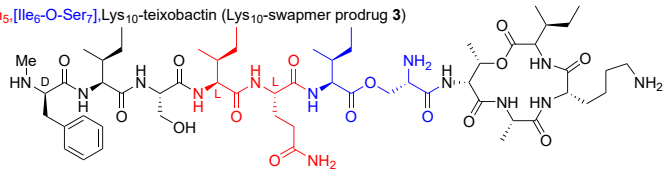

N-Me-L-Phe$_1$,Ile$_4$,Gln$_5$,[Ile$_6$-O-Ser$_7$],Lys$_{10}$-teixobactin (L-tail swapmer **4**)

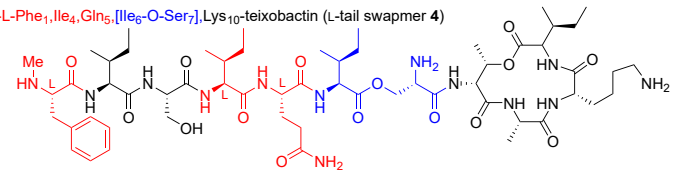

N-Bn-Gly$_1$,Ile$_4$,Gln$_5$,[Ile$_6$-O-Ser$_7$],Lys$_{10}$-teixobactin (peptoid swapmer **5**)

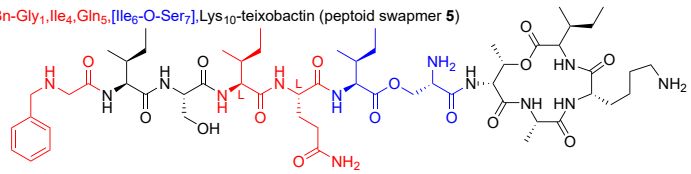

Arg$_{10}$-teixobactin **6**

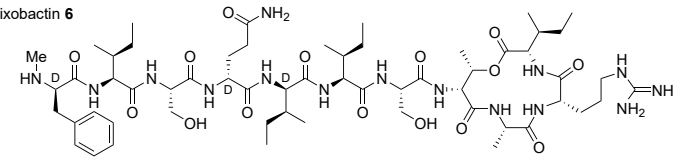

[Ile$_6$-O-Ser$_7$],Arg$_{10}$-teixobactin (Arg$_{10}$-teixobactin prodrug **7**)

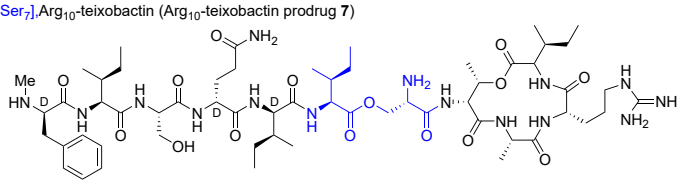

Ile$_4$,Gln$_5$,[Ile$_6$-O-Ser$_7$],Arg$_{10}$-teixobactin (Arg$_{10}$-swapmer prodrug **8**)

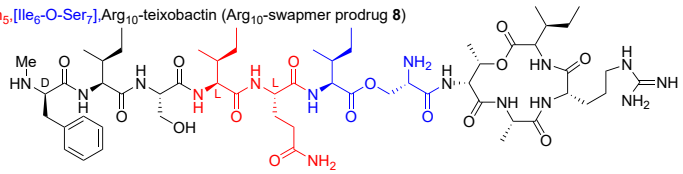

N-Me-Phe$_0$,Gln$_1$,Ile$_4$,Gln$_5$,[Ile$_6$-O-Ser$_7$],Arg$_{10}$-teixobactin (extended-tail swapmer **9**)

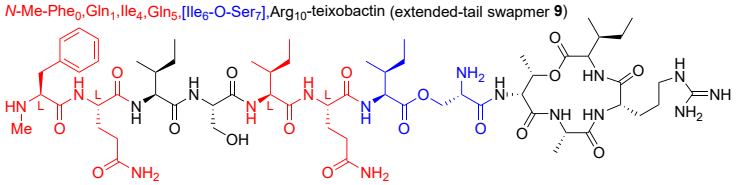

Figure 3.4. Chemical structures of teixobactin analogues prepared and studied. Amino acid stereochemistry is indicated for residues 1, 4, and 5. Stereochemically modified residues are highlighted in red. *O*-acyl dipeptide units are highlighted in blue. We studied prodrugs containing *O*-acyl dipeptide units to overcome problems with solubility.

I determined the MIC values of these teixobactin swapmer prodrugs against the Gram-positive bacteria *Bacillus subtilis*, *Staphylococcus epidermidis*, methicillin-susceptible *Staphylococcus aureus* (MSSA), and methicillin-resistant *Staphylococcus aureus* (MRSA) in a broth microdilution assay as described previously.[10,11] I used the antibiotic vancomycin as a positive control and the Gram-negative bacterium *Escherichia coli* as a negative control. The MIC values for Lys_{10}-teixobactin **1**, Lys_{10}-teixobactin prodrug **2**, Arg_{10}-teixobactin **6**, and Arg_{10}-teixobactin prodrug **7** are shown in Table 3.1 for comparison to the swapmer analogues.

Lys_{10} swapmer prodrug **3** has MIC values between 4–8 μg/mL against the Gram-positive bacteria tested, and Arg_{10} swapmer prodrug **8** has MIC values between 2–4 μg/mL against the Gram-positive bacteria tested (Table 3.1). Compared to the unswapped analogues **1**, **2**, **6**, and **7**, swapmers **3** and **8** have 2–4-fold reduced activity against *S. epidermidis*, MSSA, and MRSA. The activities of Lys_{10}-swapmer prodrug **3** and Arg_{10}-swapmer prodrug **8** support the hypothesis that pairwise swapping of residues 4 and 5 with inversion of stereochemistry in teixobactin preserves antibiotic activity. However, the reduction in activity of these swapmers shows that there is still some loss of activity associated with the incorporation of L amino acids at these positions. *B. subtilis* is exceptionally sensitive to the unswapped teixobactin analogues **1**, **2**, **6**, and **7**, with MICs of ≤0.0625 μg/mL. Although the swapmers **3** and **8** do not reflect this extraordinary activity, their activities against *B. subtilis* are consistent with their activities against the other Gram-positive bacteria.

Table 3.1. MIC values of teixobactin, isobactin, and "swapmer" analogues in μg/mL. MIC assays were performed in the presence of 0.002% polysorbate 80.

	Bacillus subtilis ATCC 6051	*Staphylococcus epidermidis* ATCC 14990	*Staphylococcus aureus* (MSSA) ATCC 29213	*Staphylococcus aureus* (MRSA) ATCC 700698	*Escherichia coli* ATCC 10798
Lys_{10}-teixobactin (**1**)	≤0.0313	1	2	2	>32
[Ile_6-O-Ser_7],Lys_{10}-teixobactin (Lys_{10}-teixobactin prodrug **2**)	≤0.0313	1	2	1–2	>32
Ile_4,Gln_5,[Ile_6-O-Ser_7],Lys_{10}-teixobactin (Lys_{10}-swapmer prodrug **3**)	4	4	8	8	>32
N-Me-L-Phe_1,Ile_4,Gln_5,[Ile_6-O-Ser_7],Lys_{10}-teixobactin (L-tail swapmer **4**)	≥32	>32	>32	>32	>32
N-Bn-Gly_1,Ile_4,Gln_5,[Ile_6-O-Ser_7],Lys_{10}-teixobactin (peptoid swapmer **5**)	32	>32	>32	>32	>32
Arg_{10}-teixobactin (**6**)	≤0.0313	0.5	2	2	>32
[Ile_6-O-Ser_7],Arg_{10}-teixobactin (Arg_{10}-teixobactin prodrug **7**)	0.0625	0.5	2	1	>32
Ile_4,Gln_5,[Ile_6-O-Ser_7],Arg_{10}-teixobactin (Arg_{10}-swapmer prodrug **8**)	2	2	4	4	>32
N-Me-Phe_0,Gln_1,Ile_4,Gln_5,[Ile_6-O-Ser_7],Arg_{10}-teixobactin (extended-tail swapmer prodrug **9**)	>32	>32	>32	>32	>32
vancomycin	0.125–0.25	1–2	1–2	4	>32

To test whether a teixobactin analogue with all-L tail stereochemistry would retain antibiotic activity, I prepared *N*-Me-L-Phe_1,Ile_4,Gln_5,[Ile_6-O-Ser_7],Lys_{10}-teixobactin (L-tail swapmer **4**), in which the only remaining D-amino acid in the tail, *N*-Me-D-Phe_1, is instead L. While this design does not preserve amphiphilicity in the idealized β-strand, I envisioned that the

flexibility of the *N*-terminal residue might still allow the peptide to adopt an amphiphilic conformation. Nevertheless, L-tail swapmer **4** is virtually inactive against all bacteria in the concentration range tested. I next hypothesized that removal of stereochemistry at position 1 would allow activity in an analogue with an otherwise all-L tail, and subsequently prepared *N*-Bn-Gly$_1$,Ile$_4$,Gln$_5$,[Ile$_6$-O-Ser$_7$],Lys$_{10}$-teixobactin (peptoid swapmer **5**), in which the *N*-terminal residue is achiral. Peptoid swapmer **5** is only very weakly active against *B. subtilis* and is inactive against all other bacteria tested. These two results indicate that, even in a swapmer analogue with otherwise all-L tail stereochemistry, D stereochemistry at position 1 is necessary for antibiotic activity. Other researchers have reported similar observations in teixobactin analogues that modify the *N*-terminus in this way.[5,7,9]

In a third and final attempt to introduce L-stereochemistry at the *N*-terminus of teixobactin analogues, I prepared a tail-extended analogue. To preserve an *N*-terminal phenylalanine side chain in an idealized, all-L, amphiphilic β-strand, I prepared *N*-Me-Phe$_0$,Gln$_1$,Ile$_4$,Gln$_5$,[Ile$_6$-O-Ser$_7$],Arg$_{10}$-teixobactin (extended-tail swapmer **9**), in which the linear tail is extended by one amino acid residue. I incorporated L-glutamine at position 1 to duplicate the pattern of residues 4 and 5 and incorporated *N*-Me-L-phenylalanine at "position 0" to match the *N*-terminal residue of teixobactin. As with my two preceding attempts to eliminate the D-stereochemistry at position 1, extended-tail swapmer **9** was completely inactive against all bacteria tested. This result indicates that I cannot create an active all-L swapmer in which the *N*-terminal *N*-Me-D-phenylalanine is replaced with an amphiphilic L-L dipeptide unit, and further cements that the *N*-Me-D-Phe$_1$ residue is critical to the antibiotic activity of teixobactin.

"Chimeric" Teixobactin Analogues

In addition to teixobactin swapmers, I sought to engineer new peptide antibiotics that were very structurally dissimilar to teixobactin while utilizing the same mechanism of action to kill Gram-positive bacteria. My initial hypothesis was that teixobactin achieves bacterial killing through (1) supramolecular assembly of the amphiphilic tail, which forms antiparallel β-sheets that then (2) create high avidity for lipid II pyrophosphate by bringing many macrolactone rings into the same assembly (Figure 3.5). While the teixobactin macrolactone has evolved high specificity for lipid II and related bacterial cell wall precursors, I reasoned that the amphiphilic tail could be exchanged for a structurally dissimilar β-sheet-forming peptide sequence while retaining antibiotic activity.

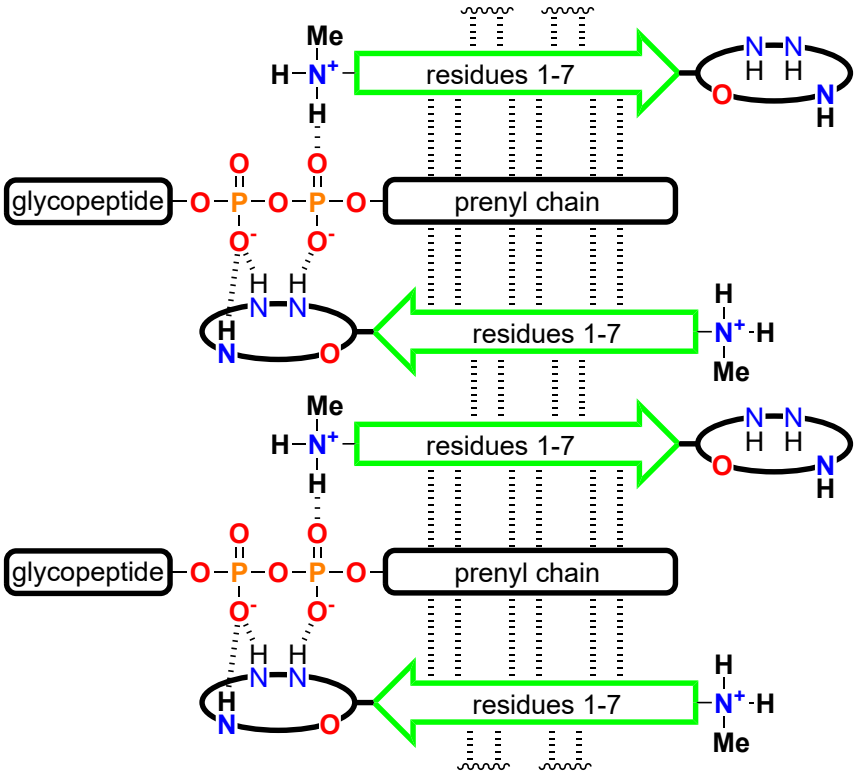

Figure 3.5. Cartoon representation of a supramolecular teixobactin assembly bound to lipid II molecules.

To prepare these "chimeric" teixobactin analogues, I chose the tail sequence MAX1. Schneider and coworkers at the National Cancer Institute (NCI) have developed MAX1 and

many related β-hairpin peptides as biocompatible hydrogels for use in tissue regeneration, delivery of drugs and cells, and as antimicrobial agents.[13,14,15,16,17,18,19] As illustrated in Figure 3.6, MAX1 forms an amyloid-like network of antiparallel β-sheets. The MAX1 peptide — VKVKVKVKV-^{D}PP-TKVKVKVKV — is a β-hairpin composed of two amphipathic nonapeptide β-strands connected by a turn forming unit. I began my studies of MAX1-based supramolecular antibiotics by synthesizing a teixobactin analogue with three valine-lysine repeat units in place of the natural teixobactin tail (Figure 3.7).

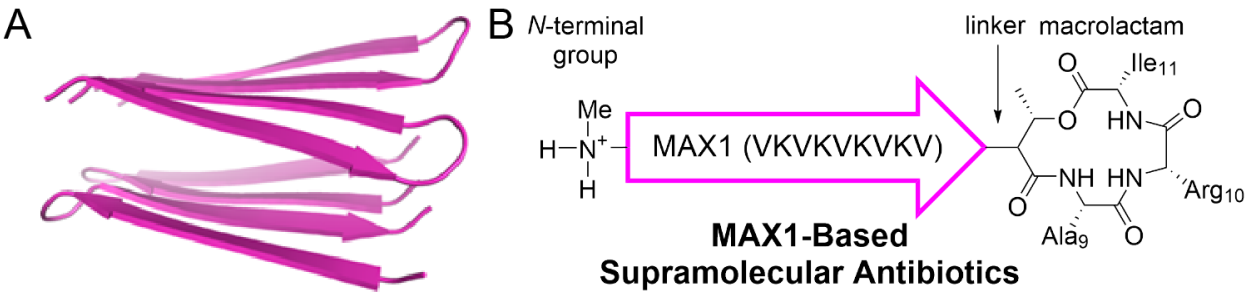

Figure 3.6. Design of MAX1-teixobactin "chimeras." (A) Solid-state NMR structure of MAX1 ((VK)$_4$V-^{D}PP-T(KV)$_4$, PDB 2N1E19). (B) Cartoon representation of teixobactin "chimera" design.

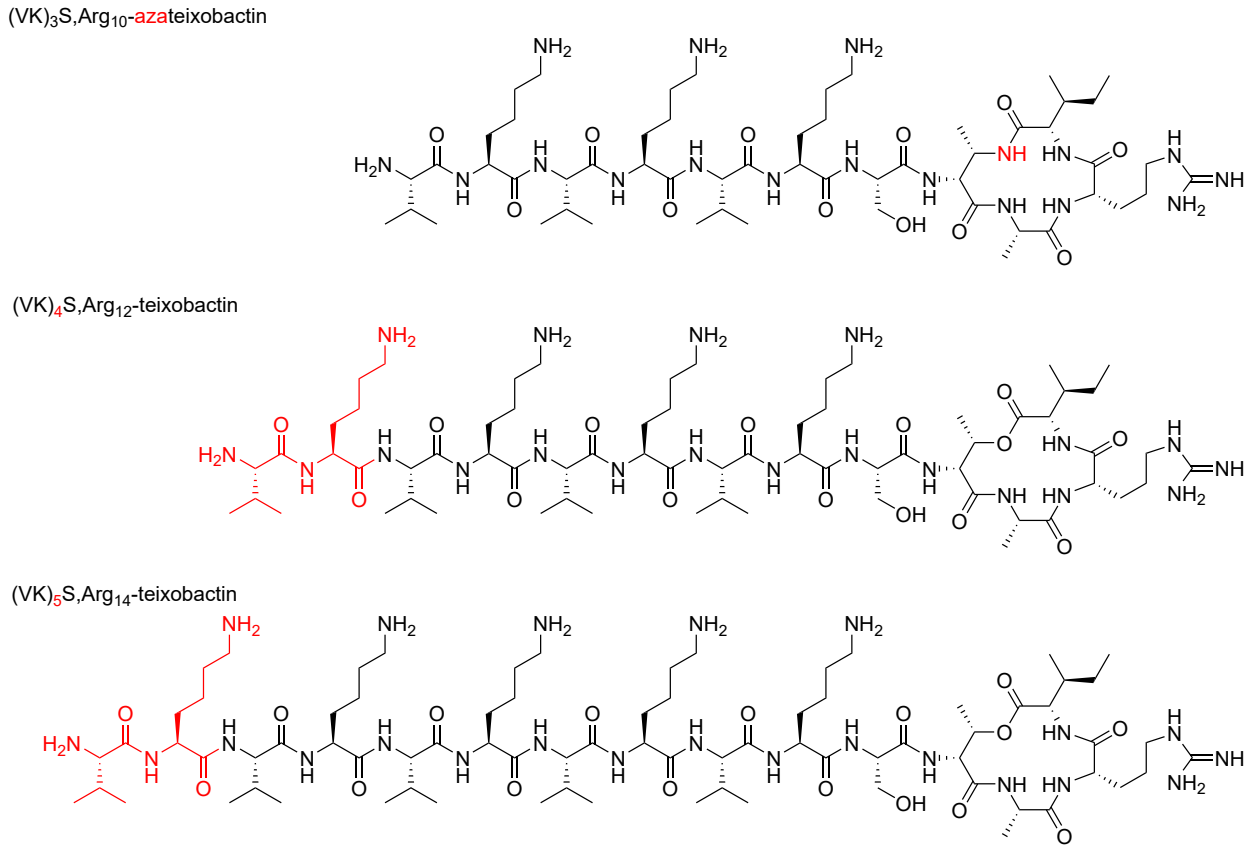

Figure 3.7. MAX1-teixobactin "chimeras" prepared in this study.

In each of the MAX1-teixobactin chimeras prepared, the serine residue adjacent to the macrolactone ring was preserved as a linker between the ring and the tail. In multiple crystallographic structures determined by our group, the side-chain hydroxy group of this serine residue makes an intermolecular hydrogen bond to the amide NH group of the ring alanine.[2,9,20] This hydrogen bond enforces a specific conformation in which the ring is presented on the external face of the supramolecular assembly and able to bind lipid II pyrophosphate.

For the first chimera only, the macrolactone is replaced with a macrolactam. Our group previously demonstrated that macrolactam teixobactin has greater antibiotic activity than macrolactone teixobactin, presumably due to the additional hydrogen bond donor to lipid II

pyrophosphate anion.[5] However, the on-resin synthetic approach for introducing the additional nitrogen atom significantly reduces peptide yields, and so was not pursued in further analogues.

$(VK)_4S,Arg_{12}$-teixobactin and $(VK)_5S,Arg_{14}$-teixobactin were obtained as an inseparable mixture of diastereomers. Similarly for the PEGylated teixobactins prepared in Chapter II, I hypothesize that the diastereomers resulting from epimerization during Ile esterification as less able to be differentiated by reversed-phase preparative HPLC purification techniques.

$(VK)_3S,Arg_{10}$-azateixobactin is completely inactive against all bacteria in the concentration range tested (Table 3.2). $(VK)_4S,Arg_{12}$-teixobactin — with one additional valine-lysine repeat unit, but a macrolactone ring — is similarly inactive. Only $(VK)_5S,Arg_{14}$-teixobactin, with the longest VK-repeat tail, exhibited any antibiotic activity, with an MIC of 16–32 μg/mL against all bacteria tested. Because $(VK)_5S,Arg_{14}$-teixobactin has weak antibiotic activity against the Gram-negative *E. coli*, I hypothesize that this chimeric peptide may have a nonspecific lytic mechanism of action.

Table 3.2. MIC values of MAX1-teixobactin "chimeras" in μg/mL. MIC assays were performed in the presence of 0.002% polysorbate 80.

	Bacillus subtilis ATCC 6051	*Staphylococcus epidermidis* ATCC 14990	*Escherichia coli* ATCC 10798
Arg_{10}-teixobactin	≤0.0313	0.5	>32
$(VK)_3S,Arg_{10}$-azateixobactin	>32	>32	>32
$(VK)_4S,Arg_{12}$-teixobactin	>32	>32	>32
$(VK)_5S,Arg_{14}$-teixobactin	16–32	16	32

Conclusion

The chirality of the peptide tail of teixobactin is remarkably important to its activity. Although stereochemical mutation of individual residues abrogates the activity of teixobactin analogues, pairwise swapping of residues 4 and 5 with inversion of stereochemistry does not. This pairwise swapping of D-Gln_4 and D-*allo*-Ile_5 to L-Ile_4 and L-Gln_5 allows for retention of the critical amphiphilic structure and results in only a 2–4-fold loss in activity. Nevertheless, further

efforts to alter the stereochemistry of the tail, specifically the *N*-terminal *N*-Me-D-phenylalanine residue, did not result in active analogues. A separate project in which the linear tail was exchanged for repeating, β-sheet forming amphiphilic units was also unsuccessful in preparing active analogues. I envision that my exploration of these principles of amphiphilicity in the tail of teixobactin could enable the development of new antibiotics consisting of (1) an all-L or all-D amphiphilic tail that self-assembles through β-sheet interactions and (2) a macrocycle that targets the pyrophosphate group of lipid II and related bacterial cell wall precursors.

Supporting Information for Chapter III

General Information.

Methylene chloride (CH_2Cl_2) was passed through alumina under argon prior to use. Amine-free *N*,*N*-dimethylformamide (DMF) was purchased from Alfa Aesar. Fmoc-D-*allo*-Ile-OH was purchased from Santa Cruz Biotechnology. Boc-Ser(Fmoc-Ile)-OH was purchased from AAPPTec. Fmoc-*N*-Bn-Gly-OH and other protected amino acids were purchased from Chem-Impex. Vancomycin was purchased from Sigma-Aldrich. All peptides were prepared and studied as the trifluoroacetate salts. Peptides were first purified on a Biotage Isolera One flash column chromatography instrument equipped with a Biotage® SfarBio C18 D – Duo 300 Å 20 µm 25 g column. Peptides were then further purified by preparative reversed-phase HPLC on a Shimadzu instrument equipped with an Agilent Zorbax 7 µm 300SB-C18 column (21.2×250 mm). Analytical reversed-phase HPLC was performed on an Agilent 1260 Infinity II instrument equipped with a Phenomonex bioZen PEPTIDE 2.6 um XB-C18 column (150×4.6 mm). LC-MS analysis was performed using a Waters Acuity QDa UPLC/MS. HPLC grade acetonitrile (MeCN) and deionized water (18 MΩ) containing 0.1% trifluoroacetic acid (TFA) were used as solvents for both preparative and analytical reverse-phase HPLC. Deionized water (18 MΩ) was obtained from a ThermoScientific Barnstead GenPure Pro water purification system. Glass solid-phase peptide synthesis vessels with fritted disks and BioRad Polyprep columns were used for solid-phase peptide synthesis. Bacteria were incubated in a Thermo Fisher Scientific MaxQ Shaker 6000.

Peptide Synthesis of Teixobactin Analogues.

I synthesized teixobactin analogues as the trifluoroacetate (TFA) salt by manual solid-phase peptide synthesis of the corresponding linear peptide on 2-chlorotrityl resin, followed by

on-resin esterification, solution-phase cyclization, deprotection, and purification as previously described.[10] A step-by-step procedure is detailed below.

Resin loading. 2-Chlorotrityl chloride resin (300 mg, 1.07 mmol/g, 0.32 mmol total) was swelled with dry CH_2Cl_2 (8 mL) in a Bio-Rad Poly-Prep chromatography column (10 mL) for 30 minutes with gentle rocking. The CH_2Cl_2 was drained from resin, a solution of Fmoc-Lys(Boc)-OH (150 mg, 0.32 mmol) or Fmoc-Arg(Pbf)-OH (208 mg, 0.32 mmol) in 2,4,6-collidine (300 μL) and CH_2Cl_2 (8 mL) was added, and the suspension was gently rocked for 12–16 h. The solution was drained from resin, a mixture of CH_2Cl_2/CH_3OH/*N*,*N*-diisopropylethylamine (DIPEA) (8.5:1:0.5, 10 mL) was immediately added, and the resin was gently rocked for 1 h to cap unreacted 2-chlorotrityl resin sites. The solution was drained from resin, and the resin was washed three times with CH_2Cl_2. Resin loading was quantified as previously described.[21] Briefly, ca. 1.0 mg of dried, loaded resin was transferred to a scintillation vial containing 3.0 mL of 20% (v/v) piperidine/DMF and gently shaken for 10 minutes. The absorbance of the solution was measured at 290 nm to determine the concentration of piperidine-dibenzofulvene (Fmoc) adduct, which is proportional to the amount of loaded amino acid. Typical resin loadings of 0.43–0.56 mmol/g were observed for lysine, and typical resin loadings of 0.11–0.16 mmol/g were observed for arginine.

Linear peptide synthesis. The loaded resin was suspended in dry DMF and transferred to a solid-phase peptide synthesis vessel. Residues 9 through 1 were manually coupled using Fmoc-protected amino acid building blocks. Note the following: For residue 8, side-chain unprotected Fmoc-D-Thr-OH is used to enable the later esterification step in macrolactone analogues (for macrolactam analogues, Fmoc-D-*allo*-Thr-OH is used to enable on-resin azide substitution — see *Alloc protection*, *Mesylation*, *S_N2 with NaN_3*, and *Alloc deprotection* below); for residue 1,

Boc-*N*-Me-D-Phe-OH or Boc-Val-OH is used to prevent cross-reactivity during the cyclization step; for "swapmer" analogues, Boc-Ser(Fmoc-Ile)-OH is used in place of Fmoc-Ser(Boc)-OH and Fmoc-Ile-OH when coupling residues 7 and 6; for MAX1-teixobactin "chimera" analogues, Fmoc-Lys(Boc)-OH and Fmoc-Val-OH are used in place of residues 1–7 as indicated. For all other amino acid couplings, Fmoc-protected amino acids with orthogonal side-chain protecting groups are used. Amino acids were coupled through the following cycles: *i.* Fmoc-deprotection with 20% (v/v) piperidine in DMF (5 mL) for 20 min, *ii.* washing with DMF (3×5 mL), *iii.* coupling of the amino acid (4 equiv.) with HCTU (4 equiv.) in 20% (v/v) 2,4,6-collidine in DMF (5 mL) for 30 min (60 min for L-to-D or D-to-L couplings, or when coupling to β-branched amino acids), and *iv.* washing with DMF (3×5 mL).

(The *Alloc protection*, *Mesylation*, *S_N2 with NaN_3*, and *Alloc deprotection* steps were performed only for $(VK)_3S$,Arg_{10}-azateixobactin, following procedure established by our group for preparing macrolactam teixobactin analogues.[8])

Alloc protection. Following Fmoc-D-*allo*-Thr-OH coupling, the resin was transferred to a Poly-Prep column with dry DMF, and the solution was drained with a flow of nitrogen. The resin was washed with dry CH_2Cl_2 (3×5 mL). To the resin in the PolyPrep column, dry CH_2Cl_2 (5 mL), DIPEA (38 μL, 0.23 mmol, 1.5 equiv), and allyl chloroformate (23 μL, 0.23 mmol, 1.5 equiv) were added sequentially. The column was then capped and rocked for 1 h. The resin was washed with dry CH_2Cl_2 (3×5 mL).

Mesylation. Dry CH_2Cl_2 (6 mL) was added to the resin in the PolyPrep column. The column was then capped and rocked in a cold room (4 °C) for 15 min. DIPEA (254 μL, 1.5 mmol, 10 equiv) was added, and the mixture was rocked in a cold room (4 °C) for an additional 15 min. Methanesulfonyl chloride (113 μL, 1.5 mmol, 10 equiv) was added, and mixture was

rocked in a cold room (4 °C) for an additional 15 min. The resin was then washed with dry CH_2Cl_2 (3x) and then with dry DMF (3×5 mL). The resin was transferred to the hand coupling vessel.

S_N2 with NaN_3. NaN_3 (474 mg, 7.5 mmol, 50 equiv) was added to the resin in a jacketed hand coupling vessel. Dry DMF (1 mL) and 15-crown-5 (1 mL) were added to the hand coupling vessel. (Not all of the NaN_3 dissolves in the solvent mixture.) A continuous water flow at 55 °C was flowed through the jacketed hand coupling vessel to provide heating. Using a gentle nitrogen flow, the mixture was bubbled for 12 h at 55 °C. The resin was washed with 10 mL of 20% H_2O in THF (3×5 mL) to remove excess NaN_3. The resin was transferred to a Poly-Prep column with dry DMF and then washed with dry CH_2Cl_2 (3×5 mL).

Alloc deprotection. A mixture of CH_2Cl_2 (5 mL), $(Ph_3P)_4Pd$ (16.9 mg, 0.015 mmol, 0.1 equiv) and $PhSiH_3$ (360 µL, 3 mmol, 20 equiv) was added to the resin in the Poly-Prep column, and the column was rocked for 30 min. The resin was washed with dry CH_2Cl_2 (3×5 mL) and then with dry DMF (3×5 mL) and transferred to a hand coupling vessel. Following Alloc deprotection, amino acid coupling proceeded as described in *Linear peptide synthesis*.

Ile esterification. The resin was drained, washed with CH_2Cl_2 (3×5 mL), and transferred to a clean Bio-Rad Poly-Prep chromatography column. In a test tube, Fmoc-Ile-OH (10 equiv.) and diisopropylcarbodiimide (10 equiv.) were dissolved in CH_2Cl_2 (5 mL). The resulting solution was filtered through a 0.20-µm nylon filter, and 4-dimethylaminopyridine (1 equiv.) was added to the filtrate. The resulting solution was transferred to the resin and gently rocked for 1 h. The solution was drained and then washed with CH_2Cl_2 (3×5 mL) and DMF (3×5 mL).

Fmoc deprotection of Ile_{11} and cleavage of the linear peptide from chlorotrityl resin. The Fmoc protecting group on Ile_{11} was removed by adding 20% (v/v) piperidine in DMF and gently

rocking for 30 min. The solution was drained and then washed with DMF (3×5 mL) and CH_2Cl_2 (3×5 mL). The linear peptide was cleaved from the resin by rocking the resin in a solution of 20% (v/v) 1,1,1,3,3,3-hexafluoroisopropanol (HFIP) in CH_2Cl_2 (10 mL) for 1 h. Upon addition of the HFIP solution, the resin beads and solution change color from yellow and clear, respectively, to red. The suspension was filtered, and the filtrate was collected in a 250-mL round-bottomed flask. The resin was washed with additional HFIP solution (10 mL) for 30 min and then filtered into the same flask. The combined filtrates were concentrated by rotary evaporation and further dried by vacuum pump to afford the crude protected linear peptide, which was cyclized without further purification.

Cyclization of the linear peptide. The crude protected linear peptide was dissolved in dry DMF (125 mL). HOAt (6 equiv.) and HATU (6 equiv.) were dissolved in DMF (8 mL) in a test tube. The HOAt/HATU solution was added to the flask containing the dissolved peptide, and the mixture was stirred under nitrogen for 30 min. Diisopropylethylamine (300 μL) was added to the flask and the mixture was stirred under nitrogen for an additional 16–20 h. The reaction mixture was concentrated by rotary evaporation and further dried by vacuum pump to afford the crude protected cyclized peptide, which was immediately subjected to global deprotection.

Global deprotection and ether precipitation. The protected cyclic peptide was dissolved in TFA:triisopropylsilane (TIPS):H_2O (9:0.5:0.5, 10 mL) in a 250-mL round-bottomed flask equipped with a stir bar, and the solution was stirred under nitrogen for 1 h. During the 1 h deprotection, two 50-mL conical tubes containing 40 mL each of dry Et_2O were chilled on ice. After the 1 h deprotection, the peptide solution was split between the two conical tubes of chilled Et_2O. The tubes were then centrifuged at 600×*g* for 10 min and decanted. The pelleted peptides were dried under nitrogen.

Reversed-phase HPLC purifications. The peptide was dissolved in 20% (v/v) CH_3CN in H_2O (5 mL) containing 0.1% TFA, injected on the Biotage instrument (General Information) at 20% CH_3CN, and eluted with a gradient of 20%–40% CH_3CN over 15 min.. The fractions containing the desired peptide as determined by LC-MS were concentrated by rotary evaporation, diluted in 20% (v/v) CH_3CN in H_2O (5 mL) containing 0.1% TFA, injected on the Shimadzu instrument (General Information) at 20% CH_3CN, and eluted with a gradient of 20%–40% CH_3CN over 80 min. The collected fractions were analyzed by analytical HPLC and LC-MS, and the pure fractions were concentrated by rotary evaporation and lyophilized.

Minimum Inhibitory Concentration (MIC) Assays.

I performed minimum inhibitory concentration (MIC) assays as previously described.[10] A concise procedure is detailed below.

Preparing peptide stock solutions. Stock solutions of teixobactin analogues were prepared gravimetrically by dissolving an appropriate amount of peptide to 20 mg/mL in sterile DMSO. The stock solutions were stored at -20 °C for subsequent experiments.

Preparing bacterial cultures. Bacillus subtilis (ATCC 6051), *Staphylococcus epidermidis* (ATCC 14990), methicillin-susceptible *Staphylococcus aureus* (MSSA) (ATCC 29213), and *Escherichia coli* (ATCC 10798) were cultured from glycerol stocks in Mueller-Hinton broth containing 0.002% polysorbate 80 overnight in a shaking incubator at 37 °C. Methicillin-resistant *Staphylococcus aureus* (MRSA) (ATCC 700698) was cultured from a glycerol stock in brain hearth infusion broth containing 0.002% polysorbate 80 overnight in a shaking incubator at 37 °C. After overnight incubation, each culture was diluted with the appropriate media (containing 0.002% polysorbate 80) to 1×10^6 colony-forming units (CFU)/mL as previously described.[9,21] Briefly, we have previously determined the CFU/mL for each bacterium at OD_{600} =

0.075 for 200 µL of bacterial culture in a 96-well plate. The OD_{600} of each overnight culture was determined, then each culture was diluted to OD_{600} = 0.075. Cultures were further diluted to achieve 1×10^6 CFU/mL solutions.

96-well plate setup. Aliquots of the 20 mg/mL peptide stock solutions were diluted to make a 64 µg/mL solution in Mueller-Hinton broth containing 0.002% polysorbate 80 and a 64 µg/mL solution in brain heart infusion broth containing 0.002% polysorbate 80. The solutions were mixed by pipetting to ensure homogeneity. A 200-uL aliquot of a 64 µg/mL solution was transferred to a 96-well plate. Two-fold serial dilutions were made with media containing 0.002% polysorbate 80 across the 96-well plate to achieve a final volume of 100 µL in each well (initial concentrations ranging from 64 µg/mL to 0.0625 µg/mL). A 100-uL aliquot of a 1×10^6 CFU/mL bacterial solution was added to each well in the series, resulting in final bacterial concentrations of 5×10^5 CFU/mL in each well. As 100 uL of bacteria were added to each well, the concentration of peptide was also diluted twofold (final concentrations ranging from 32 µg/mL to 0.03125 µg/mL). Each plate was covered with a lid and incubated at 37 °C for 16 h. The optical density measurements were measured at 600 nm using a 96-well UV-vis plate reader (MultiSkan GO, Thermo Scientific). The MIC values were taken as the lowest concentration that had no bacterial growth. MIC assays for each compound were run in triplicate to ensure reproducibility.

Peptide Characterization Data

Solvent blank

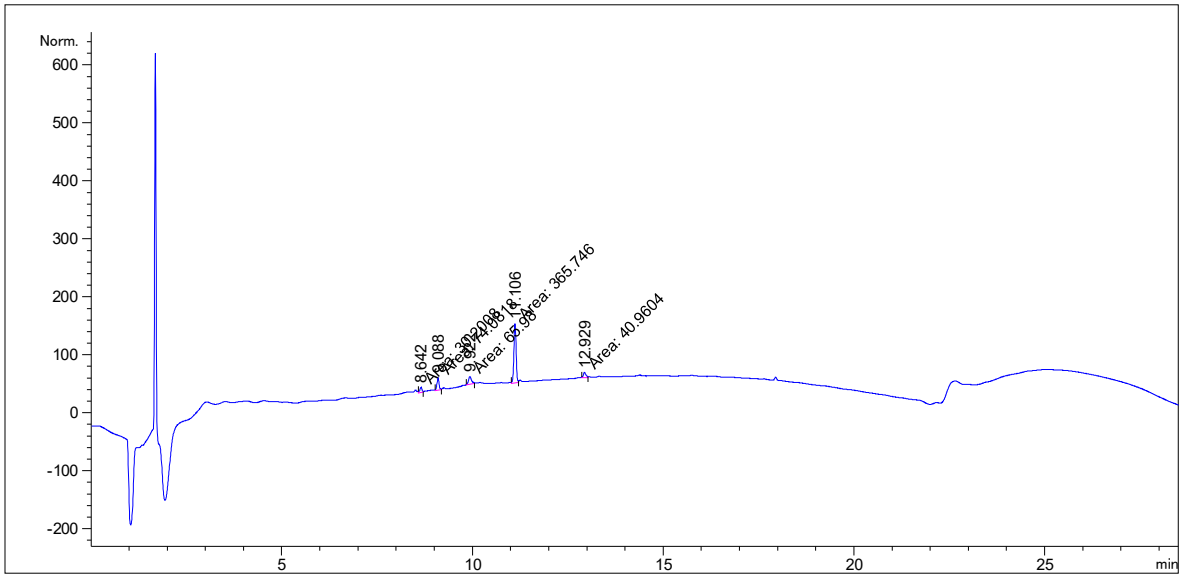

Peak #	RetTime [min]	Type	Width [min]	Area [mAU*s]	Height [mAU]	Area %	
1	8.642	MM	0.0629	30.20078	8.00599	5.234	4
2	9.088	MM	0.0628	74.08182	19.65947	12.839	8
3	9.922	MM	0.0933	65.97999	11.78372	11.435	6
4	11.106	MM	0.0656	365.74561	92.94729	63.390	9
5	12.929	MM	0.0825	40.96040	8.27779	7.099	2
Totals :				576.96859	140.67426		

Lys$_{10}$*-teixobactin* ***1***

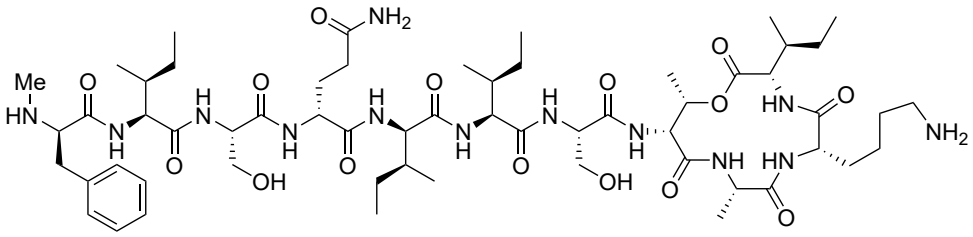

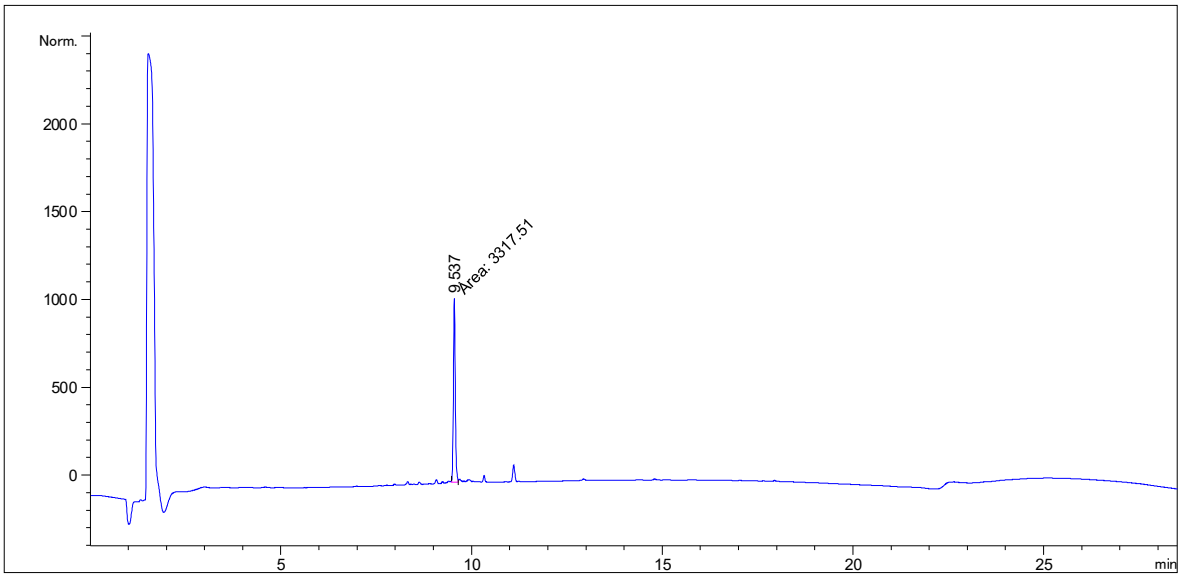

Peak #	RetTime [min]	Type	Width [min]	Area [mAU*s]	Height [mAU]	Area %
1	9.537	MM	0.0583	3317.50903	948.15326	100.000
Totals :				3317.50903	948.15326	

Calculated mass for Lys_{10}-teixobactin: 1215.7227
$[M+H]^+$ = 1216.7300
$[M+2H]^{2+}$ = 608.8689

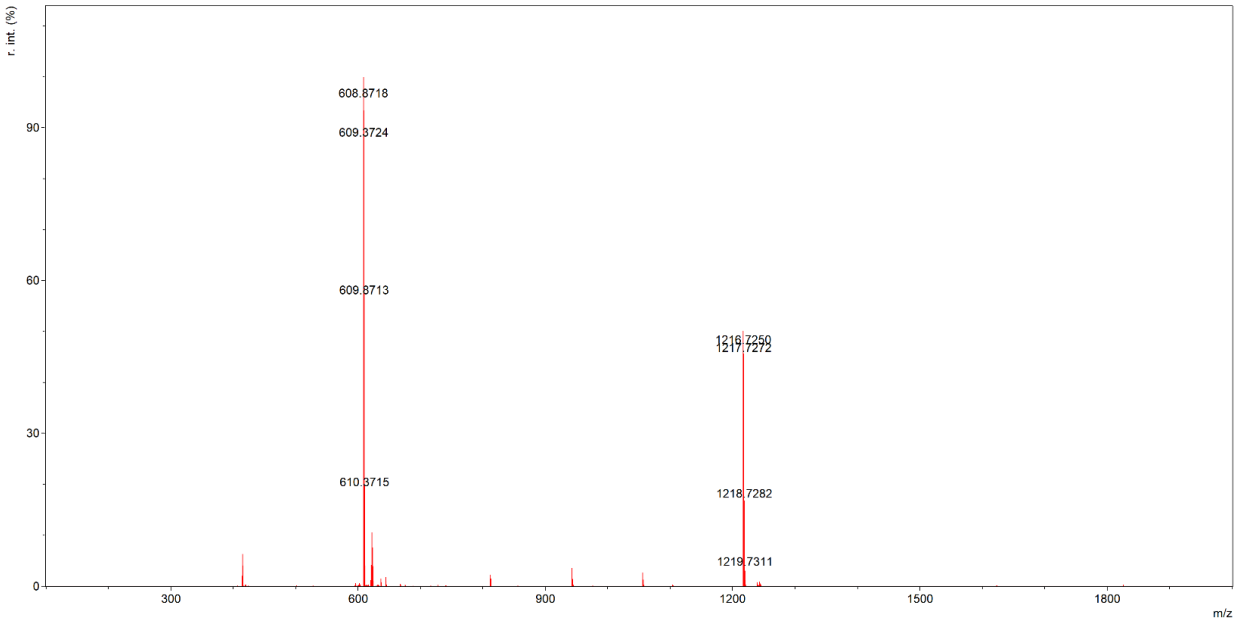

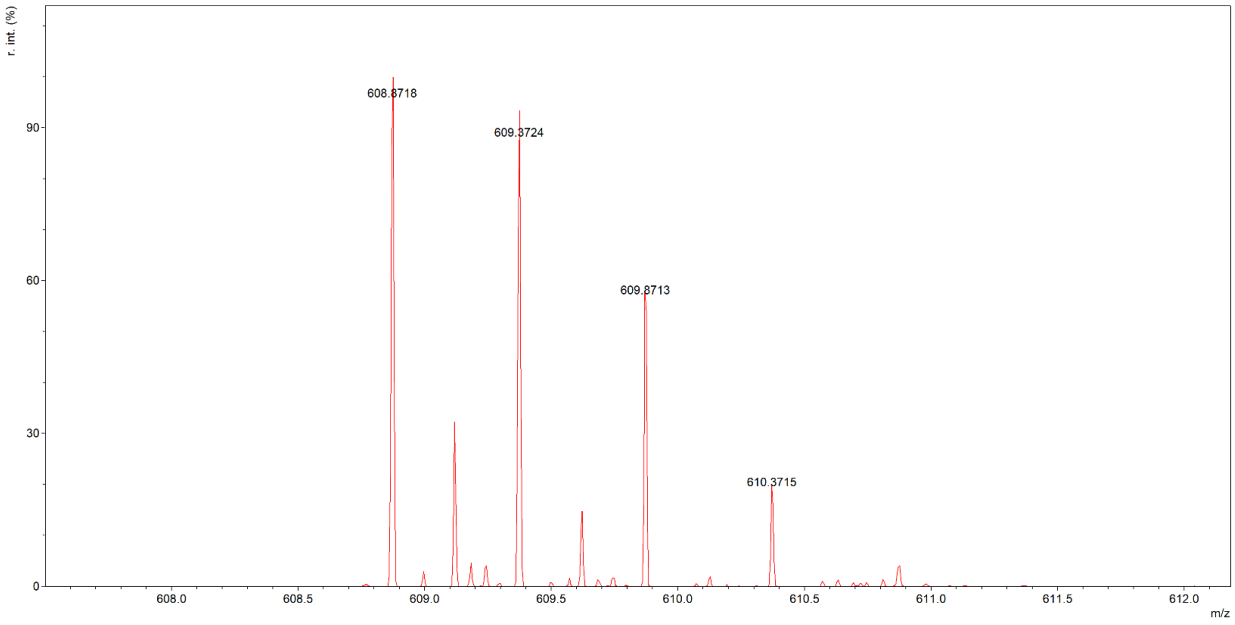

[Ile$_6$-O-Ser$_7$],Lys$_{10}$-teixobactin ***2***

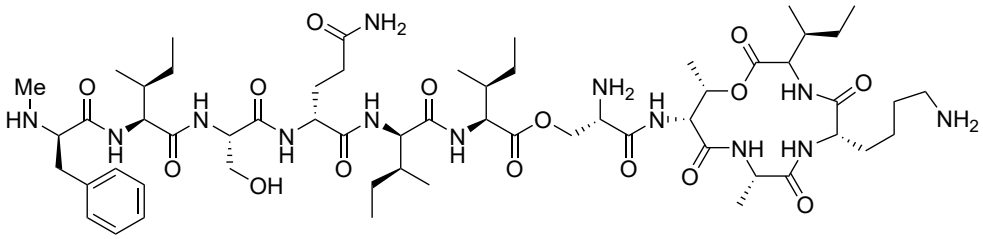

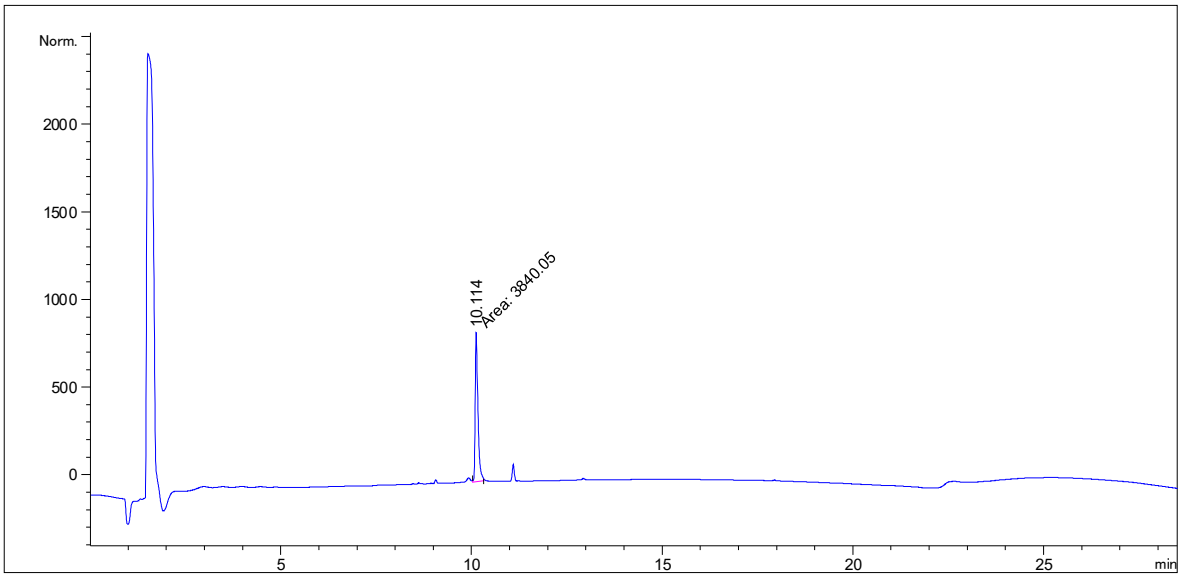

Peak #	RetTime [min]	Type	Width [min]	Area [mAU*s]	Height [mAU]	Area %	
1	10.114	MM	0.0827	3840.05347	773.84924	100.000	0
Totals :				3840.05347	773.84924		

Calculated mass for [Ile$_6$-O-Ser$_7$],Lys$_{10}$-teixobactin: 1215.7227
$[M+H]^+$ = 1216.7300
$[M+2H]^{2+}$ = 608.8689
$[M+3H]^{3+}$ = 406.2482

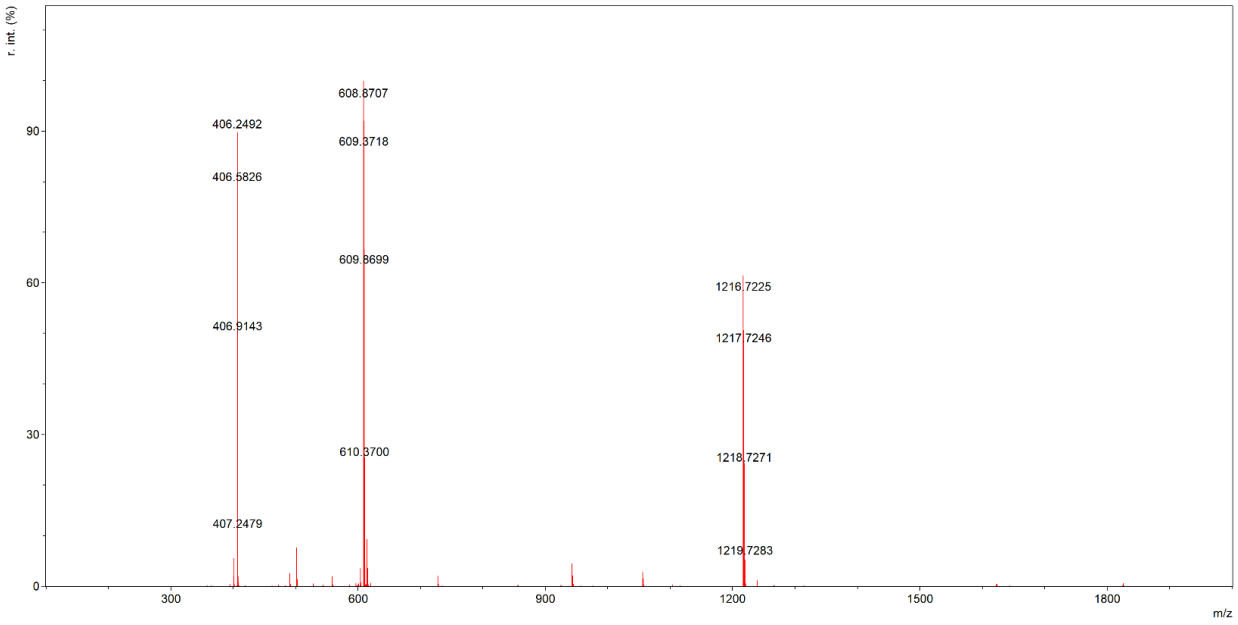

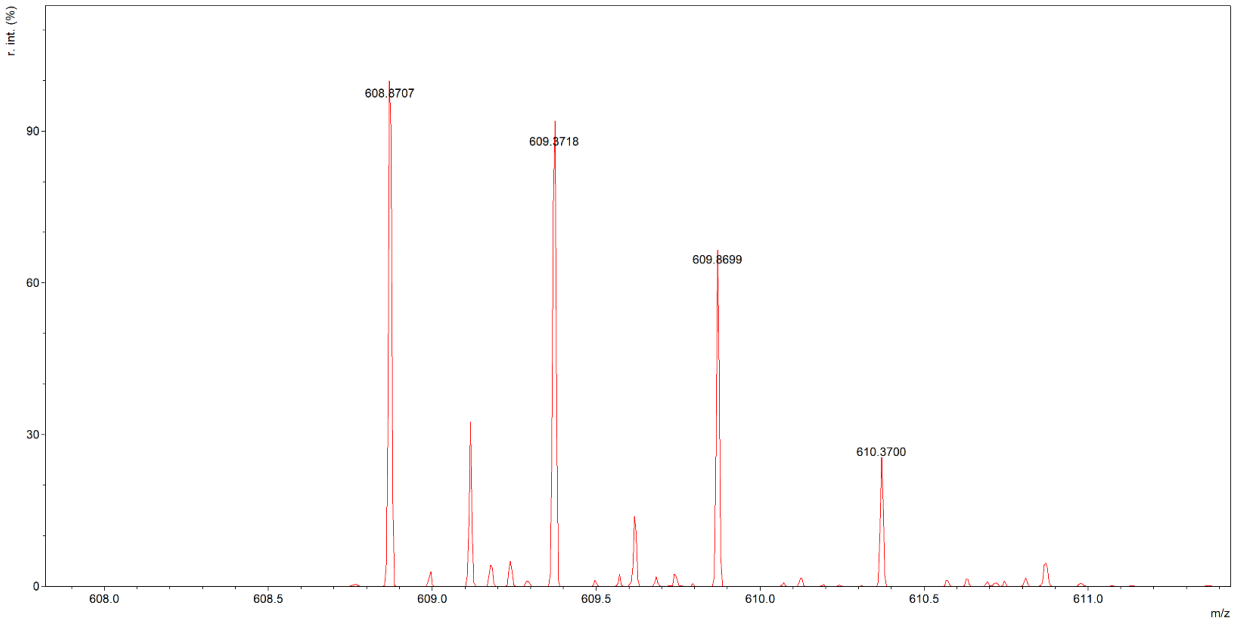

Ile$_4$,*Gln*$_5$,[*Ile*$_6$-*O*-*Ser*$_7$],*Lys*$_{10}$-teixobactin **3**

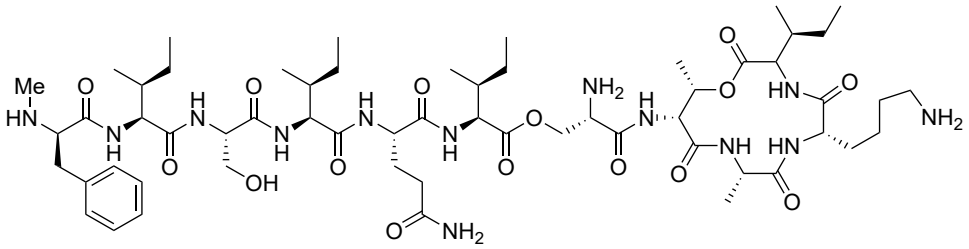

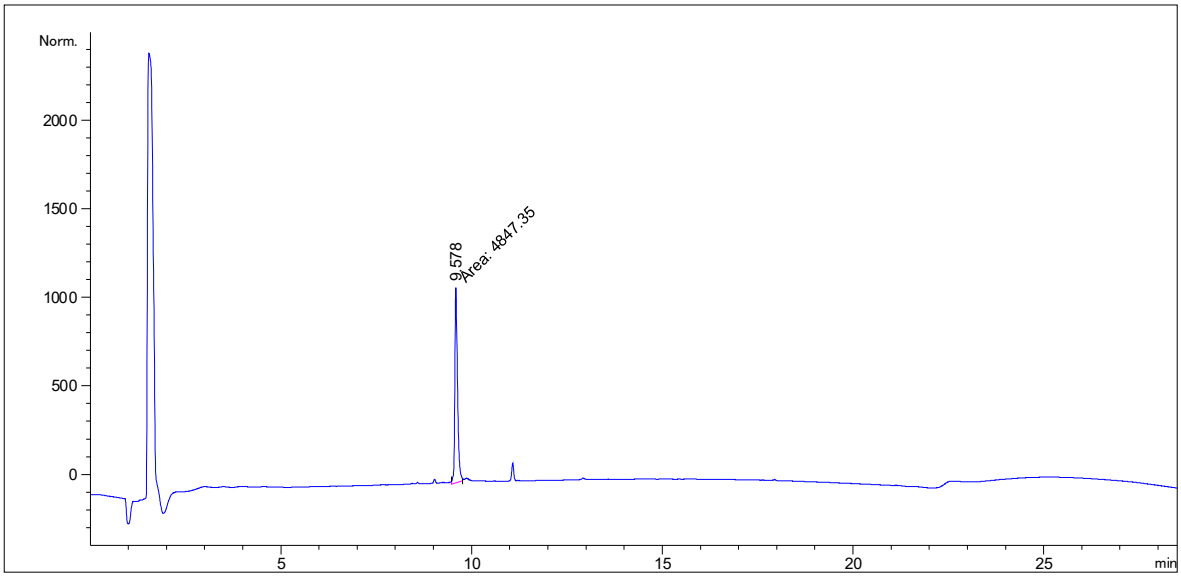

Peak #	RetTime [min]	Type	Width [min]	Area [mAU*s]	Height [mAU]	Area %
1	9.578	MM	0.0806	4847.34863	1002.93707	100.000
Totals :				4847.34863	1002.93707	

Calculated mass for $Ile_4,Gln_5,[Ile_6\text{-}O\text{-}Ser_7],Lys_{10}$-teixobactin: 1215.7227
$[M+H]^+ = 1216.7300$
$[M+2H]^{2+} = 608.8689$
$[M+3H]^{3+} = 406.2482$

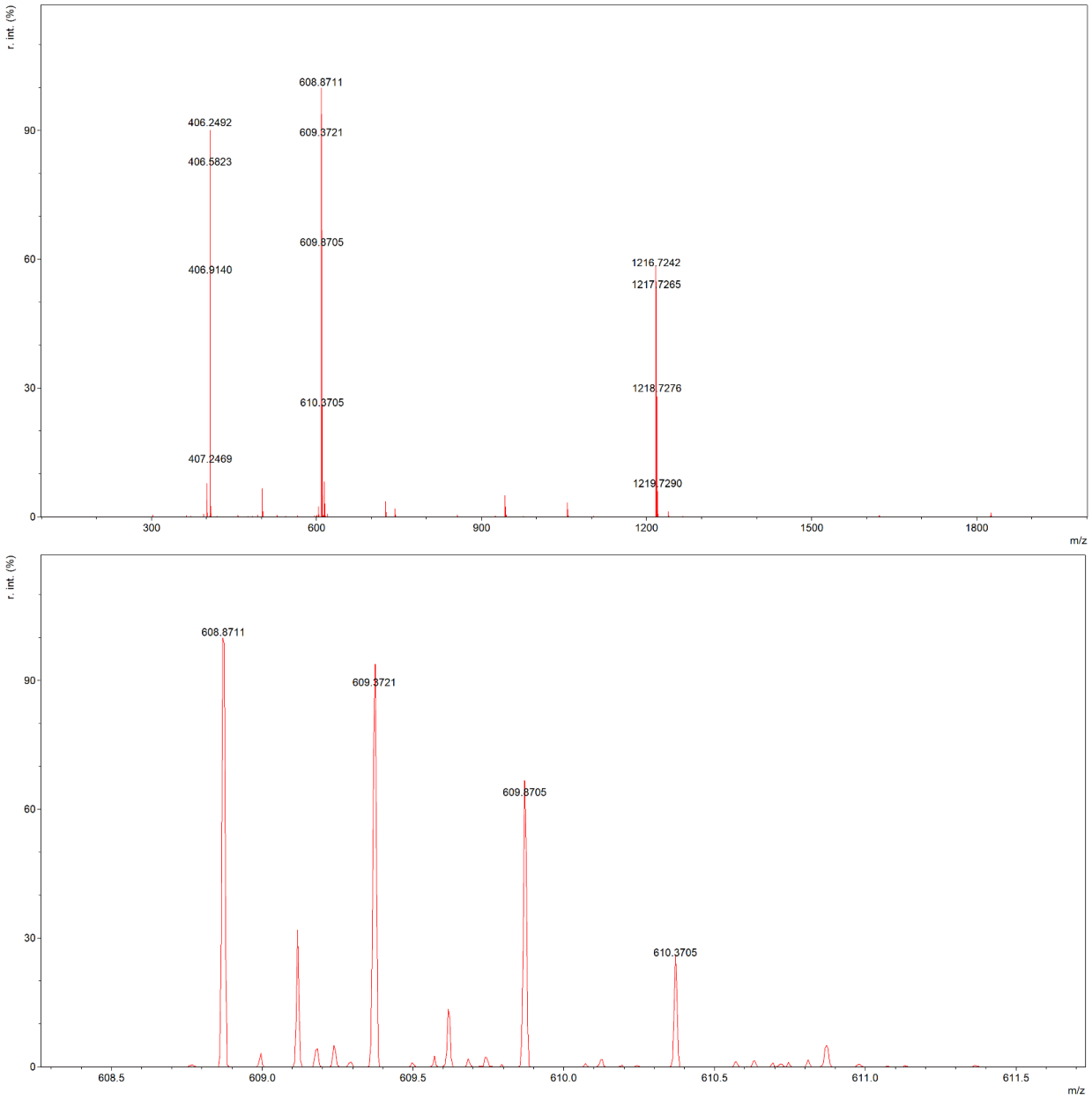

N-Me-L-Phe$_1$*,Ile*$_4$*,Gln*$_5$*,[Ile*$_6$*-O-Ser*$_7$*],Lys*$_{10}$*-teixobactin* ***4***

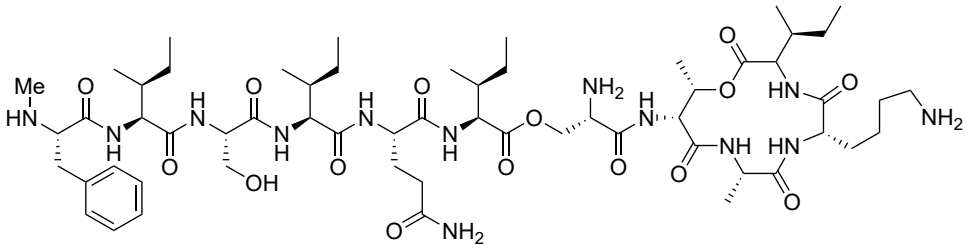

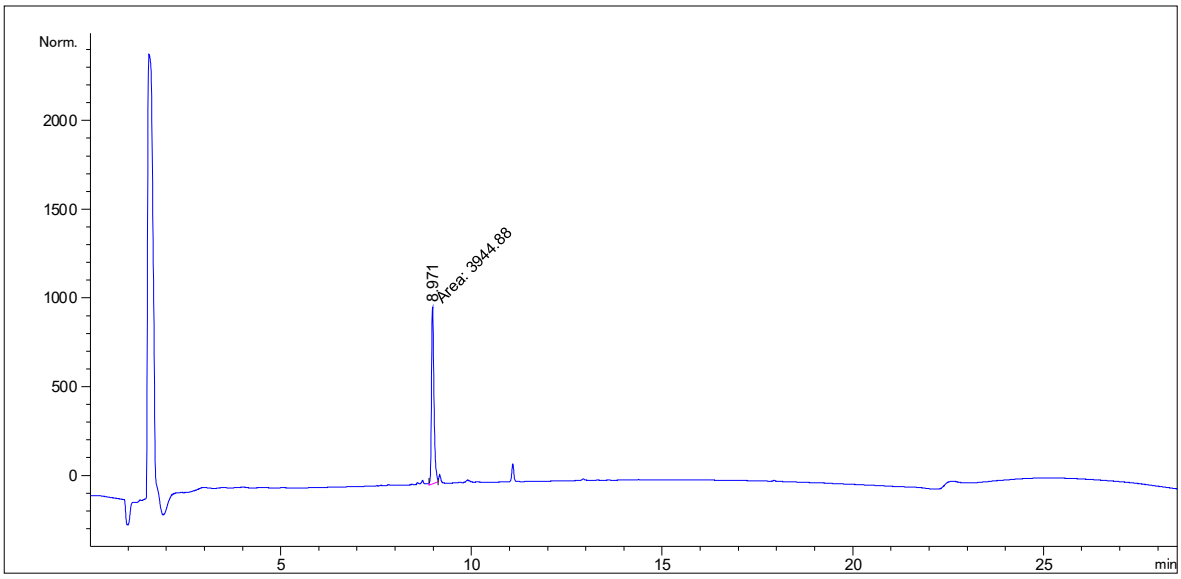

Peak #	RetTime [min]	Type	Width [min]	Area [mAU*s]	Height [mAU]	Area %
1	8.971	MM	0.0729	3944.88159	902.38306	100.000
0						

Totals :	3944.88159	902.38306

Calculated mass for *N*-Me-L-Phe$_1$,Ile$_4$,Gln$_5$,[Ile$_6$-O-Ser$_7$],Lys$_{10}$-teixobactin: 1215.7227
$[M+H]^+$ = 1216.7300
$[M+2H]^{2+}$ = 608.8689
$[M+3H]^{3+}$ = 406.2482

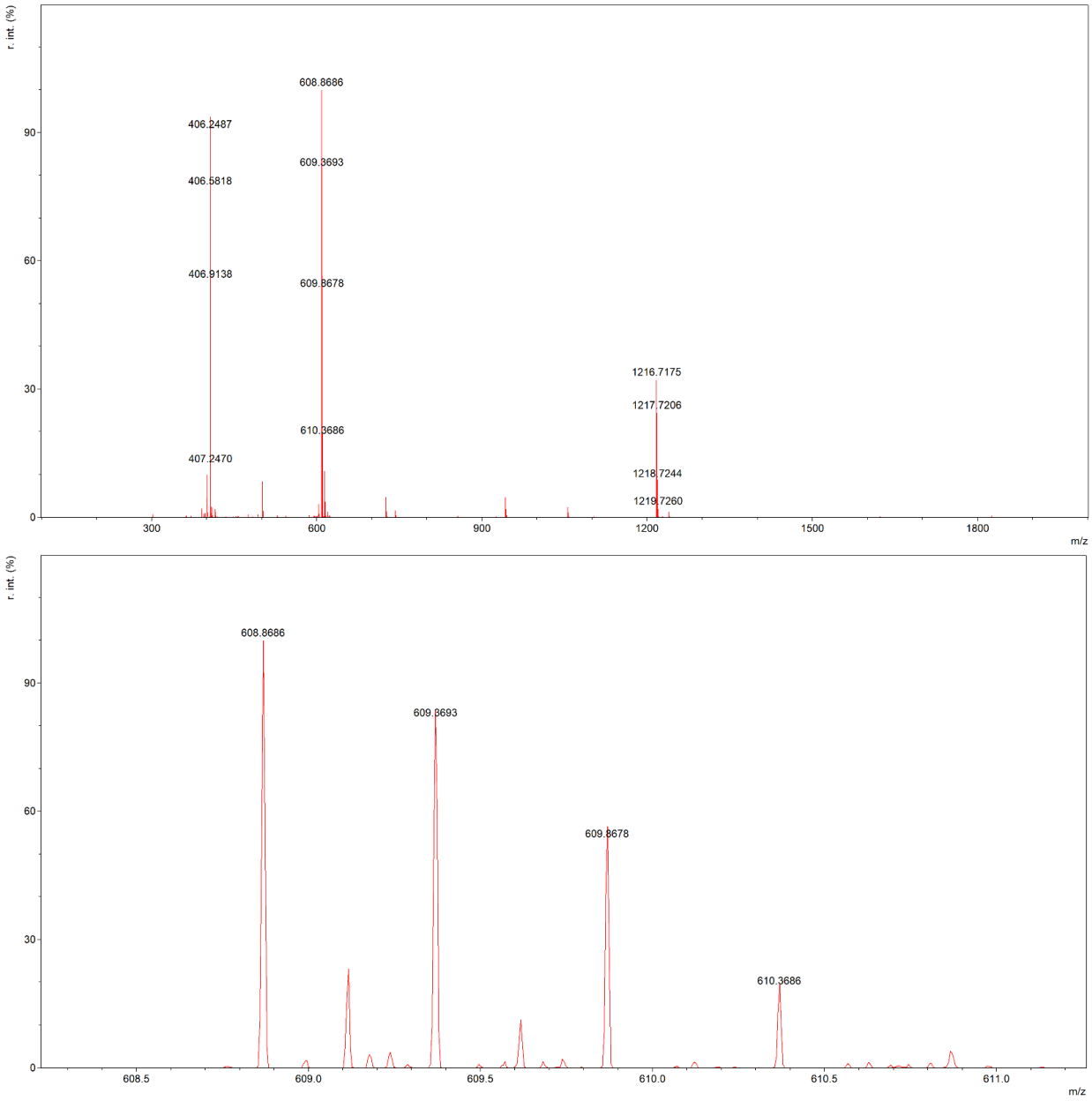

N-Bn-Gly$_1$*,Ile*$_4$*,Gln*$_5$*,[Ile*$_6$*-O-Ser*$_7$*],Lys*$_{10}$*-teixobactin* ***5***

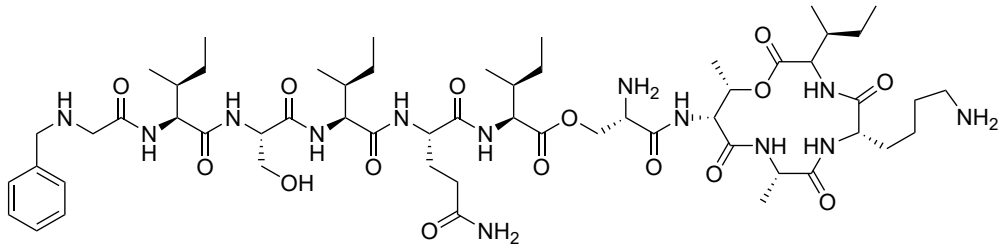

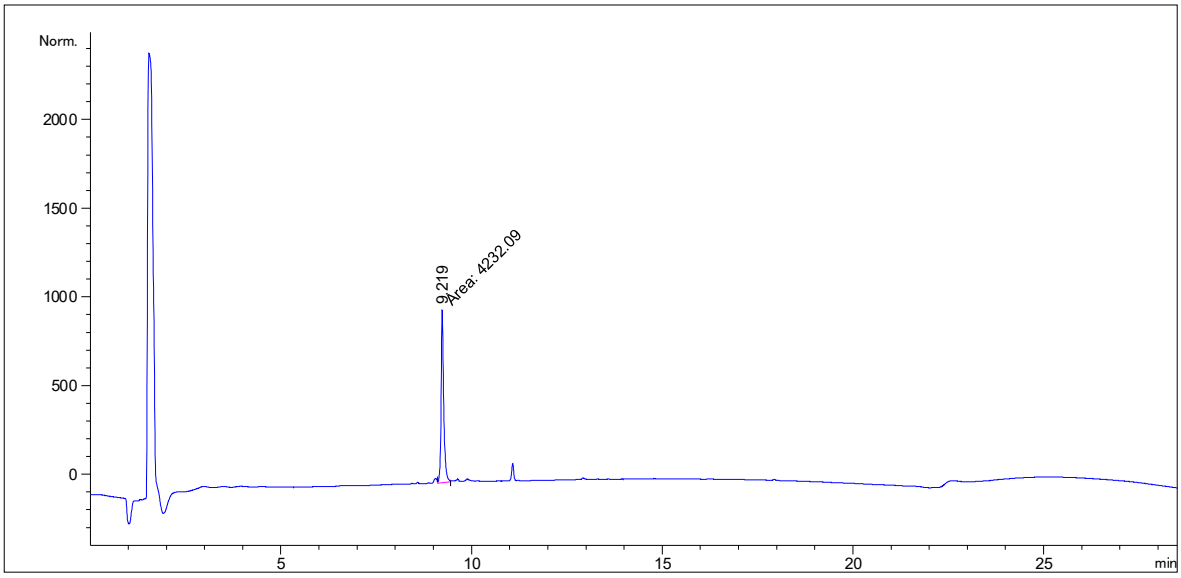

Peak #	RetTime [min]	Type	Width [min]	Area [mAU*s]	Height [mAU]	Area %
1	9.219	MM	0.0797	4232.09375	884.69745	100.000
Totals :				4232.09375	884.69745	

Calculated mass for *N*-Bn-Gly$_1$,Ile$_4$,Gln$_5$,[Ile$_6$-O-Ser$_7$],Lys$_{10}$-teixobactin: 1201.7071
$[M+H]^+$ = 1202.7143
$[M+2H]^{2+}$ = 601.8608
$[M+3H]^{3+}$ = 401.5763

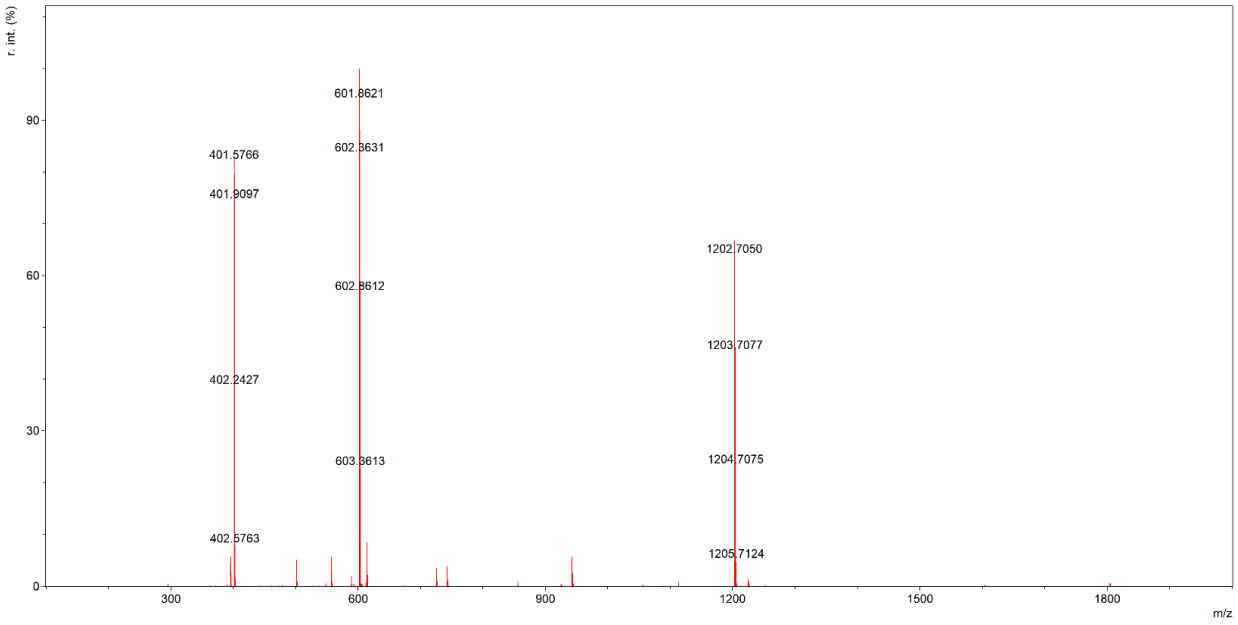

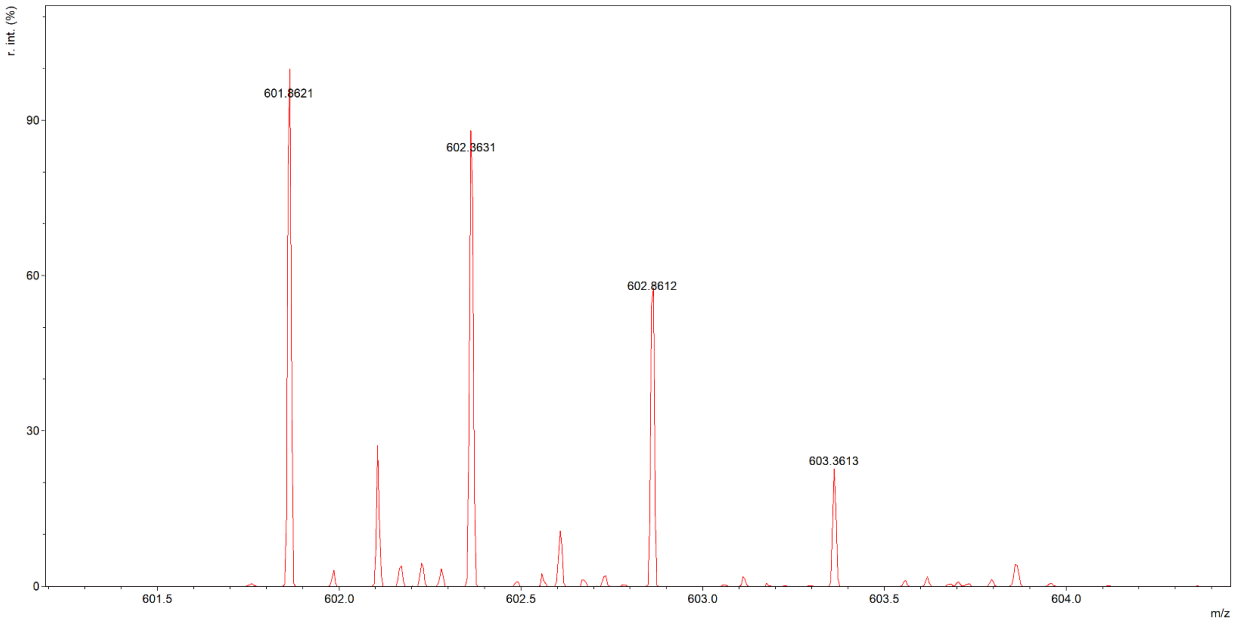

Arg_{10}-teixobactin ***6***

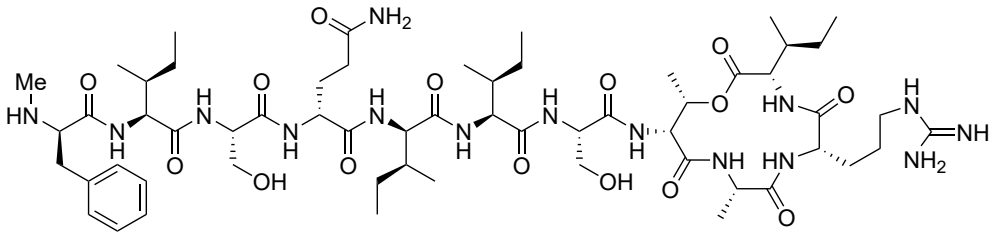

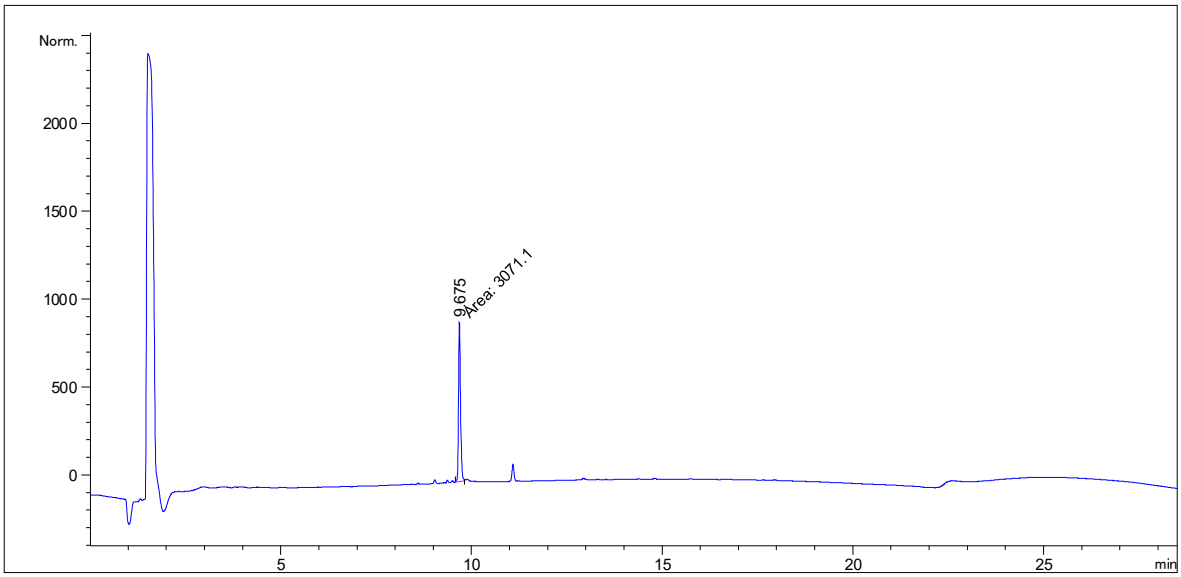

Peak #	RetTime [min]	Type	Width [min]	Area [mAU*s]	Height [mAU]	Area %
1	9.675	MM	0.0622	3071.09692	823.41827	100.000
Totals :				3071.09692	823.41827	

Calculated mass for Arg_{10}-teixobactin: 1243.7289
$[M+H]^+$ = 1244.7361
$[M+2H]^{2+}$ = 622.8717

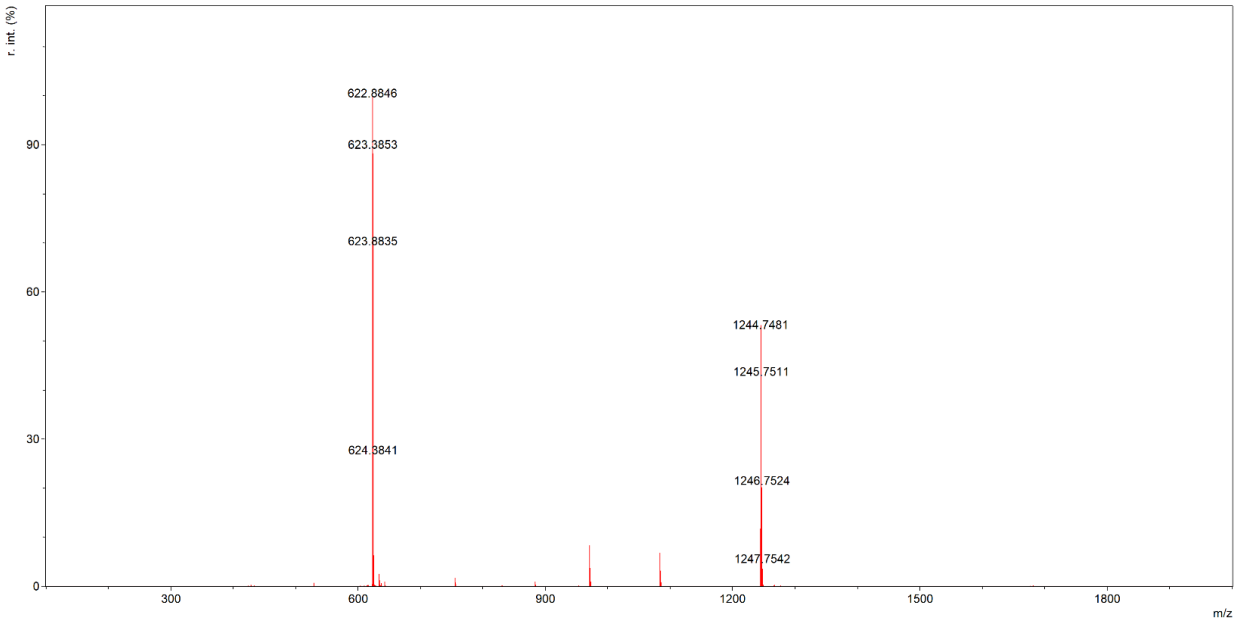

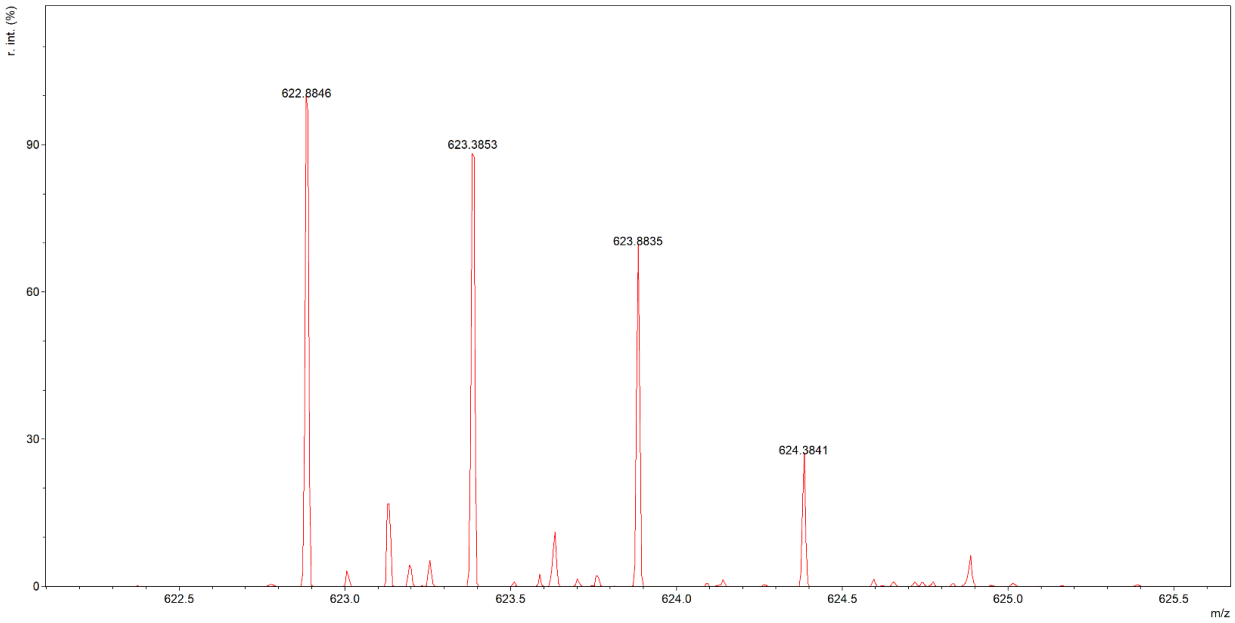

[Ile$_6$-O-Ser$_7$],Arg$_{10}$-teixobactin 7

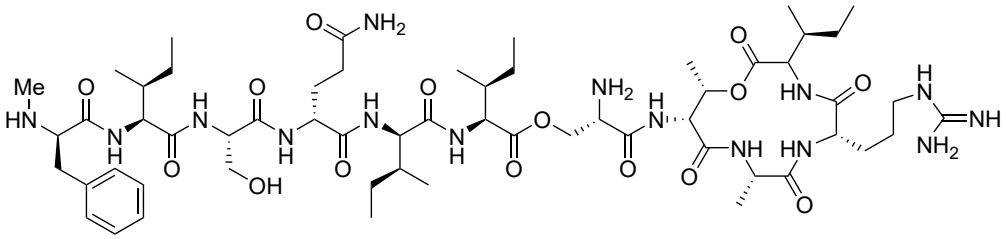

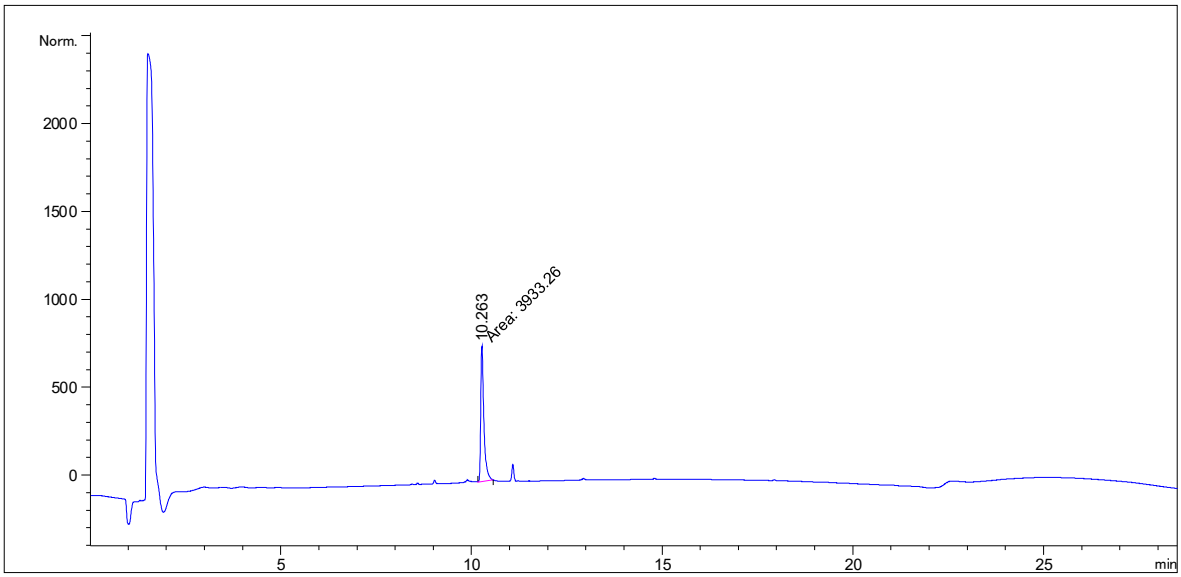

Peak #	RetTime [min]	Type	Width [min]	Area [mAU*s]	Height [mAU]	Area %
1	10.263	MM	0.0938	3933.26465	698.89679	100.000
Totals :				3933.26465	698.89679	

Calculated mass for [Ile$_6$-O-Ser$_7$],Arg$_{10}$-teixobactin: 1243.7289
$[M+H]^+$ = 1244.7361
$[M+2H]^{2+}$ = 622.8717
$[M+3H]^{3+}$ = 415.5836

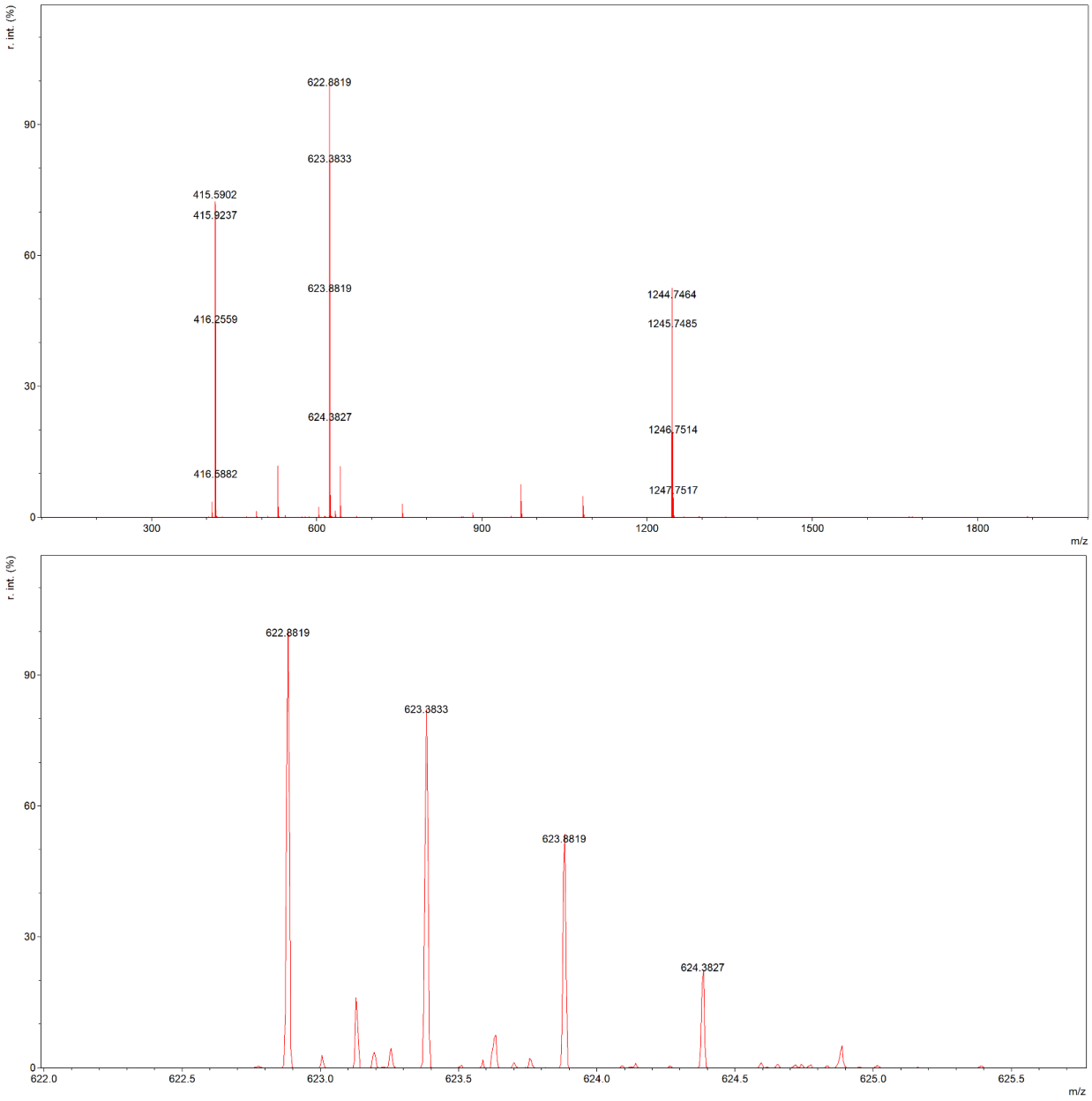

Ile$_4$,*Gln*$_5$,[*Ile*$_6$-*O*-*Ser*$_7$],*Arg*$_{10}$-*teixobactin* ***8***

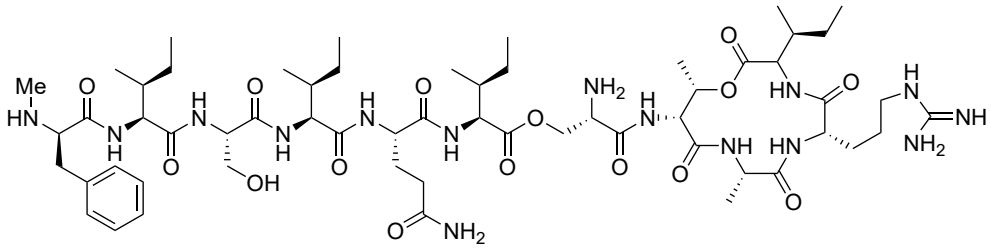

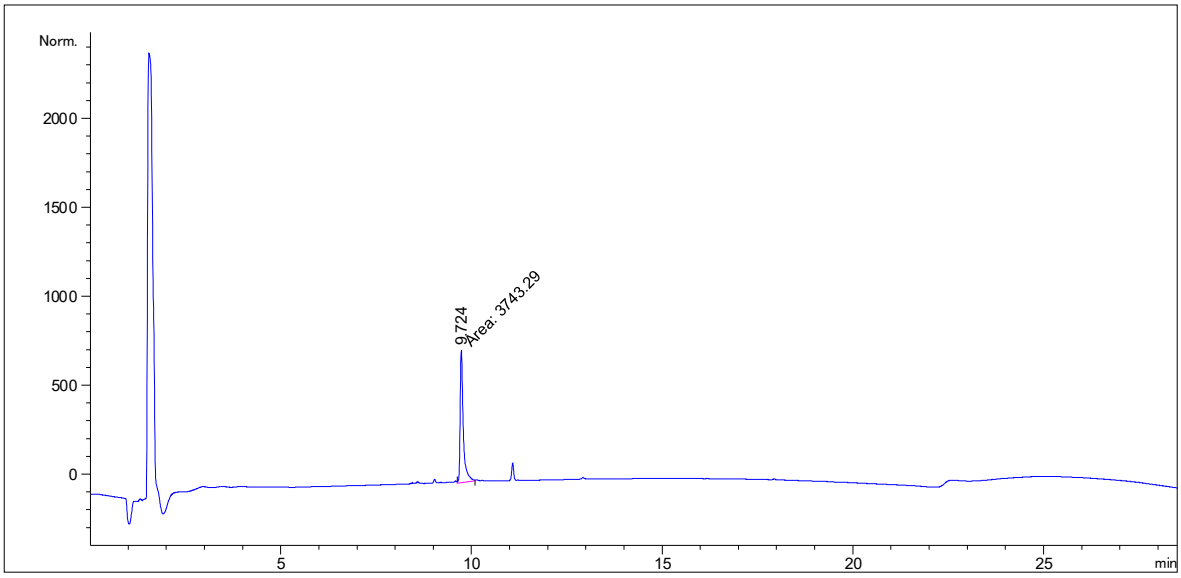

Peak #	RetTime [min]	Type	Width [min]	Area [mAU*s]	Height [mAU]	Area %
1	9.724	MM	0.0928	3743.28955	672.38824	100.000
Totals :				3743.28955	672.38824	

Calculated mass for Ile_4,Gln_5,[Ile_6-O-Ser_7],Arg_{10}-teixobactin: 1243.7289
$[M+H]^+$ = 1244.7361
$[M+2H]^{2+}$ = 622.8717
$[M+3H]^{3+}$ = 415.5836

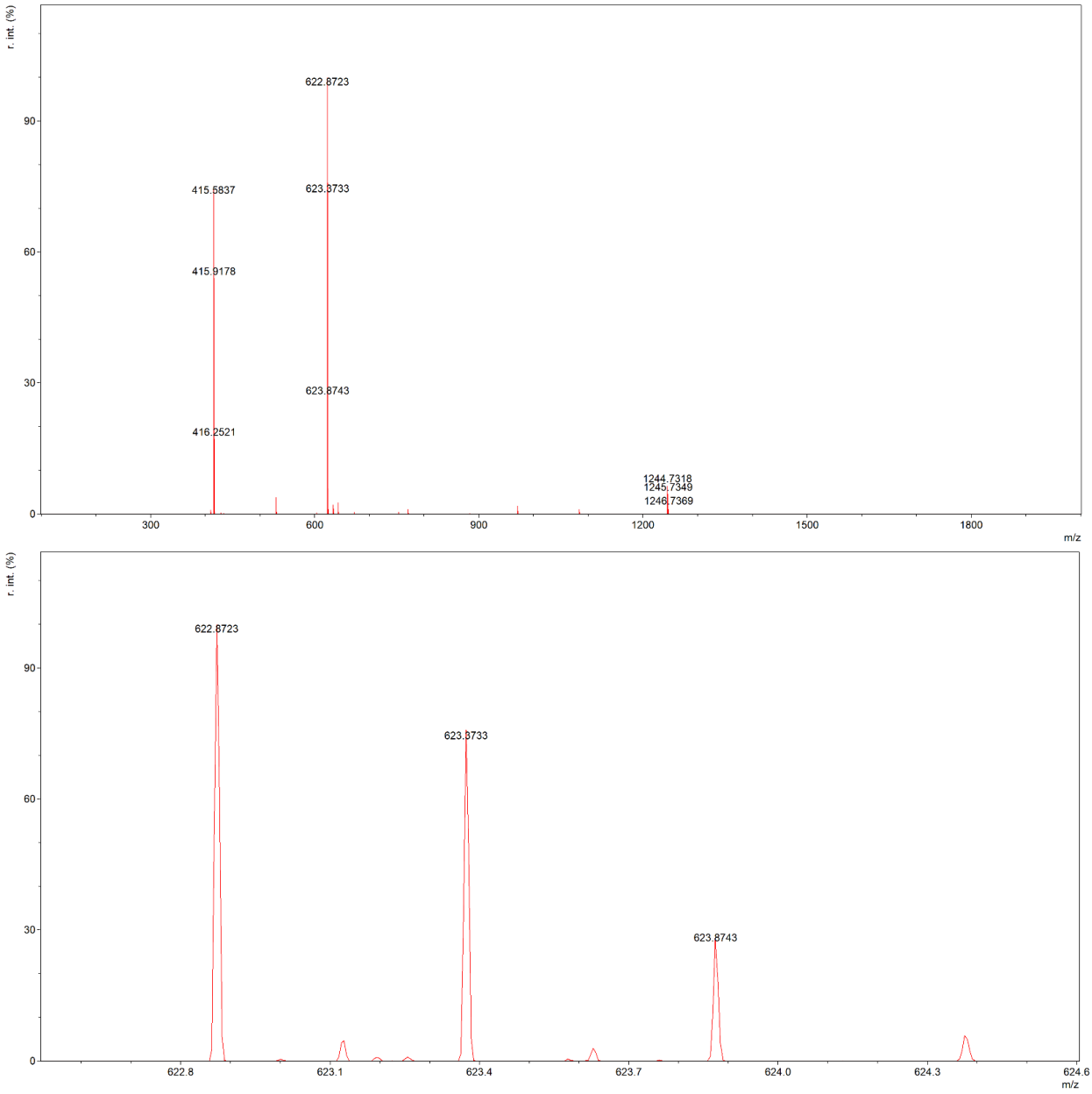

N-Me-Phe$_0$,Gln$_1$,Ile$_4$,Gln$_5$,[Ile$_6$-O-Ser$_7$],Arg$_{10}$-teixobactin ***9***

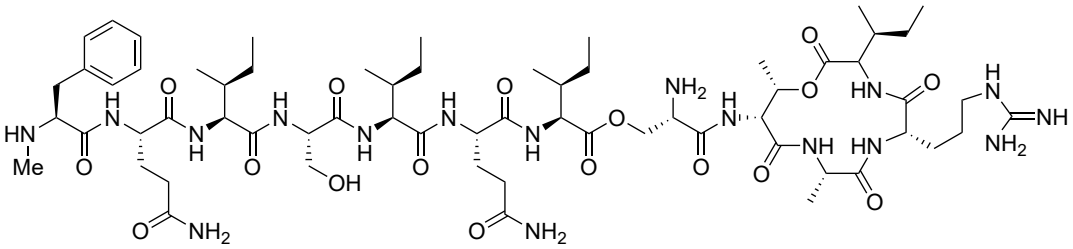

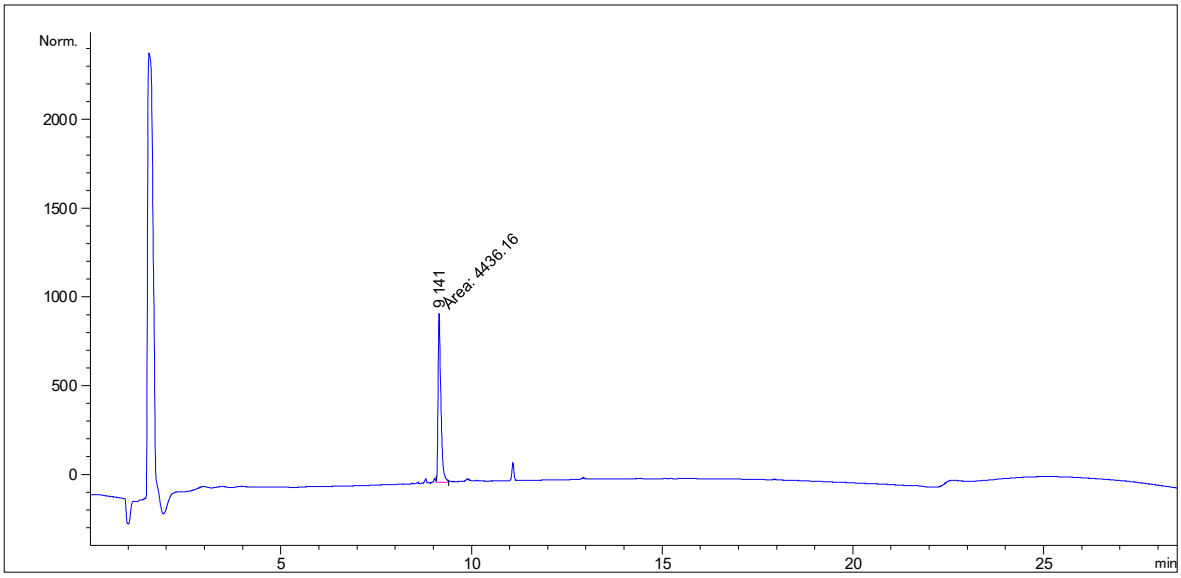

Signal 1: MWD1 A, Sig=214,4 Ref=off

Peak #	RetTime [min]	Type	Width [min]	Area [mAU*s]	Height [mAU]	Area %
1	9.141	MM	0.0858	4436.16162	861.54309	100.000
Totals :				4436.16162	861.54309	

Calculated mass for *N*-Me-Phe$_0$,Gln$_1$,Ile$_4$,Gln$_5$,[Ile$_6$-O-Ser$_7$],Arg$_{10}$-teixobactin: 1371.7874
$[M+H]^+$ = 1372.7947
$[M+2H]^{2+}$ = 686.9010
$[M+3H]^{3+}$ = 458.2698

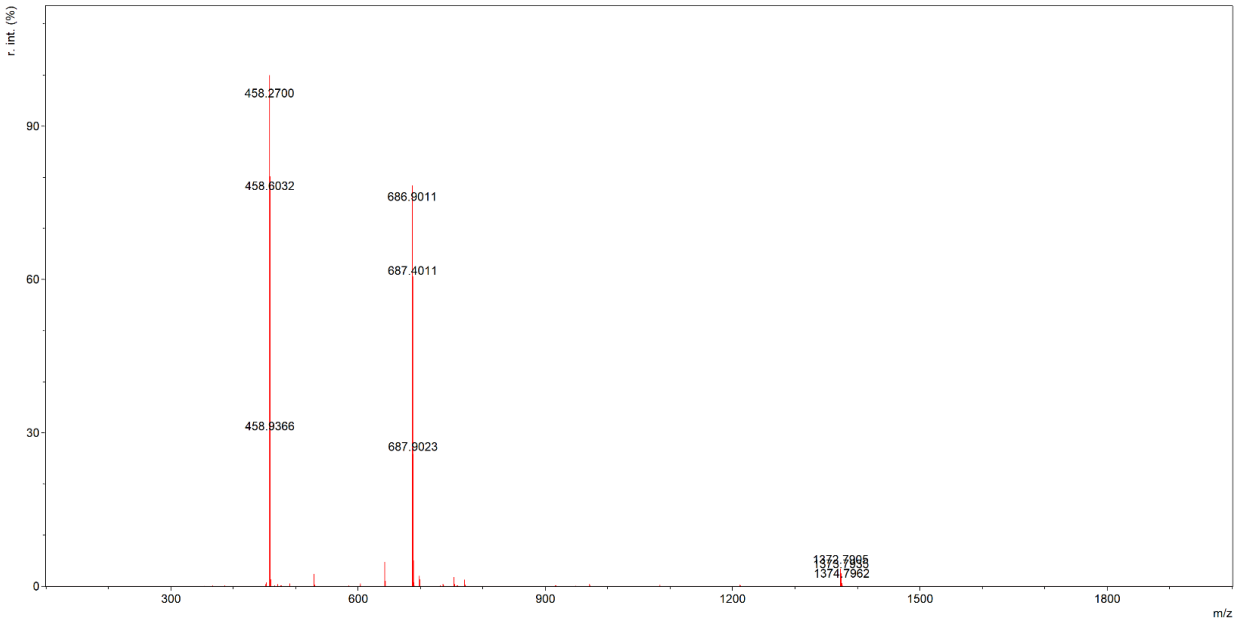

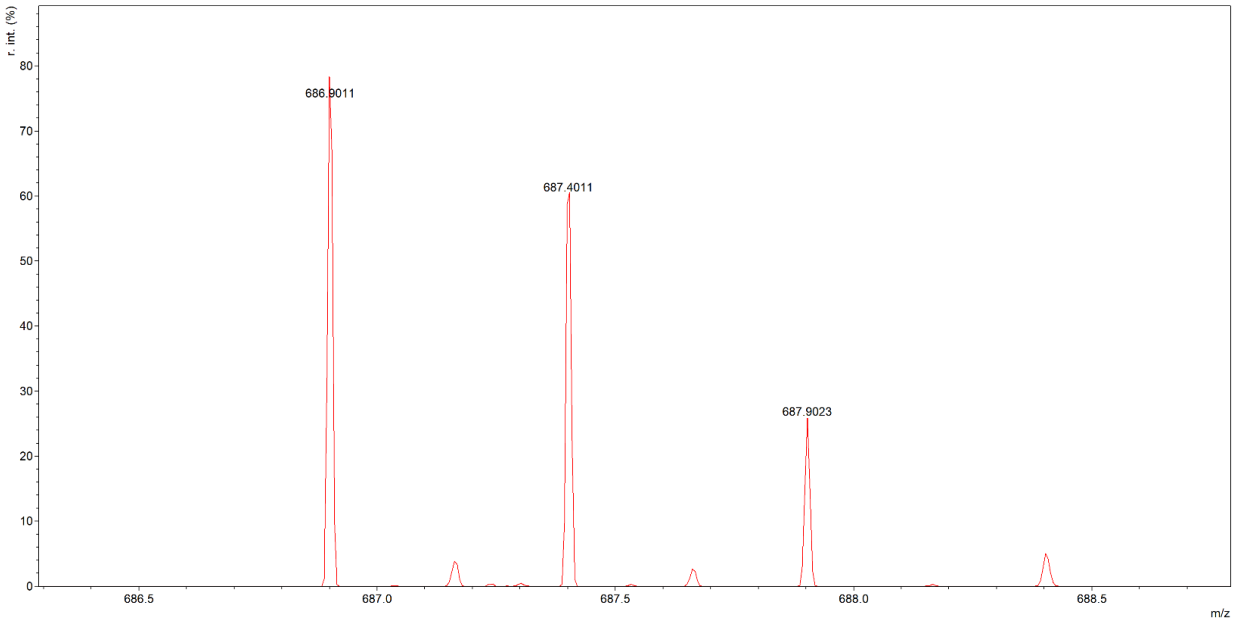

(VK)$_3$S,Arg$_{10}$-azateixobactin

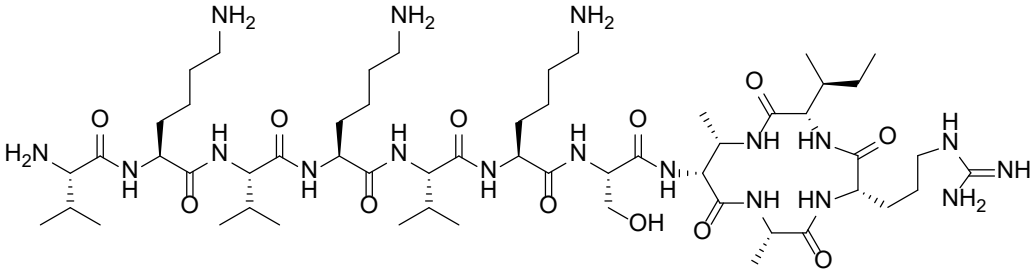

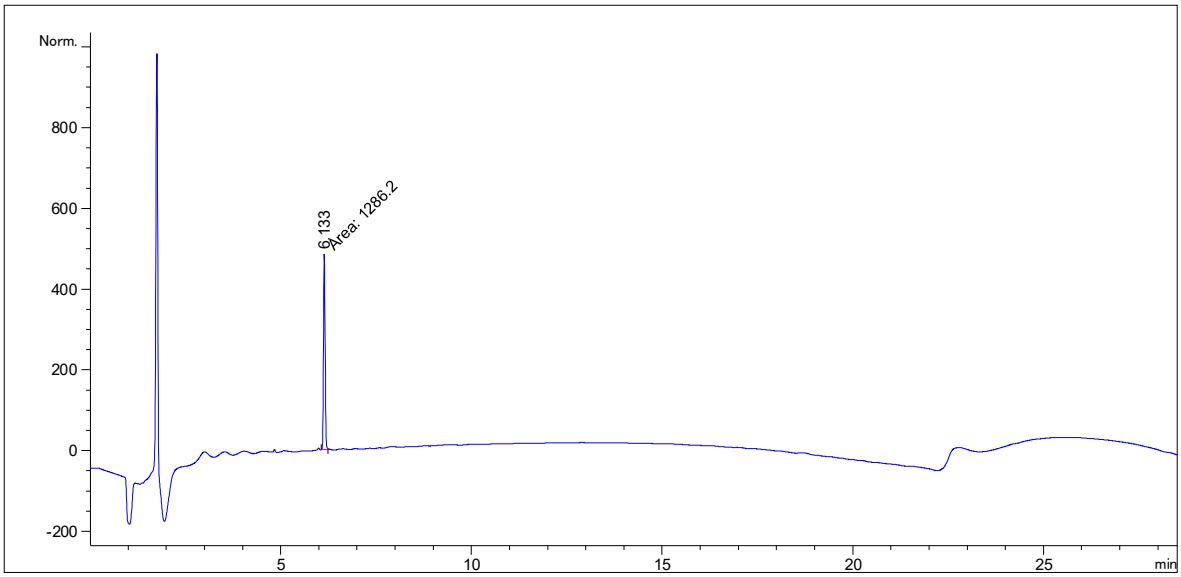

Peak #	RetTime [min]	Type	Width [min]	Area [mAU*s]	Height [mAU]	Area %
1	6.133	MM	0.0488	1286.20093	438.89722	100.000
Totals :				1286.20093	438.89722	

Calculated mass for $(VK)_3S,Arg_{10}$-azateixobactin: 1208.8081
$[M+H]^+$ = 1209.8154
$[M+Na]^{1+}$ = 1231.7973

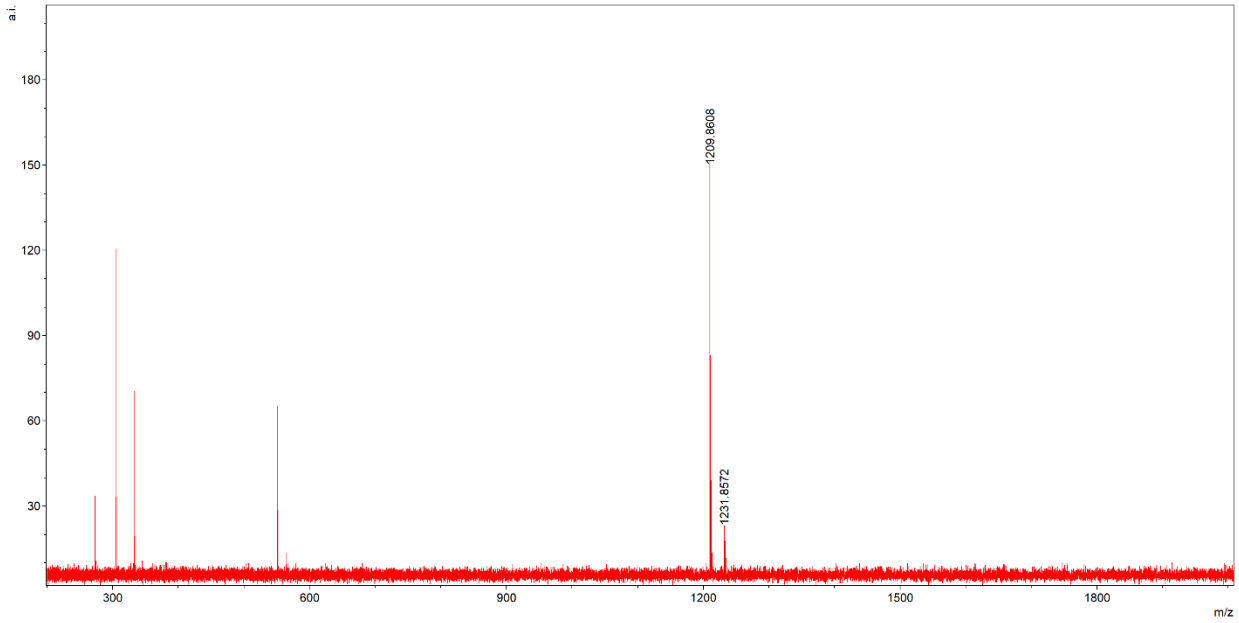

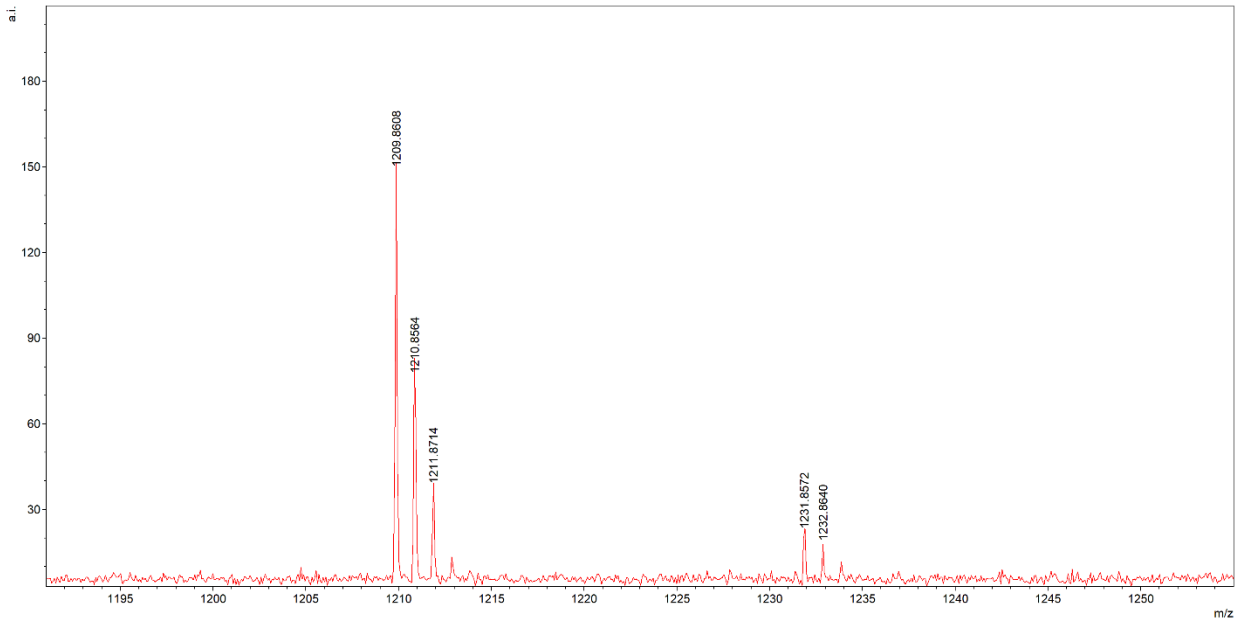

(VK)$_4$S,Arg$_{12}$-teixobactin

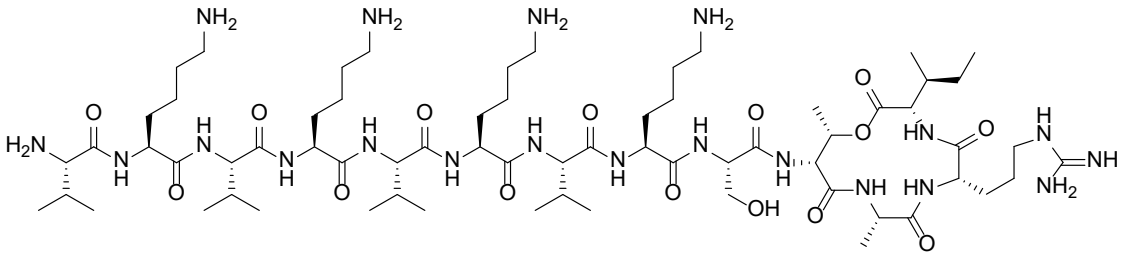

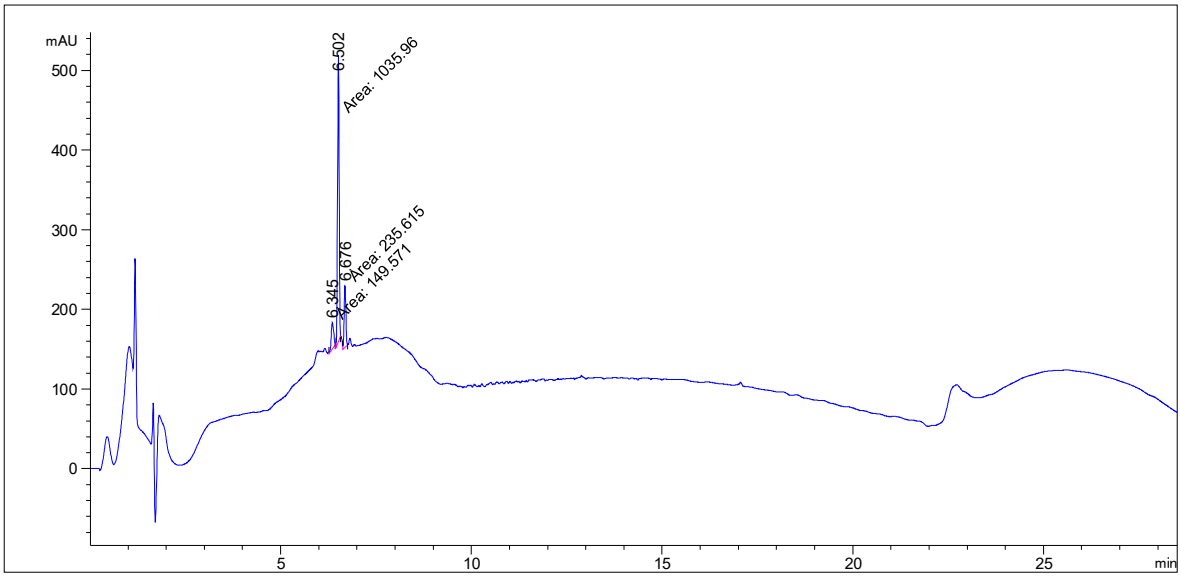

Peak #	RetTime [min]	Type	Width [min]	Area [mAU*s]	Height [mAU]	Area %	
1	6.345	MM	0.0748	149.57097	33.33830	10.524	6
2	6.502	MM	0.0476	1035.96301	362.50137	72.896	2
3	6.676	MM	0.0500	235.61514	78.46061	16.579	2

Calculated mass for $(VK)_4S,Arg_{12}$-teixobactin: 1436.9555
$[M+H]^+$ = 1437.9628
$[M+Na]^{1+}$ = 1459.9447

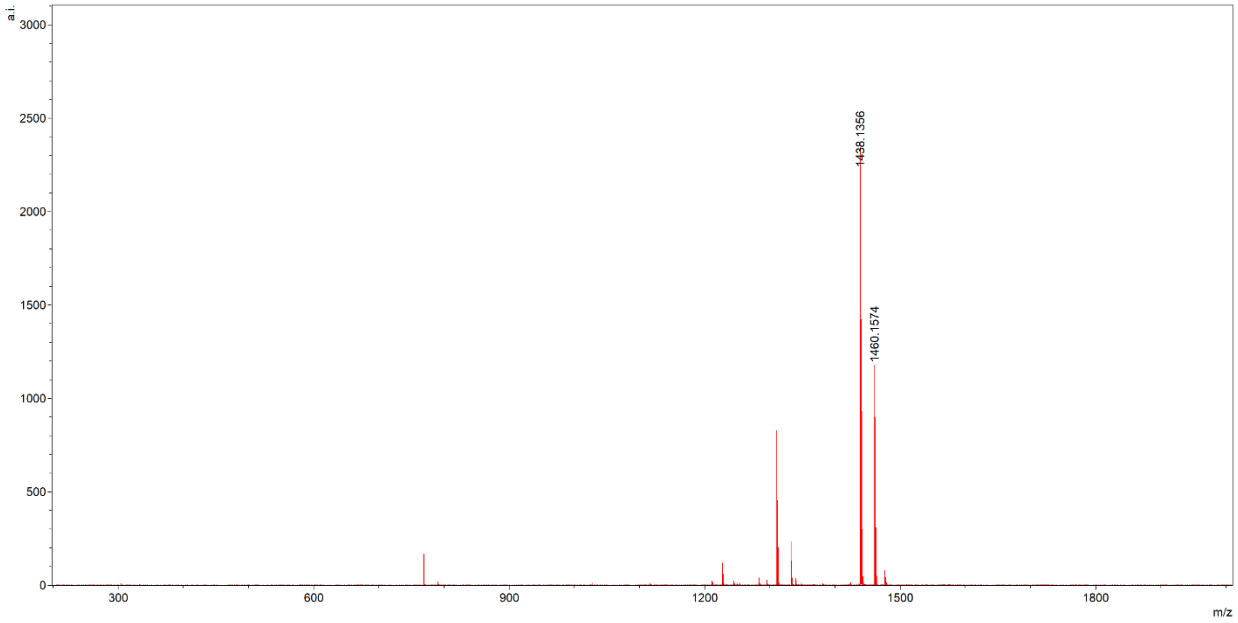

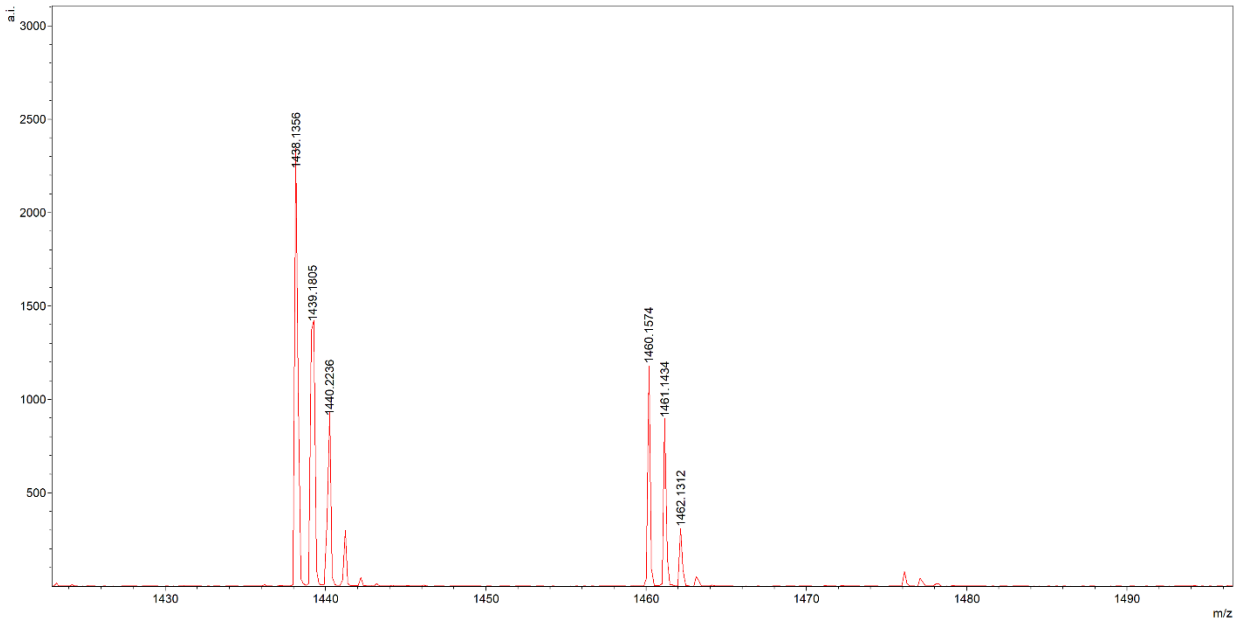

(VK)$_5$S,Arg$_{14}$-teixobactin

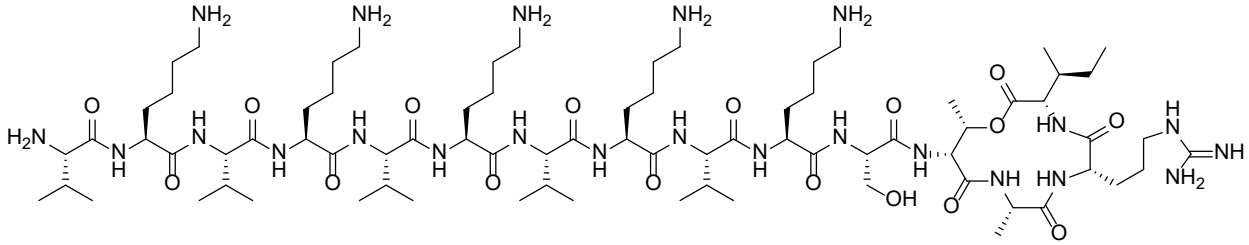

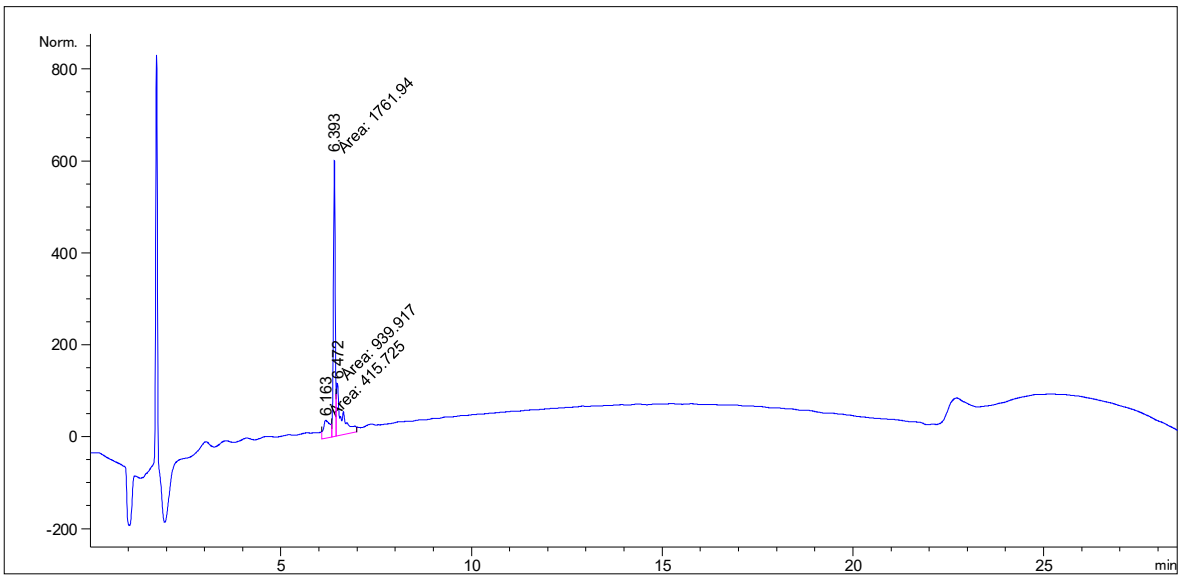

Peak #	RetTime [min]	Type	Width [min]	Area [mAU*s]	Height [mAU]	Area %
1	6.163	MF	0.1955	415.72540	35.43221	13.334
2	6.393	MF	0.0535	1761.93665	548.74261	56.516
3	6.472	FM	0.1526	939.91687	102.65623	30.148
Totals :				3117.57892	686.83106	

Calculated mass for $(VK)_5S,Arg_{14}$-teixobactin: 1664.1189
$[M+H]^+$ = 1665.1262

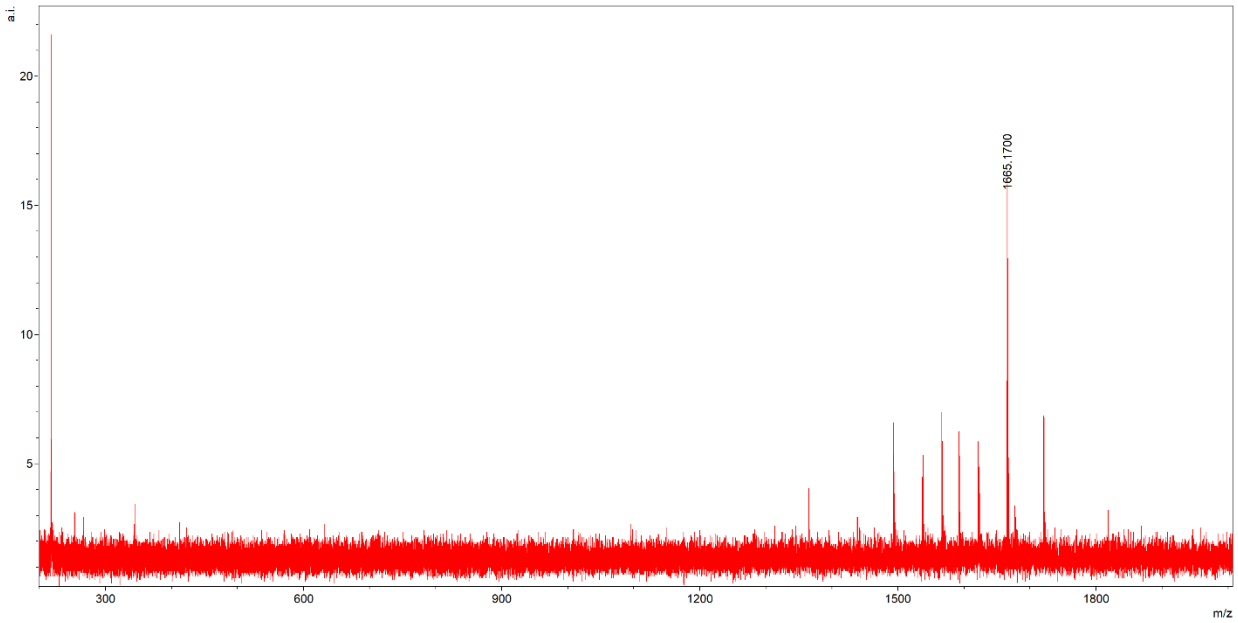

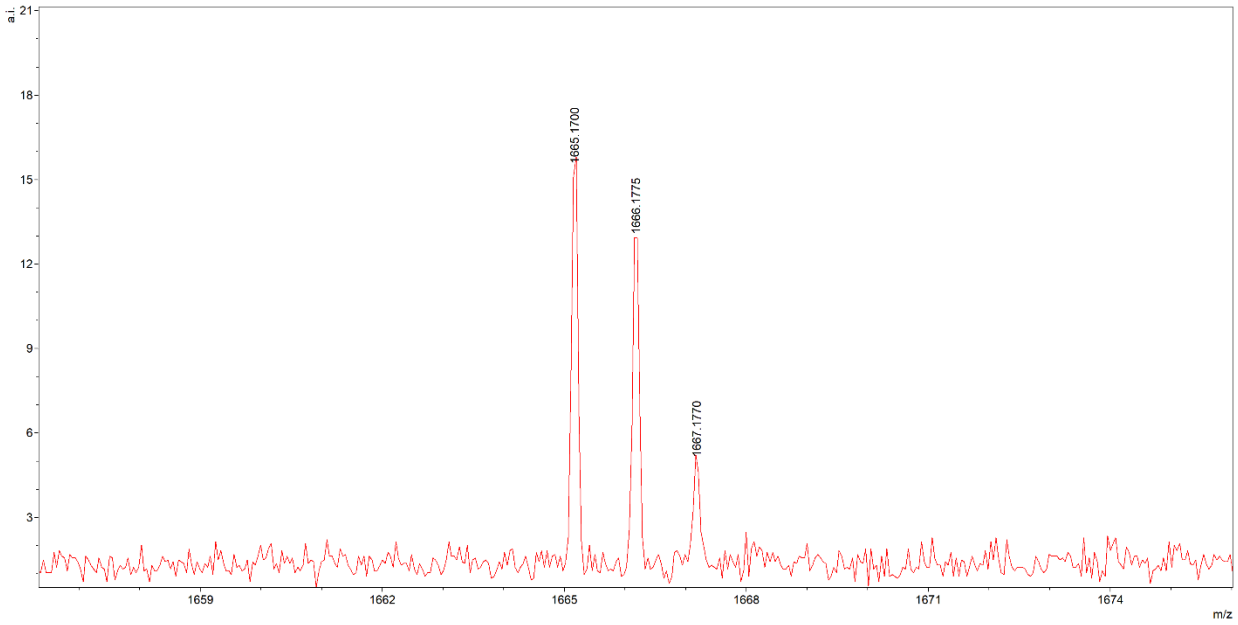

References for Chapter III

[1] Ling, L. L.; Schneider, T.; Peoples, A. J.; Spoering, A. L.; Engels, I.; Conlon, B. P.; Mueller, A.; Schäberle, T. F.; Hughes, D. E.; Epstein, S.; Jones, M.; Lazarides, L.; Steadman, V. A.; Cohen, D. R.; Felix, C. R.; Fetterman, K. A.; Millett, W. P.; Nitti, A. G.; Zullo, A. M.; Chen, C.; Lewis, K. A New Antibiotic Kills Pathogens without Detectable Resistance. Nature **2015**, *517* (7535), 455–459. DOI: 10.1038/nature14098

[2] Yang, H.; Wierzbicki, M.; Du Bois, D. R.; Nowick, J. S. X-Ray Crystallographic Structure of a Teixobactin Derivative Reveals Amyloid-like Assembly. *J. Am. Chem. Soc.* **2018**, *140* (43), 14028–14032. DOI: 10.1021/jacs.8b07709

[3] Shukla, R.; Lavore, F.; Maity, S.; Derks, M. G. N.; Jones, C. R.; Vermeulen, B. J. A.; Melcrová, A.; Morris, M. A.; Becker, L. M.; Wang, X.; Kumar, R.; Medeiros-Silva, J.; Van Beekveld, R. A. M.; Bonvin, A. M. J. J.; Lorent, J. H.; Lelli, M.; Nowick, J. S.; MacGillavry, H. D.; Peoples, A. J.; Spoering, A. L.; Ling, L. L.; Hughes, D. E.; Roos, W. H.; Breukink, E.; Lewis, K.; Weingarth, M. Teixobactin Kills Bacteria by a Two-Pronged Attack on the Cell Envelope. *Nature* **2022**, *608* (7922), 390–396. DOI: doi.org/10.1038/s41586-022-05019-y

[4] Parmar, A.; Iyer, A.; Vincent, C. S.; Van Lysebetten, D.; Prior, S. H.; Madder, A.; Taylor, E. J.; Singh, I. Efficient Total Syntheses and Biological Activities of Two Teixobactin Analogues. *Chem. Commun.* **2016**, *52* (36), 6060–6063. DOI: 10.1039/C5CC10249A

[5] Abdel Monaim, S. A. H.; Jad, Y. E.; Acosta, G. A.; Naicker, T.; Ramchuran, E. J.; El-Faham, A.; Govender, T.; Kruger, H. G.; De La Torre, B. G.; Albericio, F. Re-Evaluation of the N-

Terminal Substitution and the D-Residues of Teixobactin. *RSC Adv.* **2016**, *6* (77), 73827–73829. DOI: 10.1039/C6RA17720D

[6] Parmar, A.; Prior, S. H.; Iyer, A.; Vincent, C. S.; Van Lysebetten, D.; Breukink, E.; Madder, A.; Taylor, E. J.; Singh, I. Defining the Molecular Structure of Teixobactin Analogues and Understanding Their Role in Antibacterial Activities. *Chem. Commun.* **2017**, *53* (12), 2016–2019. DOI: 10.1039/C6CC09490B

[7] Jin, K.; Po, K. H. L.; Wang, S.; Reuven, J. A.; Wai, C. N.; Lau, H. T.; Chan, T. H.; Chen, S.; Li, X. Synthesis and Structure-Activity Relationship of Teixobactin Analogues via Convergent Ser Ligation. *Bioorg. Med. Chem.* **2017**, *25* (18), 4990–4995. DOI: 10.1016/j.bmc.2017.04.039

[8] Yang, H.; Pishenko, A. V.; Li, X.; Nowick, J. S. Design, Synthesis, and Study of Lactam and Ring-Expanded Analogues of Teixobactin. *J. Org. Chem.* **2020**, *85* (3), 1331–1339. DOI: 10.1021/acs.joc.9b02631

[9] Chen, K. H.; Le, S. P.; Han, X.; Frias, J. M.; Nowick, J. S. Alanine Scan Reveals Modifiable Residues in Teixobactin. *Chem. Commun.* **2017**, *53* (82), 11357–11359. DOI: 10.1039/C7CC03415F

[10] Jones, C. R.; Guaglianone, G.; Lai, G. H.; Nowick, J. S. Isobactins: *O*-Acyl Isopeptide Prodrugs of Teixobactin and Teixobactin Derivatives. *Chem. Sci.* **2022**, *13* (44), 13110–13116. DOI: 10.1039/D2SC02670H

[11] Jones, C. R.; Lai, G. H.; Padilla, M. S. T. L.; Nowick, J. S. Investigation of Isobactin Analogues of Teixobactin. *ACS Med. Chem. Lett.* **2024**, *15* (7), 1136–1142. DOI: 10.1021/acsmedchemlett.4c00215

[12] Sohma, Y.; Yoshiya, T.; Taniguchi, A.; Kimura, T.; Hayashi, Y.; Kiso, Y. Development of *O*-acyl Isopeptide Method. *Biopolymers* **2007**, *88* (2), 253–262. DOI: 10.1002/bip.20683

[13] Schneider, J. P.; Pochan, D. J.; Ozbas, B.; Rajagopal, K.; Pakstis, L.; Kretsinger, J. Responsive Hydrogels from the Intramolecular Folding and Self-Assembly of a Designed Peptide. *J. Am. Chem. Soc.* **2002**, *124* (50), 15030–15037. DOI: 10.1021/ja027993g

[14] Pochan, D. J.; Schneider, J. P.; Kretsinger, J.; Ozbas, B.; Rajagopal, K.; Haines, L. Thermally Reversible Hydrogels via Intramolecular Folding and Consequent Self-Assembly of a de Novo Designed Peptide. *J. Am. Chem. Soc.* **2003**, *125* (39), 11802–11803. DOI: 10.1021/ja0353154

[15] Ozbas, B.; Kretsinger, J.; Rajagopal, K.; Schneider, J. P.; Pochan, D. J. Salt-Triggered Peptide Folding and Consequent Self-Assembly into Hydrogels with Tunable Modulus. *Macromolecules* **2004**, *37* (19), 7331–7337. DOI: 10.1021/ma0491762

[16] Ozbas, B.; Rajagopal, K.; Schneider, J. P.; Pochan, D. J. Semiflexible Chain Networks Formed via Self-Assembly of Beta-Hairpin Molecules. *Phys. Rev. Lett.* **2004**, *93* (26), 268106. DOI: 10.1103/PhysRevLett.93.268106

[17] Rajagopal, K.; Ozbas, B.; Pochan, D. J.; Schneider, J. P. Probing the Importance of Lateral Hydrophobic Association in Self-Assembling Peptide Hydrogelators. *Eur. Biophys. J.* **2006,** *35* (2), 162–169. DOI: 10.1007/s00249-005-0017-7

[18] Sathaye, S.; Zhang, H.; Sonmez, C.; Schneider, J. P.; MacDermaid, C. M.; Von Bargen, C. D.; Saven, J. G.; Pochan, D. J. Engineering Complementary Hydrophobic Interactions to Control β-Hairpin Peptide Self-Assembly, Network Branching, and Hydrogel Properties. *Biomacromolecules* **2014**, *15* (11), 3891–3900. DOI: 10.1021/bm500874t

[19] Nagy-Smith, K.; Moore, E.; Schneider, J.; Tycko, R. Molecular Structure of Monomorphic Peptide Fibrils within a Kinetically Trapped Hydrogel Network. *Proc. Natl. Acad. Sci. U.S.A.* **2015**, *112* (32), 9816–9821. DOI: 10.1073/pnas.1509313112

[20] Yang, H.; Chen, K. H.; Nowick, J. S. Elucidation of the Teixobactin Pharmacophore. *ACS Chem. Biol.* **2016**, *11* (7), 1823–1826. DOI: 10.1021/acschembio.6b00295

[21] Morris, M. A.; Malek, M.; Hashemian, M. H.; Nguyen, B. T.; Manuse, S.; Lewis, K.; Nowick, J. S. A Fluorescent Teixobactin Analogue. *ACS Chem. Biol.* **2020**, *15* (5), 1222–1231. DOI: 10.1021/acschembio.9b00908

CHAPTER IV: Structure-Activity Relationship Studies of the Peptide Antibiotic Clovibactin*

Abstract

Our laboratory previously reported the chemical synthesis and stereochemical assignment of the recently discovered peptide antibiotic clovibactin. An alanine scan of clovibactin reveals that the residues Phe_1, D-Leu_2, Ser_4, Leu_7, and Leu_8 are important for antibiotic activity. The side chain amide group of the rare D-Hyn_5 residue is not essential to activity and can be replaced with a methyl group with moderate loss of activity. The macrolactone ring is essential to antibiotic activity. The enantiomer of clovibactin is active, albeit somewhat less so than clovibactin. A conformationally constrained clovibactin analogue retains moderate antibiotic activity, while a backbone *N*-methylated analogue is almost completely inactive. X-ray crystallography of these two analogues reveals that the macrolactone ring adopts a crownlike conformation that binds anions. In contrast to the related antibiotic teixobactin, conversion of the macrolactone to a macrolactam appears to decrease, rather than increase, activity.

Introduction

Clovibactin is a newly reported antibiotic that is active against Gram-positive bacteria, including drug-resistant human pathogens such as MRSA and VRE, without detectable

* Portions of this chapter have been submitted to and are under review by *The Journal of Organic Chemistry* as of 2024-08-02. The sections pertaining to the alanine scan and X-ray crystallography are adapted or taken verbatim from the submitted manuscript. Jackson Brunicardi and Jeramiah Small produced the protected hydroxyasparagine amino acid used to prepare clovibactin analogues. Jackson Brunicardi, Jeramiah Small, and Ana-Teresa Mendoza contributed to the peptide synthesis of alanine scan analogues. Prof. Michael Ferracane prepared stapled D-Thr_5-clovibactin and its precursors. Dr. Adam Kreutzer and Dr. Joseph Ziller contributed to the X-ray crystallography of D-Thr_5-clovibactin analogues. Jackson Brunicardi, Prof. Michael Ferracane, and Prof. James Nowick participated in writing and editing the submitted manuscript.

resistance.[1] It is an eight-residue depsipeptide comprising a linear tail (residues 1–4) and macrolactone ring (residues 5–8). Clovibactin kills bacteria by inhibiting cell-wall biosynthesis, specifically targeting the pyrophosphate moiety of multiple peptidoglycan precursors. Weingarth and coworkers have recently reported an NMR-based model of clovibactin binding lipid II pyrophosphate. On the basis of this model, they propose a mechanism of action in which clovibactin forms antiparallel β-sheet assemblies upon binding to the pyrophosphate group. This mechanism is similar to the related antibiotic teixobactin, which our group has also studied.[2,3,4,5,6,7,8]

Our group previously reported the chemical synthesis of clovibactin and a stereochemical assignment of the rare noncanonical amino acid hydroxyasparagine at position 5.[9] In the current study, we perform an alanine scan and other structure-activity relationship studies. These studies allow us to identify critical amino acid residues and thus better understand how clovibactin interacts with Gram-positive bacteria. We obtain X-ray crystallographic structures of two clovibactin analogues designed to probe the relationship between the conformation and supramolecular assembly of clovibactin and its antibiotic activity, and we show that both analogues bind anions in the crystallographic structures.

To further compare teixobactin, clovibactin, and the related antibiotic hypeptin, I perform further structure-activity relationship studies of clovibactin and hypeptin analogues. Following a synthetic route originally developed for macrolactam teixobactin analogues, I prepare and evaluate the activity of a macrolactam clovibactin analogue. Using the same synthetic route for preparing clovibactin analogues, and using commercially available amino acids, I prepare two analogues of hypeptin to study the importance of its unusual β-hydroxylated amino acids.

Results and Discussion

Structure-Activity Relationship Studies

We performed structure-activity relationship (SAR) studies to identify the features of clovibactin that contribute to its strong antibiotic activity. We first performed an alanine scan to identify individual amino acid residues in clovibactin that contribute to its antibiotic activity. Each residue was sequentially replaced with alanine while maintaining the native stereochemistry: L-alanine for positions 1, 4, 7, and 8, and D-alanine for positions 2 and 3. Position 6 was not modified, as it is already alanine. Additionally, we prepared D-Thr_5-clovibactin, in which the primary amide group of D-Hyn_5 is replaced with a methyl group (Figure 4.1).[10] This substitution is analogous to an alanine mutation in determining the significance of the side-chain amide group of hydroxyasparagine. To probe the importance of the absolute configuration of clovibactin, we also prepared the enantiomer of clovibactin, *ent*-clovibactin. To probe the importance of the macrolactone ring, we prepared the acyclic analogue, *seco*-clovibactin.

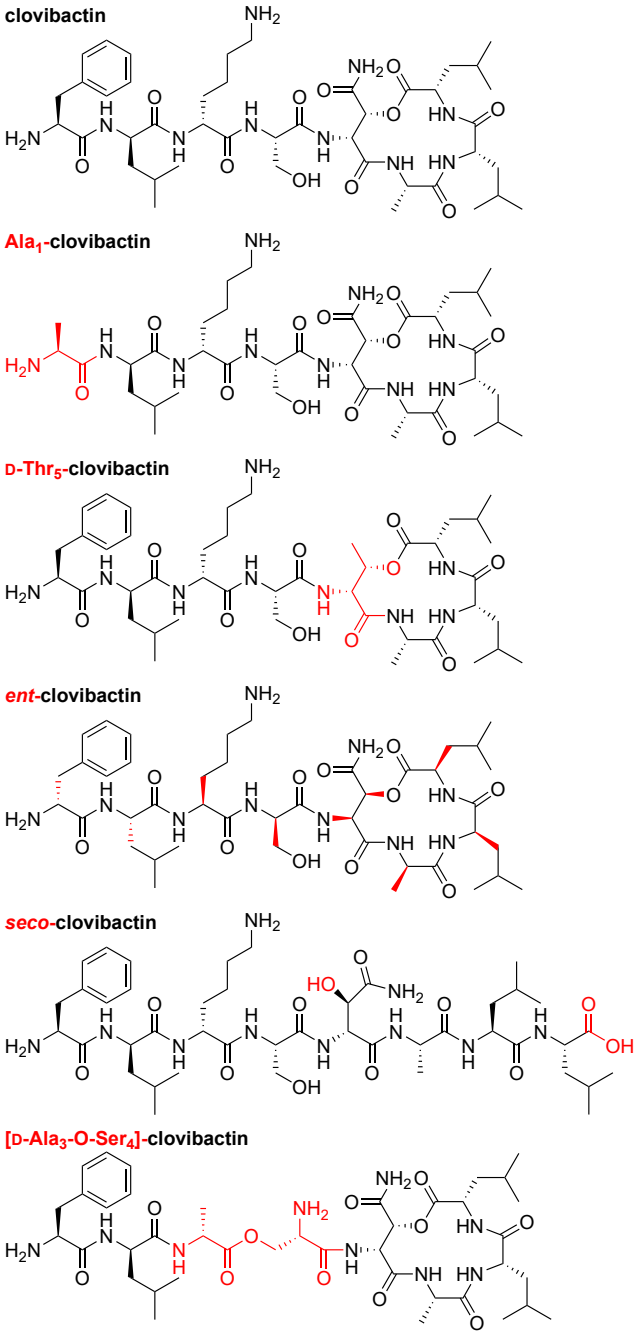

Figure 4.1. Clovibactin and representative analogues for SAR studies.

We synthesized these analogues as the trifluoroacetate (TFA) salts by solid-phase peptide synthesis and solution-phase cyclization as described previously (Scheme 4.2), and we assessed their antibiotic activities against the Gram-positive bacteria *Bacillus subtilis*, *Staphylococcus epidermidis*, methicillin-susceptible *Staphylococcus aureus* (MSSA), and methicillin-resistant

Staphylococcus aureus (MRSA).[9] We used natural clovibactin and vancomycin in these experiments as positive controls and the Gram-negative bacterium *Escherichia coli* as a negative control. Table 4.1 summarizes the minimum inhibitory concentrations (MICs) of the different analogues.

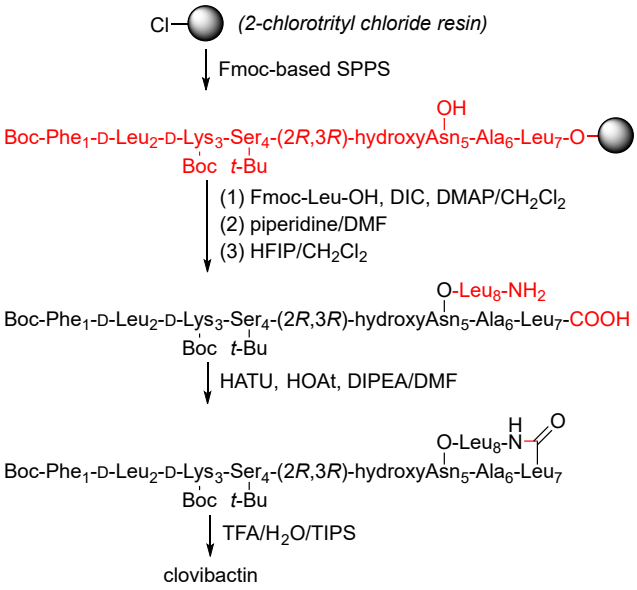

Scheme 4.1. Synthesis of clovibactin.

Table 4.1. MIC values of clovibactin and SAR analogues of clovibactin in μg/mL.

	Bacillus subtilis ATCC 6051	*Staphylococcus epidermidis* ATCC 14990	*Staphylococcus aureus* (MSSA) ATCC 29213	*Staphylococcus aureus* (MRSA) ATCC 700698	*Escherichia coli* ATCC 10798
natural clovibactin	0.0625–0.125	0.5	0.5	0.25	16
synthetic clovibactin	0.125	0.25–0.5	0.5	0.25–0.5	16
Ala_1-clovibactin	2–4	8–16	16	16	>32
D-Ala_2-clovibactin	4–8	16	16–32	32	>32
Ala_4-clovibactin	2	4–8	8	8	32
D-Thr_5-clovibactin	1	2	8	8	>32
Ala_7-clovibactin	0.5–1	4	4	4	>32
Ala_8-clovibactin	16	32	>32	>32	>32
ent-clovibactin	0.5–1	1	1	1–2	16
seco-clovibactin	>32	>32	>32	>32	>32

[D-Ala$_3$-O-Ser$_4$]-clovibactin	>32	>32	>32	>32	>32
D-Thr$_5$-clovibactin diene	0.5	2	4	4	32
stapled D-Thr$_5$-clovibactin	4	8	16	16	>32
N-Me-D-Leu$_2$,D-Thr$_5$-clovibactin	32	>32	>32	>32	>32
vancomycin	0.125–0.25	2	1	4	>32

Clovibactin is highly active against these Gram-positive bacteria, exhibiting MIC values of 0.0625–0.5 μg/mL. Alanine mutation of clovibactin residues 1, 2, 4, 7, or 8 reduces antibiotic activity in all cases, but none of the resulting analogues are completely inactive. Leu$_8$, D-Leu$_2$, and Phe$_1$ are most sensitive to alanine replacement: Replacing Leu$_8$ with alanine resulted in 64–256-fold decreased activity against *B. subtilis* and *S. epidermidis* and loss of activity (MIC >32 μg/mL) against MSSA and MRSA, and replacing Phe$_1$ or D-Leu$_2$ with D-alanine resulted in 16–128-fold decreased activity against all Gram-positive bacteria. Replacing Ser$_4$ or Leu$_7$ with alanine resulted in 8–32-fold decreased activity against all Gram-positive bacteria.

Replacing D-Hyn$_5$ with D-threonine resulted in 4–32-fold decreased activity against the Gram-positive bacteria tested.[10] Thus, the primary amide group of the unusual D-Hyn$_5$ residue is important, but not necessary, for antibiotic activity. The macrolactone ring of clovibactin is critical for antibiotic activity: The acyclic analogue *seco*-clovibactin is completely inactive against all bacteria tested (MIC >32 μg/mL).

The enantiomer of clovibactin exhibits MICs of 0.5–2 μg/mL against the Gram-positive bacteria studied. Although *ent*-clovibactin is 2–8-fold less active than clovibactin, these MIC values are comparable to vancomycin. The activity of *ent*-clovibactin indicates that it is still capable of recognizing the achiral pyrophosphate group of lipid II and related

cell wall precursors; however, interactions with chiral components (such as MurNAc) must also be important for recognition of the target.[1]

We observed modest activity (MIC 16–32 μg/mL) against the Gram-negative bacterium *E. coli* for clovibactin, Ala_4-clovibactin, and *ent*-clovibactin. We have previously observed both natural and synthetic clovibactin to have an MIC of 8 μg/mL against *E. coli* ATCC 10798.[9] Weingarth and coworkers reported natural clovibactin to have an MIC of 64 μg/mL against this same strain of *E. coli*.[1] These differing results may reflect subtle differences in the procedures for the MIC assays.

Weingarth and coworkers recently proposed a model for the mechanism of action of clovibactin.[1] In this model, the four tail residues form an amphiphilic β-strand in which the polar residues (D-Lys_3 and Ser_4) and the nonpolar residues (Phe_1 and D-Leu_2) are displayed on opposite faces. D-Lys_3 and Ser_4 then make hydrogen bond contacts with the pyrophosphate group of lipid II while Leu_2 anchors clovibactin in the bacterial cell membrane. The amide NH groups of the macrolactone ring of clovibactin form hydrogen bonds to lipid II pyrophosphate in a fashion similar to teixobactin.[11,12,13,14] The hydrophobic side chains Ala_6, Leu_7, and Leu_8 on the macrolactone ring form a "hydrophobic glove" that wraps around the pyrophosphate group and facilitates its desolvation while making hydrophobic contacts with the MurNAc group of lipid II and related cell wall precursors.

The structure-activity relationships we have observed against Gram-positive bacteria are largely consistent with the model proposed by Weingarth and coworkers. The reduction in activity upon alanine mutation of Leu_8 and Leu_7 is consistent with reduced ability to form a "hydrophobic glove" and desolvate lipid II pyrophosphate and participate in hydrophobic interactions with the MurNAc group. The reduction in activity upon alanine mutation of Ser_4

is consistent with the importance of proposed polar interactions of the serine OH group with the pyrophosphate group. The reduction in activity upon D-alanine mutation of D-Leu_2 is consistent with the proposed role of D-Leu_2 in membrane anchoring. The reduction in activity upon alanine mutation of Phe_1 suggest that Phe_1 may also be involved in membrane anchoring or important hydrophobic interactions.

Despite repeated attempts, we were unable to synthesize and purify D-Ala_3-clovibactin. We hypothesize that removal of a positive charge renders the peptide insoluble in the aqueous conditions necessary for purification and subsequent MIC assays. Following a strategy previously employed by our laboratory to prepare tractable prodrugs of aggregation-prone teixobactin peptides, we prepared [D-Ala_3-O-Ser_4]-clovibactin, in which the D-Ala_3-Ser_4 peptide linkage is replaced with an *O*-acyl linkage (Figure 4.2).[6,7] Peptides containing *O*-acyl linkages to serine are stable at acidic pH but convert quantitatively to the corresponding amide-linked peptides at neutral pH. [D-Ala_3-O-Ser_4]-clovibactin should thus generate D-Ala_3-clovibactin under the conditions of the MIC assays.[15,16] [D-Ala_3-O-Ser_4]-clovibactin proved completely inactive against all bacteria in the concentration range tested (Table 1). This finding suggests that D-Lys_3 may be important to the antibiotic activity of clovibactin.

X-ray Crystallography

Our group previously reported a model for the conformation and supramolecular assembly of clovibactin based on the X-ray crystallographic structure of a clovibactin epimer.[9] In this model, clovibactin adopts an amphiphilic conformation, with the hydrophobic side chains of Phe_1, D-Leu_2, Ala_6, Leu_7, and Leu_8 on one face of the molecule and the hydrophilic side chains of D-Lys_3, Ser_4, and D-Hyn_5 on the opposite face (Figure 4.2A). The molecules assemble in a linear

head-to-tail fashion, with the amide NH groups of D-Leu$_2$ and D-Lys$_3$ in one molecule hydrogen bonding to the carbonyl groups of Ala$_6$ and Leu$_7$ in an adjacent molecule. We have now prepared an analogue of clovibactin designed to probe the relationship between its conformation and antibiotic activity (stapled D-Thr$_5$-clovibactin) and a second analogue designed to probe the relationship between its supramolecular assembly and antibiotic activity (*N*-Me-D-Leu$_2$,D-Thr$_5$-clovibactin) (Figure 4.3). We incorporated commercially available D-threonine at position 5 instead of (2*R*,3*R*)-3-hydroxyasparagine in these analogues to expedite their syntheses. We have obtained X-ray crystallographic structures of both analogues and determined their MIC values.

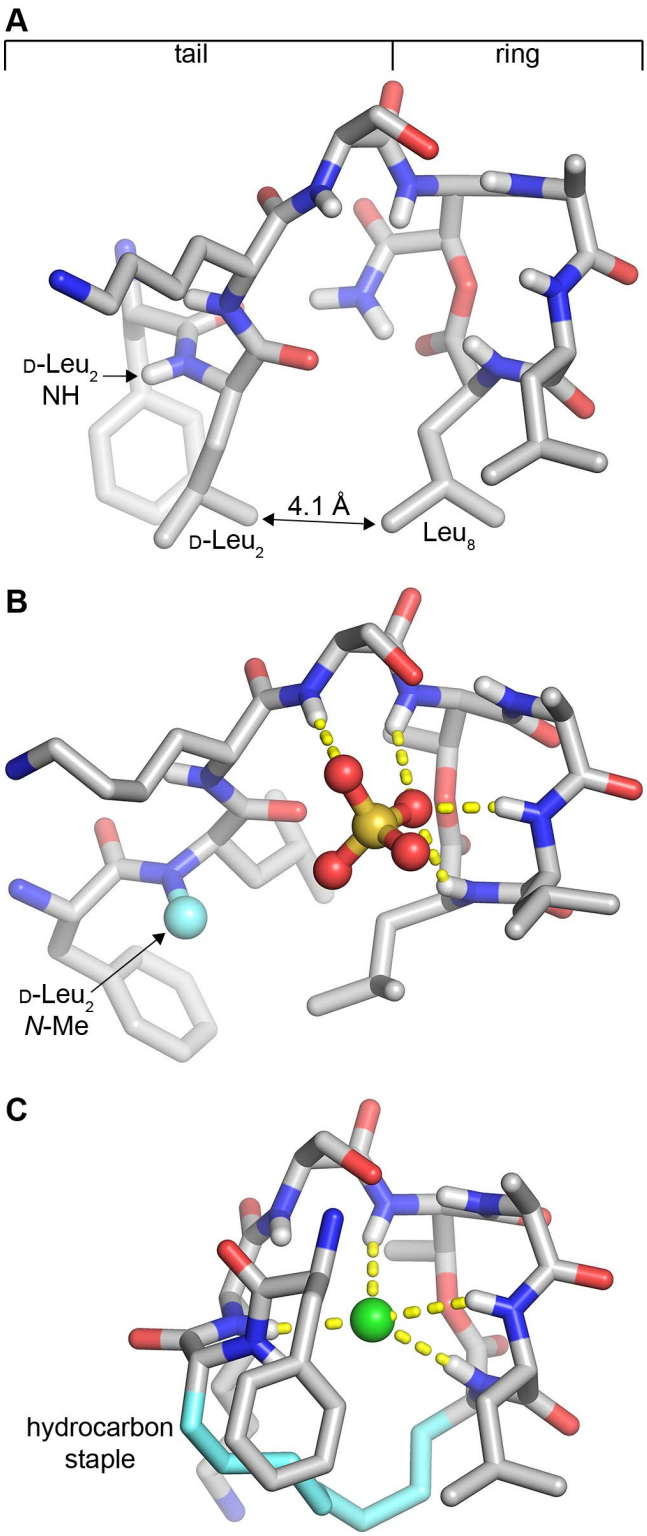

Figure 4.2. Crystallographically based molecular model of clovibactin and X-ray crystallographic structures of *N*-methylated and stapled clovibactin analogues. (A) Crystallographically based molecular model of clovibactin.9 (B) X-ray crystallographic structure of *N*-Me-D-Leu$_2$,D-Thr$_5$-clovibactin bound to a sulfate anion. Eight peptide molecules comprise

the asymmetric unit; a representative molecule is shown. The *N*-Me carbon of *N*-Me-D-Leu$_2$ is highlighted in cyan. Hydrogen bonds are shown as yellow dashed lines. (C) X-ray crystallographic structure of stapled D-Thr$_5$-clovibactin bound to a chloride anion. Three peptide molecules comprise the asymmetric unit; a representative molecule is shown. The hydrocarbon staple is highlighted in cyan.

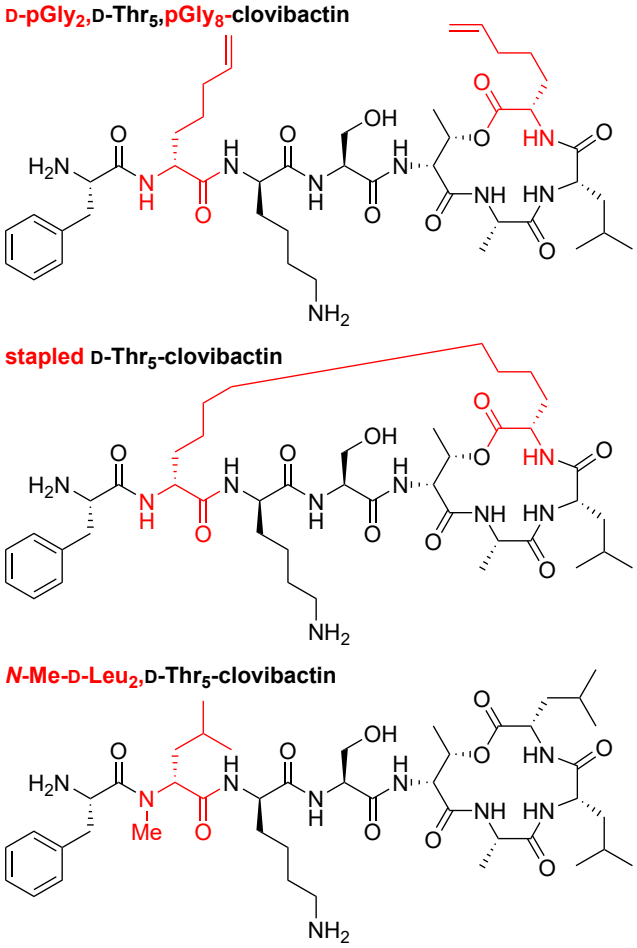

Figure 4.3. D-Thr$_5$-clovibactin analogues.

In our crystallographically based molecular model of clovibactin, the side chains of D-Leu$_2$ and Leu$_8$ are proximal to one another (Figure 4.2A). To help enforce this conformation, we prepared a stapled analogue in which positions 2 and 8 are linked by an eight-carbon chain (stapled D-Thr$_5$-clovibactin, Figure 4.3). We crystallized stapled D-Thr$_5$-clovibactin in conditions containing $MgCl_2$ and determined its X-ray crystallographic structure (Figure 4.2C). Three peptide molecules comprise the asymmetric unit, and each

molecule forms a cage that binds a chloride anion. The macrolactone ring adopts a crownlike conformation in which the amide NH groups of D-Lys$_3$, D-Hyn$_5$, Leu$_7$, and stapled residue 8 form hydrogen bonds with the chelated chloride anion. The amide NH group of Ala$_6$ hydrogen bonds to the side chain oxygen atom of Ser$_4$. We have observed similar ring conformations and anion binding in the X-ray crystallographic structures of four different analogues of teixobactin.[2,4,5,7]

Stapled D-Thr$_5$-clovibactin is 2–4-fold less potent than D-Thr$_5$-clovibactin in MIC assays against the Gram-positive bacteria tested (Table 4.1). The retention of antibiotic activity despite a dramatic change to the overall flexibility of the molecule indicates that a conformation in which residues 2 and 8 are proximal is active. The diene precursor to stapled D-Thr$_5$-clovibactin (D-pGly$_2$,D-Thr$_5$,pGly$_8$-clovibactin, Figure 4.3) is 2-fold more potent than D-Thr$_5$-clovibactin. These results suggest that enforcing proximity between positions 2 and 8, while tolerated, does not enhance antibiotic activity.

In our crystallographically based model of clovibactin assembly, the molecules align such that the amide NH group of D-Leu$_2$ forms an intermolecular hydrogen bond with the carbonyl group of Leu$_7$ in an adjacent molecule (Figure 4.2A).[9] To probe whether the D-Leu$_2$ amide NH group is important for antibiotic activity, we prepared a clovibactin analogue in which the amide NH group of D-Leu$_2$ is *N*-methylated. We crystallized *N*-Me-D-Leu$_2$,D-Thr$_5$-clovibactin in conditions containing $CdSO_4$ and determined its X-ray crystallographic structure (Figure 4.2B). Eight peptide molecules comprise the asymmetric unit (Figure 4.4A, B). The molecules pack through hydrophobic interactions among their side chains and coordinate to Cd^{2+} ions through their *N*-terminal amino groups.

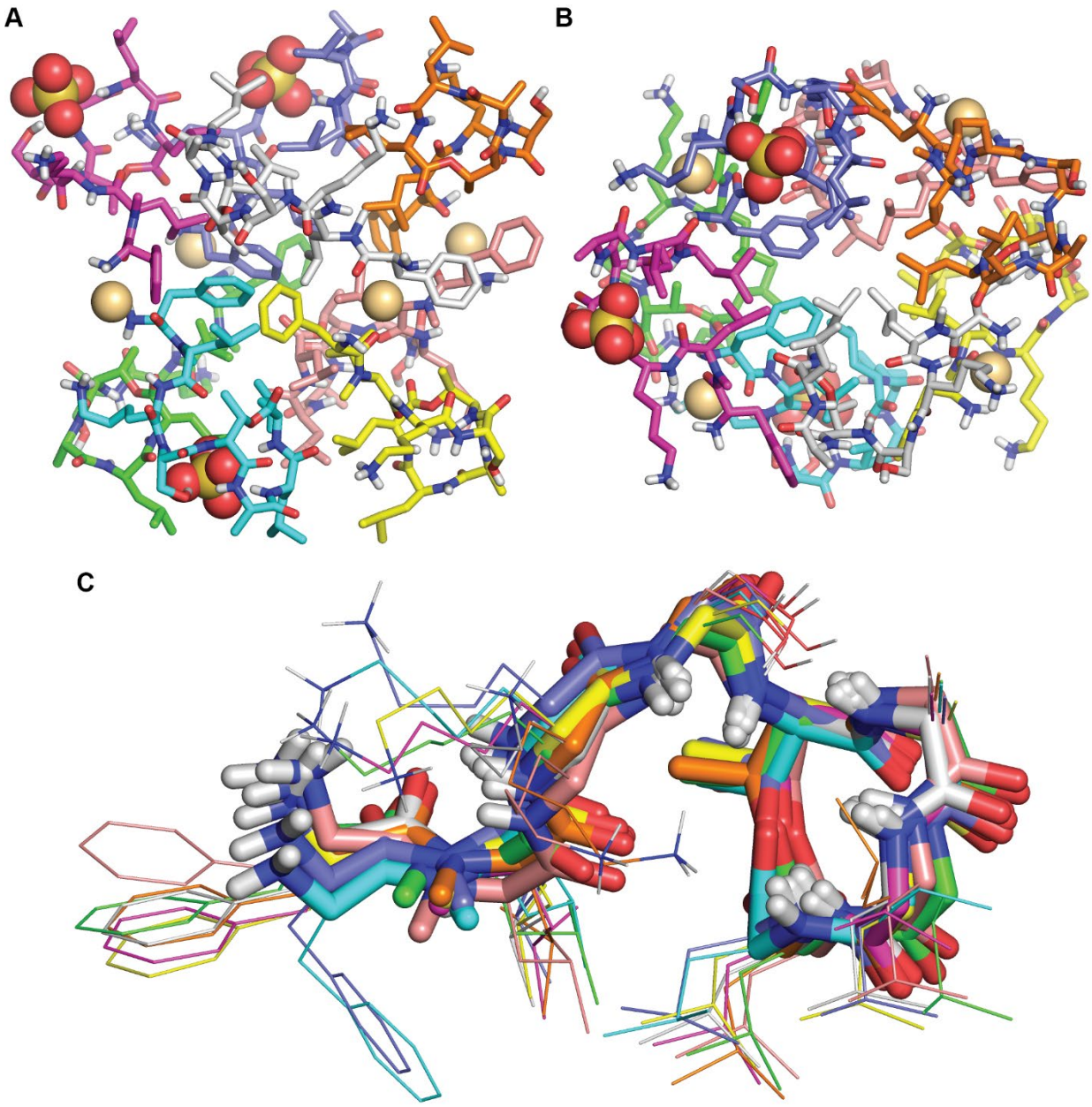

Figure 4.4. X-ray crystallographic structures of *N*-Me-D-Leu$_2$,D-Thr$_5$-clovibactin. (A and B) The asymmetric unit is an octamer. The macrolactone rings of three of the eight monomers bind sulfate anions. Four Cd^{2+} cations bridge the *N*-termini of four individual pairs of monomers. (C) Overlay of all eight monomers. The backbone conformation is very similar in each monomer. The side chains of Phe$_1$, *N*-Me-D-Leu$_2$, D-Lys$_3$, Ser$_4$, Ala$_6$, Leu$_7$, and Leu$_8$ are shown as sticks.

In each of the molecules, the macrolactone ring adopts a crownlike conformation and the NH group of Ala$_6$ hydrogen bonds to the side chain oxygen atom of Ser$_4$ (Figure 4.4C).

Three of the molecules bind sulfate anions, with the backbone NH groups of Ser$_4$, D-Thr$_5$,

Leu$_7$, and Leu$_8$ hydrogen bonding to the oxygen atoms of the sulfate anion. These interactions are similar to how teixobactin binds to the phosphate group of lipid II and related cell wall precursors.[14] All eight molecules share identical conformations of residues 3–8 in the peptide backbone. This backbone conformation is similar to that observed in our previous model of clovibactin assembly, differing only at Phe$_1$ and D-Leu$_2$, presumably due to the *N*-methyl group (Figure 4.5).

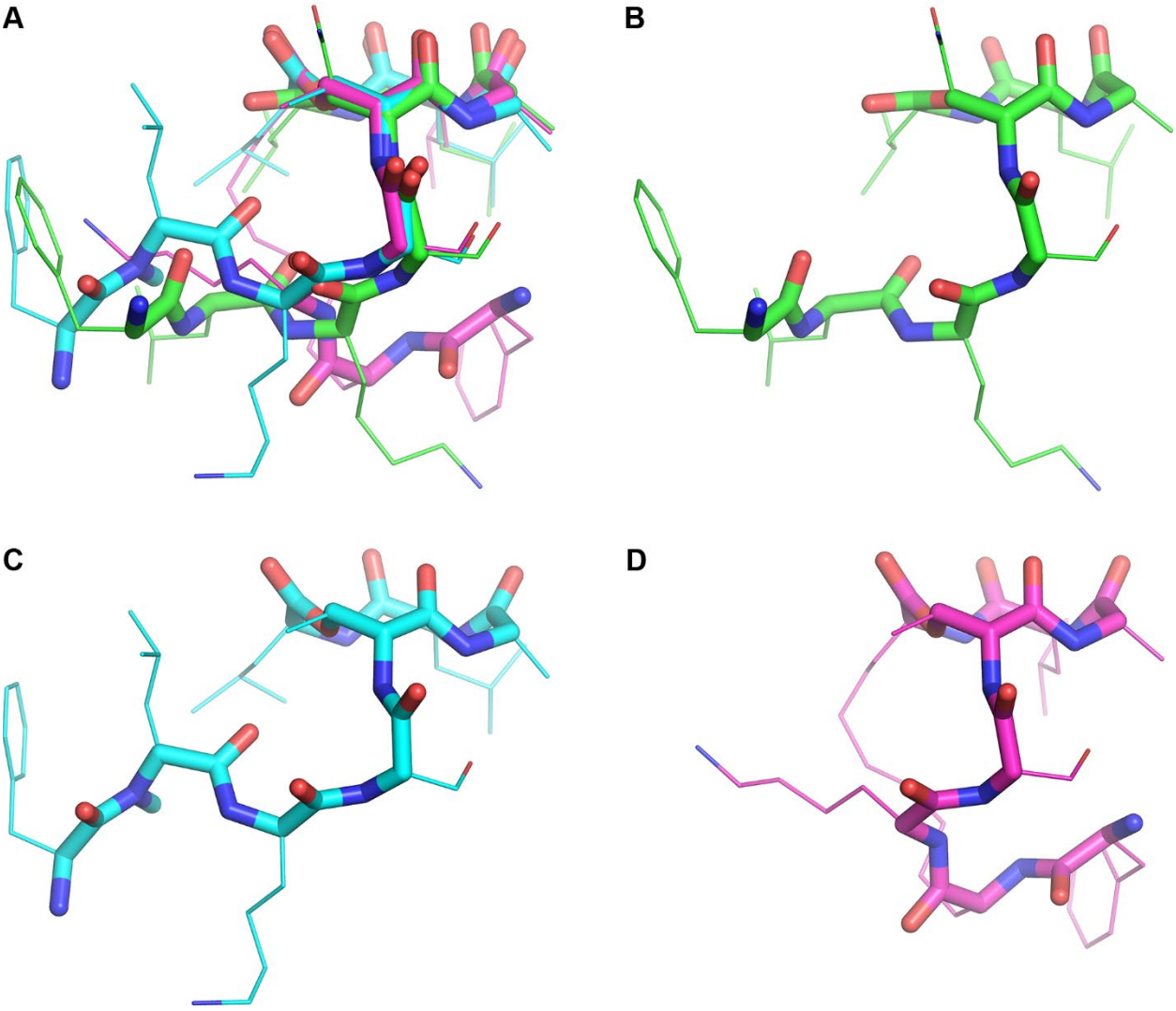

Figure 4.5. Comparison of the backbone conformation of three clovibactin analogue crystal structures, aligned by their macrolactone rings. A representative molecule from the asymmetric unit of each structure is shown. Non-backbone atoms are shown as sticks. (A) Overlay. (B) *Epi*-clovibactin (PDB 8CUG).[1] (C) *N*-Me-D-Leu$_2$,D-Thr$_5$-clovibactin. (D) Stapled D-Thr$_5$-clovibactin.

In an MIC assay, *N*-Me-D-Leu$_2$,D-Thr$_5$-clovibactin is weakly active against *B. subtilis* (MIC = 32 ug/mL) and inactive against all other bacterial strains tested (Table 4.1). This inactivity is consistent with a model in which supramolecular assembly of clovibactin through intermolecular hydrogen bonding of the D-Leu$_2$ amide NH group is important to its antibiotic activity. These findings support both our laboratory's model, in which clovibactin assembles in a linear head-to-tail fashion,[9] and the Weingarth group's model, in which clovibactin forms antiparallel dimers.[1]

Further Study of D-Thr$_5$-clovibactin and Analogues

Aza-D-Thr$_5$-clovibactin

Our laboratory has previously demonstrated that replacement of the macrolactone ring in teixobactin with a macrolactam improves antibiotic activity.[5] We propose that this increase in activity is due to the presence of an additional amide NH hydrogen bond donor in the ring, which increases binding affinity to pyrophosphate anion in lipid II. This hypothesis is supported by a crystallographic structure of a macrolactam teixobactin analogue, in which the additional amide NH group makes a hydrogen bond to chlorine anion. I proposed preparing a similar macrolactam analogue of clovibactin. I prepared aza-D-Thr$_5$-clovibactin using commercially available Fmoc-D-Thr-OH, as with the SAR analogues described previously (Figure 4.6).

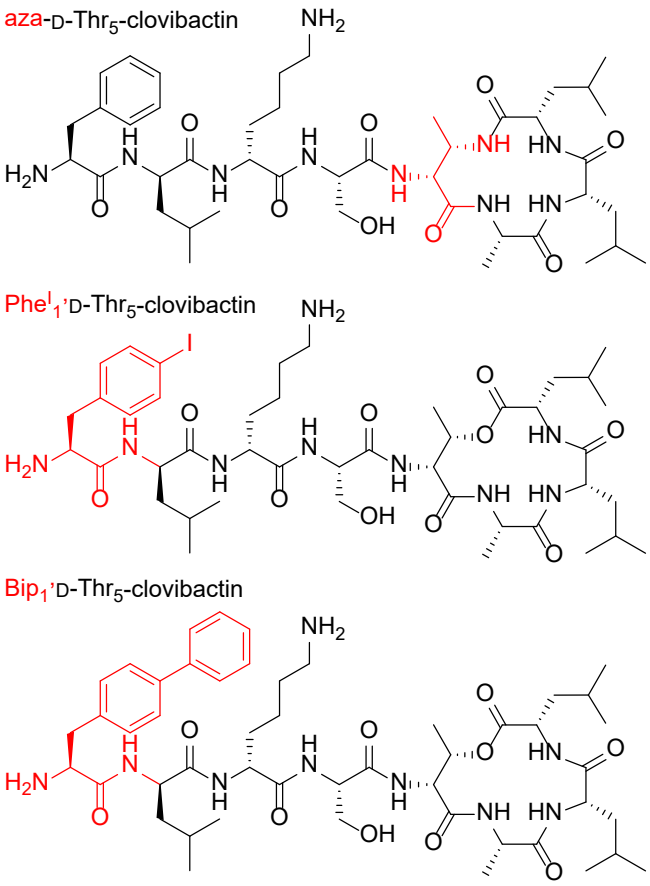

Figure 4.6. Additional D-Thr$_5$-clovibactin analogues.

Aza-D-Thr$_5$-clovibactin was prepared in a similar fashion to aza-teixobactin analogues (Scheme 4.2). Briefly, following resin loading with Ala$_6$ and coupling of side-chain unprotected D-Thr$_5$, the *N*-terminal amino group of the peptide was orthogonally protected with Alloc-Cl, and the β-hydroxyl group of D-Thr$_5$ was mesylated at 4 °C. The threonine oxygen was then substituted for a nitrogen atom by S_N2 with sodium azide in a jacketed peptide coupling vessel with heating to 55 °C. During this step, crown ether must be used to solubilize the sodium azide in DMF. Once the azide was installed, the Alloc group was orthogonally deprotected with $Pd(PPh_3)_4$ and phenylsilane in CH_2Cl_2, and linear peptide coupling continued. Once the linear peptide was constructed, the azide was reduced in modified Staudinger conditions using triphenylphosphine-2-carboxamide.[17] Leu$_8$ was coupled to the newly-revealed aza-D-Thr$_5$ amino

group, followed by Leu$_7$ to complete peptide coupling. Cleavage of the branched peptide from resin followed by cyclization and global side chain deprotection were performed using standard conditions to give crude aza-D-Thr$_5$-clovibactin.

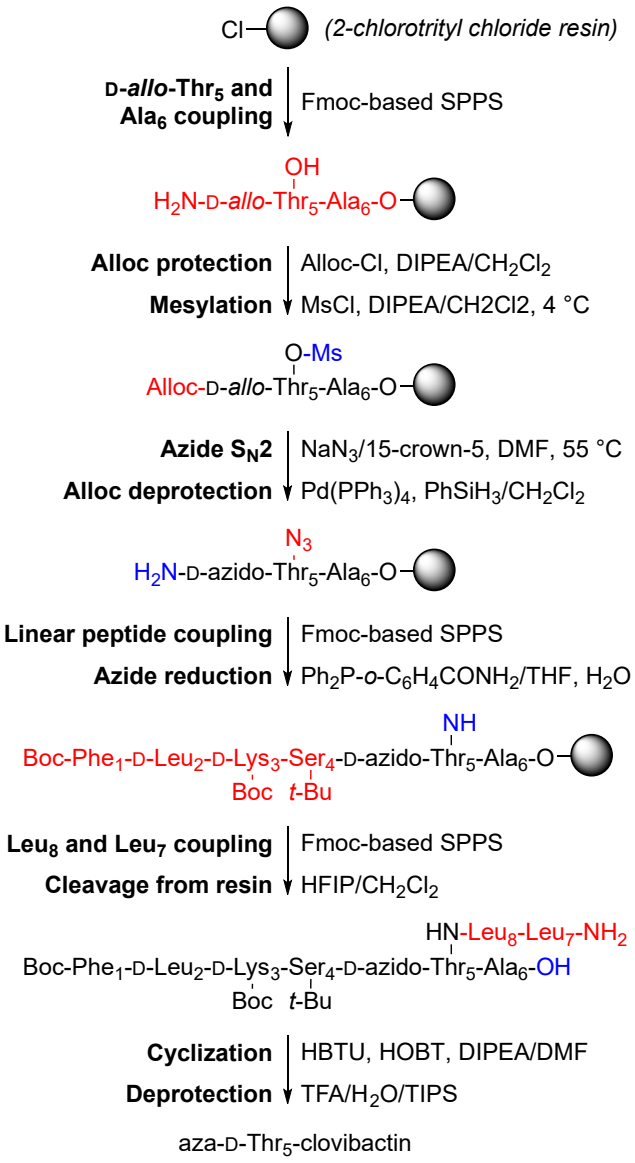

Scheme 4.2. Synthesis of aza-D-Thr$_5$-clovibactin.

Unlike aza-teixobactin and teixobactin, aza-D-Thr$_5$-clovibactin exhibited 2–4-fold reduced antibiotic activity compared to the parent compound D-Thr$_5$-clovibactin (Table 4.2). Furthermore, unlike for teixobactin analogues, the presence or absence of the surfactant

polysorbate 80 (PS80) does not appear to impact MIC values in our assay conditions. In the initial report of teixobactin and subsequent studies of its antibiotic activity, very low concentrations of PS80 (0.002%) are commonly used in the antibiotic peptide stock solutions and bacterial culture media.[18] The surfactant is proposed to reduce either self-aggregation of the peptide or adhering of aggregated peptide to the bottom and walls of the plastic plates used in these assays.[6] The lack of an observed effect in the presence of PS80 may be explained by the shorter clovibactin tail, which is less able than teixobactin to form extended antiparallel β-sheet assemblies. The reduced activity of the lactam analogue compared to the lactone may indicate that the D-Thr$_5$ oxygen atom plays an as-yet undiscovered role in either conformation or target binding, and substitution of this atom for an additional hydrogen bond donor is not beneficial to antibiotic activity.

Table 4.2. MIC values of additional D-Thr$_5$-clovibactin analogues and hypeptin analogues in μg/mL.

	Bacillus subtilis ATCC 6051	*Staphylococcus epidermidis* ATCC 14990	*Escherichia coli* ATCC 10798
D-Thr$_5$-clovibactin	1[a] 0.5–1[b]	2[a] 2–4[b]	>32[a] >32[b]
aza-D-Thr$_5$-clovibactin	2[a] 1–2[b]	8[a] 8[b]	>32[a] >32[b]
Bip$_1$,D-Thr$_5$-clovibactin	0.5–1[b]	2[b]	≥32[b]
hypeptin	0.0625[c]	*NR*[c]	16[c]
Asn$_4$,D-Thr$_5$,Tyr$_6$,Leu$_7$-hypeptin	>32[a]	>32[a]	>32[a]
Ser$_4$,D-Thr$_5$,Tyr$_6$,Leu$_7$-hypeptin[d]	16–32[a]	>32[a]	>32[a]

[a] Assays performed without PS80
[b] Assays performed with 0.002% PS80
[c] The antibiotic activity of hypeptin is reported in ref. 21
[d] Mixture of diastereomers

Additional Crystallography Screening

While the X-ray crystallographic structures of stapled D-Thr$_5$-clovibactin and *N*-Me-D-Leu$_2$,D-Thr$_5$-clovibactin provide interesting insights into how clovibactin may bind lipid II pyrophosphate, these structures differ from previous crystallography of teixobactin in important

ways. First, we are not able to make inferences about supramolecular assembly of clovibactin, as supramolecular assembly is not observed in either of these structures. Second, each structure is made distinct from natural clovibactin in significant ways: For stapled D-Thr$_5$-clovibactin, the binding pocket appears too small for pyrophosphate, and for *N*-Me-D-Leu$_2$,D-Thr$_5$-clovibactin, the parent compound does not have antibiotic activity. In a prior study, our group encountered difficulty obtaining crystals of natural clovibactin, presumably due to hydrolysis of the macrolactone ring.[9] For these reasons, I attempted to obtain a crystallographic structure of D-Thr$_5$-clovibactin.

I screened D-Thr$_5$-clovibactin and aza-D-Thr$_5$-clovibactin in the same conditions as for stapled D-Thr$_5$-clovibactin and *N*-Me-D-Leu$_2$,D-Thr$_5$-clovibactin and observed crystallization in some conditions. Both D-Thr$_5$-clovibactin and aza-D-Thr$_5$-clovibactin crystals grew in conditions containing 19% v/v *tert*-butanol and 0.5 M sodium fluoride buffered to pH 8.8 with Tris. However, even following crystallization condition optimization, none of the obtained crystals produced crystallographic datasets amenable to structure solving. Specifically, the datasets exhibited hallmarks of crystal "twinning," in which multiple orientations of the same crystal lattice grow in parallel to one another; such datasets cannot be solved by traditional methods.[19]

Our group has previously prepared side-chain iodinated teixobactin analogues in order to solve X-ray crystallographic structures using single anomalous diffraction (SAD) phasing.[4] I prepared the iodinated clovibactin analogue Phe$^{I}_1$,D-Thr$_5$-clovibactin and screened for crystallization in the same conditions as for previous analogues (Figure 4.6). Crystals of Phe$^{I}_1$,D-Thr$_5$-clovibactin grew in multiple conditions; however, these crystals grew as dense clusters of very thin needles which could not be mounted for data collection.

Biphenyl D-Thr$_5$-clovibactin (Bip$_1$,D-Thr$_5$-clovibactin)

The most active teixobactin analogue reported thus far extends the hydrophobic area of the *N*-terminal *N*-Me-D-Phe$_1$ residue by mutation to a biphenyl group.[20] Increased hydrophobicity of residue 1 is hypothesized to promote amphiphilic β-strand formation and increase bacterial membrane anchoring. I prepared a biphenyl clovibactin analogue, Bip$_1$,D-Thr$_5$-clovibactin, to investigate whether this same effect is observed in clovibactin (Figure 4.6). The MIC values for Bip$_1$,D-Thr$_5$-clovibactin are comparable to D-Thr$_5$-clovibactin, indicating no benefit to activity from the increased hydrophobic area at residue 1.

Hypeptin-like Peptides

Hypeptin is an eight-residue cyclodepsipeptide antibiotic belonging to the same family as teixobactin and clovibactin (Chapter I).[21,22] Hypeptin contains four unnatural β-hydroxylated amino acids, one of which being the same D-Hyn$_5$ present in clovibactin. The remaining unnatural amino acids — β-hydroxyasparagine$_4$, β-hydroxytyrosine$_6$, and β-hydroxyleucine$_7$ — have no published syntheses. I prepared two analogues of hypeptin containing commercially-available amino acids: non-hydroxylated residues at positions 4, 6, and 7, and either asparagine or serine at position 5 (Figure 4.7) For Ser$_4$,D-Thr$_5$,Tyr$_6$,Leu$_7$-hypeptin, I was not able to separate a mixture of compounds characterized by distinct peaks by analytical HPLC analysis. I hypothesize that these peaks are diastereomers differing in their stereochemistry at the α-carbon of Leu$_8$, which we observe in some synthetic peptides due to epimerization during the on-resin ester-forming step, as only a single mass species is observed an aliquot of peptide containing both diastereomers.[23]

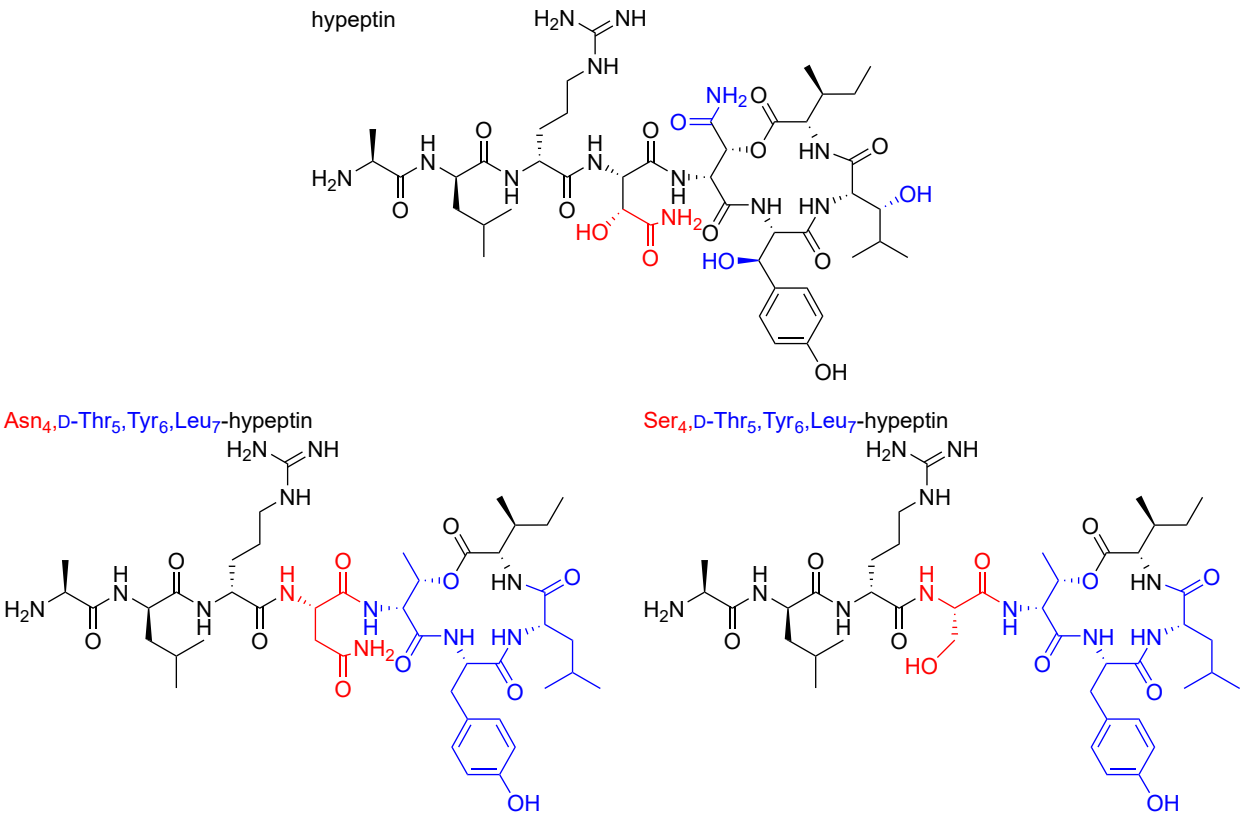

Figure 4.7. Hypeptin and prepared hypeptin analogues.

Hypeptin is reported to have excellent activity against Gram-positive bacterial pathogens, including an MIC of 0.0625 against *B. subtilis*. Asn$_4$,D-Thr$_5$,Tyr$_6$,Leu$_7$-hypeptin is completely inactive against all bacteria in the concentration range tested. A mixture of Ser$_4$,D-Thr$_5$,Tyr$_6$,Leu$_7$-hypeptin diastereomers is similarly inactive against *S. epidermidis* and *E. coli*, but has activity at 16–32 µg/mL against *B. subtilis*. This result implies that one or more of either the side-chain amide group of D-Hyn$_5$ or the β-hydroxyl groups of residues 4, 6, and 7 are necessary for antibiotic activity. This result additionally suggests that, at position 4, the β-hydroxyl group is more important to antibiotic activity than the side-chain amide group.

Investigation of Supramolecular Assembly of D-Thr$_5$-clovibactin and N-Me-D-Leu$_2$,D-Thr$_5$-clovibactin by SDS-PAGE

Clovibactin is proposed to assemble in antiparallel β-sheets and bind with high avidity to lipid II and other bacterial cell wall precursor molecules, similarly to teixobactin.[1] This hypothesis is based on NMR and microscopy characterization of clovibactin fibrils bound to lipid II. I previously prepared and described *N*-Me-D-Leu$_2$,D-Thr$_5$-clovibactin, a clovibactin analogue designed to disrupt the proposed supramolecular assembly by blocking hydrogen-bonding interactions along the linear peptide tail. In addition to MIC and crystallographic characterization of this *N*-methylated analogue, I compared D-Thr$_5$-clovibactin and *N*-Me-D-Leu$_2$,D-Thr$_5$-clovibactin by sodium dodecyl sulfate–polyacrylamide gel electrophoresis (SDS-PAGE) with silver staining (Figure 4.8).

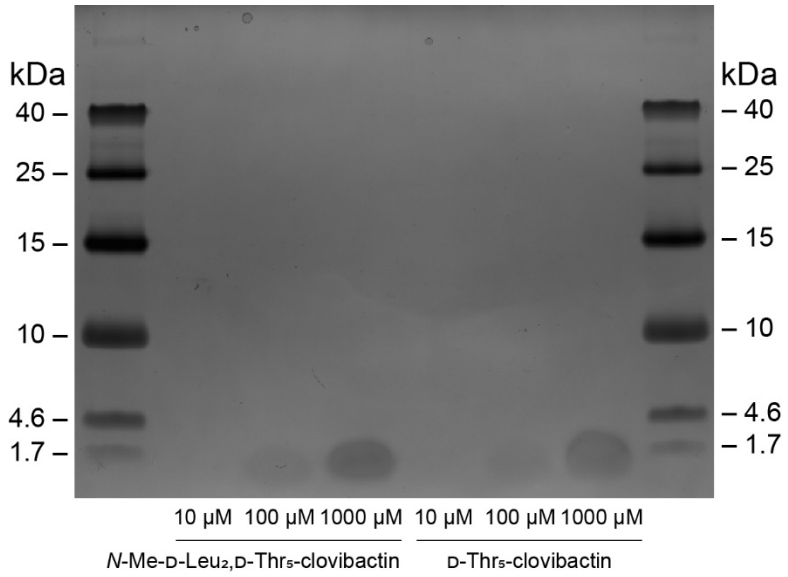

Figure 4.8. SDS-PAGE studies of D-Thr$_5$-clovibactin and *N*-Me-D-Leu$_2$,D-Thr$_5$-clovibactin at various concentrations (10, 100, and 1000 μM). A 10 μL aliquot of each peptide was run on the gel.

Both D-Thr$_5$-clovibactin and *N*-Me-D-Leu$_2$,D-Thr$_5$-clovibactin run below the 1.7 KDa band, consistent with their molecular weights of 874.1 and 888.1 Da, respectively. The bands for both peptides travelled virtually the same distance across the gel and with no streaking, indicating no observable oligomerization or higher supramolecular assembly. Collectively, these

results indicate that supramolecular assembly of neither D-Thr$_5$-clovibactin nor *N*-Me-D-Leu$_2$,D-Thr$_5$-clovibactin is observable by the conditions of SDS-PAGE.

Conclusion

Structure-activity relationship studies of the peptide antibiotic clovibactin provide insights into the roles of various residues in its activity. Replacement of Phe$_1$, D-Leu$_2$, Ser$_4$, D-Hyn$_5$, Leu$_7$, or Leu$_8$ with Ala, D-Ala, or D-Thr indicates that the side chains of these residues are important, but not essential, to the antibiotic activity of clovibactin. The nonpolar residue Leu$_8$, and to a lesser extent Phe$_1$ and D-Leu$_2$, is most important for antibiotic activity. The enantiomer of clovibactin is less active than clovibactin but still exhibits good antibiotic activity against Gram-positive bacteria, while a linear clovibactin analogue with no macrolactone ring is completely inactive. X-ray crystallography of clovibactin analogues shows that the backbone amide NH groups of residues D-Hyn$_5$, Leu$_7$, and Leu$_8$ chelate anions and suggests that clovibactin binds to the pyrophosphate group of lipid II and related cell wall precursors through similar hydrogen-bonding interactions. Conversion of the clovibactin macrolactone to a macrolactam appears to decrease activity. The results of the alanine scan and other SAR studies should facilitate the development of additional analogues of clovibactin with improved pharmacological properties.

Supporting Information for Chapter IV

Supplementary Tables

Table S4.1. Dihedral angles of *epi*-clovibactin (PDB 8CUG), *N*-Me-D-Leu$_2$,D-Thr$_5$-clovibactin, and stapled D-Thr$_5$-clovibactin. The angles provided correspond to the representative molecules depicted in Figure 4.5.

***epi*-clovibactin**			***N*-Me-D-Leu$_2$,D-Thr$_5$-clovibactin**			**stapled D-Thr$_5$-clovibactin**		
Residue	**Phi**	**Psi**	**Residue**	**Phi**	**Psi**	**Residue**	**Phi**	**Psi**
Phe$_1$	*NA*	159	Phe$_1$	*NA*	143	Phe$_1$	*NA*	155
D-Leu$_2$	76	29	*N*-Me-D-Leu$_2$	119	-34	D-pGly$_2$	80	20
D-Lys$_3$	89	-156	D-Lys$_3$	77	-157	D-Lys$_3$	120	4
Ser$_4$	-84	-17	Ser$_4$	-71	-24	Ser$_4$	-70	-32
(2*R*,3*S*)-Hyn$_5$	107	-10	D-Thr$_5$	110	-15	D-Thr$_5$	111	-16
Ala$_6$	-69	-66	Ala$_6$	-64	-63	Ala$_6$	-64	-42
Leu$_7$	-75	-49	Leu$_7$	-78	-41	Leu$_7$	-100	-51
Leu$_8$	-128	13	Leu$_8$	-123	-35	pGly$_8$	-103	-40

Table S4.2. Crystallographic properties, crystallization conditions, and data collection and model refinement statistics for stapled D-Thr$_5$-clovibactin (CCDC 2358085).

peptide	stapled D-Thr$_5$-clovibactin
CCDC ID	2358085
Empirical formula	C_{43} H_{70} Cl N_9 O_{10} • 7(H_2O)
Formula weight	1034.64
Temperature	93(2) K
Wavelength	1.54178 Å
Crystal system	Orthorhombic
Space group	$P2_12_12_1$
Unit cell dimensions	a = 11.4938(4) Å b = 35.8430(15) Å c = 40.0966(15) Å
Volume	16518.7(11) Å^3
Z	12
Density (calculated)	1.248 Mg/m^3
Absorption coefficient	1.227 mm^{-1}
F(000)	6696
Crystal color	colorless
Crystal size	0.130 x 0.110 x 0.110 mm^3
Theta range for data collection	2.525 to 68.428°
Index ranges	$-13 \leq h \leq 11$, $-42 \leq k \leq 43$, $-48 \leq l \leq 48$
Reflections collected	200977
Independent reflections	30211 [R(int) = 0.1388]
Completeness to theta = 67.679°	100.0 %
Absorption correction	Semi-empirical from equivalents
Max. and min. transmission	0.8643 and 0.5732
Refinement method	Full-matrix least-squares on F^2
Data / restraints / parameters	30211 / 0 / 871
Goodness-of-fit on F^2	1.078
Final R indices [I>2sigma(I) = 27142 data]	R1 = 0.1137, wR2 = 0.2642
R indices (all data, 0.83 Å)	R1 = 0.1237, wR2 = 0.2716
Absolute structure parameter	0.079(7)
Largest diff. peak and hole	2.039 and -0.732 e.Å^{-3}
crystallization conditions	0.2 M magnesium chloride hexahydrate and 25% w/v PEG 3,350 buffered to pH 8.5 with 0.1 M Tris

Table S4.3. Crystallographic properties, crystallization conditions, and data collection and model refinement statistics for *N*-Me-D-Leu$_2$,D-Thr$_5$-clovibactin (PDB ID 9BIC).

peptide	*N*-Me-D-Leu$_2$,D-Thr$_5$-clovibactin
PDB ID	9BIC
space group	$P22_12_1$
a, *b*, *c* (Å)	23.504 47.773 54.078
α, β, λ (°)	90, 90, 90
molecules per asymmetric unit	8
wavelength (Å)	1.54
resolution (Å)	27.04–2.05 (2.21–2.05)
total reflections	108880 (18464)
unique reflections	4452 (866)
multiplicity	24.5 (21.3)
completeness (%)	100.00 (100.00)
mean I/σ(I)	21.19 (14.64)
Wilson B factor	9.67
R_{merge}	0.2555 (0.2541)
$R_{measure}$	0.261 (0.2603)
$CC_{1/2}$	0.846 (0.94)
CC^*	0.958 (0.984)
R_{work}	0.1549 (0.1521)
R_{free}	0.2037 (0.2251)
number of non-hydrogen atoms	602
RMS_{bonds}	0.124
RMS_{angles}	4.47
Ramachandran favored (%)	75.00
Ramachandran allowed (%)	25.00
Ramachandran outliers (%)	0
rotamer outliers (%)	3.12
clashscore	0.90
average B-factor	14.36
macromolecules	12.90
ligands/ions	16.38
solvent	17.58
crystallization conditions	0.05 M cadmium sulfate hydrate and 1.0 M sodium acetate trihydrate buffered to pH 7.5 with 0.1 M HEPES

Materials and Methods

Chemicals and Supplies

All chemicals were used as received unless otherwise noted. Dry methylene chloride (CH_2Cl_2), tetrahydrofuran (THF), methanol (MeOH), and *N*,*N*-dimethylformamide (DMF) were obtained by passing through alumina under argon prior to use. 1,4-Dioxane (dioxane) was used without added stabilizers. Anhydrous, amine-free *N*,*N*-dimethylformamide (DMF), DIPEA, 2,4,6-collidine, and piperidine were purchased from Alfa Aesar. HPLC-grade acetonitrile and deionized water (18 MΩ), each containing 0.1% trifluoroacetic acid (TFA), were used for analytical and preparative reverse-phase HPLC, as well as reverse-phase flash chromatography using a Biotage® Isolera One flash column chromatography instrument; normal-phase flash chromatography was performed using CH_2Cl_2 and MeOH. Deionized water (18 MΩ) was obtained from a Barnstead NANOpure Diamond water purification system. Commercial agents were used without purification, unless otherwise stated. All amino acids, coupling agents, 2-chlorotrityl chloride resin, DIC, and triisopropylsilane were purchased from Chem-Impex.

Instrumentation

Bacteria were incubated in a Thermo Fisher Scientific MaxQ Shaker 6000. Analytical reverse-phase HPLC was performed on an Agilent 1260 Infinity II instrument equipped with a Phenomonex bioZen PEPTIDE 2.6 um XB-C18 column (150 x 4.6 mm), eluting with a gradient of acetonitrile and water (each containing 0.1% TFA) from 5–100% over 20 minutes. Peptides were first purified on a Biotage Isolera One flash column chromatography instrument with a Biotage® SfarBio C18 D – Duo 300 Å 20 µm 25 g column. Peptides were then further purified by preparative reverse-phase HPLC on a Shimadzu equipped with an Agilent Zorbax 7 µm 300SB-C18 column (21.2 x 250 mm). All peptides were prepared and used as the trifluoroacetate

(TFA) salts and were assumed to have one trifluoroacetic acid molecule per amine group on each peptide. Natural clovibactin was provided by NovoBiotic Pharmaceuticals LLC as the trifluoroacetate (TFA) salt. SDS-PAGE gel images were obtained using a Bio-Rad ChemiDoc MP Imaging System. Peptide mass spectrometry was performed using an AB Sciex 5800 MALDI TOF/TOF or Waters Xevo TQ Absolute with Acquity UPLC Premier.

Synthesis of Peptides

Synthesis of Clovibactin and Alanine Scan Analogues of Clovibactin

Peptide synthesis procedure. Alanine scan analogues of clovibactin were synthesized by manual solid-phase peptide synthesis of the corresponding linear peptide on 2-chlorotrityl resin, followed by on-resin esterification, solution-phase cyclization, deprotection, and purification. A step-by-step procedure is detailed below.

a. Loading the resin. 2-Chlorotrityl chloride resin (300 mg, 1.42 mmol/g) was added to a Bio-Rad Poly-Prep chromatography column (10 mL). Dry CH_2Cl_2 (8 mL) was used to suspend and swell the resin for 30 min with gentle rocking. After the solution was drained from the resin, a separate solution of Fmoc-Leu-OH (75 mg, 0.7 equiv., 0.21 mmol) or Fmoc-Ala-OH (65 mg, 0.7 equiv., 0.21 mmol) in 6% (v/v) 2,4,6-collidine in dry CH_2Cl_2 (8 mL) was added, and the suspension was gently rocked for 12–16 h. The solution was then drained, and a mixture of CH_2Cl_2/CH_3OH/*N*,*N*-diisopropylethylamine (DIPEA) (17:2:1, 8 mL) was added immediately. The resin was gently rocked for 1 h to cap the unreacted 2-chlorotrityl chloride resin sites. The resin was then washed three times with dry CH_2Cl_2 and dried by passing nitrogen through the vessel. This procedure typically yields 0.15–0.20 mmol of loaded resin, as assessed by spectrophotometric analysis.[24]

b. Manual peptide coupling. The loaded resin was suspended in dry DMF and then

transferred to a solid-phase peptide synthesis vessel. Residues 6 through 1 were manually coupled using Fmoc-protected amino acid building blocks. Fmoc-Ala-OH, Fmoc-(2*R*,3*R*)-3-hydroxyAsn-OH, Fmoc-Ser(*t*-Bu)-OH or Fmoc-Ala-OH, Fmoc-D-Lys(Boc)-OH or Fmoc-D-Ala-OH, Fmoc-D-Leu-OH or Fmoc-D-Ala-OH, and Boc-Phe-OH or Boc-Ala-OH were coupled through the following cycles: *i*. Fmoc-deprotection with 20% (v/v) piperidine in DMF (5 mL) for 10–20 min at room temperature, *ii*. washing with dry DMF (3 x 5 mL), *iii*. coupling of the amino acid (4 equiv.) with HCTU (4 equiv.) for commercial amino acids or HATU (4 equiv.) for Fmoc-(2*R*,3*R*)-3-hydroxyAsn-OH in 20% (v/v) 2,4,6-collidine in dry DMF (5 mL) for 30–60 min, and *iv.* washing with dry DMF (3 x 5 mL). The last amino acid coupling of the linear sequence is Boc-Phe-OH or Boc-Ala-OH, which intentionally protects the *N*-terminus from being reactive during the esterification step and cyclization steps. The resin was then transferred to a clean Bio-Rad PolyPrep chromatography column.

c. *Esterification.* In a test tube, Fmoc-Leu-OH (10 equiv.) or Fmoc-Ala-OH (10 equiv.) and diisopropylcarbodiimide (10 equiv.) were dissolved in dry CH_2Cl_2 (5 mL). The resulting solution was filtered through a 0.20-μm nylon filter, and 4-dimethylaminopyridine (1 equiv.) was added to the filtrate. The resulting solution was transferred to the resin and gently agitated for 1 h. The solution was then drained, and the resin was washed with dry CH_2Cl_2 (3 x 5 mL) and DMF (3 x 5 mL).

d. *Fmoc deprotection of* Leu_8 *or* Ala_8. The Fmoc protecting group on Leu_8 or Ala_8 was removed by adding 20% (v/v) piperidine in DMF for 30 min. The solution was drained, and the resin was washed with dry DMF (3 x 5 mL) and CH_2Cl_2 (3 x 5 mL).

e. *Cleavage of the linear peptide from chlorotrityl resin*. The linear peptide was cleaved from the resin by rocking the resin in a solution of 20% (v/v) 1,1,1,3,3,3-hexafluoroispropanol

(HFIP) in CH_2Cl_2 (8 mL) for 1 h. The suspension was filtered, and the filtrate was collected in a 250-mL round-bottomed flask. The resin was washed with additional cleavage solution (8 mL) for 30 min and filtered into the same 250 mL round bottom-bottomed flask. The combined filtrates were concentrated by rotary evaporation and further dried by vacuum pump to afford the crude protected linear peptide, which was cyclized without further purification.

f. Cyclization of the linear peptide. The crude protected linear peptide was dissolved in dry DMF (125 mL). HOAt (6 equiv.) and HATU (6 equiv.) were dissolved in 8 mL of dry DMF in a test tube. The HOAt/HATU solution was then added to the round-bottom flask containing the dissolved peptide and the mixture was stirred at room temperature for 30 min. Diisopropylethylamine (300 μL) was added to the round-bottom flask containing the dissolved peptide and the mixture was stirred for an additional 16–20 h. The reaction mixture was concentrated by rotary evaporation and further dried by vacuum pump to afford the crude protected cyclized peptide, which was immediately subjected to global deprotection.

g. Global deprotection of the cyclic peptide. The protected cyclic peptides were dissolved in TFA:triisopropylsilane (TIPS):H_2O (18:1:1, 10 mL) in a 250-mL round-bottomed flask equipped with a stir bar. The solution was stirred for 1 h. During the 1 h deprotection, two 50-mL conical tubes containing 40 mL of dry Et_2O each were chilled on ice. After the 1 h deprotection, the peptide solution was split between the two conical tubes of chilled Et_2O. The tubes were then centrifuged at 600x*g* for 10 min and decanted. The pelleted peptides were dried under air for 15–20 min. The deprotected cyclic peptide was then purified by reverse-phase HPLC (RP-HPLC).

h. Reverse-phase HPLC purification. The peptide was dissolved in 20% CH_3CN in H_2O (5 mL) and pre-purified on a Biotage Isolera One flash chromatography instrument equipped

with a Biotage® Sfär Bio C18 D - Duo 300 Å 20 µm 25 g column. The solution of crude cyclic peptide was injected at 20% CH_3CN and eluted with a gradient of 20–40% CH_3CN. The fractions containing the desired peptide were concentrated by rotary evaporation, diluted in 20% CH_3CN, injected on a Shimadzu instrument, and eluted over a gradient of 20–40% CH_3CN over 80 min. The collected fractions were analyzed by analytical HPLC and LC-MS, and the pure fractions were concentrated by rotary evaporation and lyophilized. These procedures typically yielded 5 mgs (~1 % yield) of synthetic peptides as the TFA salts.

Synthesis of D*-Thr$_5$-clovibactin*

D-Thr$_5$-clovibactin was prepared in the same way as the alanine scan analogues, with the following modification: Fmoc-D-Thr-OH was used in place of Fmoc-(2*R*,3*R*)-hydroxyAsn-OH.

*Synthesis of [*D*-Ala$_3$-O-Ser$_4$]-clovibactin*

[D-Ala$_3$-O-Ser$_4$]-clovibactin was prepared in the same way as the alanine scan analogues, with the following modification: Boc-Ser(Fmoc-D-Ala)-OH was used in place of Fmoc-Ser(Boc)-OH and Fmoc-D-Ala-OH. Boc-Ser(Fmoc-D-Ala)-OH was prepared according to the method described by Kiso and coworkers.[25]

*Synthesis of N-Me-*D*-Leu$_{2,}$*D*-Thr$_5$-clovibactin*

N-Me-D-Leu$_2$,D-Thr$_5$-clovibactin was prepared in the same way as D-Thr$_5$-clovibactin, with the following modification: Fmoc-*N*-Me-D-Leu-OH was used in place of Fmoc-D-Leu-OH.

*Synthesis of Phe$^I{}_{1,}$*D*-Thr$_5$-clovibactin*

Phe$^I{}_1$,D-Thr$_5$-clovibactin was prepared in the same way as D-Thr$_5$-clovibactin, with the following modification: Boc-Phe^I-OH was used in place of Boc-Phe-OH.

*Synthesis of Bip$_{1,}$*D*-Thr$_5$-clovibactin*

Bip$_1$,D-Thr$_5$-clovibactin was prepared in the same way as D-Thr$_5$-clovibactin, with the following modification: Boc-Bip-OH was used in place of Boc-Phe-OH.

Synthesis of Asn$_{4,D}$-Thr$_5$,Tyr$_6$,Leu$_7$-hypeptin

Asn$_4$,D-Thr$_5$,Tyr$_6$,Leu$_7$-hypeptin was prepared in the same way as D-Thr$_5$-clovibactin, with the following modifications: (1) Fmoc-Asn(Trt)-OH and Tyr(*t*-Bu)-OH were used in place of Fmoc-Ser(*t*-Bu)-OH and Fmoc-Ala-OH during linear amino acid coupling, respectively. (2) Fmoc-Ile-OH was used in place of Fmoc-Leu-OH during the esterification step.

Synthesis of Ser$_{4,D}$-Thr$_5$,Tyr$_6$,Leu$_7$-hypeptin

Ser$_4$,D-Thr$_5$,Tyr$_6$,Leu$_7$-hypeptin was prepared in the same way as Asn$_4$,D-Thr$_5$,Tyr$_6$,Leu$_7$-hypeptin, with the following modification: Fmoc-Ser(*t*-Bu)-OH was used in place of Fmoc-Asn(Trt)-OH.

MIC Assays

Preparing the Peptide Stocks

Solutions of clovibactin and clovibactin analogues were prepared gravimetrically by dissolving an appropriate amount of peptide in an appropriate volume of sterile DMSO to make 20 mg/mL stock solutions. The stock solutions were stored at -20 °C for subsequent experiments.

Preparation and Tray Setup

Bacillus subtilis (ATCC 6051), *Staphylococcus epidermidis* (ATCC 14990), *Staphylococcus aureus* (MSSA) (ATCC 29213), and *Escherichia coli* (ATCC 10798) were cultured from glycerol stocks in Mueller-Hinton broth overnight in a shaking incubator at 37 °C. *Staphylococcus aureus* (MRSA) (ATCC 700698) was cultured from a glycerol stock in brain heart infusion broth overnight in a shaking incubator at 37 °C. Aliquots of the 20 mg/mL antibiotic stock solutions were diluted with pipette mixing to make a 64 μg/mL solution with

Mueller-Hinton broth and a 64 μg/mL solution with brain heart infusion broth. A 200-μL aliquot of the 64 μg/mL solution was transferred to a 96-well plate and mixed by pipetting. Two-fold serial dilutions were made with media and pipette mixing across a 96-well plate to achieve a final volume of 100 μL in each well. These solutions had the following concentrations: 64, 32, 16, 8, 4, 2, 1, 0.5, 0.25, 0.125, and 0.0625 μg/mL. The overnight cultures of each bacterium were diluted with Mueller-Hinton broth to an OD_{600} of 0.075 as measured for 200 μL in a 96-well plate. The diluted mixtures were further diluted to 1×10^6 CFU/mL with the appropriate media.[24] A 100-μL aliquot of the 1×10^6 CFU/mL bacterial solution was added to each well in 96-well plates, resulting in final bacteria concentrations of 5×10^5 CFU/mL in each well. As 100 μL of bacteria were added to each well, clovibactin and clovibactin analogues were also diluted to the following concentrations: 32, 16, 8, 4, 2, 1, 0.5, 0.25, 0.125, 0.0625, and 0.03125 μg/mL. The plate was covered with a lid and incubated at 37 °C for 16 h. The optical density measurements were recorded at 600 nm and were measured using a 96-well UV/vis plate reader (MultiSkan GO, Thermo Scientific). The MIC values were taken as the lowest concentration that had no bacteria growth ($OD_{600} < 0.0100$). Each MIC assay was run in triplicate to ensure reproducibility.

X-ray Crystallography

X-ray crystallography of stapled D-Thr$_5$-clovibactin

Crystallization of stapled D-Thr$_5$-clovibactin. The hanging-drop vapor-diffusion method was used to determine initial crystallization conditions for stapled D-Thr$_5$-clovibactin. Each peptide was screened in 96-well plate format using seven crystallization kits (Crystal Screen, Index, and PEG/ION from Hampton Research; and Morpheus, MemSys, MemPlus, and PGA from Molecular Dimensions). A TTP LabTech Mosquito nanodisperse was used to make

three 150 nL hanging drops for each well condition. The three hanging drops differed in the ratio of peptide to well solution for each condition in the 96-well plate. A 10 mg/mL solution of stapled D-Thr$_5$-clovibactin peptide in deionized water was combined with a well solution in ratios of 1:1, 1:2, and 2:1 peptide:well solution at appropriate volumes to create the three 150 nL hanging drops. Crystals of stapled D-Thr$_5$-clovibactin grew in well conditions of 0.2 M magnesium chloride hexahydrate and 25% w/v polyethylene glycol (PEG) 3,350 buffered to pH 8.5 with 0.1 M Tris.

Crystallization conditions for stapled D-Thr$_5$-clovibactin were optimized using a 4 x 6 matrix Hampton 24-well plate. For stapled D-Thr$_5$-clovibactin, the pH of the Tris buffer was varied in each row (7.5, 8.0, 8.5, and 9.0). The concentration of PEG 3,350 in each column was varied in increments of 2 % w/v (19, 21, 23, 25, 27, 29). Three hanging-drops were prepared on borosilicate glass slides by combing a 10 mg/mL solution of stapled D-Thr$_5$-clovibactin in deionized water with the well solution in the following amounts: 1 µL:1 µL, 2 µL:1 µL, and 1 µL:2 µL. Slides were inverted and pressed firmly against the silicone grease surrounding each well.

Data collection, data processing, and structure determination. A colorless crystal of approximate dimensions 0.110 x 0.110 x 0.130 mm was mounted in a cryoloop and transferred to a Bruker X8 Prospector diffractometer system. The APEX3[26] program package was used to determine the unit-cell parameters and for data collection (10-20 sec/frame scan time). The raw frame data was processed using SAINT[27] and SADABS[28] to yield the reflection data file. Subsequent calculations were carried out using the SHELXTL[29] program package. The diffraction symmetry was *mmm* and the systematic absences were consistent with the orthorhombic space group $P2_12_12_1$ that was later determined to be correct.

The structure was solved by direct methods and refined on F2 by full-matrix least-squares techniques. The analytical scattering factors[30] for neutral atoms were used throughout the analysis. Hydrogen atoms were included using a riding model. There were three molecules of the formula-unit present. There were at least seven (7) water molecules present per formula-unit. The hydrogen atoms associated with the water molecules were not included in the refinement.

Least squares analysis yielded wR2 = 0.2716 and Goof = 1.078 for 871 variables refined against 30211 data (0.83 Å), R1 = 0.1137 for those 27142 data with I > 2.0σ(I). The absolute structure was assigned by refinement of the Flack parameter.[31] Data collection and refinement statistics are shown in Table S4.2.

X-ray crystallography of N-Me-D-Leu$_{2}$,D-Thr$_{5}$-clovibactin

Crystallization of N-Me-D-Leu$_{2}$,D-Thr$_{5}$-clovibactin. Initial crystallization conditions for *N*-Me-D-Leu$_{2}$,D-Thr$_{5}$-clovibactin were determined in the same manner as for stapled D-Thr$_{5}$-clovibactin. Crystals of *N*-Me-D-Leu$_{2}$,D-Thr$_{5}$-clovibactin grew in well conditions of 0.05 M cadmium sulfate hydrate and 1.0 M sodium acetate trihydrate buffered to pH 7.5 with 0.1 M HEPES.

Crystallization conditions for *N*-Me-D-Leu$_{2}$,D-Thr$_{5}$-clovibactin were optimized in the same manner as for hydrocarbon-stapled D-Thr$_{5}$-clovibactin. For *N*-Me-D-Leu$_{2}$,D-Thr$_{5}$-clovibactin, the pH of the HEPES buffer was varied in each row (7.2, 7.5, 7.8, and 8.1). The concentration of sodium acetate trihydrate in each column was varied in increments of 0.2 M (0.6, 0.8, 1.0, 1.2, 1.4, 1.6).

Data collection, data processing, and structure determination. Diffraction data for *N*-Me-D-Leu$_{2}$,D-Thr$_{5}$-clovibactin were collected on a Rigaku Micromax-007HF X-ray diffractometer with a rotating copper anode at 1.54 Å wavelength with 0.5° oscillation.

Diffraction data were collected using CrystalClear. Diffraction data were scaled and merged using XDS and pointless and aimless.[32] Coordinates for the anomalous signals from cadmium were determined using HySS and then used in Autosol in the Phenix software suite to generate an electron density map.[33] Molecular manipulations of the model were performed with Coot.[34] Coordinates were refined with phenix.refine.[35,36] The optimal number and composition of the TLS groups were chosen automatically by phenix.refine. Data collection and refinement statistics are shown in Table S4.3.

X-ray crystallography of D*-Thr*$_5$*-clovibactin*

D-Thr$_5$-clovibactin crystallized in well conditions of 19% v/v *tert*-butanol and 0.5 M sodium fluoride buffered to pH 8.8 with Tris.

*X-ray crystallography of aza-*D*-Thr*$_5$*-clovibactin*

Aza-D-Thr$_5$-clovibactin crystallized in well conditions of 19% v/v *tert*-butanol and 0.5 M sodium fluoride buffered to pH 8.8 with Tris.

X-ray crystallography of Phe$^{I}_{1,D}$*-Thr*$_5$*-clovibactin*

Phe$^{I}_1$,D-Thr$_5$-clovibactin crystallized in three different well conditions: (1) 0.2 M ammonium acetate and 30% v/v 2-propanol buffered to pH 8.5 with 0.1 M Tris, (2) 0.2 M ammonium acetate and 30% v/v (±)-2-methyl-2,4-pentanediol buffered to pH 5.6 with 0.1 M sodium citrate tribasic dihydrate, (3) 0.2 M potassium phosphate monobasic and 20% w/v PEG 3,350.

SDS-PAGE with Silver Staining

SDS-PAGE was performed according to a standard procedure previously described by our group.[37] A step-by-step procedure is provided herein. Solutions of D-Thr$_5$-clovibactin and *N*-Me-D-Leu$_2$,D-Thr$_5$-clovibactin were prepared gravimetrically by dissolving lyophilized peptide

in the appropriate amount of deionized water to achieve 10 mg/mL stock solutions. For each of D-Thr$_5$-clovibactin and *N*-Me-D-Leu$_2$,D-Thr$_5$-clovibactin, the 10 mg/mL stock solution was further diluted to 1.2 mM, 1200 μM, and 120 μM in deionized water. A 20 μL aliquot of each of these 1.2 mM, 1200 μM, and 120 μM peptide stock solutions was combined with 4 μL of 6X SDS-PAGE loading buffer (100 mM Tris buffer at pH 6.8, 20% (v/v) glycerol, and 4% w/v SDS) to give 24 μL of peptide working solution at 1000 μM, 100 μM, and 10 μM for each of D-Thr$_5$-clovibactin and *N*-Me-D-Leu$_2$,D-Thr$_5$-clovibactin. A 10 μL aliquot of each working solution was run on a 16% polyacrylamide gel with a 4% stacking polyacrylamide gel. The gel was run at a constant 90 volts at room temperature for approximately 2 hours.

Staining with silver nitrate was used to visualize peptides in the SDS-PAGE gel. Briefly, the gel was first rocked in fixing solution (50% (v/v) methanol and 5% (v/v) acetic acid in deionized water) for 20 min. Next, the fixing solution was discarded, and the gel was rocked in 50% (v/v) aqueous methanol for 10 min. Next, the 50% methanol was discarded, and the gel was rocked in deionized water for 10 min. Next, the water was discarded, and the gel was rocked in 0.02% (w/v) sodium thiosulfate in deionized water for 1 min. The sodium thiosulfate was discarded, and the gel was rinsed twice with deionized water for 1 min each. After the second rinse, the gel was submerged in chilled 0.1% (w/v) silver nitrate in deionized water and rocked at 4 °C for 20 min. Next, the silver nitrate solution was discarded, and the gel was rinsed twice with deionized water for 1 min each. To develop the gel, the gel was incubated in developing solution (2% (w/v) ultrapure sodium carbonate and 0.04% (w/v) formaldehyde) until the desired intensity of staining was reached (~1–3 min). When the desired intensity of staining was reached, the development was stopped by discarding the developing solution and submerging the gel in 5% aqueous acetic acid.

Characterization Data

Solvent Blank

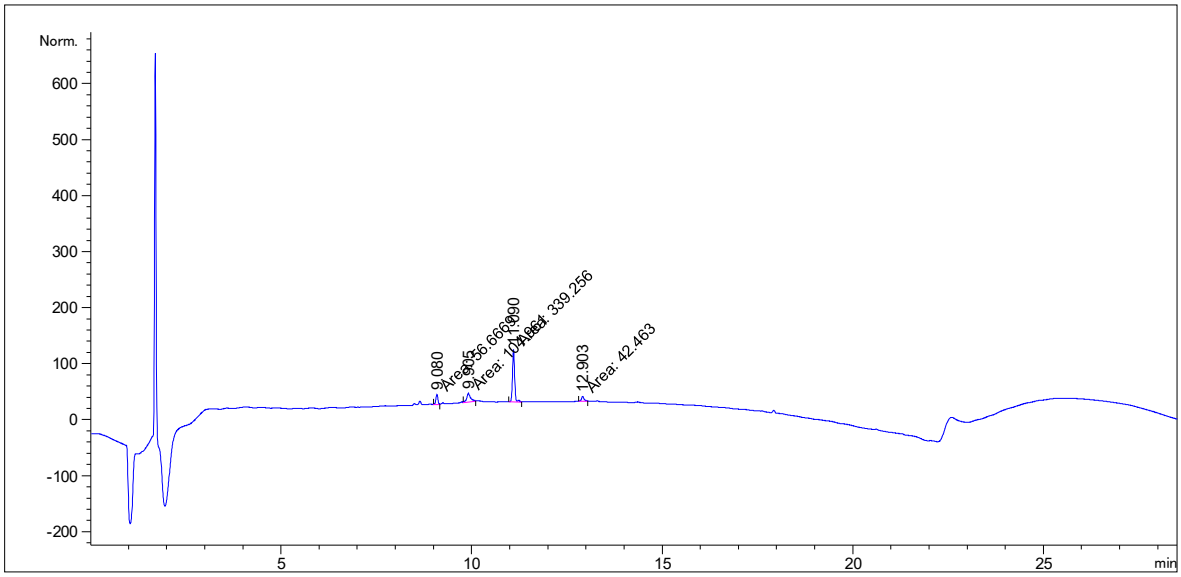

Signal 1: MWD1 A, Sig=214,4 Ref=off

Peak #	RetTime [min]	Type	Width [min]	Area [mAU*s]	Height [mAU]	Area %	
1	9.080	MM	0.0592	56.66687	15.95016	10.429	2
2	9.905	MM	0.1230	104.96137	14.22245	19.317	6
3	11.090	MM	0.0665	339.25589	84.99799	62.438	1
4	12.903	MM	0.0854	42.46304	8.28448	7.815	1

Characterization of Ala1-clovibactin

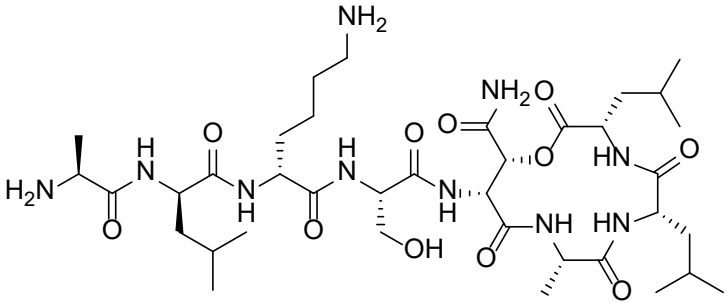

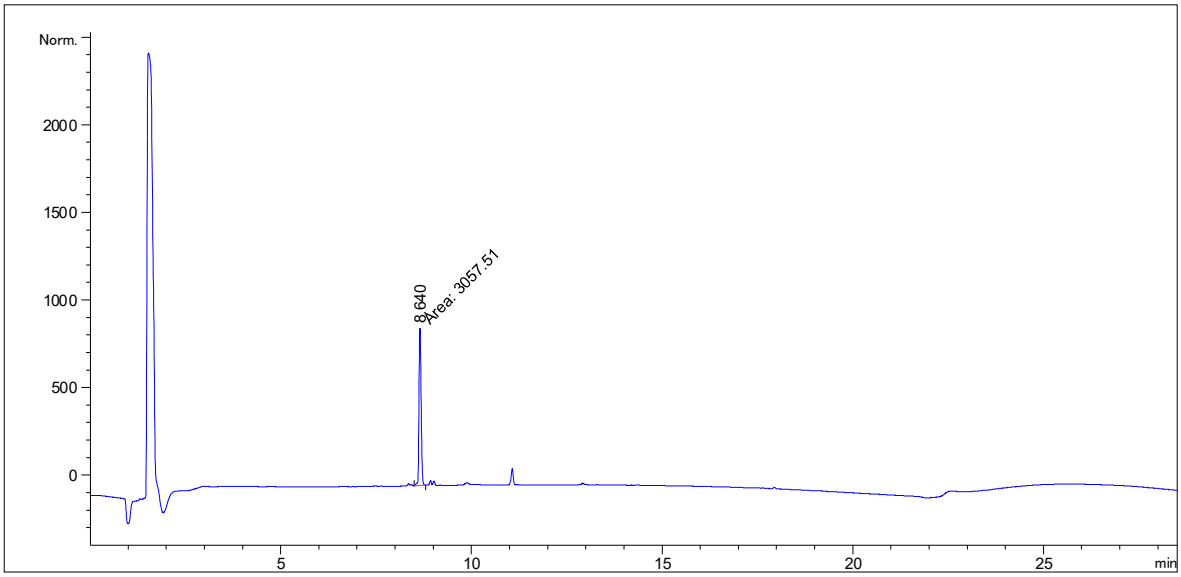

Signal 1: MWD1 A, Sig=214,4 Ref=off

Peak #	RetTime [min]	Type	Width [min]	Area [mAU*s]	Height [mAU]	Area %	
1	8.640	MM	0.0627	3057.51099	812.31726	100.000	0

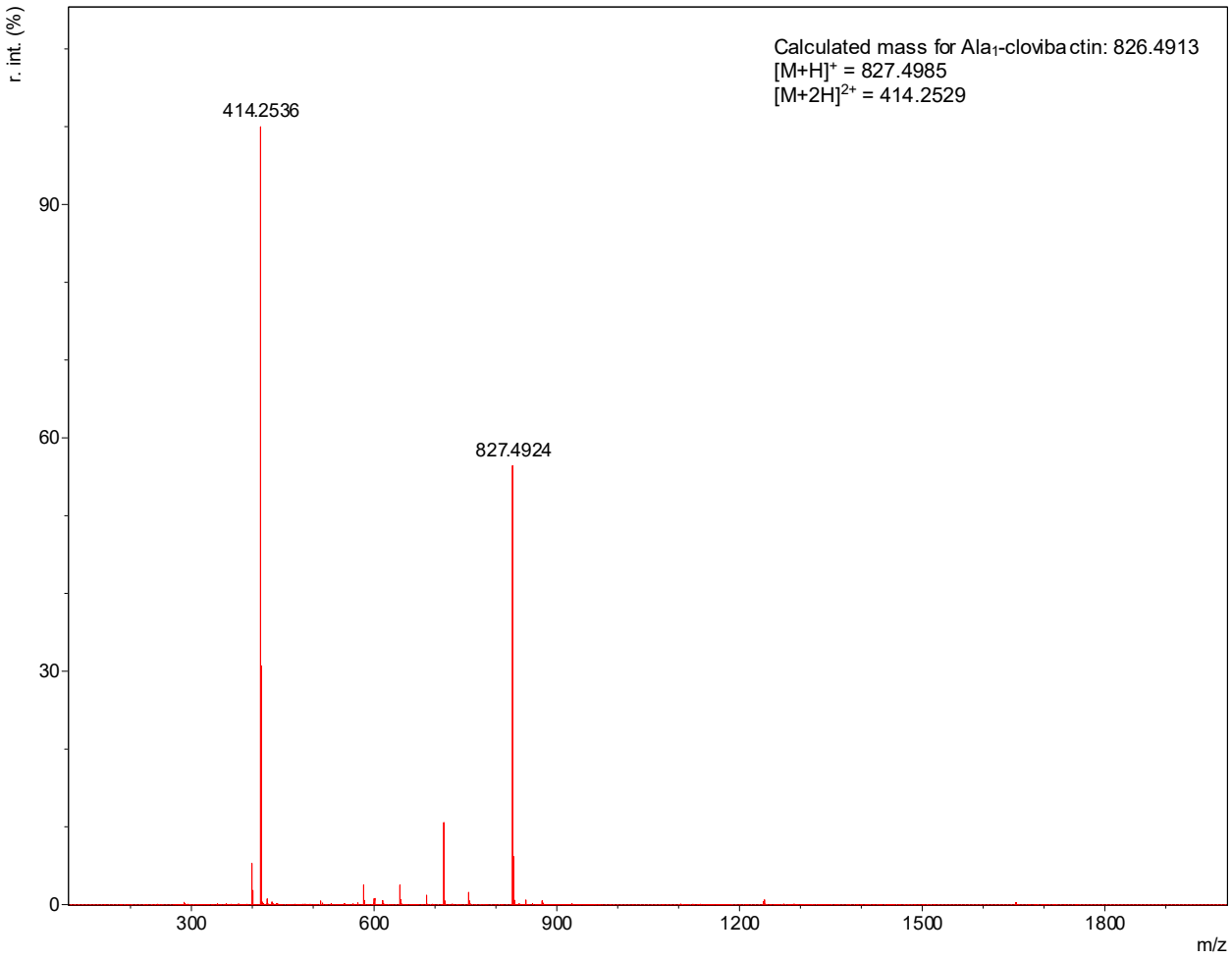
r. int. (%)
Calculated mass for Ala1-clovibactin: 826.4913
[M+H]+ = 827.4985
[M+2H]2+ = 414.2529
414.2536
827.4924
90
60
30
0
300
600
900
1200
1500
1800
m/z

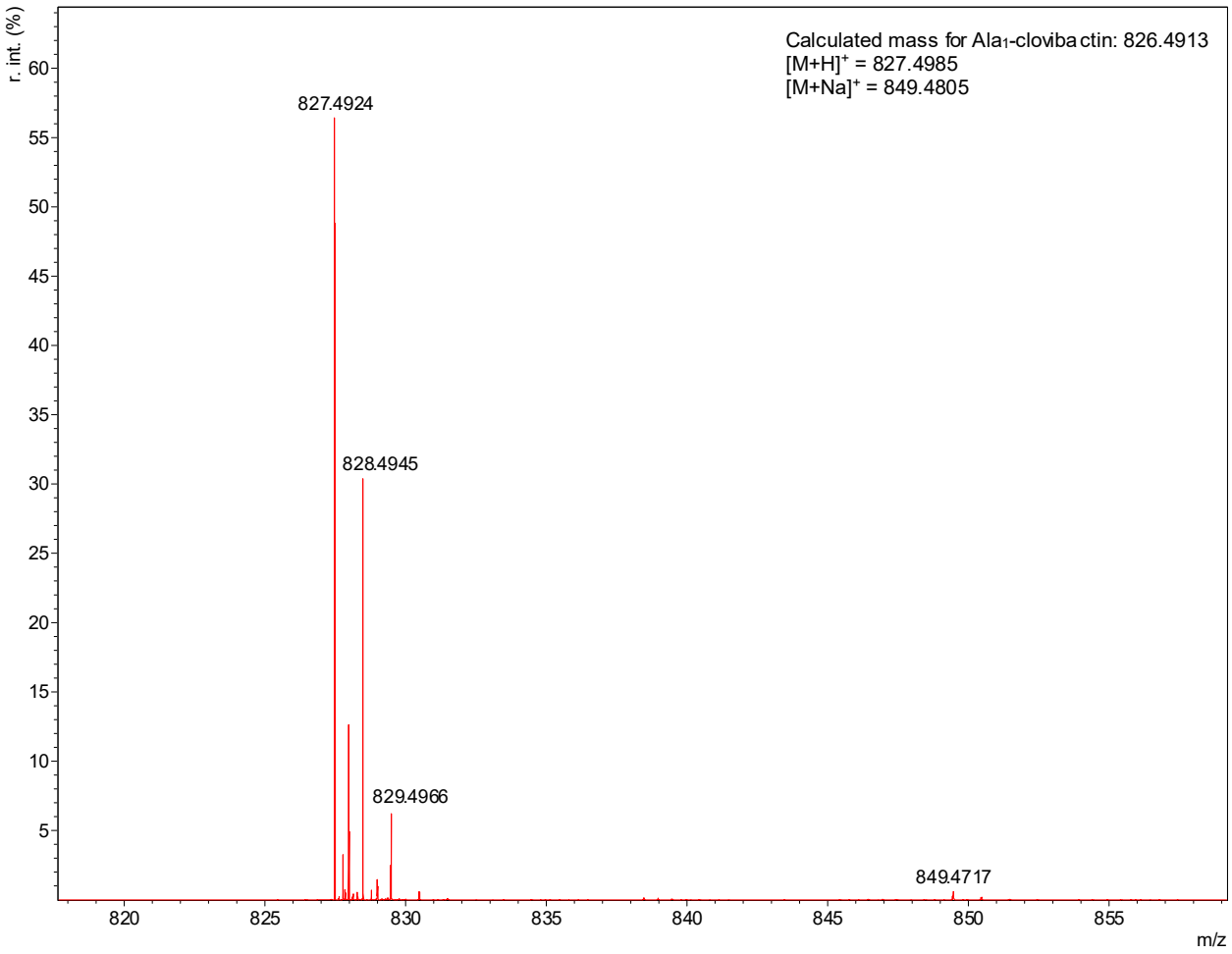
Calculated mass for Ala1-clovibactin: 826.4913
[M+H]+ = 827.4985
[M+Na]+ = 849.4805
827.4924
828.4945
829.4966
849.4717
r. int. (%)
m/z

Characterization of D-Ala$_2$-clovibactin

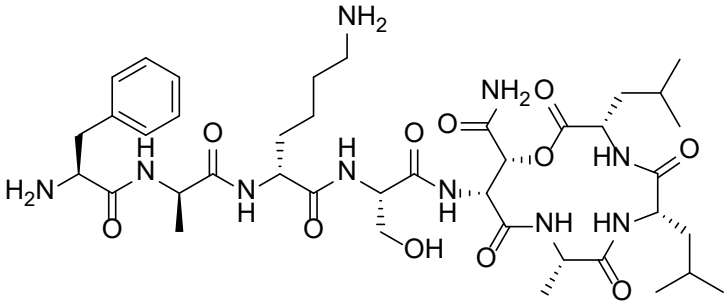

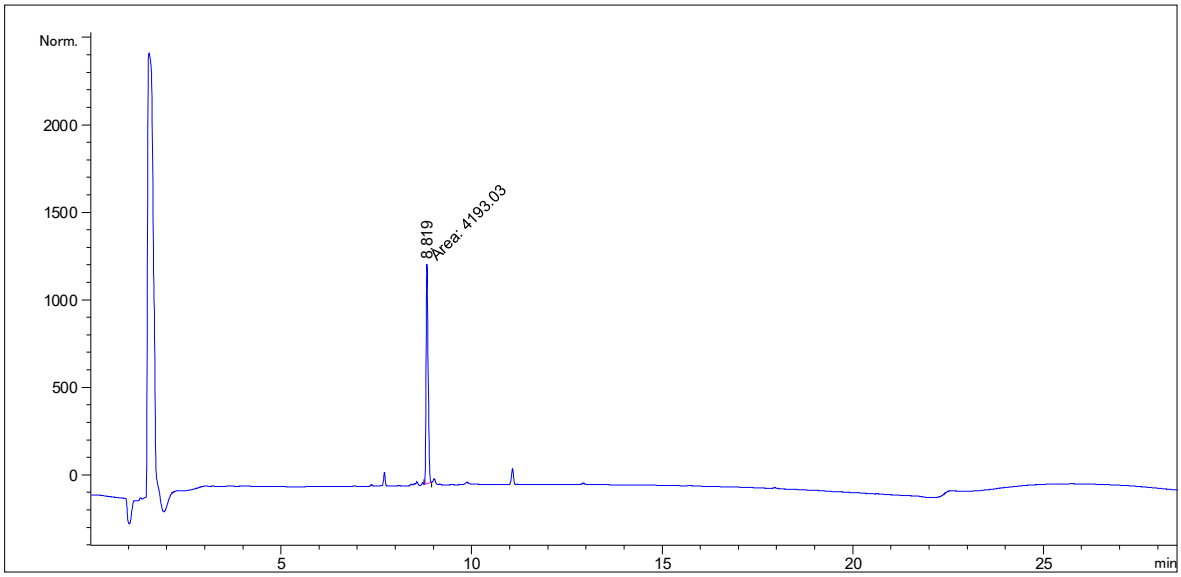


```
Signal 1: MWD1 A, Sig=214,4 Ref=off

Peak RetTime Type  Width     Area      Height     Area
#    [min]        [min]   [mAU*s]     [mAU]         %
----|-------|----|-------|----------|----------|--------|
1   8.819 MM    0.0616 4193.03418 1134.06335 100.000   0
```

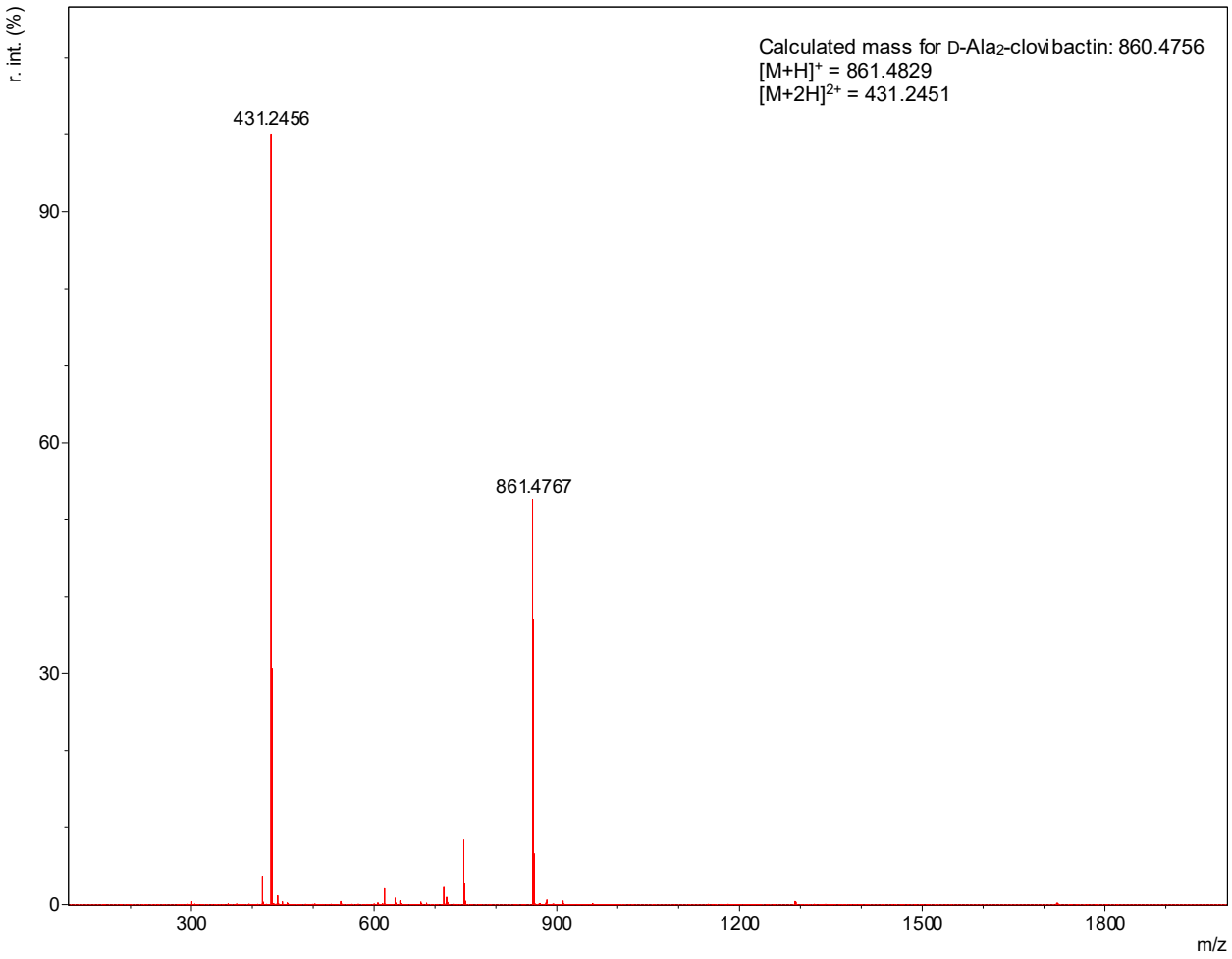
r. int. (%)
Calculated mass for D-Ala2-clovibactin: 860.4756
[M+H]+ = 861.4829
[M+2H]2+ = 431.2451
431.2456
861.4767
90
60
30
0
300
600
900
1200
1500
1800
m/z

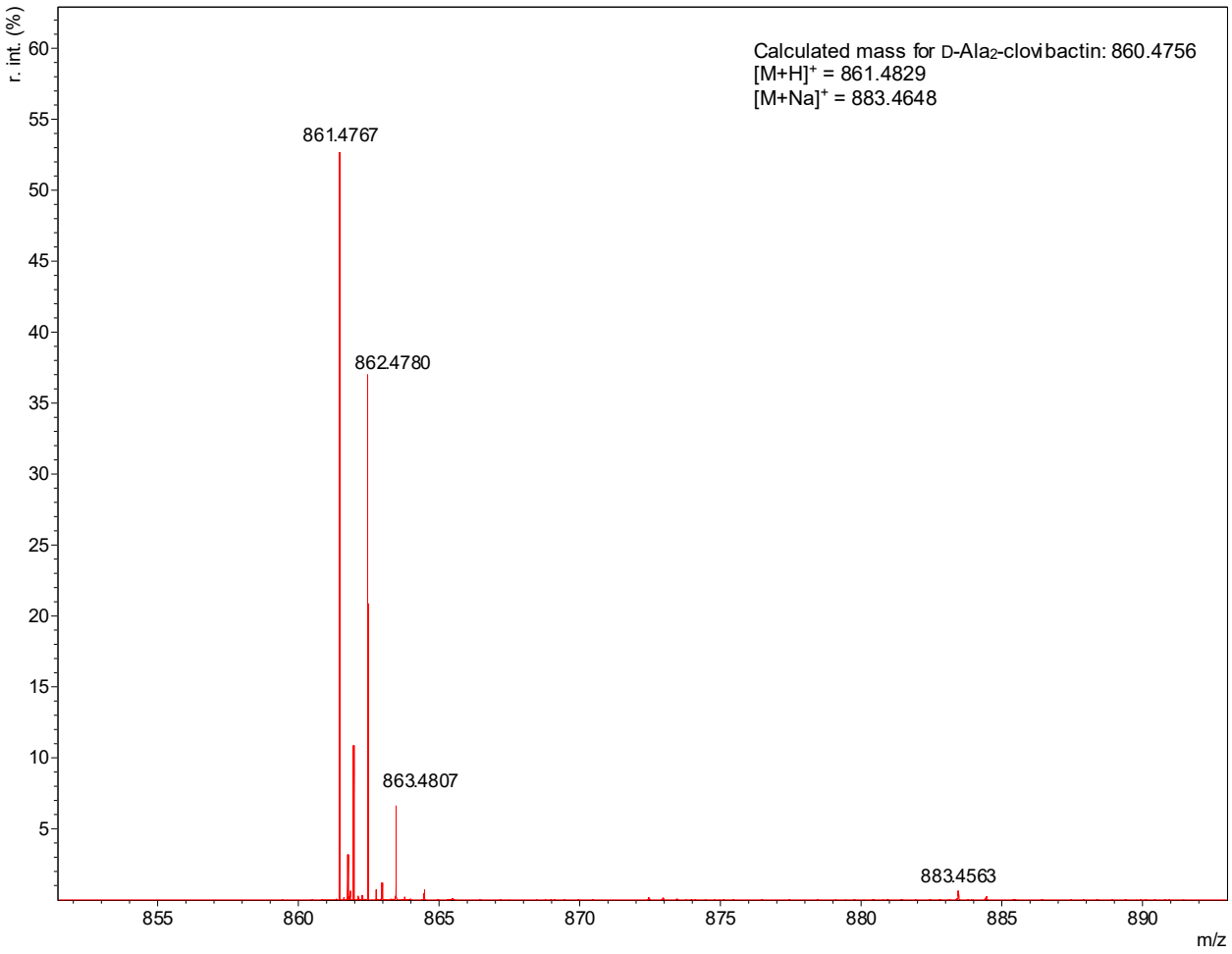
Calculated mass for D-Ala2-clovibactin: 860.4756
[M+H]+ = 861.4829
[M+Na]+ = 883.4648
861.4767
862.4780
863.4807
883.4563
r. int. (%)
m/z

Characterization of [D-Ala$_3$-O-Ser$_4$]-clovibactin

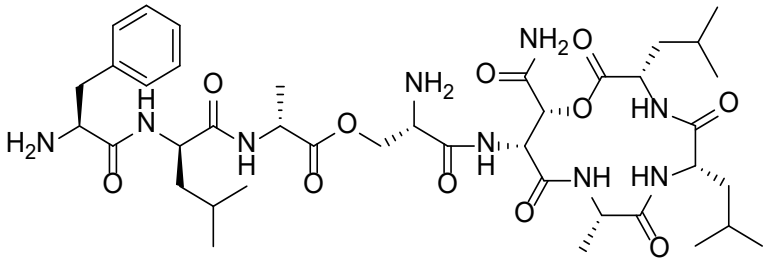

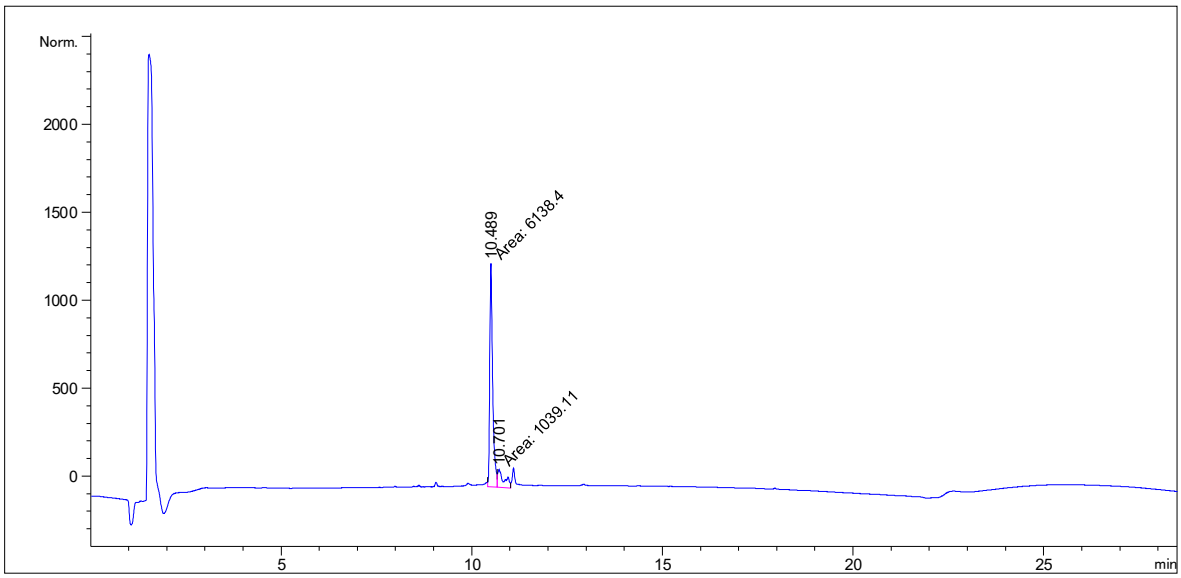

Signal 1: MWD1 A, Sig=214,4 Ref=off

Peak #	RetTime [min]	Type	Width [min]	Area [mAU*s]	Height [mAU]	Area %
1	10.489	MF	0.0891	6138.40332	1148.75098	85.522
2	10.701	FM	0.1907	1039.10754	90.82335	14.477

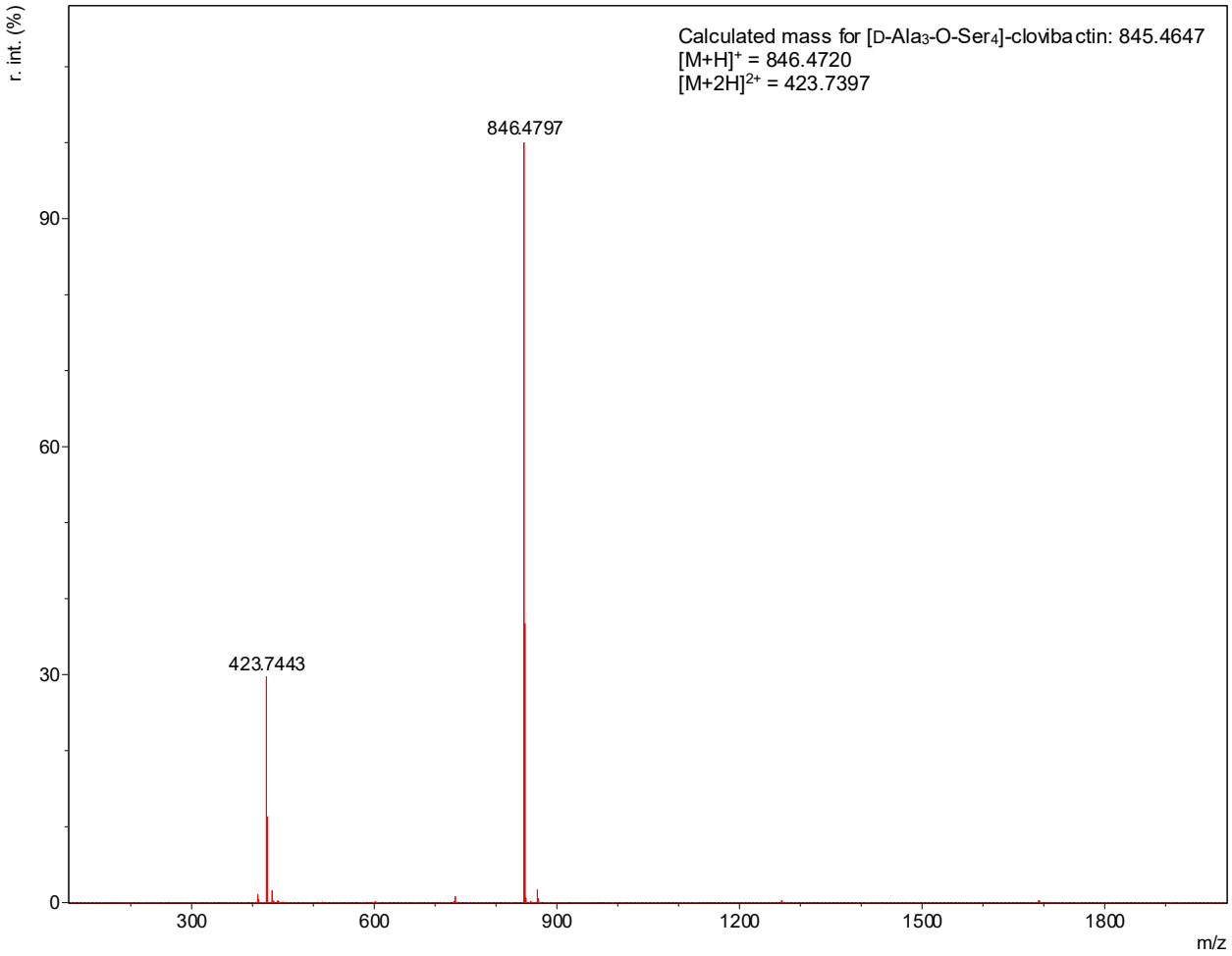
Calculated mass for [D-Ala3-O-Ser4]-clovibactin: 845.4647
[M+H]+ = 846.4720
[M+2H]2+ = 423.7397
846.4797
423.7443
r. int. (%)
0
30
60
90
300
600
900
1200
1500
1800
m/z

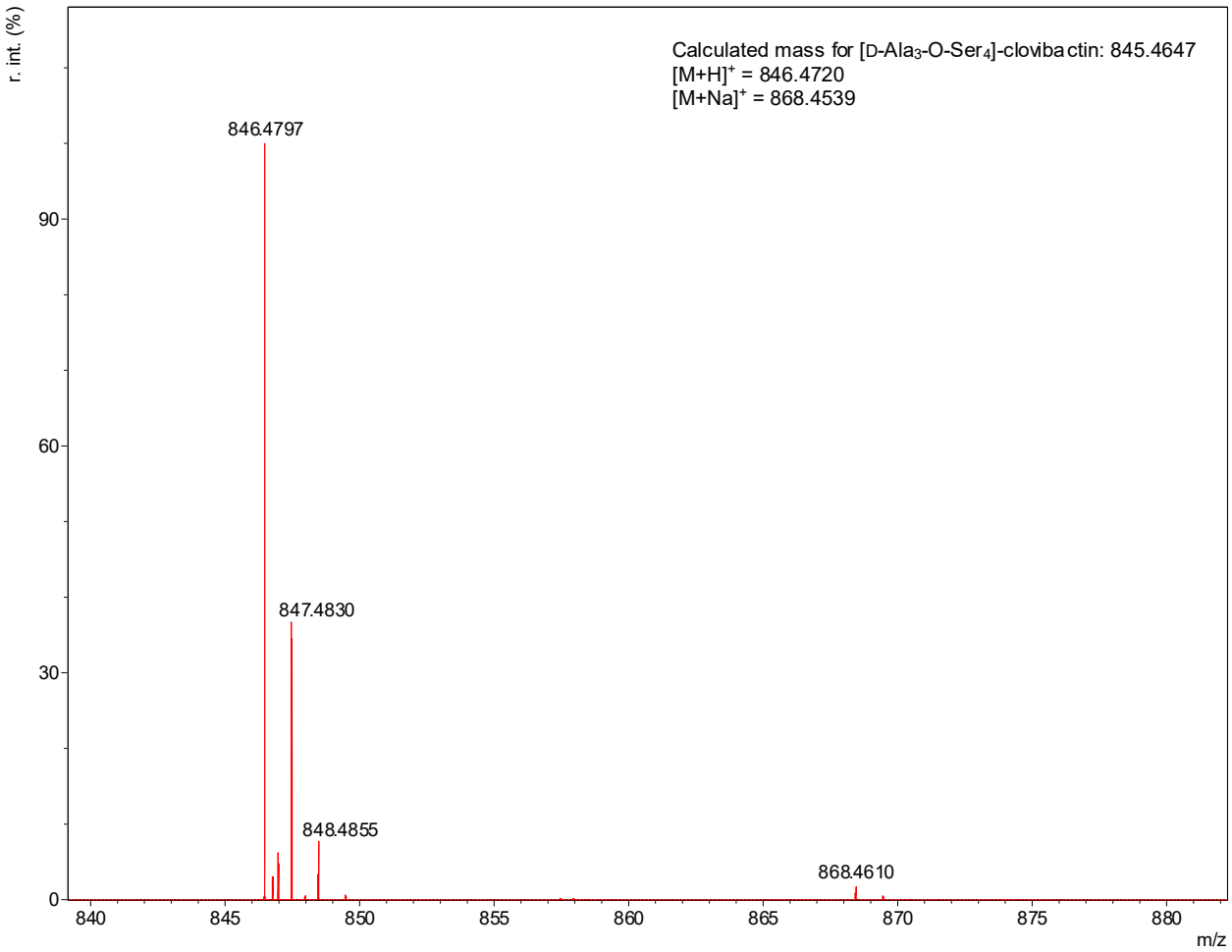
Calculated mass for [D-Ala3-O-Ser4]-clovibactin: 845.4647
[M+H]+ = 846.4720
[M+Na]+ = 868.4539
846.4797
847.4830
848.4855
868.4610
r. int. (%)
0
30
60
90
840
845
850
855
860
865
870
875
880
m/z

Characterization of Ala$_4$-clovibactin

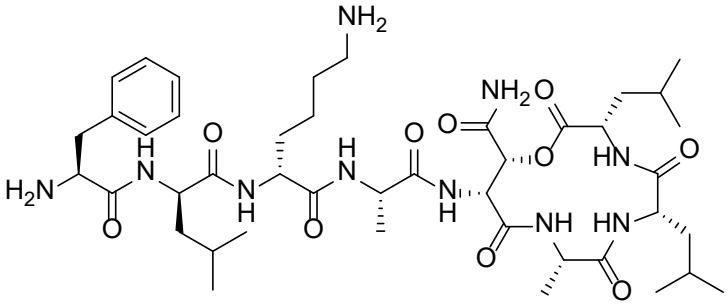

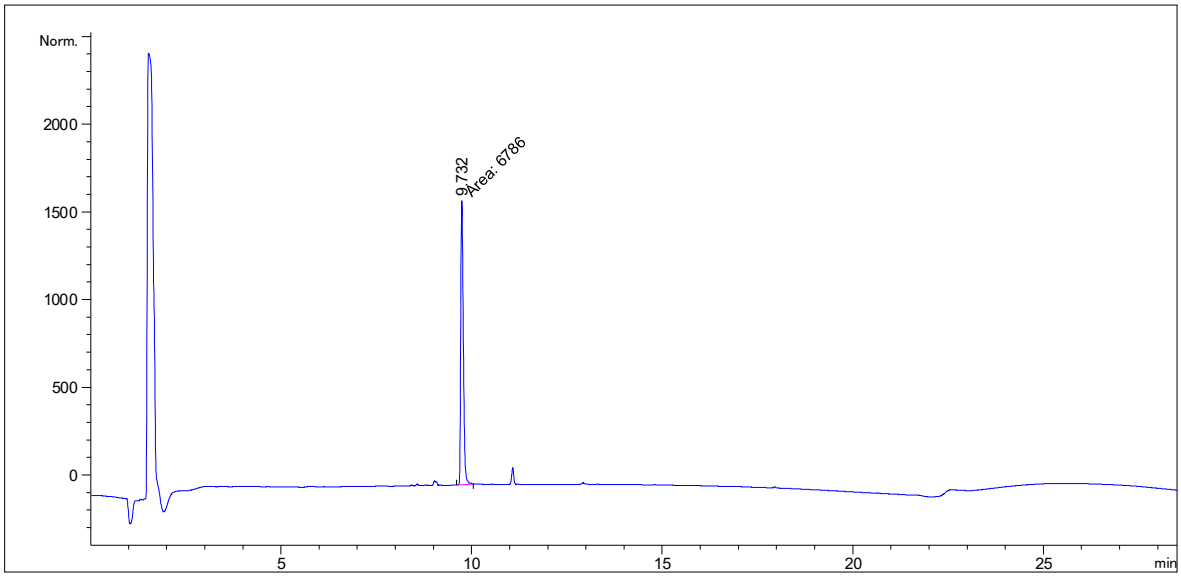


```
Signal 1: MWD1 A, Sig=214,4 Ref=off

Peak RetTime Type  Width     Area      Height     Area
#    [min]        [min]   [mAU*s]     [mAU]         %
----|-------|----|-------|----------|----------|--------|
1   9.732 MM    0.0773 6786.00488 1463.88306 100.000   0
```

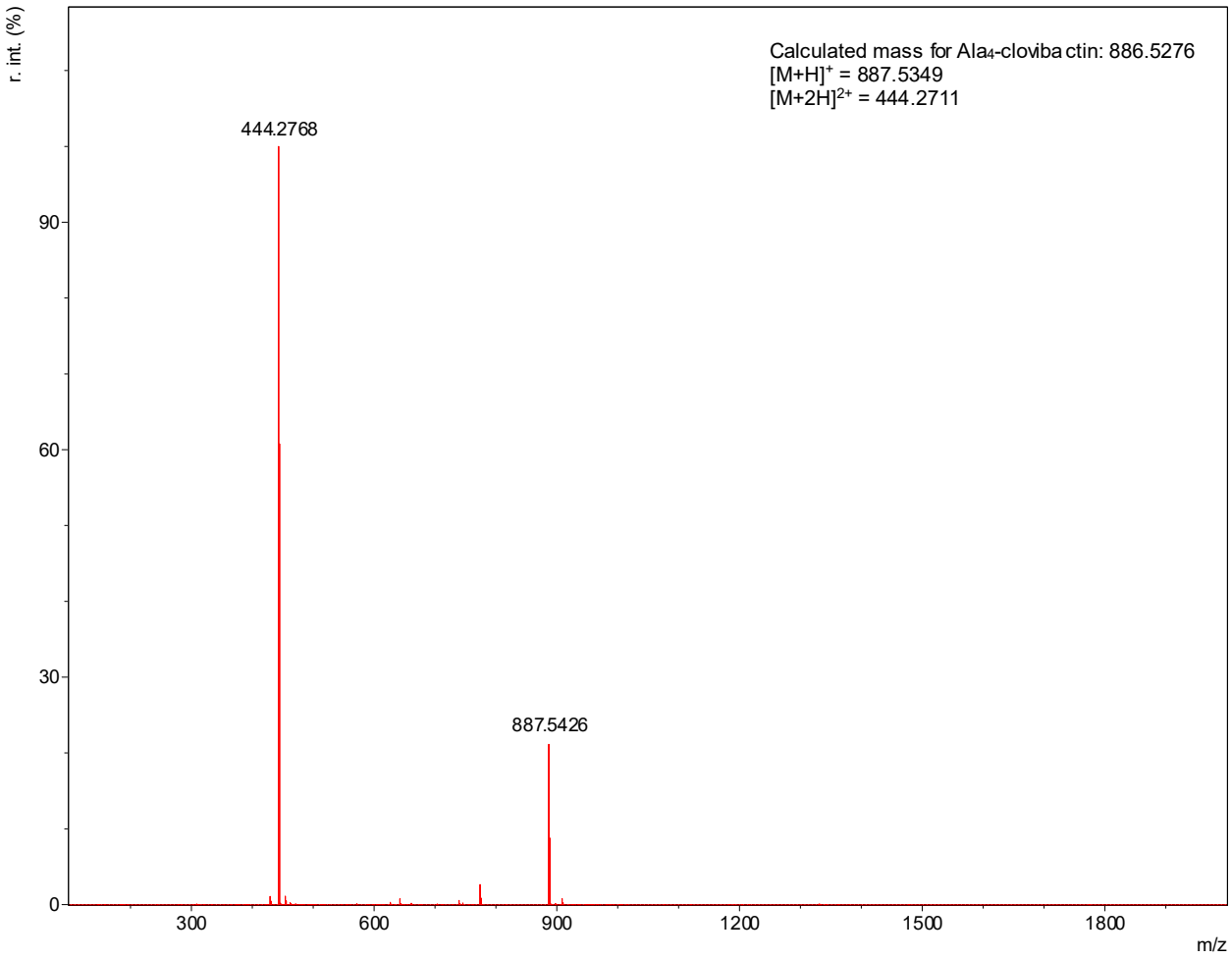
r. int. (%)
Calculated mass for Ala4-clovibactin: 886.5276
[M+H]+ = 887.5349
[M+2H]2+ = 444.2711
444.2768
887.5426
90
60
30
0
300
600
900
1200
1500
1800
m/z

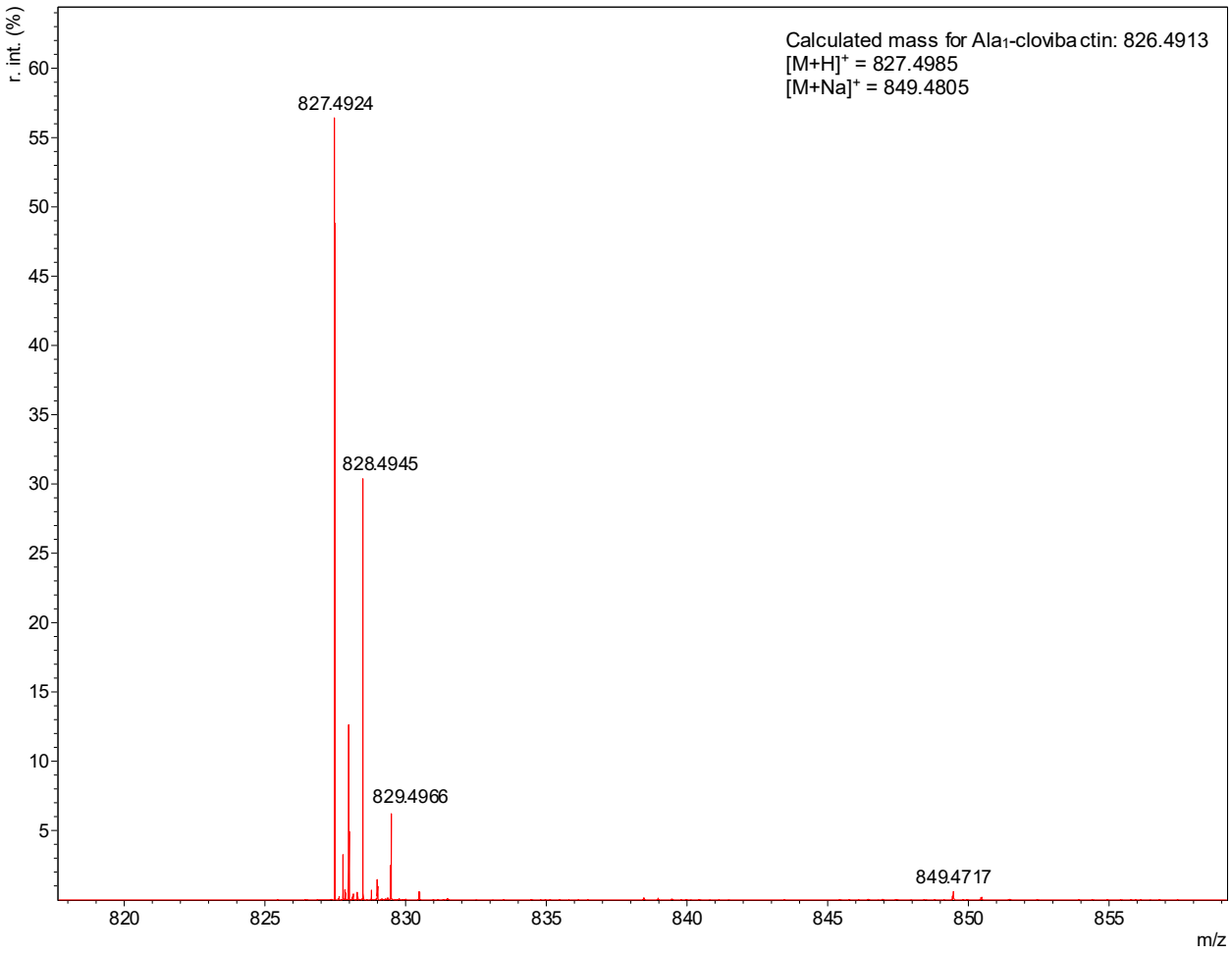
Calculated mass for Ala1-clovibactin: 826.4913
[M+H]+ = 827.4985
[M+Na]+ = 849.4805
827.4924
828.4945
829.4966
849.4717
r. int. (%)
m/z

Characterization of D-Thr5-clovibactin

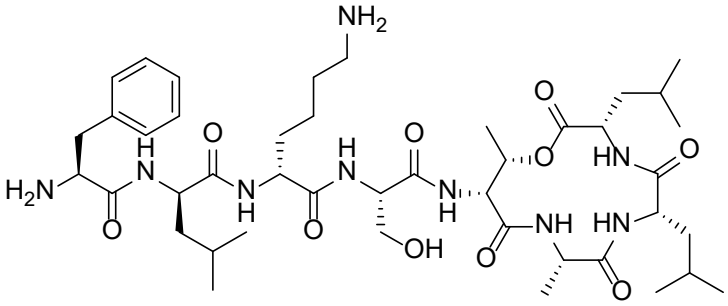

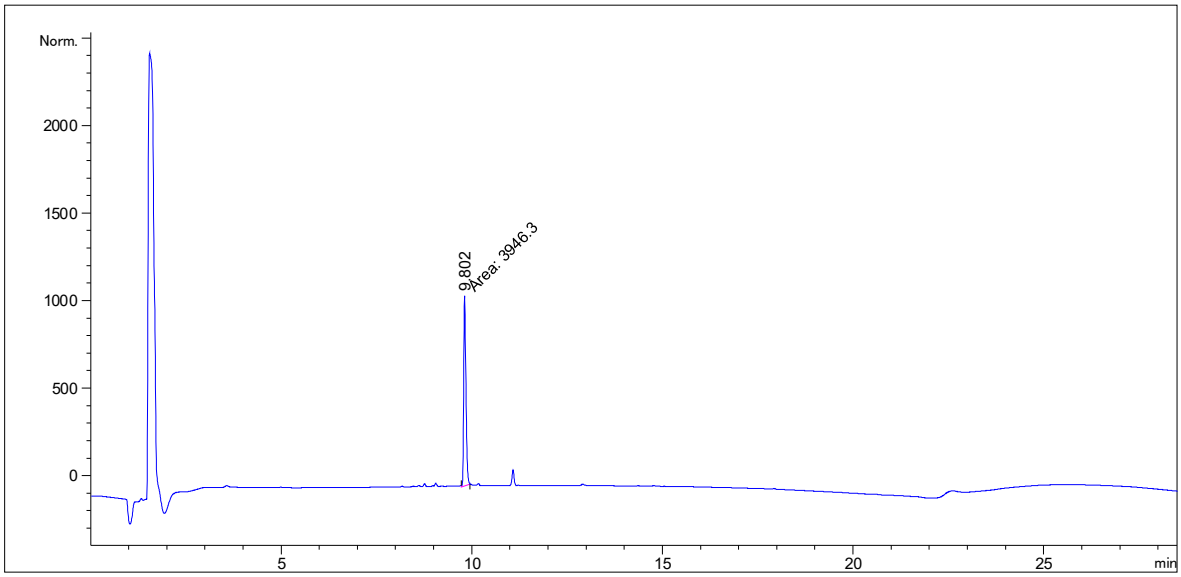

Signal 1: MWD1 A, Sig=214,4 Ref=off

Peak #	RetTime [min]	Type	Width [min]	Area [mAU*s]	Height [mAU]	Area %	
1	9.802	MM	0.0668	3946.29614	984.83063	100.000	0

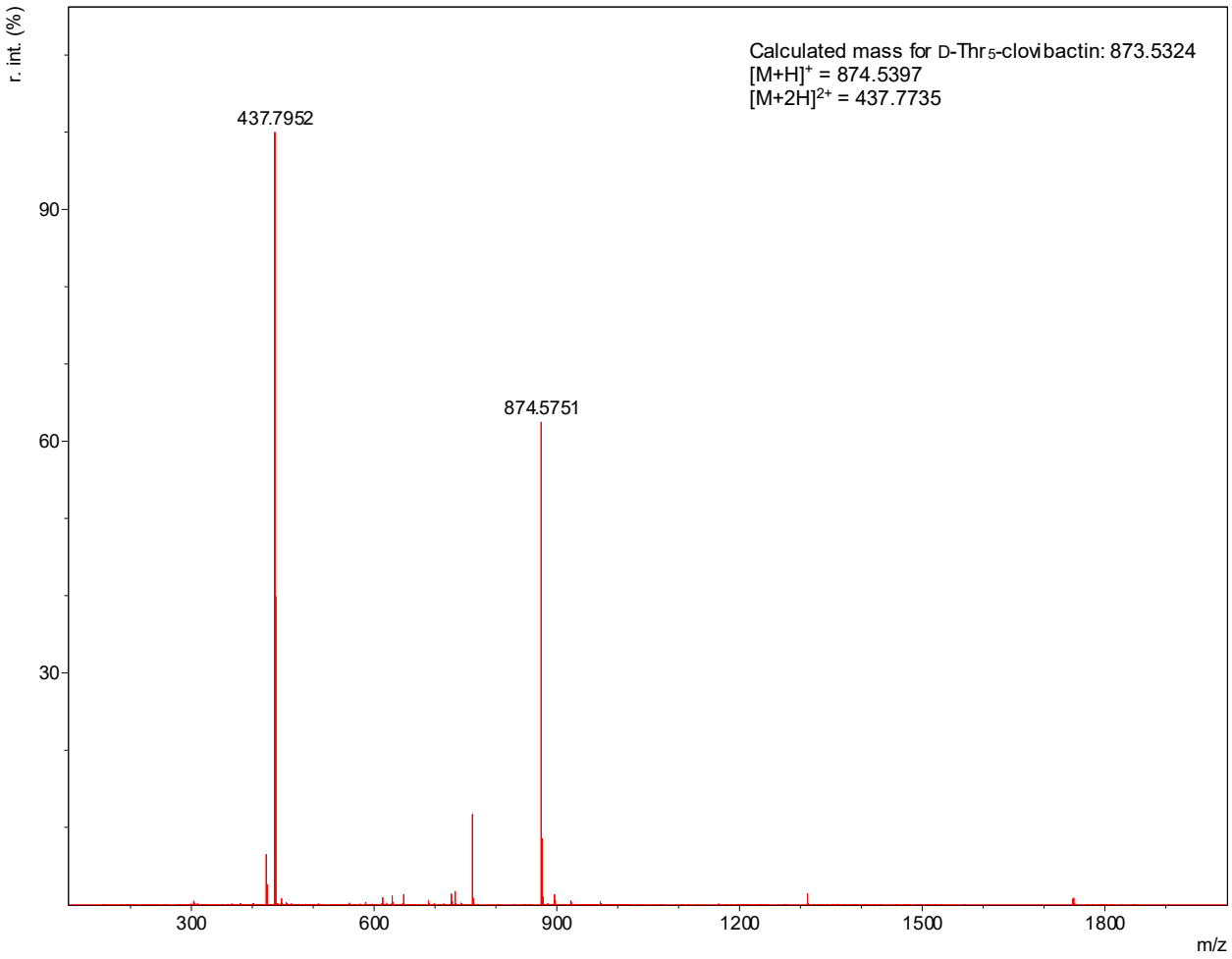
r. int. (%)
Calculated mass for D-Thr5-clovibactin: 873.5324
[M+H]+ = 874.5397
[M+2H]2+ = 437.7735
437.7952
874.5751
90
60
30
300
600
900
1200
1500
1800
m/z

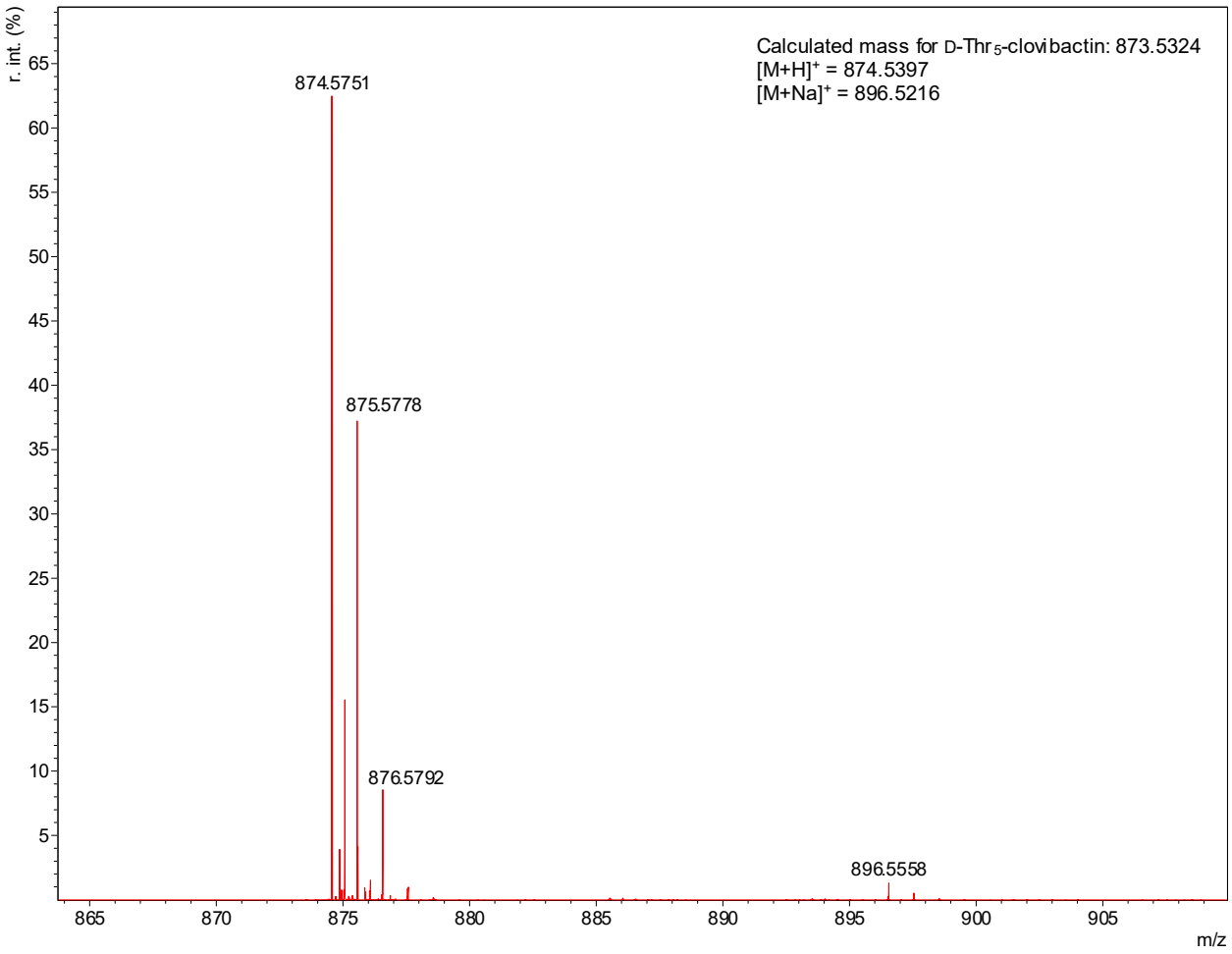
Calculated mass for D-Thr5-clovibactin: 873.5324
[M+H]+ = 874.5397
[M+Na]+ = 896.5216
874.5751
875.5778
876.5792
896.5558
r. int. (%)
m/z

Characterization of Ala$_7$-clovibactin

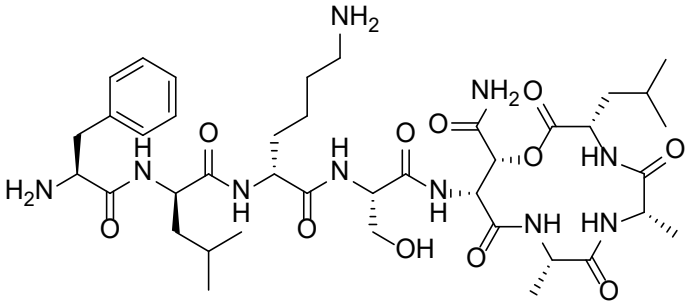

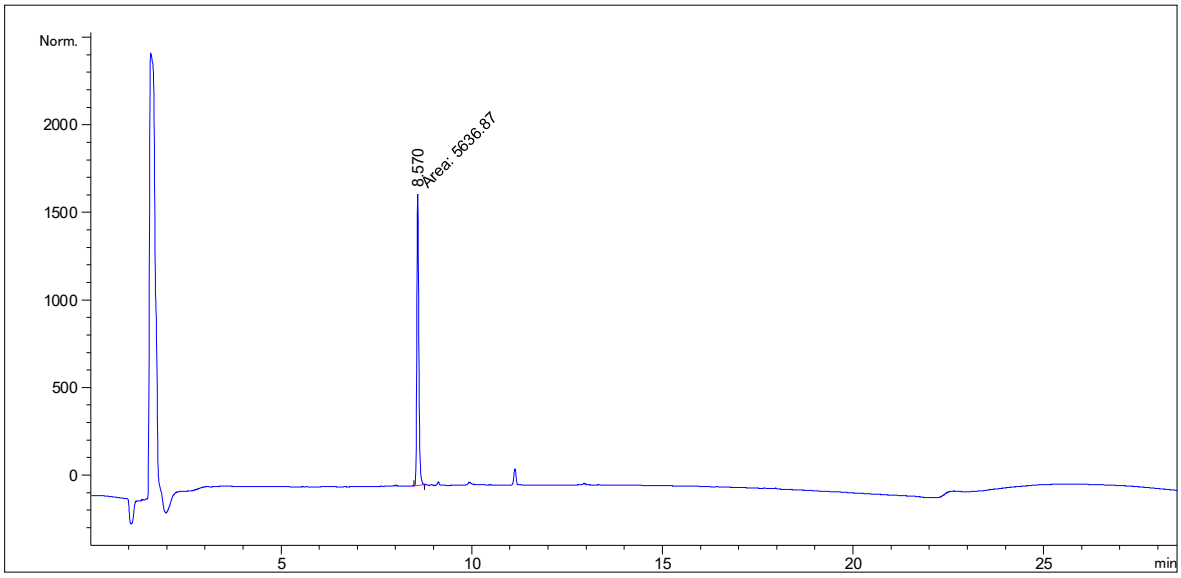


```
Signal 1: MWD1 A, Sig=214,4 Ref=off

Peak RetTime Type  Width     Area      Height     Area
#    [min]        [min]   [mAU*s]     [mAU]         %
----|-------|----|-------|----------|----------|--------|
1   8.570 MM    0.0620 5636.86768 1514.32629 100.000   0
```

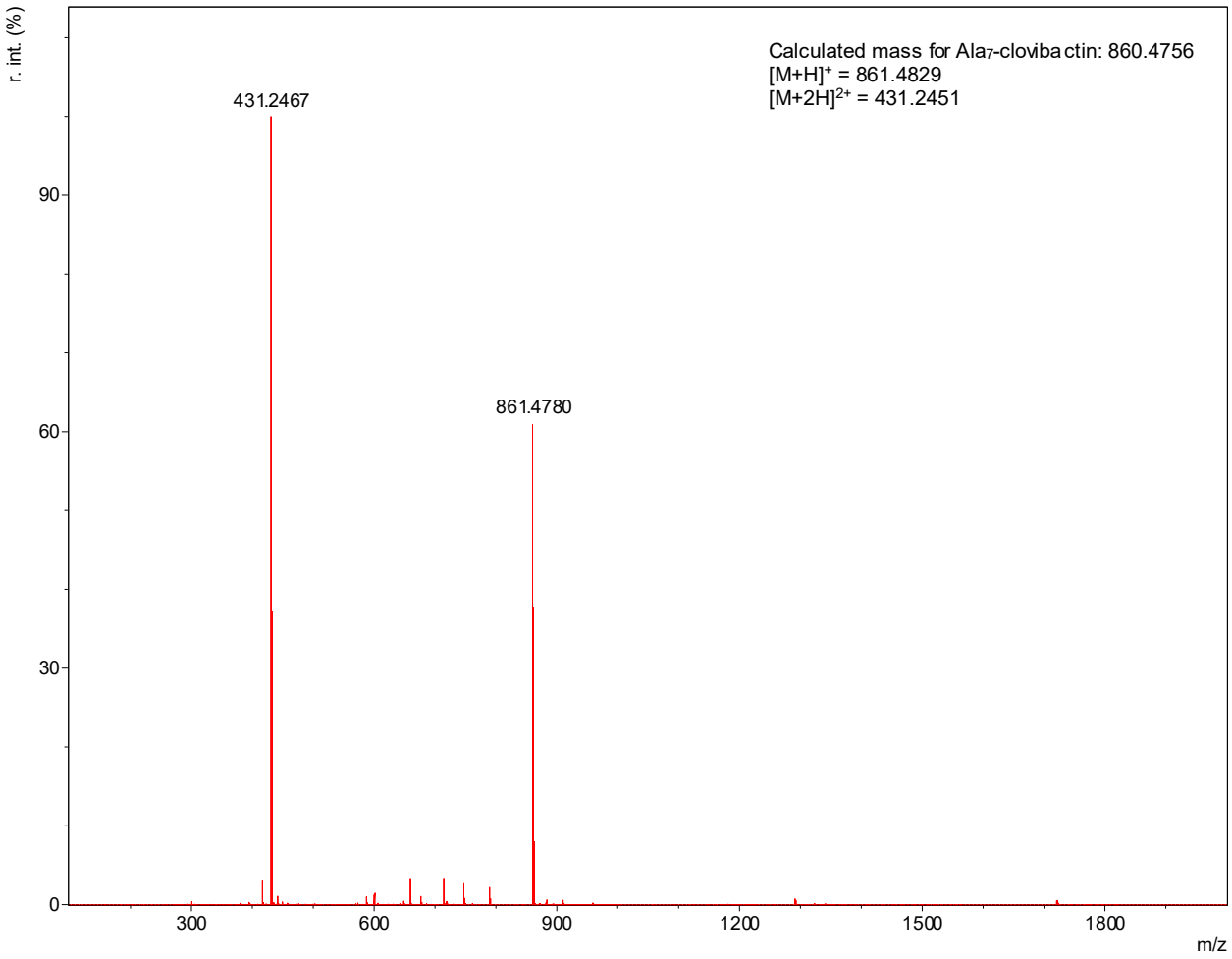
r. int. (%)
Calculated mass for Ala7-clovibactin: 860.4756
[M+H]+ = 861.4829
[M+2H]2+ = 431.2451
431.2467
861.4780
90
60
30
0
300
600
900
1200
1500
1800
m/z

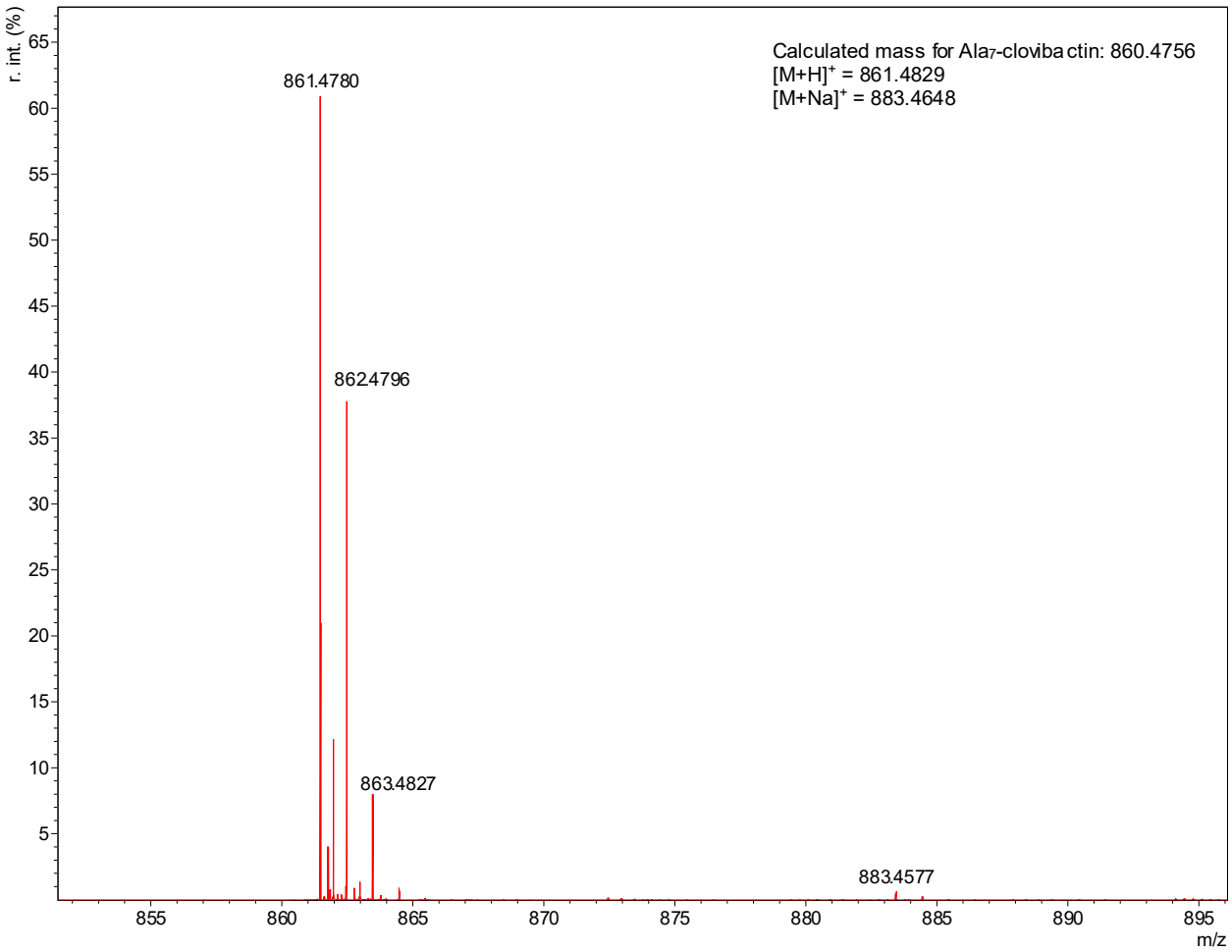
r. int. (%)
65
60
55
50
45
40
35
30
25
20
15
10
5
861.4780
862.4796
863.4827
883.4577
Calculated mass for Ala7-clovibactin: 860.4756
[M+H]+ = 861.4829
[M+Na]+ = 883.4648
855
860
865
870
875
880
885
890
895
m/z

Characterization of Ala$_8$-clovibactin

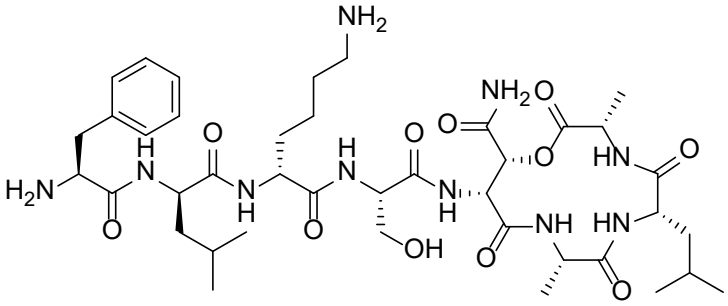

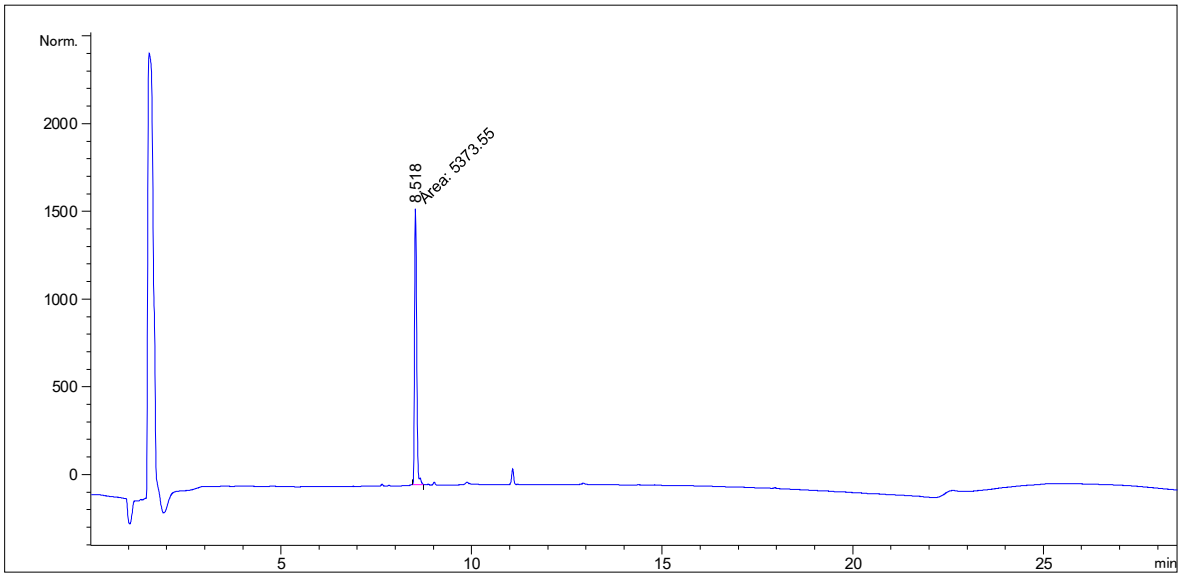


```
Signal 1: MWD1 A, Sig=214,4 Ref=off

Peak RetTime Type  Width     Area      Height     Area
#    [min]        [min]   [mAU*s]     [mAU]         %
----|-------|----|-------|----------|----------|--------|
1   8.518 MM    0.0627 5373.54785 1427.77112 100.000   0
```

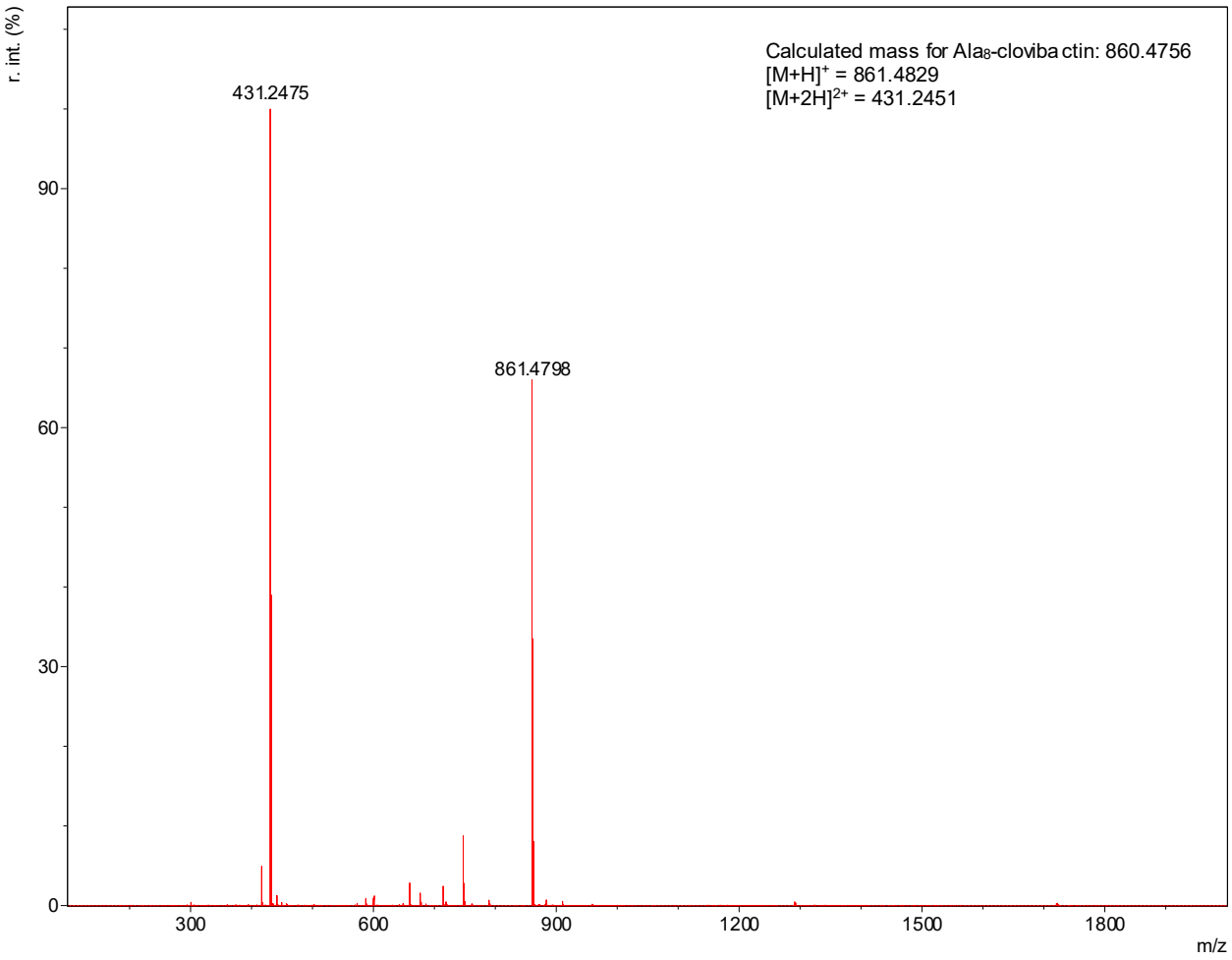
r. int. (%)
Calculated mass for Ala8-clovibactin: 860.4756
[M+H]+ = 861.4829
[M+2H]2+ = 431.2451
431.2475
861.4798
90
60
30
0
300
600
900
1200
1500
1800
m/z

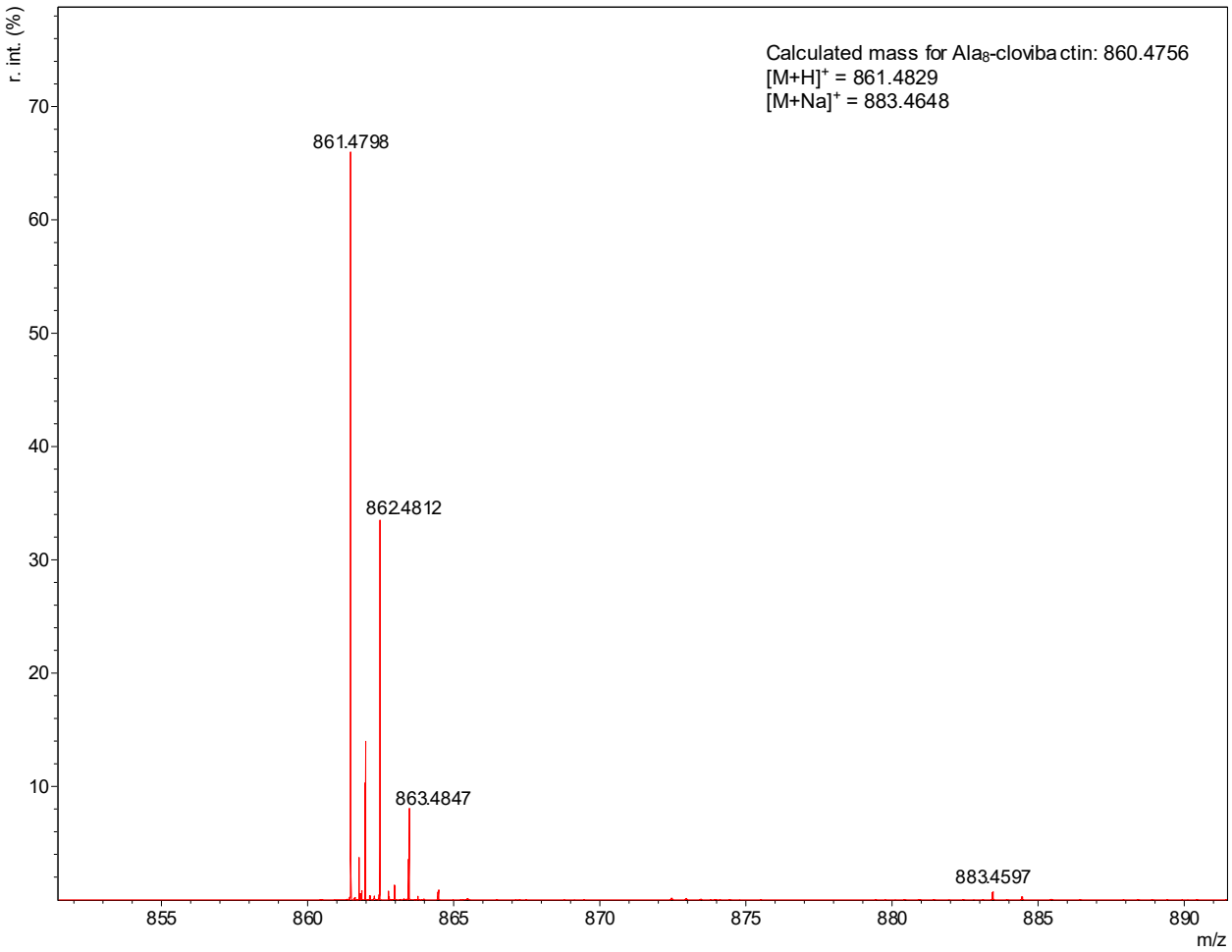
r. int. (%)
70
60
50
40
30
20
10
Calculated mass for Ala8-cloviba ctin: 860.4756
[M+H]+ = 861.4829
[M+Na]+ = 883.4648
861.4798
862.4812
863.4847
883.4597
855
860
865
870
875
880
885
890
m/z

Characterization of ent-clovibactin

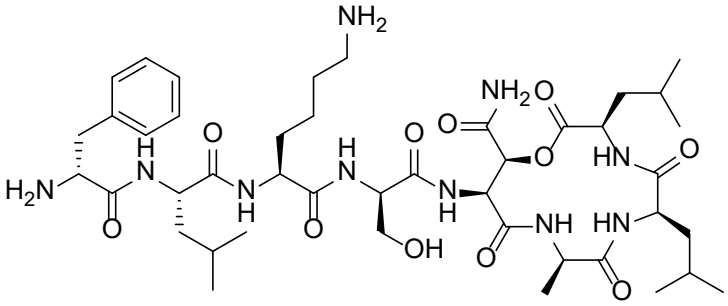

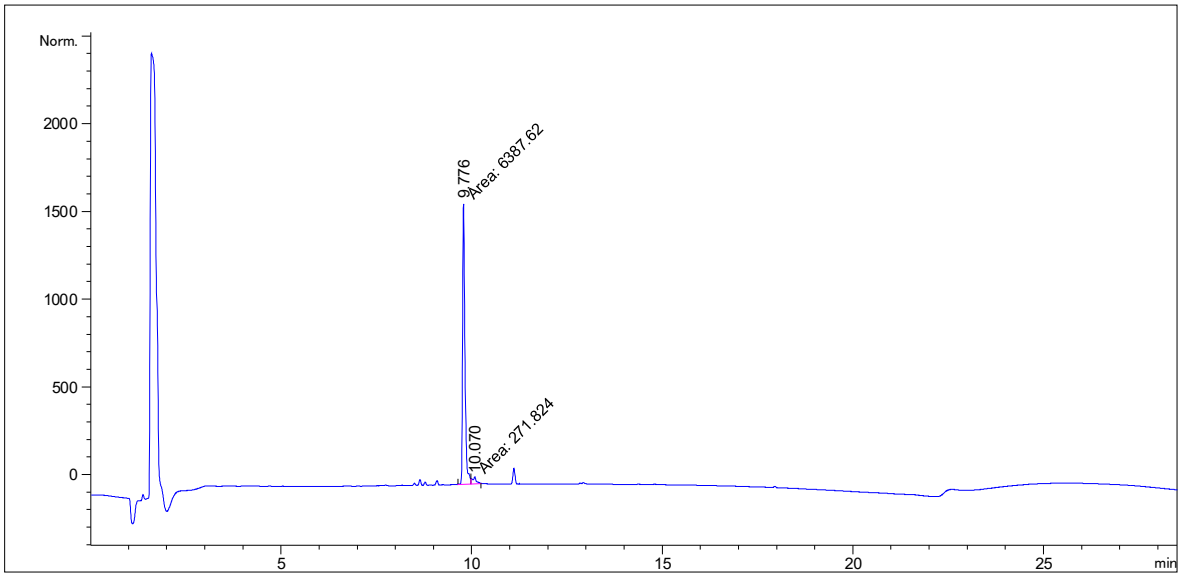

Signal 1: MWD1 A, Sig=214,4 Ref=off

Peak #	RetTime [min]	Type	Width [min]	Area [mAU*s]	Height [mAU]	Area %	
1	9.776	MF	0.0735	6387.62354	1448.05359	95.918	2
2	10.070	FM	0.1219	271.82364	37.15057	4.081	8

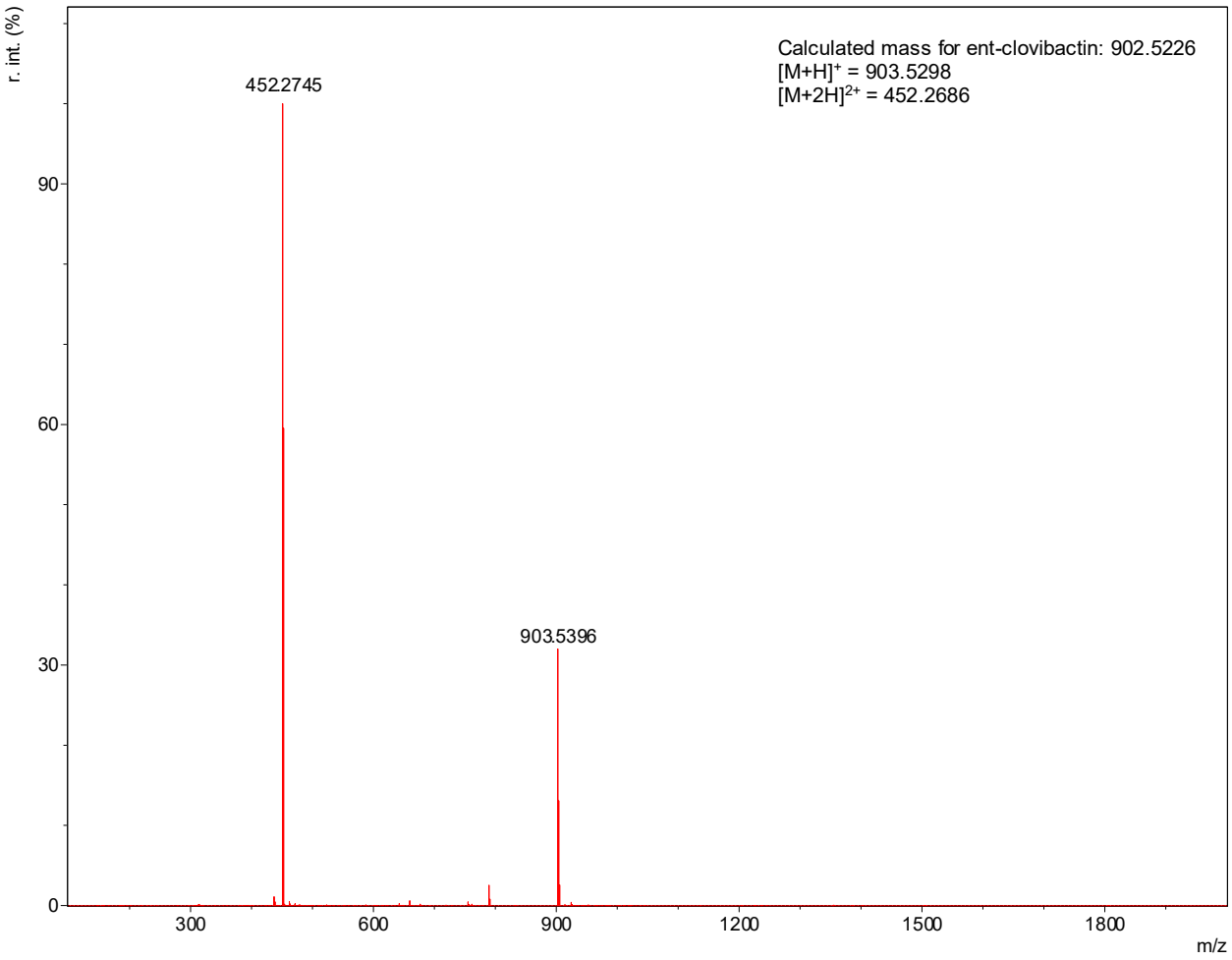
r. int. (%)
Calculated mass for ent-clovibactin: 902.5226
[M+H]+ = 903.5298
[M+2H]2+ = 452.2686
452.2745
903.5396
90
60
30
0
300
600
900
1200
1500
1800
m/z

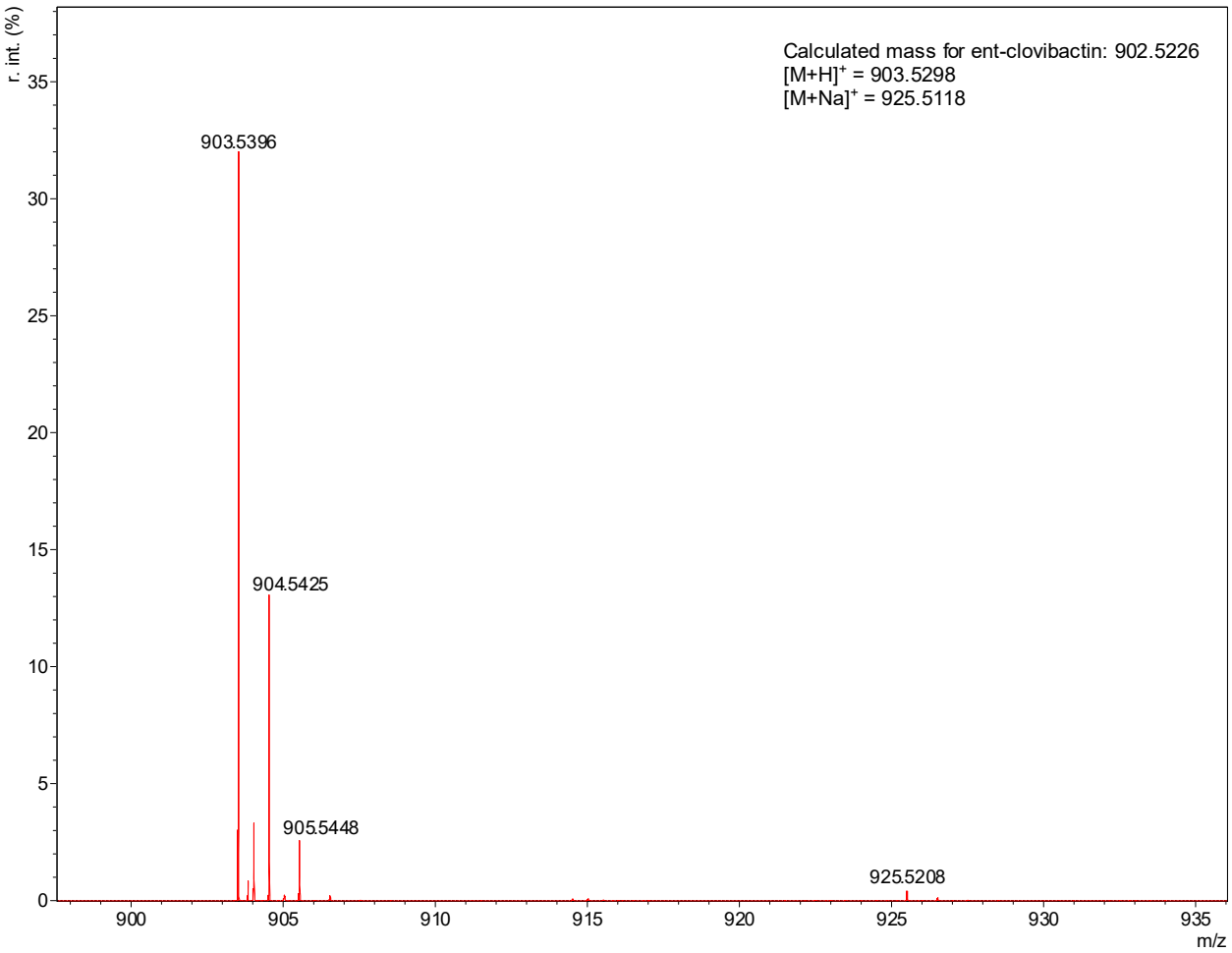
Calculated mass for ent-clovibactin: 902.5226
[M+H]+ = 903.5298
[M+Na]+ = 925.5118
903.5396
904.5425
905.5448
925.5208
r. int. (%)
m/z

Characterization of seco-clovibactin

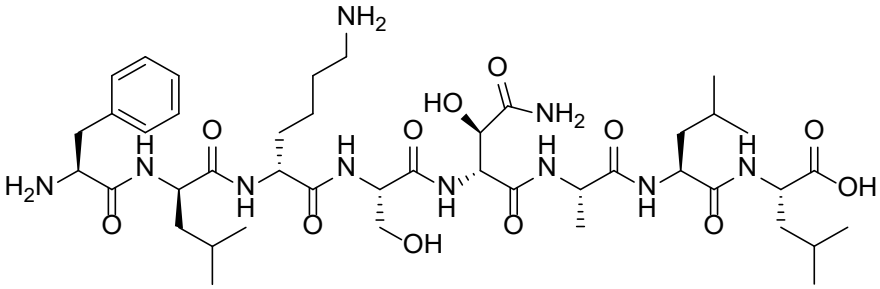

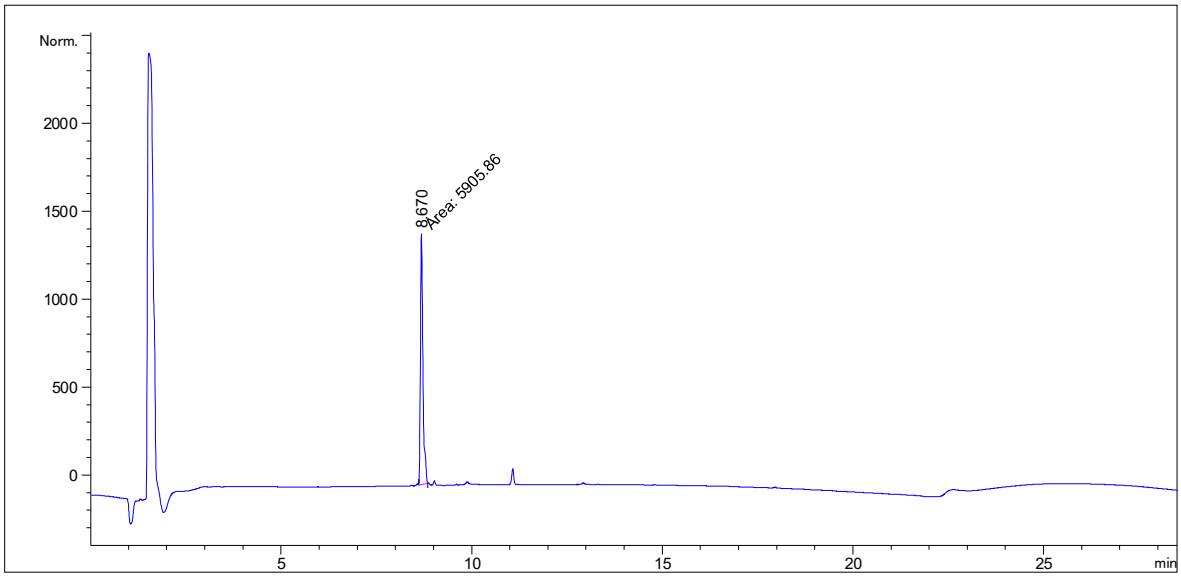

Signal 1: MWD1 A, Sig=214,4 Ref=off

Peak #	RetTime [min]	Type	Width [min]	Area [mAU*s]	Height [mAU]	Area %
1	8.670	MM	0.0763	5905.85742	1289.52185	100.000

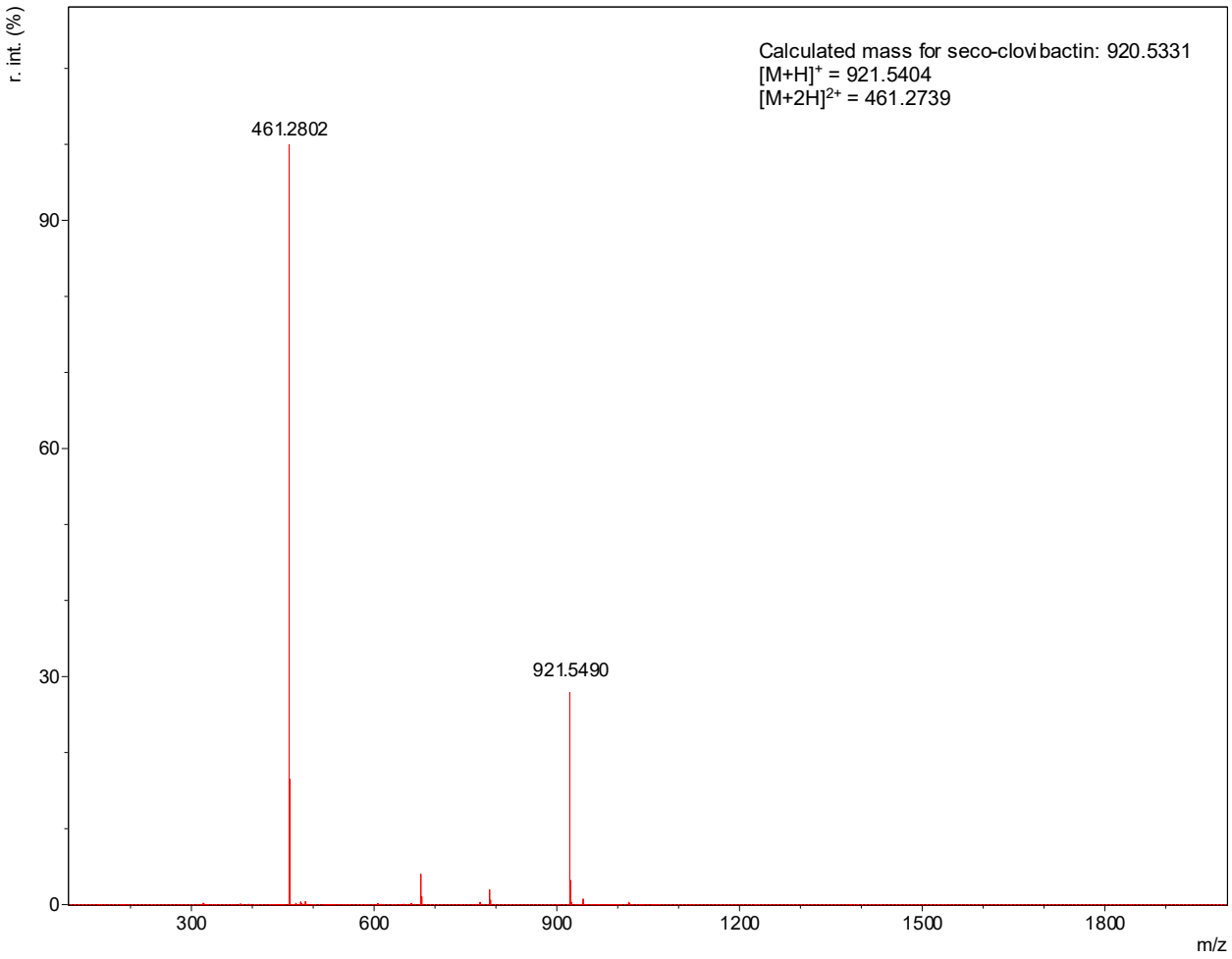
Calculated mass for seco-clovibactin: 920.5331
[M+H]+ = 921.5404
[M+2H]2+ = 461.2739
461.2802
921.5490
r. int. (%)
90
60
30
0
300
600
900
1200
1500
1800
m/z

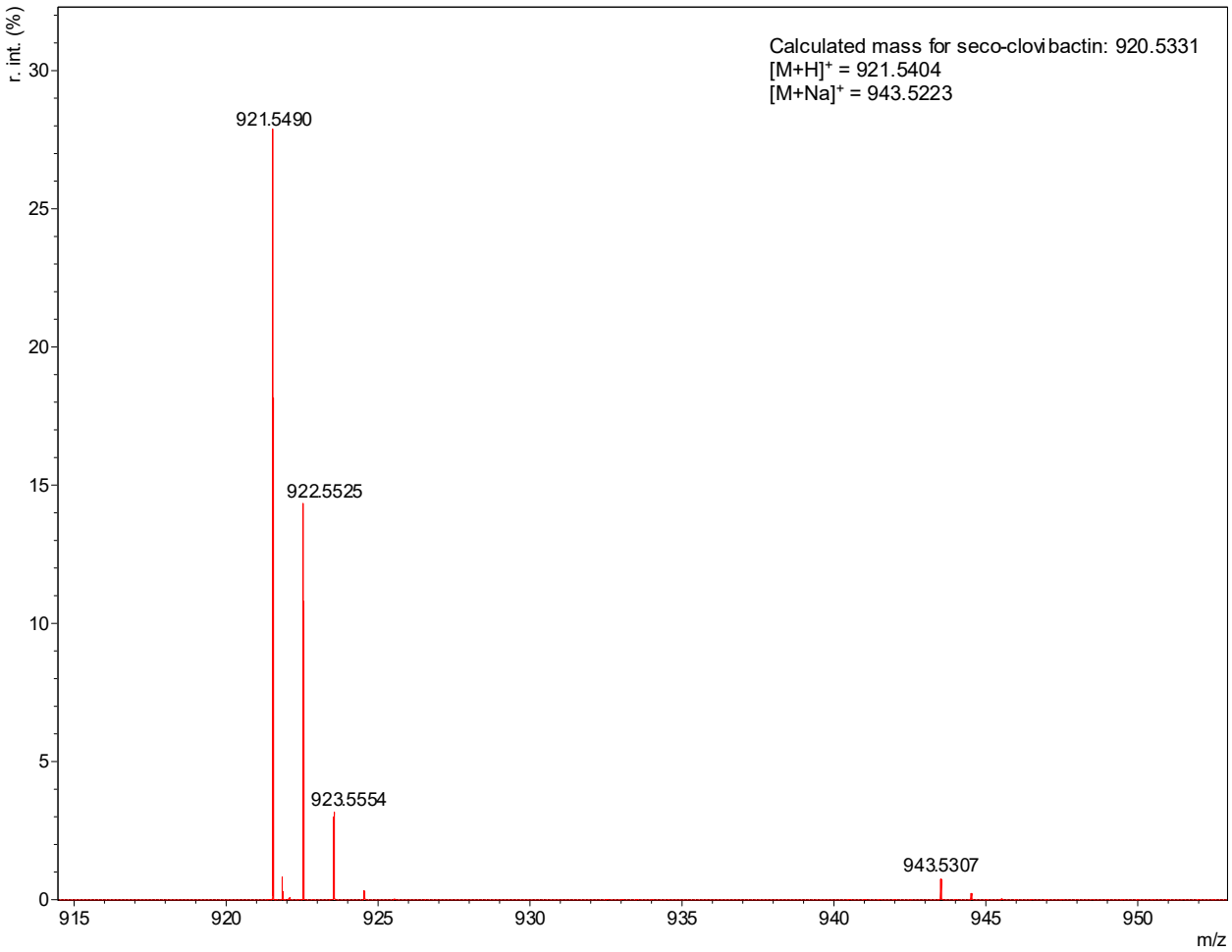
Calculated mass for seco-clovibactin: 920.5331
[M+H]+ = 921.5404
[M+Na]+ = 943.5223
r. int. (%)
921.5490
922.5525
923.5554
943.5307
m/z

Characterization of D-Thr5-clovibactin diene

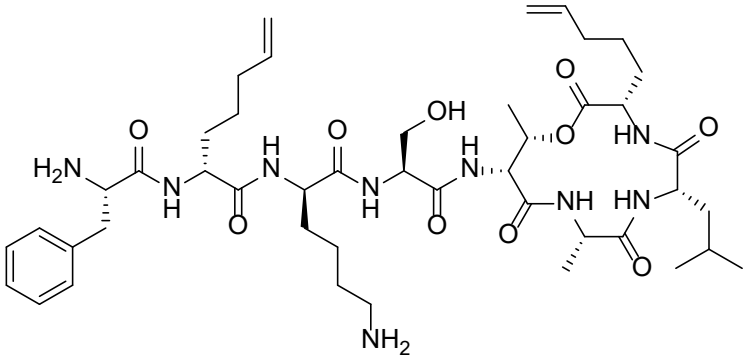

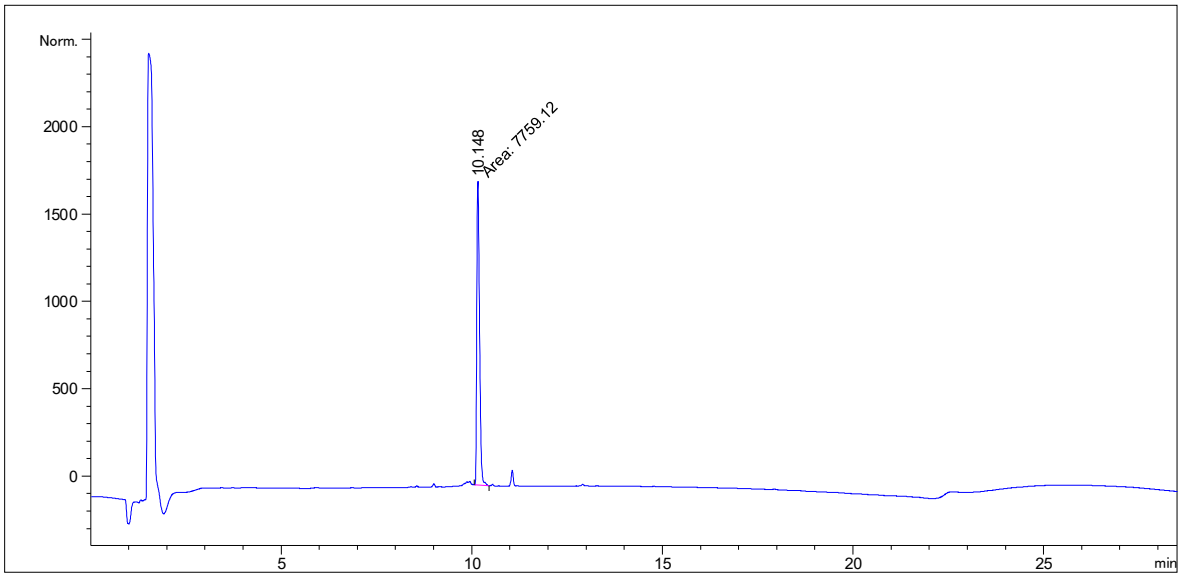

Signal 1: MWD1 A, Sig=214,4 Ref=off

Peak #	RetTime [min]	Type	Width [min]	Area [mAU*s]	Height [mAU]	Area %
1	10.148	MM	0.0823	7759.12207	1570.76721	100.000

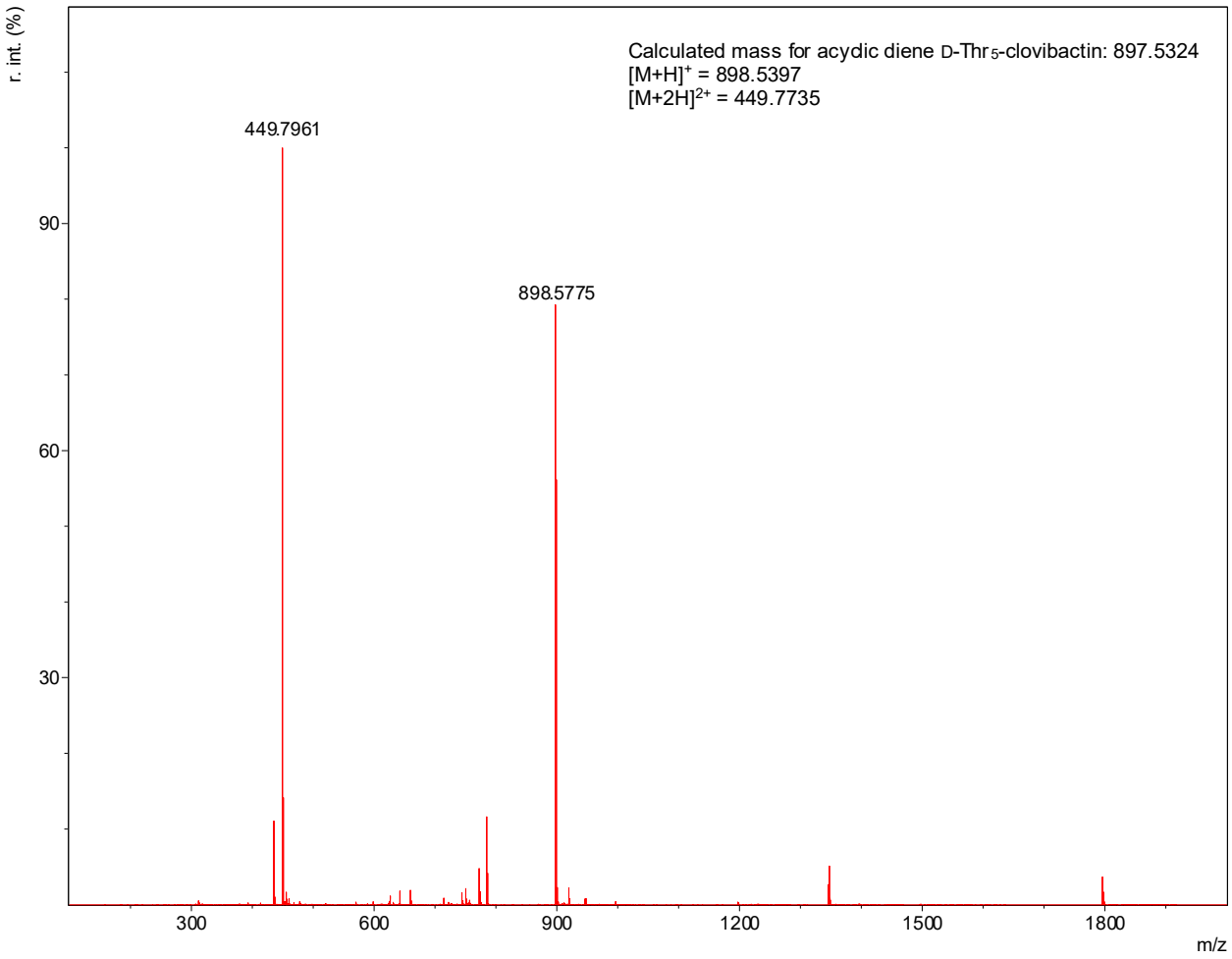
r. int. (%)
Calculated mass for acydic diene D-Thr5-clovibactin: 897.5324
[M+H]+ = 898.5397
[M+2H]2+ = 449.7735
449.7961
898.5775
90
60
30
300
600
900
1200
1500
1800
m/z

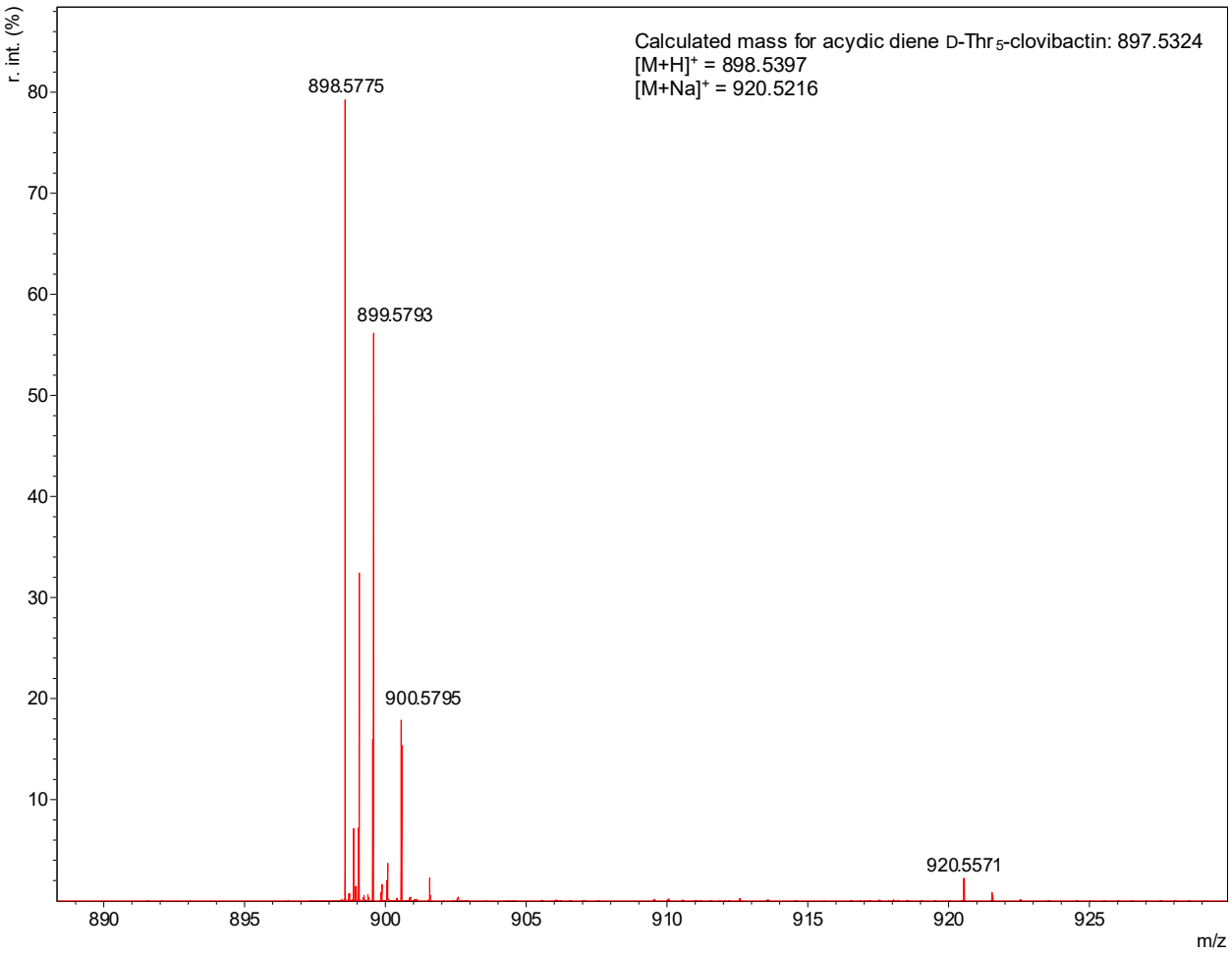
Calculated mass for acydic diene D-Thr5-clovibactin: 897.5324
[M+H]+ = 898.5397
[M+Na]+ = 920.5216
898.5775
899.5793
900.5795
920.5571
r. int. (%)
m/z

Characterization of stapled D-Thr5-clovibactin

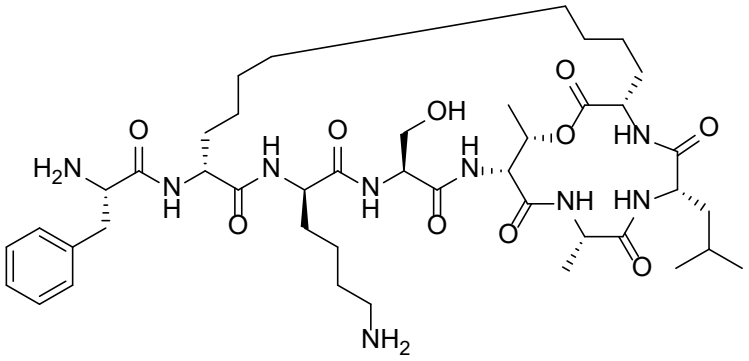

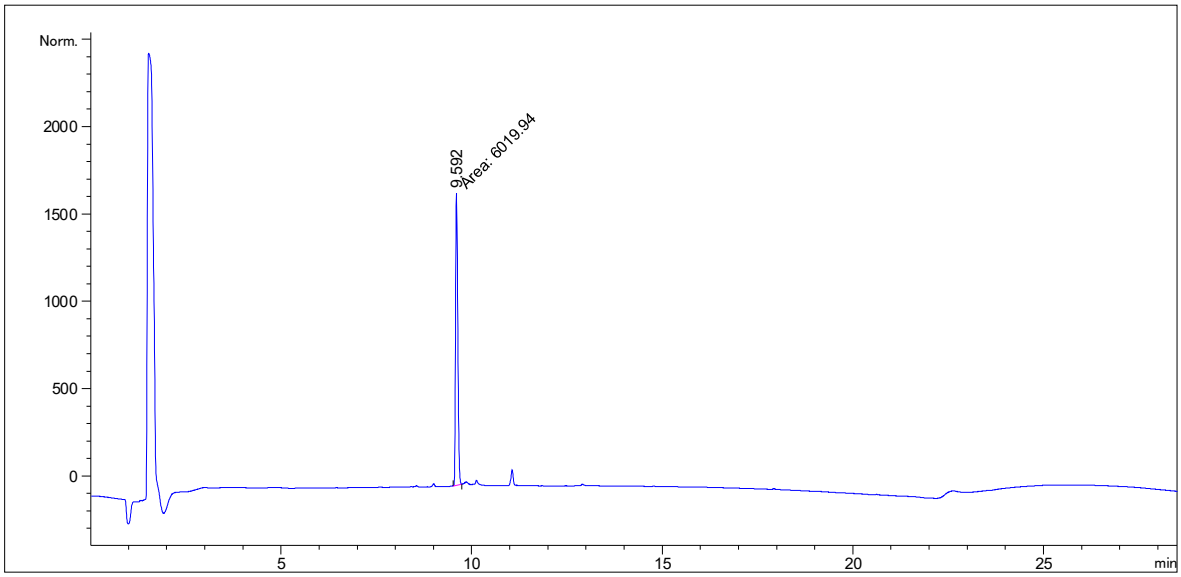

Signal 1: MWD1 A, Sig=214,4 Ref=off

Peak #	RetTime [min]	Type	Width [min]	Area [mAU*s]	Height [mAU]	Area %
1	9.592	MM	0.0663	6019.93701	1514.35608	100.000

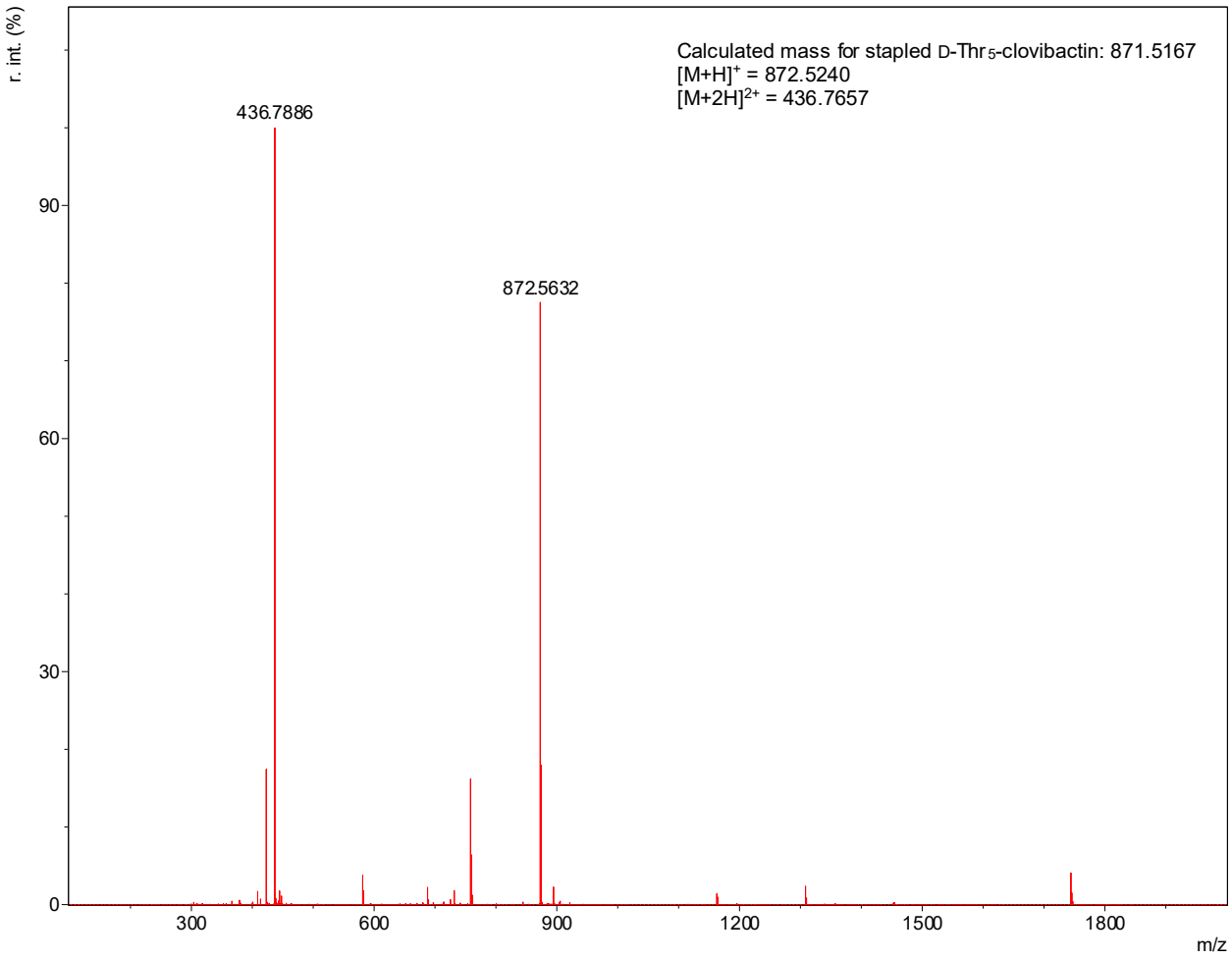
r. int. (%)
Calculated mass for stapled D-Thr5-clovibactin: 871.5167
[M+H]+ = 872.5240
[M+2H]2+ = 436.7657
436.7886
872.5632
90
60
30
0
300
600
900
1200
1500
1800
m/z

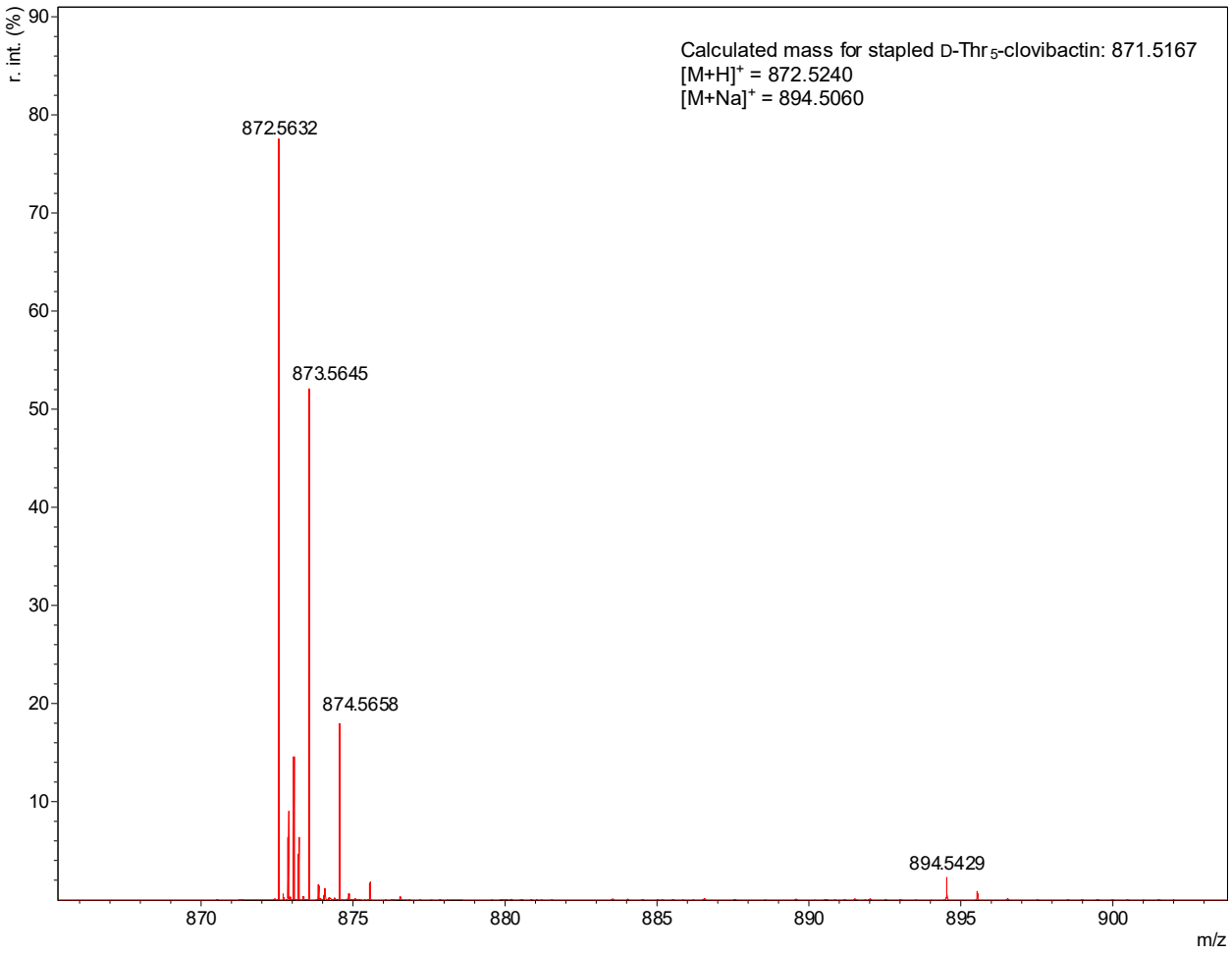
Calculated mass for stapled D-Thr5-clovibactin: 871.5167
[M+H]+ = 872.5240
[M+Na]+ = 894.5060
872.5632
873.5645
874.5658
894.5429
r. int. (%)
m/z

Characterization of N-Me-D-Leu$_{2,D}$-Thr$_5$-clovibactin

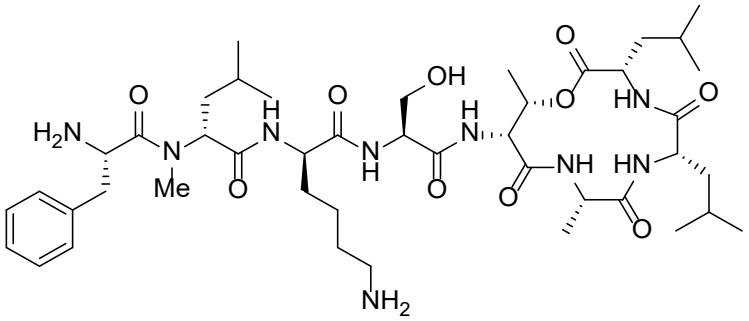

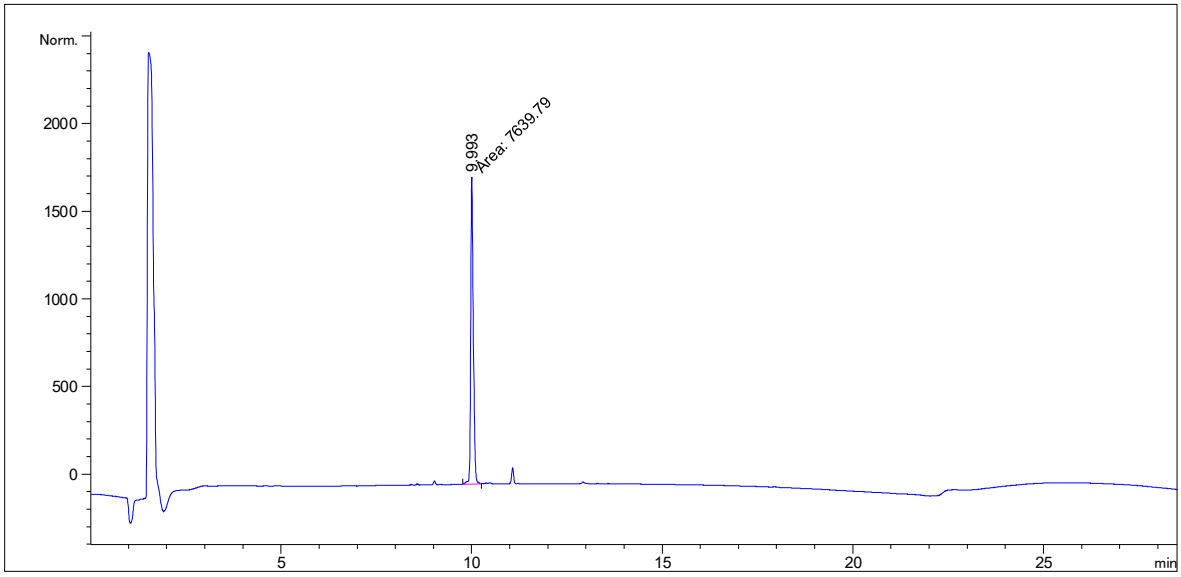

Signal 1: MWD1 A, Sig=214,4 Ref=off

Peak #	RetTime [min]	Type	Width [min]	Area [mAU*s]	Height [mAU]	Area %
1	9.993	MM	0.0804	7639.78613	1583.50024	100.000

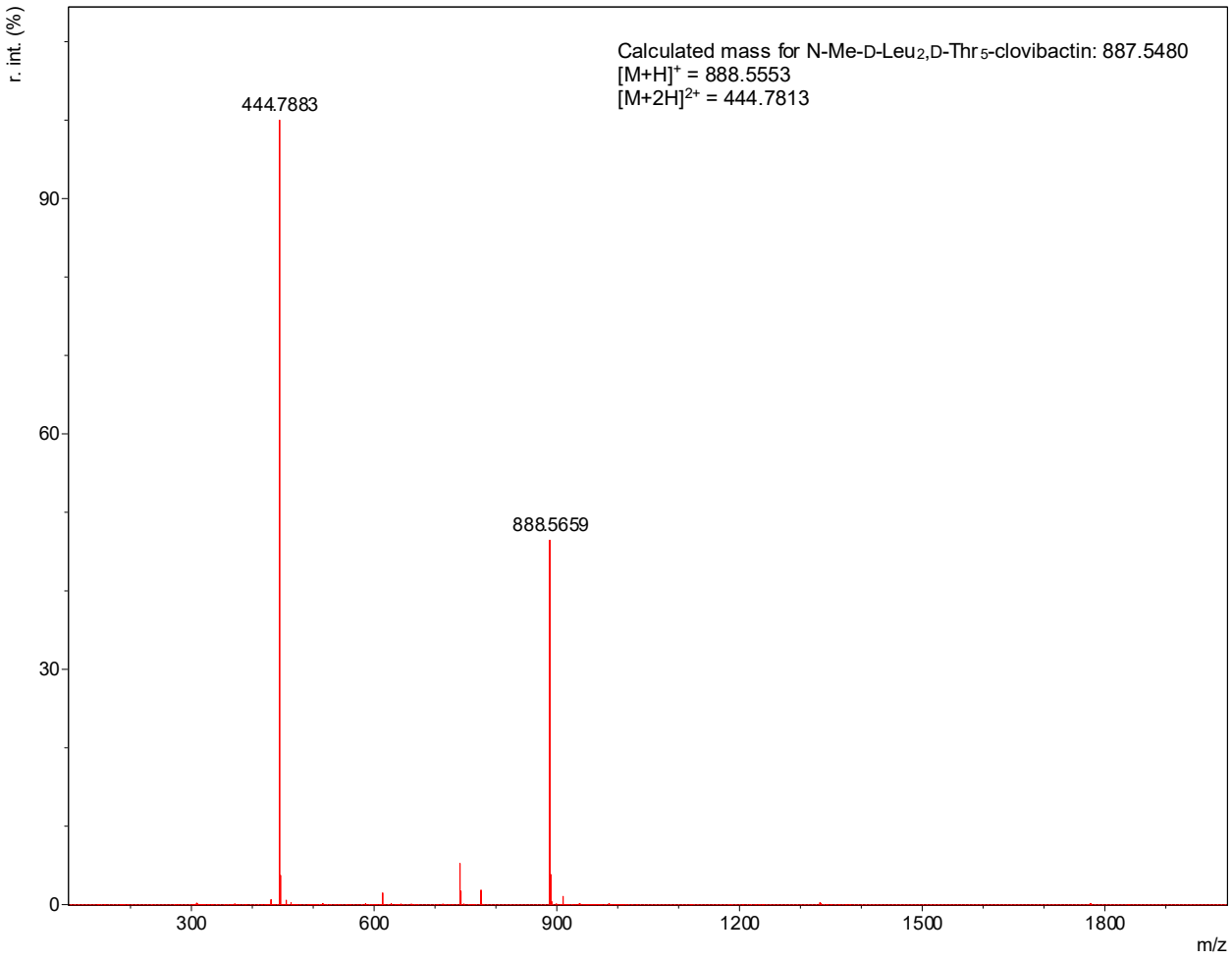
r. int. (%)
Calculated mass for N-Me-D-Leu2,D-Thr5-clovibactin: 887.5480
[M+H]+ = 888.5553
[M+2H]2+ = 444.7813
444.7883
888.5659
90
60
30
0
300
600
900
1200
1500
1800
m/z

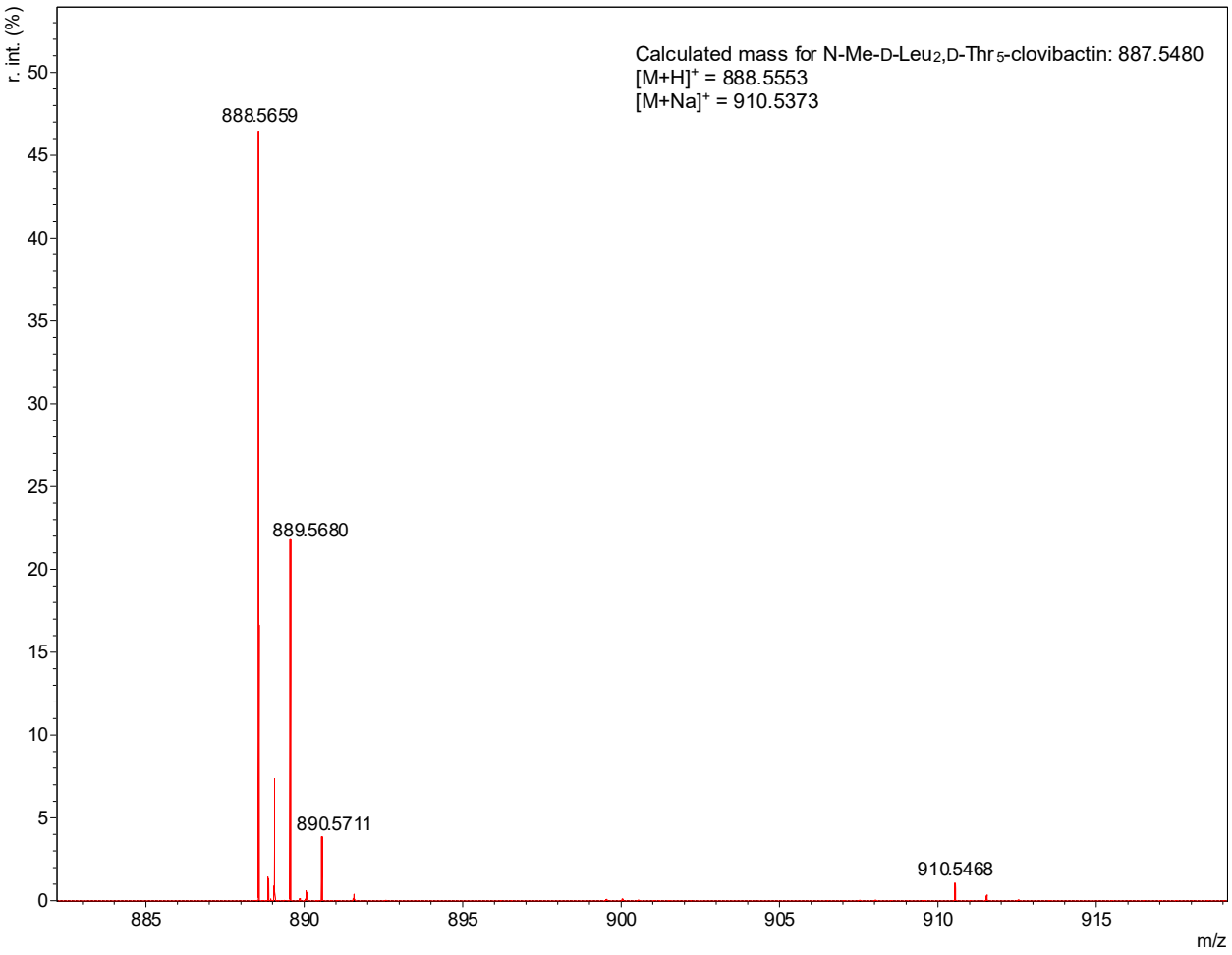
Calculated mass for N-Me-D-Leu2,D-Thr5-clovibactin: 887.5480
[M+H]+ = 888.5553
[M+Na]+ = 910.5373
888.5659
889.5680
890.5711
910.5468
r. int. (%)
m/z

Characterization of Aza-D-Thr5-clovibactin

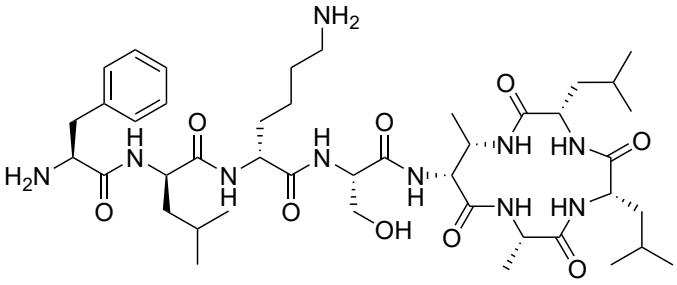

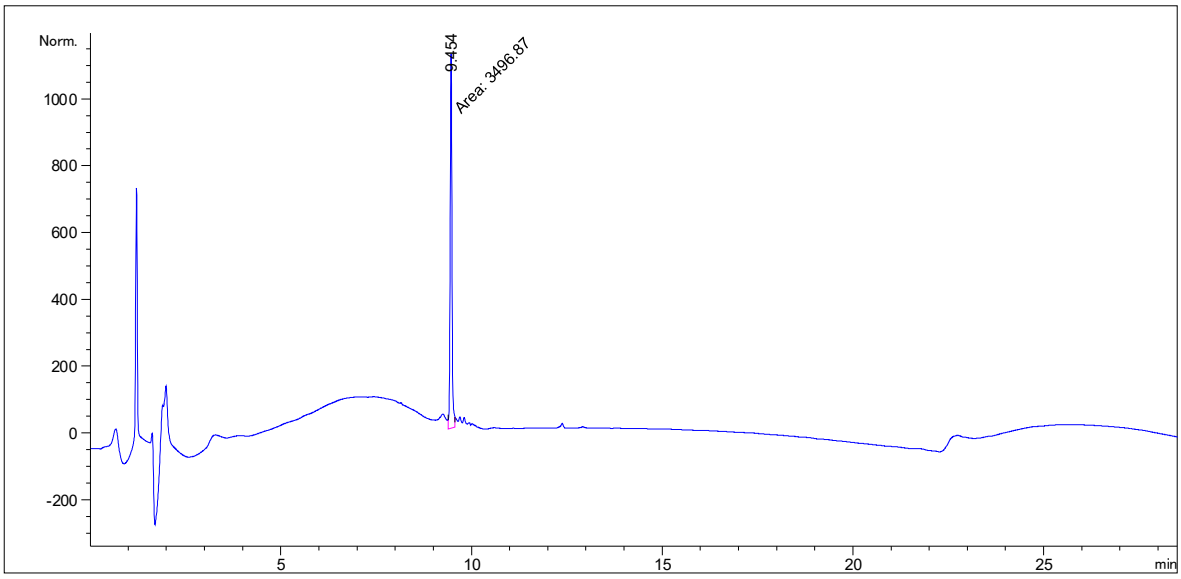

Peak #	RetTime [min]	Type	Width [min]	Area [mAU*s]	Height [mAU]	Area %
1	9.454	MM	0.0571	3496.86938	1021.21082	100.000
Totals :				3496.86938	1021.21082	

Calculated mass for Aza-D-Thr$_5$-clovibactin: 872.5484
[M+H]+ = 873.5557
[M+Na]+ = 895.5376
[M+K]+ = 911.5115

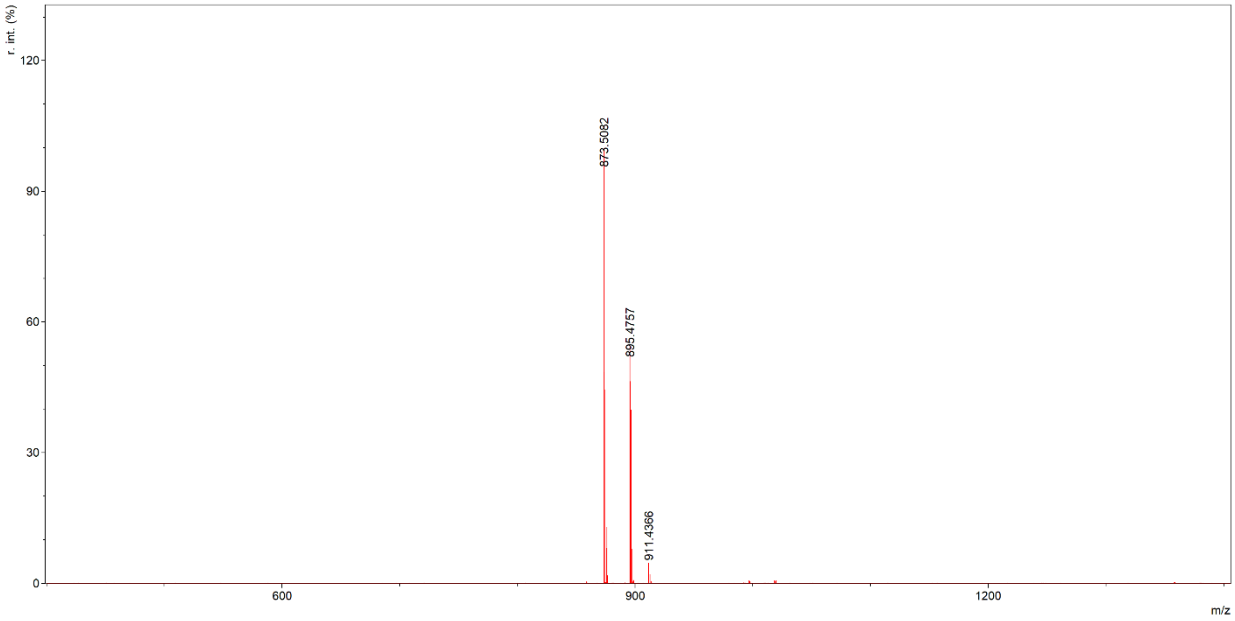

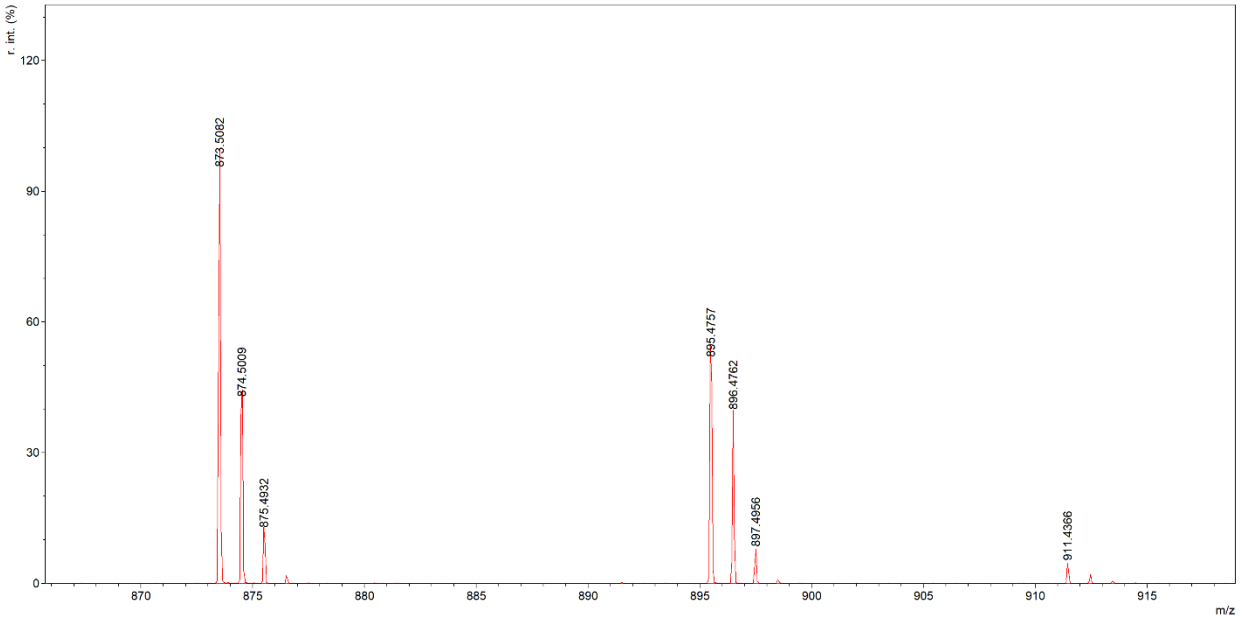

Characterization of Phe^{I}$_{1,d}$-Thr$_5$-clovibactin

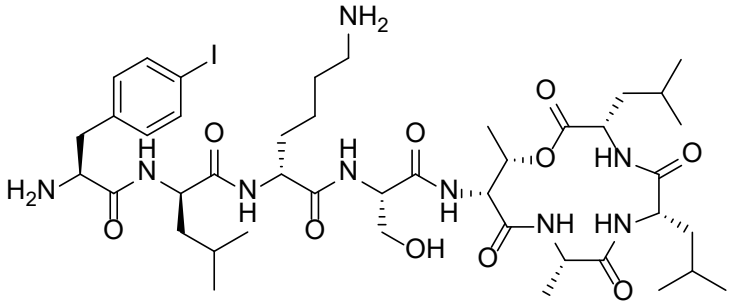

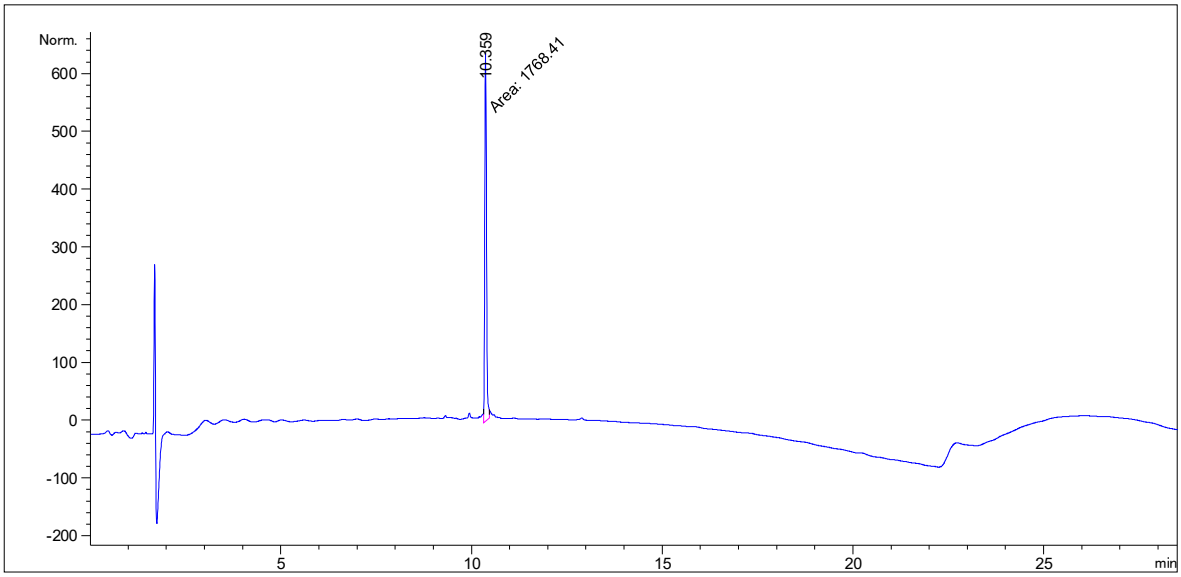

Peak #	RetTime [min]	Type	Width [min]	Area [mAU*s]	Height [mAU]	Area %
1	10.359	MM	0.0508	1768.40881	580.67322	100.000
Totals :				1768.40881	580.67322	

Calculated mass for Phe$^{I}_{1,d}$-Thr$_5$-clovibactin: 999.4290
[M+H]+ = 1000.4363
[M+Na]+ = 1022.4183

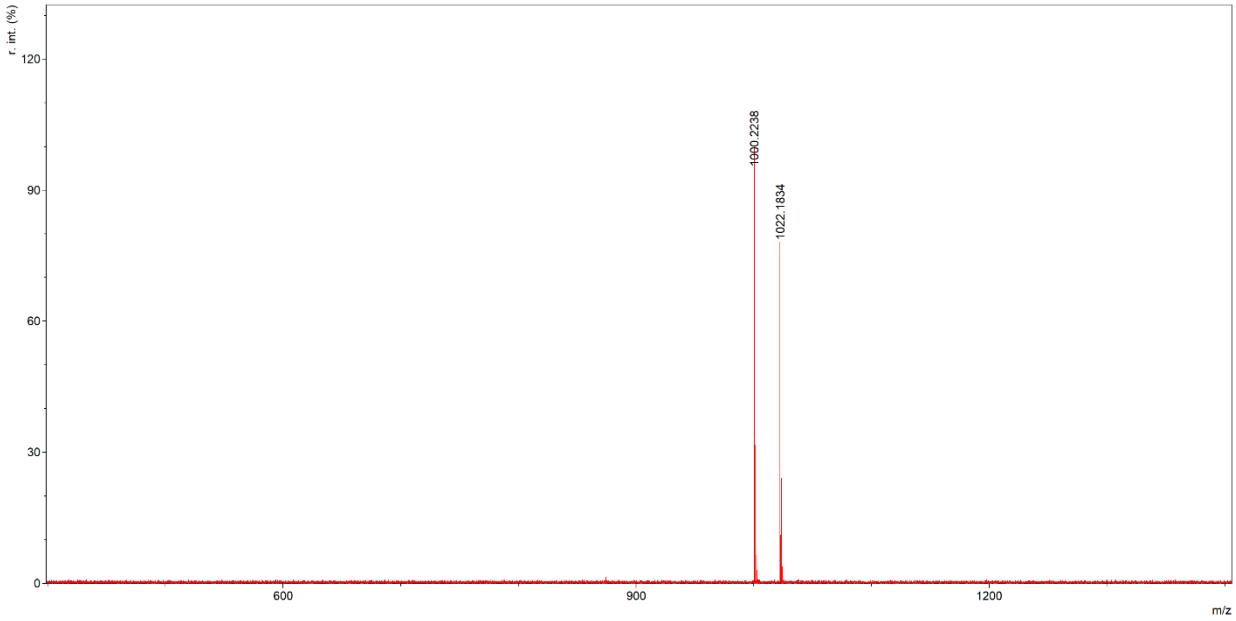

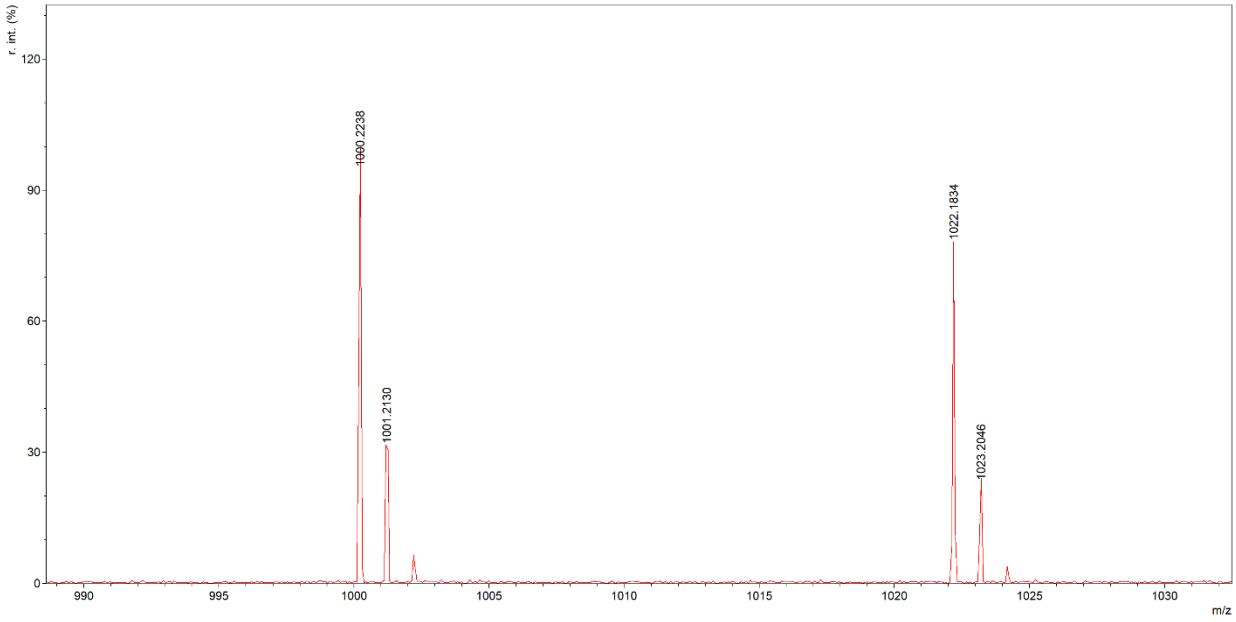

Characterization of Bip$_{1,D}$-Thr$_5$-clovibactin

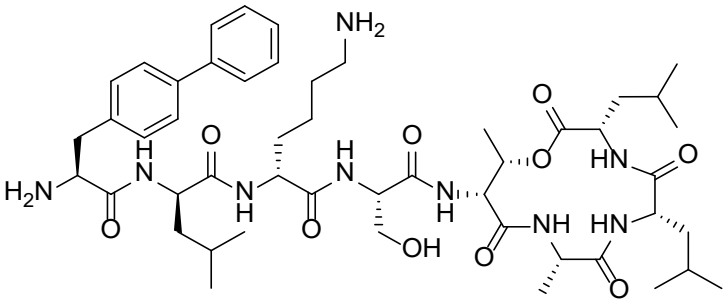

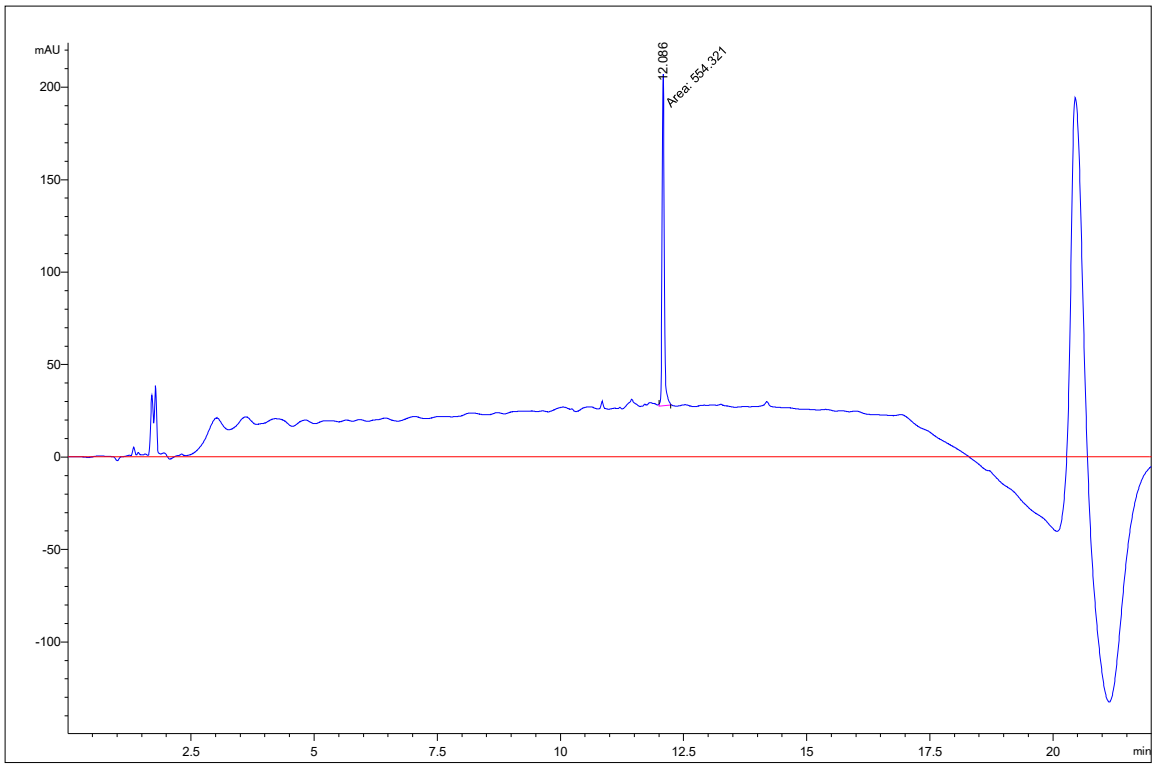

Peak #	RetTime [min]	Type	Width [min]	Area [mAU*s]	Height [mAU]	Area %
1	12.086	MM	0.0512	554.32147	180.59857	100.000
Totals :				554.32147	180.59857	

Calculated mass for Bip$_1$,D-Thr$_5$-clovibactin: 949.5637
[M+H]+ = 950.5710
[M+Na]+ = 972.5529
[M+K]+ = 988.5268

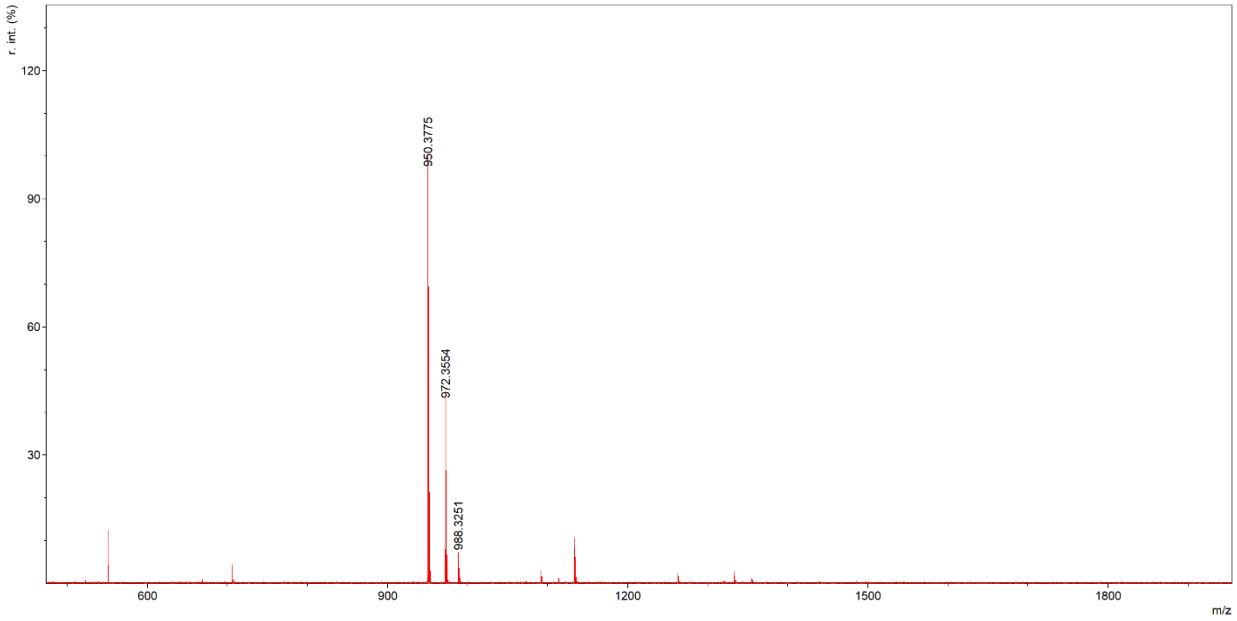

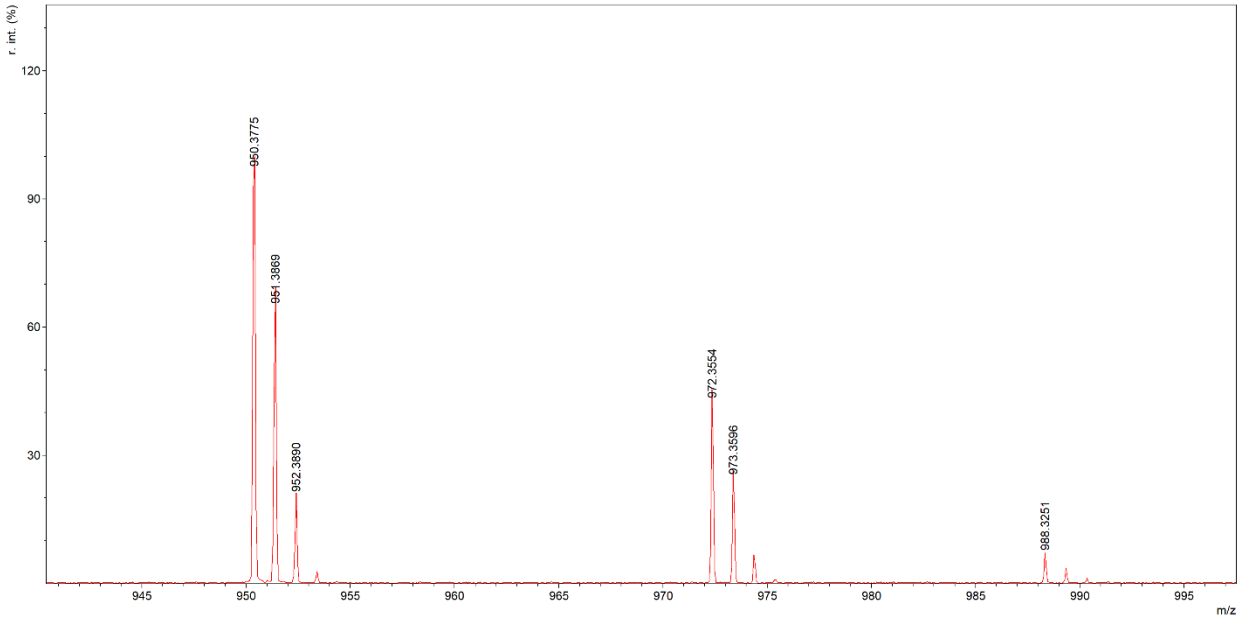

Characterization of Asn$_{4,D}$-Thr$_5$,Tyr$_6$,Leu$_7$-hypeptin

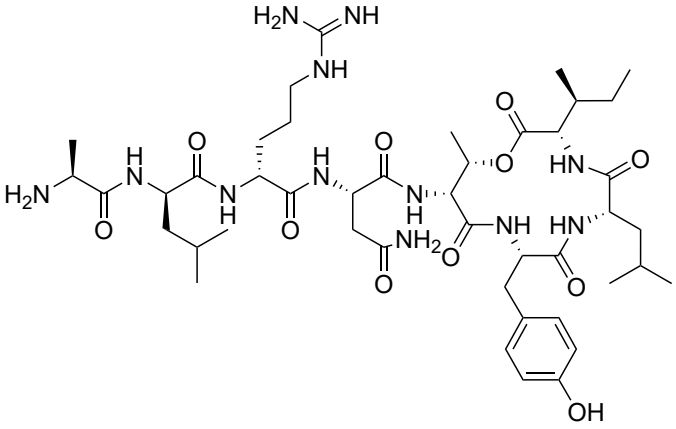

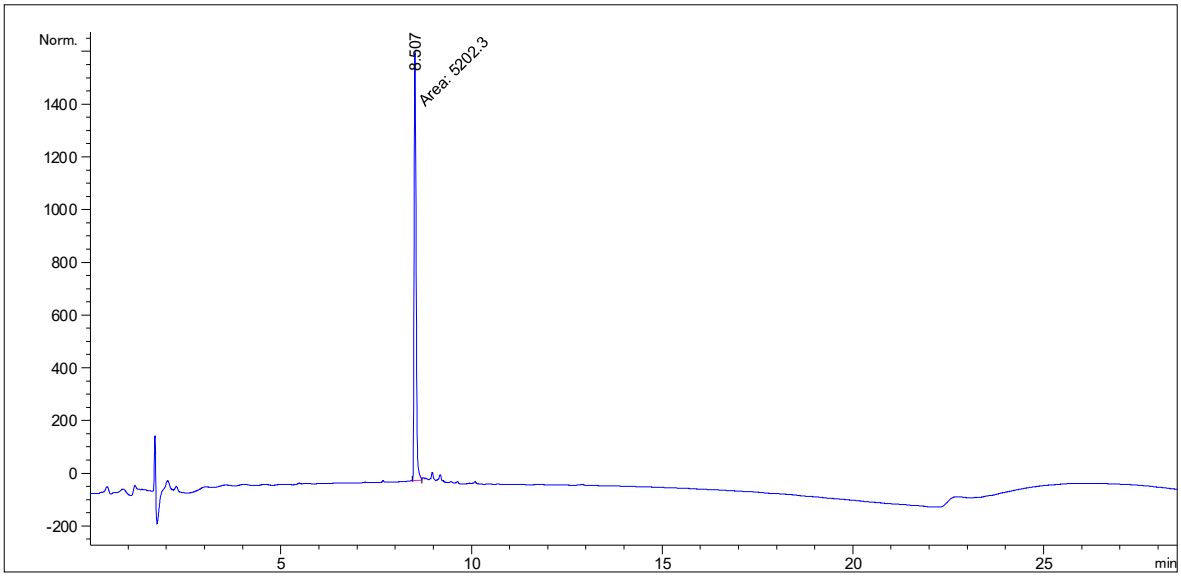

Peak #	RetTime [min]	Type	Width [min]	Area [mAU*s]	Height [mAU]	Area %
1	8.507	MM	0.0586	5202.30420	1478.69873	100.000
Totals :				5202.30420	1478.69873	

Calculated mass for Asn$_4$,D-Thr$_5$,Tyr$_6$,Leu$_7$-hypeptin: 944.5444
[M+H]+ = 945.5516
[M+Na]+ = 967.5336

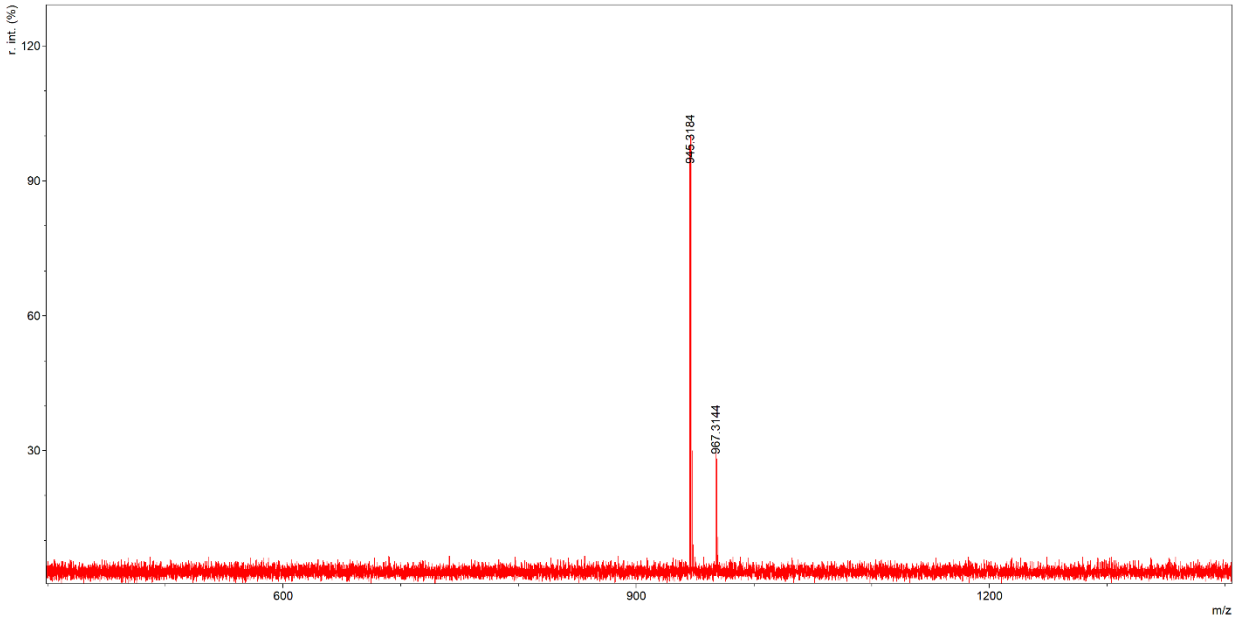

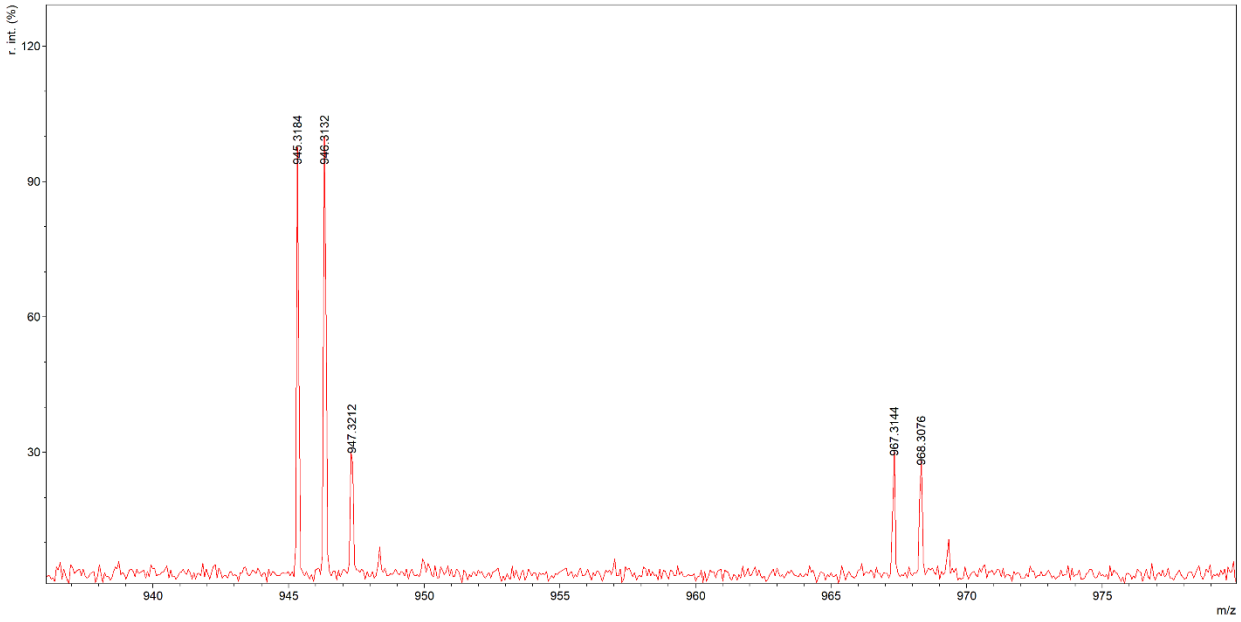

Characterization of Ser$_{4,D}$-Thr$_5$,Tyr$_6$,Leu$_7$-hypeptin

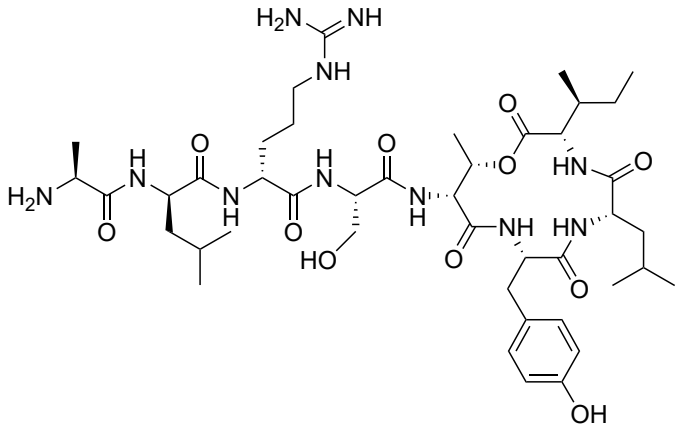

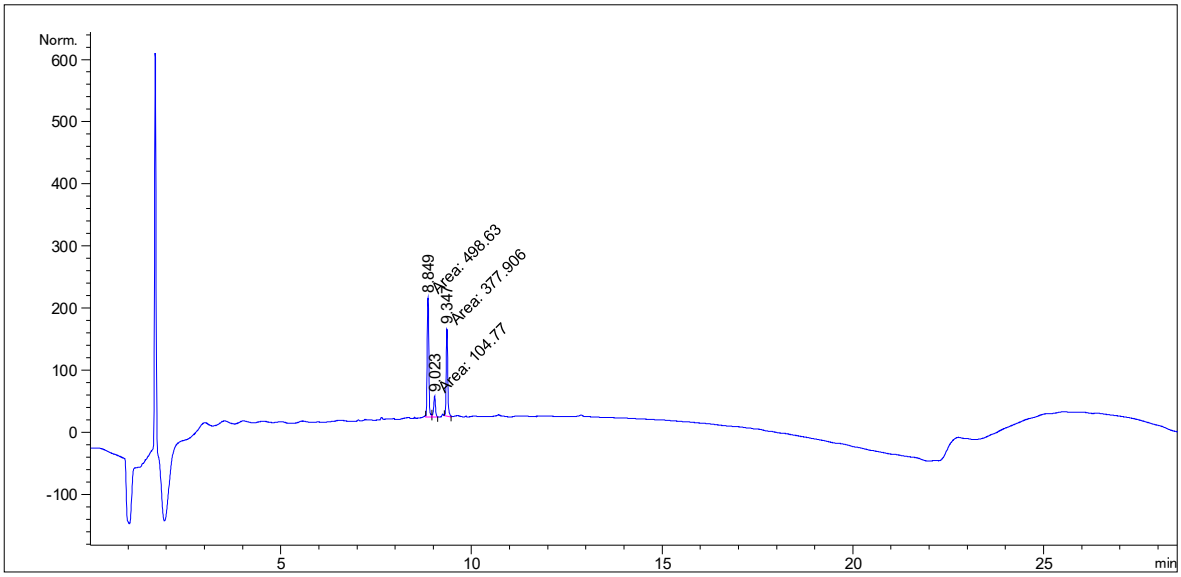

Peak #	RetTime [min]	Type	Width [min]	Area [mAU*s]	Height [mAU]	Area %	
1	8.849	MF	0.0477	498.62967	174.17307	50.812	9
2	9.023	FM	0.0574	104.76980	30.40982	10.676	6
3	9.347	MM	0.0492	377.90570	128.04916	38.510	5
Totals :				981.30517	332.63205		

Calculated mass for Ser_4,D-Thr_5,Tyr_6,Leu_7-hypeptin: 917.5335
[M+H]+ = 918.5407
[M+Na]+ = 940.5227

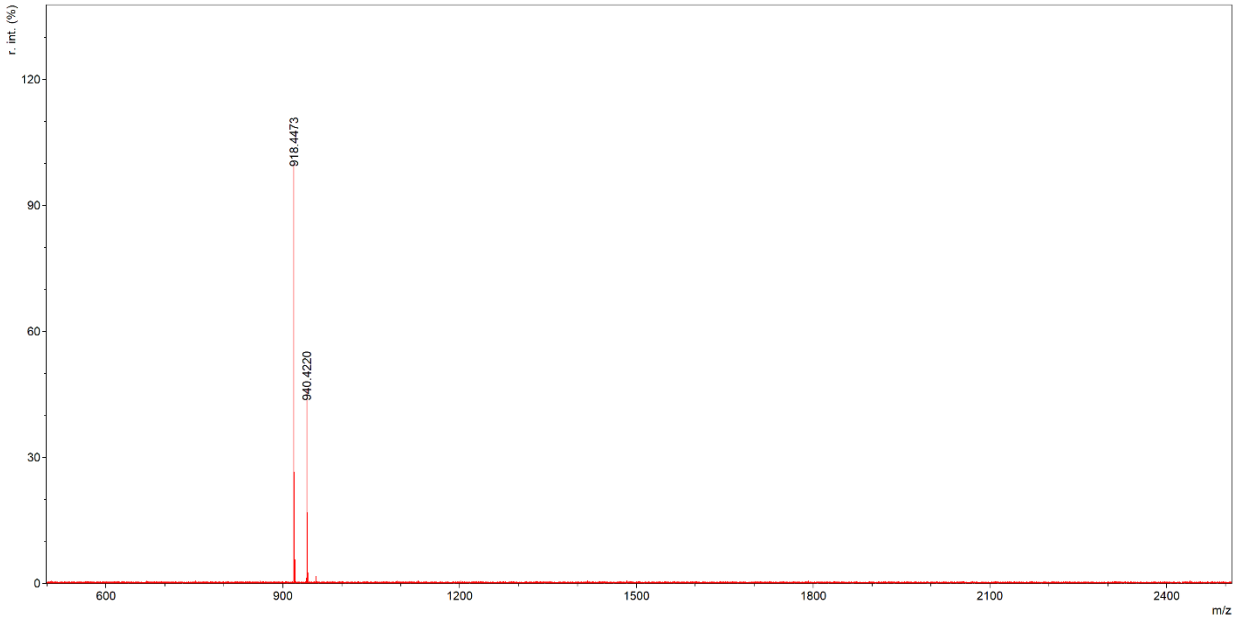

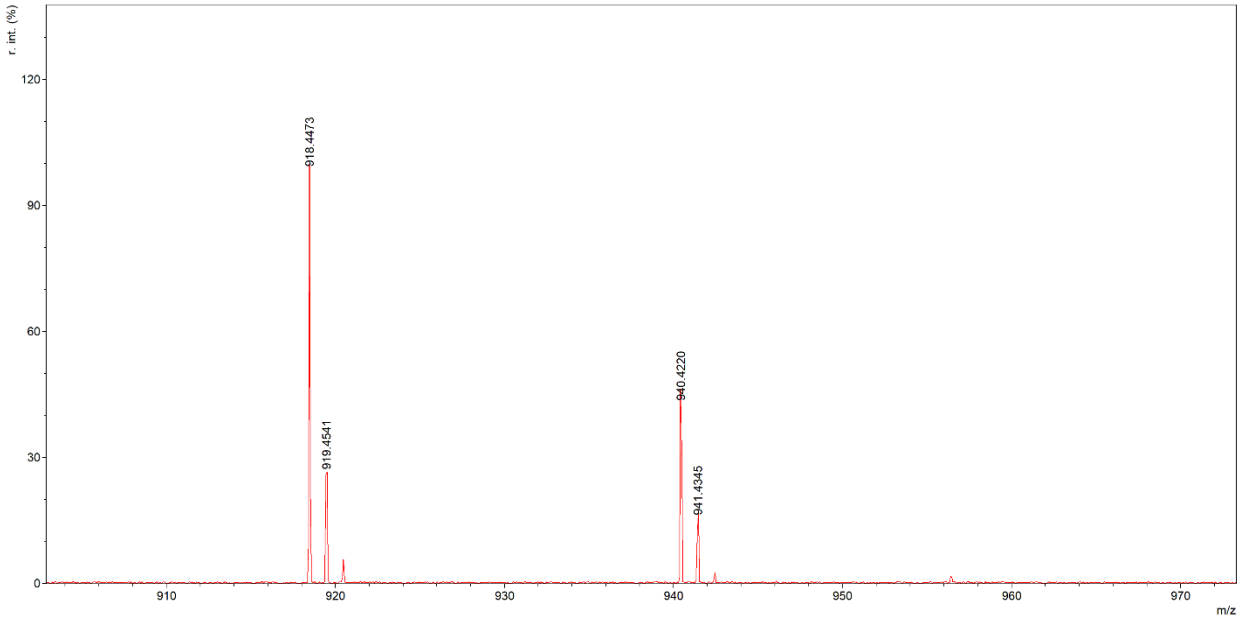

References for Chapter IV

[1] Shukla, R.; Peoples, A. J.; Ludwig, K. C.; Maity, S.; Derks, M. G. N.; De Benedetti, S.; Kreuger, A. M.; Vermeulen, B. J. A.; Harbig, T.; Lavore, F.; Kumar, R.; Honorato, R. V.; Grein, F.; Nieselt, K.; Liu, Y.; Bonvin, A. M. J. J.; Baldus, M.; Kubitscheck, U.; Breukink, E.; Achorn, C.; Nitti, A.; Schwalen, C. J.; Spoering, A. L.; Ling, L. L.; Hughes, D.; Lelli, M.; Roos, W. H.; Lewis, K.; Schneider, T.; Weingarth, M. An antibiotic from an uncultured bacterium binds to an immutable target. *Cell* **2023**, *186*, 1−15. DOI: 10.1016/j.cell.2023.07.038

[2] Yang, H.; Du Bois, D. R.; Ziller, J. W.; Nowick, J. S. X-ray Crystallographic Structure of a Teixobactin Analogue Reveals Key Interactions of the Teixobactin Pharmacophore. *Chem. Commun.* **2017**, *53*, 2772−2775. DOI: 10.1039/C7CC00783C

[3] Chen, K.H.; Le, S. P.; Han, X.; Frias, J. M.; Nowick, J. S. Alanine Scan Reveals Modifiable Residues in Teixobactin. *Chem. Commun.* **2017**, *53*, 11357−11359. DOI: 10.1039/C7CC03415F

[4] Yang, H; Wierzbicki, M.; Du Bois, D. R.; Nowick, J. S. X-ray Crystallographic Structure of a Teixobactin Derivative Reveals Amyloid-like Assembly. *J. Am. Chem. Soc.* **2018**, *140*, 14028−14032. DOI: 10.1021/jacs.8b07709

[5] Yang, H; Pishenko, A. V.; Li, X.; Nowick, J. S. Design, Synthesis, and Study of Lactam and Ring-Expanded Analogues of Teixobactin. *J. Org. Chem.* **2020**, *85*, 1331−1339. DOI: https://doi.org/10.1021/acs.joc.9b02631

[6] Jones, C. R.; Guaglianone, G.; Lai, G. H.; Nowick, J. S. Isobactins: O-acyl isopeptide prodrugs of teixobactin and teixobactin derivatives. *Chem. Sci.* **2022**, *13*, 13110−13116. DOI: 10.1039/D2SC02670H

[7] Jones, C. R.; Lai, G. H.; Padilla, M. S. T. L.; Nowick, J. S. Investigation of Isobactin Analogues of Teixobactin. *ACS Med. Chem. Lett.* **2024**, *15* (7), 1136–1142. DOI: 10.1021/acsmedchemlett.4c00215

[8] Yang, H.; Kreutzer, A. G.; Nowick, J. S. Supramolecular Interactions of Teixobactin Analogues in the Crystal State. *J. Org. Chem.* **2024**, *89* (7), 5104–5108. DOI: 10.1021/acs.joc.3c02617

[9] Krumberger, M.; Li, X.; Kreutzer, A. G.; Peoples, A.J.; Nitti, A. G.; Cunningham, A. M.; Jones, C. R.; Achorn, C.; Ling, L. L.; Hughes, D. E.; Nowick, J. S. Synthesis and Stereochemical Determination of the Peptide Antibiotic Novo29. *J. Org. Chem.* **2023**, *88*, 2214−2220. DOI: https://doi.org/10.1021/acs.joc.2c02648

[10] Peoples, A. J.; Hughes, D.; Ling, L. L.; Millett, W.; Nitti, A. G.; Spoering, A.; Steadman, V. A.; Chiva, J. C.; Lazarides, L.; Jones, M. K.; Poullennes, K. G.; Lewis, K.; Epstein, S. ″Depsipeptides and uses thereof″. US11,203,616, 2021.

[11] Homma, T.; Nuxoll, A.; Gandt, A. B.; Ebner, P.; Engels, I.; Schneider, T.; Götz, F.; Lewis, K.; Conlon, B. P. Dual Targeting of Cell Wall Precursors by Teixobactin Leads to Cell Lysis. *Antimicrob. Agents Chemother.* **2016**, *60* (11), 6510–6517. DOI: 10.1128/aac.01050-16

[12] Shukla, R.; Medeiros-Silva, J.; Parmar, A.; Vermeulen, B. J. A.; Das, S.; Paioni, A. L.; Jekhmane, S.; Lorent, J.; Bonvin, A. M. J. J.; Baldus, M.; Lelli, M.; Veldhuizen, E. J. A.;

Breukink, E.; Singh, I.; Weingarth, M. Mode of action of teixobactins in cellular membranes. *Nat. Commun.* **2020**, *11*, 2848. DOI: 10.1038/s41467-020-16600-2

[13] Chiorean, S.; Antwi, I.; Carney, D. W.; Kotsogianni, I.; Giltrap, A. M.; Alexander, F. M.; Cochrane, S. A.; Payne, R. J.; Martin, N. I.; Henninot, A.; Vederas, J. C. Dissecting the Binding Interactions of Teixobactin with the Bacterial Cell-Wall Precursor Lipid II. *ChemBioChem* **2020**, *21* (6), 789–792. DOI: 10.1002/cbic.201900504

[14] Shukla, R.; Lavore, F.; Maity, S.; Derks, M. G. N.; Jones, C. R.; Vermeulen, B. J. A.; Melcrová, A.; Morris, M. A.; Becker, L. M.; Wang, X.; Kumar, R.; Medeiros-Silva, J.; Van Beekveld, R. A. M.; Bonvin, A. M. J. J.; Lorent, J. H.; Lelli, M.; Nowick, J. S.; MacGillavry, H. D.; Peoples, A. J.; Spoering, A. L.; Ling, L. L.; Hughes, D. E.; Roos, W. H.; Breukink, E.; Lewis, K.; Weingarth, M. Teixobactin Kills Bacteria by a Two-Pronged Attack on the Cell Envelope. *Nature* **2022**, *608* (7922), 390–396. DOI: 10.1038/s41586-022-05019-y

[15] Yoshiya, T.; Taniguchi, A.; Sohma, Y.; Fukao, F.; Nakamura, S.; Abe, N.; Ito, N.; Skwarczynski, M.; Kimura, T.; Hayashi, Y.; Kiso, Y. "O-Acyl Isopeptide Method" for Peptide Synthesis: Synthesis of Forty Kinds of "O-Acyl Isodipeptide Unit" Boc-Ser/Thr(Fmoc-Xaa)-OH. Org. Biomol. Chem. **2007**, *5* (11), 1720–1730. DOI: 10.1039/B702284K

[16] Sohma, Y.; Yoshiya, T.; Taniguchi, A.; Kimura, T.; Hayashi, Y.; Kiso, Y. Development of *O*-acyl Isopeptide Method. Biopolymers **2007**, *88* (2), 253–262. DOI: 10.1002/bip.20683

[17] Saneyoshi, H.; Ochikubo, T.; Mashimo, T.; Hatano, K.; Ito, Y.; Abe, H. Triphenylphosphinecarboxamide: An Effective Reagent for the Reduction of Azides and Its

Application to Nucleic Acid Detection. *Org. Lett.* **2014**, *16* (1), 30–33. DOI: 10.1021/ol402832w

[18] Ling, L. L.; Schneider, T.; Peoples, A. J.; Spoering, A. L.; Engels, I.; Conlon, B. P.; Mueller, A.; Schäberle, T. F.; Hughes, D. E.; Epstein, S.; Jones, M.; Lazarides, L.; Steadman, V. A.; Cohen, D. R.; Felix, C. R.; Fetterman, K. A.; Millett, W. P.; Nitti, A. G.; Zullo, A. M.; Chen, C.; Lewis, K. A New Antibiotic Kills Pathogens without Detectable Resistance. *Nature* **2015**, *517* (7535), 455–459. DOI: 10.1038/nature14098

[19] Yeates, T. O. [22] Detecting and Overcoming Crystal Twinning. In Methods in Enzymology; Elsevier, 1997; Vol. 276, pp 344–358. DOI: 10.1016/S0076-6879(97)76068-3.

[20] Zong, Y.; Fang, F.; Meyer, K. J.; Wang, L.; Ni, Z.; Gao, H.; Lewis, K.; Zhang, J.; Rao, Y. Gram-Scale Total Synthesis of Teixobactin Promoting Binding Mode Study and Discovery of More Potent Antibiotics. *Nat Commun* **2019**, *10* (1), 3268. DOI: 10.1038/s41467-019-11211-y

[21] Shoji, J.; Hinoo, H.; Hattori, T.; Hirooka, K.; Kimura, Y.; Yoshida, T. Isolation and Characterization of Hypeptin from Pseudomonas Sp. *J. Antibiot.* **1989**, *42* (10), 1460–1464. DOI: 10.7164/antibiotics.42.1460

[22] Wirtz, D. A.; Ludwig, K. C.; Arts, M.; Marx, C. E.; Krannich, S.; Barac, P.; Kehraus, S.; Josten, M.; Henrichfreise, B.; Müller, A.; König, G. M.; Peoples, A. J.; Nitti, A.; Spoering, A. L.; Ling, L. L.; Lewis, K.; Crüsemann, M.; Schneider, T. Biosynthesis and Mechanism of Action of the Cell Wall Targeting Antibiotic Hypeptin. *Angew Chem Int Ed* **2021**, *60* (24), 13579–13586. DOI: 10.1002/anie.202102224

[23] Yang, H.; Chen, K. H.; Nowick, J. S. Elucidation of the Teixobactin Pharmacophore. *ACS Chem. Biol.* **2016**, *11* (7), 1823–1826. DOI: 10.1021/acschembio.6b00295

[24] Morris, M. A.; Malek, M.; Hashemian, M. H.; Nguyen, B. T.; Manuse, S.; Lewis, K.; Nowick, J. S. A Fluorescent Teixobactin Analogue. *ACS Chem. Biol.* **2020**, *15* (5), 1222–1231.

[25] Sohma, Y.; Taniguchi, A.; Skwarczynski, M.; Yoshiya, T.; Fukao, F.; Kimura, T.; Hayashi, Y.; Kiso, Y. 'O-Acyl Isopeptide Method' for the Efficient Synthesis of Difficult Sequence-Containing Peptides: Use of 'O-Acyl Isodipeptide Unit.' *Tetrahedron Letters* **2006**, *47* (18), 3013–3017.

[26] APEX3 Version 2018.1-0, Bruker AXS, Inc.; Madison, WI 2018.

[27] SAINT Version 8.38a, Bruker AXS, Inc.; Madison, WI 2013.

[28] Sheldrick, G. M. SADABS, Version 2014/5, Bruker AXS, Inc.; Madison, WI 2014.

[29] Sheldrick, G. M. SHELXTL, Version 2014/7, Bruker AXS, Inc.; Madison, WI 2014.

[30] International Tables for Crystallography 1992, Vol. C., Dordrecht: Kluwer Academic Publishers.

[31] Parsons, S., Flack, H. D., Wagner, T. Acta Cryst. B69, 249-259, 2013.

[32] W. Kabsch, XDS. *Acta Crystallographica Section D Biological Crystallography* **66**, 125–132 (2010).

[33] P. D. Adams, et al., PHENIX: a comprehensive Python-based system for macromolecular structure solution. *Acta Crystallogr. D Biol. Crystallogr.* **66**, 213–221 (2010).

[34] P. Emsley, B. Lohkamp, W. G. Scott, K. Cowtan, Features and development of Coot. *Acta Crystallographica Section D Biological Crystallography* **66**, 486–501 (2010).

[35] J. Painter, E. A. Merritt, Optimal description of a protein structure in terms of multiple groups undergoing TLS motion. *Acta Crystallogr. D Biol. Crystallogr.* **62**, 439–450 (2006).

[36] J. Painter, E. A. Merritt, TLSMD web server for the generation of multi-group TLS models. *J. Appl. Crystallogr.* **39**, 109–111 (2006).

[37] Zhang, S.; Yoo, S.; Snyder, D. T.; Katz, B. B.; Henrickson, A.; Demeler, B.; Wysocki, V. H.; Kreutzer, A. G.; Nowick, J. S. A Disulfide-Stabilized Aβ That Forms Dimers but Does Not Form Fibrils. *Biochemistry* **2022**, *61* (4), 252–264. DOI: 10.1021/acs.biochem.1c00739

CHAPTER V: Leveraging Undergraduate Learning Assistants When Implementing New Laboratory Curricula*

Abstract

At University of California, Irvine, a large-enrollment research university, undergraduate chemistry courses for non-chemistry majors were delivered remotely during the 2020–2021 academic year, with a return to in-person instruction planned for January 2022. Because this return to in-person instruction coincided with the transition of second-year students from general chemistry to organic chemistry laboratory courses, the instructional staff recognized a need for remedial laboratory curricula for students with no prior in-person laboratory experience. Simultaneously, we desired to implement undergraduate Learning Assistants (LAs) in non-chemistry major organic chemistry laboratories for the first time at our university. In this paper, we describe our approach for leveraging undergraduate LAs to (1) test new laboratory curricula and (2) address feelings of comfort and safety for students with no prior in-person laboratory experience. Benefits of our LA program perceived by students include increased laboratory efficiency and improved student learning from near-peer instructors; benefits perceived by LAs include the development of professional skills and teamwork with graduate student teaching assistants. We provide an outline of resources and strategies to enable instructors to simultaneously implement undergraduate LAs and new laboratory curricula.

* This chapter is reproduced verbatim, in its entirety, and with permission from *Frontiers in Education* (*Front. Educ.* **2024**, 9:1367087). Jordan Thompson, Pía López, and Prof. Renée Link participated in the research and in writing and editing the published manuscript.

Introduction

Learning Assistants (LAs) — undergraduate students who serve as assistant instructors for courses they have previously taken — are increasingly being leveraged in STEM courses.[1,2] Peer learning, in which experienced students guide current students' learning through a zone of proximal development, underpins LA programs.[3] In traditional learning communities, students learn solely from a senior instructor, who can be perceived as unapproachable or intimidating. Vertical learning communities seek to address this student-instructor gap by introducing a near-peer instructor.[4] LAs are approachable due to closeness in age and experience and can provide mentorship to students. Additionally, LAs improve students' comfort and confidence in the classroom.[5] Student comfort and confidence fall under the affective domain, which — along with the cognitive and psychomotor domains — is an essential part of meaningful learning in the laboratory.[6,7] Therefore, peer instructors have the potential to foster an improved overall learning environment.

The COVID-19 pandemic and subsequent statewide shutdown in 2020 resulted in evacuation of our campus and remote learning that lasted until December 2021.[8] During the Spring 2021 term, the organic chemistry laboratory (OCL) course sequence for non-chemistry majors piloted an LA program to facilitate student guidance during a time of isolation and uncertainty.

Returning to in-person learning presented unique challenges for the OCL instructional team. Under usual circumstances, students would have completed two prior in-person general chemistry laboratory courses. Due to remote learning, both students entering the OCL series and pilot program LAs who completed OCL courses online would have little to no hands-on chemistry laboratory experience. Fall 2021 was an opportunity for the simultaneous testing of

new experiments and training of LAs with little prior in-person experience before a complete return to in-person teaching in Winter 2022. Herein, we outline a strategy by which we simultaneously tested remedial laboratory curricula designed for this unique cohort of students and trained an initial group of LAs to assist with teaching these modified courses. This strategy was informed by the existing literature on LAs, vertical learning communities, and addressing the affective domain in laboratory instruction. Our overarching research question was: "Does the implementation of LAs in response to instructional discontinuity lead to beneficial outcomes for a cohort of students lacking prior in-person laboratory experience?" Specifically, these beneficial outcomes would include student- and LA-perceived improvements to the laboratory learning community and affective domain.

Pedagogical Frameworks

Vertical Learning Communities with Near-Peer Instructors

Traditional undergraduate learning communities consist of students instructed by a graduate student teaching assistant (GTA) and/or professor with several years of experience and training in the subject matter. In this hierarchical organization, students may feel disconnected or even intimidated, creating a relational gap between the student and instructor.[4,9] The effects of this structure can be exacerbated in challenging courses, such as OCL.[10] Implementation of LAs in courses results in a vertical community of scholars; LAs are inserted into the traditional relationship of students and instructors, reducing the gap between their experience and labels.[4,11] An LA or near-peer instructor is an individual who is close in age and education level but is one or more years senior in their educational progress to a student and seeks to provide mentorship and guidance.[12,13] Price et al. suggest that the social element of vertical learning communities encourages students to develop collaborative problem-solving skills.[14] Our LA program was

inspired by previously-established peer-learning programs, such as the Learning Assistant Program at the University of Colorado Boulder and the Undergraduate Teacher-Scholar Program at UC Berkeley.[4,15]

Affective Domain in Laboratory Instruction

The affective domain is defined as encompassing students' attitudes, motivations, values, expectations, and emotions in the context of the learning process. Galloway has emphasized the relevance of the affective domain in Novak's framework of meaningful learning,[6,7] which requires complete integration of the cognitive and affective domains with the psychomotor domain. For meaningful learning to occur in an OCL setting, the instructor should aim for holistic treatment of motivational and attitudinal aspects in addition to conceptual and procedural aspects when designing laboratory curricula. Seery argues for preparing and supporting students by managing their expectations for challenges and difficulties in the complex learning environment of chemistry laboratory courses, which LAs could facilitate (Seery et al., 2019).[16]

Despite a relative lack of research on the affective domain in the chemistry laboratory compared to the cognitive or psychomotor domains, considerable effort has been made in assessing the effects of various learning interventions on affect.[17,18] Implementation of a process-oriented guided inquiry learning introductory chemistry course resulted in improved self-efficacy and confidence in students with little prior chemistry knowledge and experience.[19] The introduction of LAs during the return to in-person classes had the potential to positively impact students' comfort and safety in the laboratory, with the additional benefit of improving learning assistants' confidence and attitudes towards chemistry.[20,21]

Learning Environment

The courses described herein took place at University of California, Irvine, a large public research university in the western United States, designated as a Minority Serving Institution, with the federal designations of Asian American and Native American Pacific Islander-Serving Institution and Hispanic-Serving Institution. The overall student population included in the study is 66% female and 34% male, based on self-reported responses to a binary-choice question about biological sex at time of admission. Students self-reported as 55% Asian, 17% Hispanic/Latinx, 13% white, 3% Black or African American, 8% Native Hawaiian and/or Pacific Islander, less than 1% American Indian and/or Alaskan Native; 3% declined to state. Overall, 44% of students self-identified as first-generation college students and 33% were identified as low-income. First-generation status was defined as neither parent completing a 4-year degree. Students who did not self-report income were assumed to be nonlow-income.

These courses are part of an OCL series consisting of a three-course sequence for non-chemistry majors (Figure 5.1). Each term is 10 weeks. Laboratory sections meet once per week for four hours. Additionally, students are expected to attend a one-hour laboratory lecture section once per week. Although the laboratory course, including laboratory sections and laboratory lecture sections, is separate from the organic chemistry lecture course, students enroll in both courses concurrently. Depending on the term and the specific course, an OCL course may have between 150–1,200 students enrolled. Up to 34 GTAs are required during a large-enrollment quarter, with each GTA assigned as the sole instructional staff member present for two 20-student laboratory sections per week.

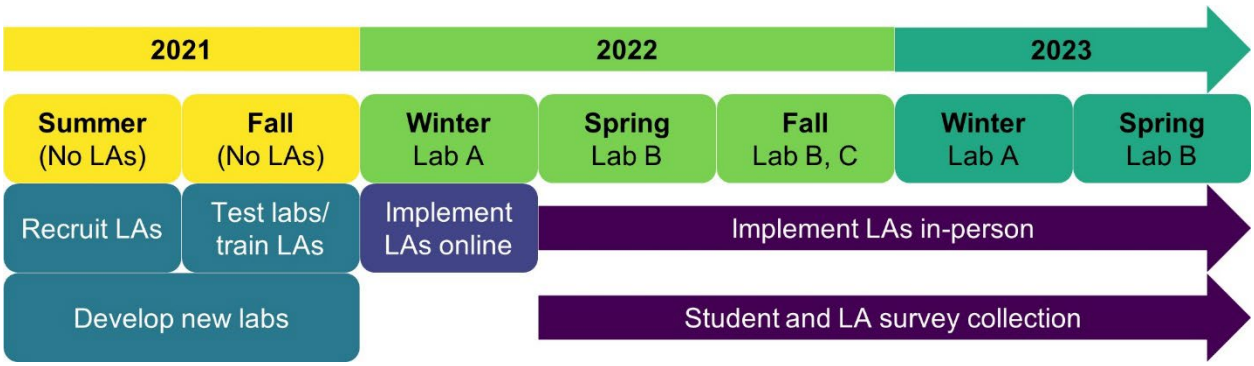

Figure 5.1. Timeline of curricula development, curricula testing, LA training, LA implementation, and survey collection.

The OCL course sequence described here is coordinated and taught by a single faculty member (RDL). Because of the scale of these courses, the instructional team includes multiple Head GTAs (JHG, JCT, PAL) who provide logistical, administrative, and pedagogical support to the instructor, including GTA scheduling, addressing grading discrepancies, writing exam questions, and hosting weekly office hours.

Results

Methods

LA Implementation

This work represents the first implementation of LAs during the laboratory component of an OCL course at UC Irvine. Students serving as an LA for the first time in any course are required to enroll in the university-wide Certified Learning Assistants Program (CLAP), in which a certified instructor trains new LAs in pedagogical theory and strategies for facilitating classroom teaching. In Summer 2021, the remedial laboratory curricula were developed, and initial recruitment applications were sent to students who had performed well in the relevant course series (B+ or better) within the two prior academic years (Figure 5.1). In Fall 2021, the first cohort of LAs was accepted, and simultaneous laboratory safety/technique training and

experiment testing took place. Implementation of LAs in lab sections occurred in Winter 2022, but continuing disruptions to instruction caused by the COVID-19 pandemic precluded survey data collection for this term. Spring 2022 represents the first term in which student and LA survey data were collected for a full in-person implementation of laboratory LAs.

Applications were sent to prospective LAs using Google Forms (Supplementary Material). The application comprises three sections: (1) potential for effective peer instruction, (2) reflection on transferable professional skills, and (3) an example of answering student questions. Applications scoring highly on a rubric were accepted without a limit on the possible number of acceptances (Supplementary Material). Application forms were distributed four weeks before the start of instruction; the application remained open for two weeks. Accepted LAs were notified two weeks before the start of instruction. One week before the start of instruction, LAs were assigned to laboratory time slots and were assigned based only on their individual availability such that each laboratory section was led by either one GTA or one GTA and one LA. In an average term of 60 individual laboratory sections, roughly 50% of sections had exactly one LA present, and the remainder did not have any LAs present.

During Fall 2021, LAs who had no prior experience handling chemicals and equipment in an instructional laboratory setting participated in training; these LAs earned the same course credit that they would have as lecture LAs. Training was carried out over five weekly two-hour periods. The first period was dedicated to safety training and familiarity with laboratory equipment. The latter four periods involved testing of both existing and new laboratory experiments. Students were provided with access to a draft version of an experiment handout where they could provide feedback. LA cohorts after Fall 2021 did not participate in training or

experiment testing, as they had prior in-person experience and no new curricula were being tested.

LA Responsibilities

All LAs attended a weekly 30-minute meeting in which the Head GTA reviewed LA feedback from the previous week's experiment and summarized the upcoming experiment. Specific time was set aside for LAs to develop a plan to address anticipated student challenges or common misconceptions and mistakes. For example: At the beginning of our laboratory sections, students complete a collaborative set of questions concerning safety, equipment, and chemical principles; accordingly, LAs were provided with follow-up questions to guide student learning.

The primary responsibilities of LAs during laboratory time were to supplement GTA instruction by facilitating student completion of experimental work and achievement of related learning outcomes (GTA duties did not change). This was accomplished by addressing challenges and answering questions related to content, equipment, and procedure. During the laboratory section, LAs were free to develop an instructional plan with their GTAs based on information discussed during the weekly meeting. We were comfortable with LAs having the freedom to develop an independent instructional plan because of their CLAP training, but instructors at institutions without a CLAP analogue may want to be more prescribed in what in-laboratory activities are expected of their LAs.

The primary responsibility of LAs between weekly laboratory sections was to provide guided feedback on the completed experiment, addressing both the experiment itself and how students were or were not able to achieve learning goals efficiently. Our framework for collecting LA feedback was inspired by the implementation of "10-minute journals" in peer-led team learning.[22] Specifically, LAs provided answers to the following five questions about the

laboratory experiment: (1) What went well? (2) What were "traps" or challenges for students? (3) Do you have suggestions for things that can be changed? (4) Do you have feedback on the writing of the experiment handout itself? (5) What information do students need clarification or additional instruction on before attending lab? This feedback was then aggregated by Head GTAs to be discussed in the following week's LA meeting. We used this feedback on a regular basis to make incremental improvements to the phrasing or organization of course materials.

Student and LA Surveys

Our surveys were adapted from work by Bourne et al. on the implementation of a large-scale laboratory LA program at UC Berkeley.[4] Specifically, their study analyzed the types of questions students approach GTAs, LAs, and/or peers with during recitation/discussion and laboratory sections. We were interested in whether these findings were consistent for our student population, who were returning from pandemic-related educational disruptions. Additionally, we investigated student and LA perceptions of (1) which LA duties were appropriate and (2) student affect in the laboratory with or without an LA present. The student survey addressed four major themes — LA duties, student learning from LAs and GTAs, student affect, and laboratory time management — using a combination of Likert-scale and open-ended questions. The LA survey included open-ended questions designed to reference the LA application, specifically the professional and academic goals and skills sections (Supplementary Material).

This study was approved by the Institutional Review Board as an exempt study (IRB #741). Surveys were available to students, LAs, and GTAs for one week during the final week of instruction through Qualtrics. Students were offered one credit toward a "token" for completing this and other research surveys in each quarter; tokens can be exchanged in the course grading

system for options such as late passes or the opportunity to revise and resubmit unsatisfactory assignments (McKnelly et al., 2023).[23]

Student survey responses (n = 1,194, 35%) were de-identified before analysis. Student survey response rates varied by term (S22 n = 564, 58%; F22 n = 131, 48%; W23 n = 140, 12%; S23 n = 359, 36%), but results remained consistent across terms regardless of response rate. Summary statistics of demographics for survey respondents matched those of the overall courses. LA survey responses (overall n = 55, 63%; S22 n = 19, 83%; F22 n = 9, 75%, W23 n = 10, 37%; S23 n = 17, 65%) were collected anonymously. GTA responses were not analyzed due to low response rates of two or fewer GTAs per term. Analysis of Likert-type questions and multiple-select questions was conducted using the statistical programming language R.[24–26] Responses from students to open-ended questions were analyzed using the Taguette free, open-source qualitative research tool.[27] Students' own wording was used to identify themes based on identified relations, similarities, and differences that were grouped conceptually.

Survey Results

LA Duties

We adapted survey questions used by Bourne et al. to confirm whether LAs were performing expected duties during laboratory sections and gauge the perceived appropriateness of those duties by students and LAs. The actual duties of LAs within the program were to (1) provide information, (2) monitor laboratory safety, (3) supervise instrument use, (4) act as a role model, and (5) facilitate discussion (Figure 2). When students were asked how appropriate these five LA duties were, the majority of respondents (57–60%) indicated that duties 1–4 were "very appropriate," while the majority deemed duty 5 "usually appropriate" (41%) (Figure 5.2A). LAs were asked to self-assess these same duties and responded that 1–5 were "very appropriate" at

higher rates than the students, particularly for duty 5, with 70% of LAs compared to 37% of students (Figure 5.2C). A similar trend emerged with student observations of their LAs during laboratory sections. The majority of students reported observing duties 1–4, but only 38% of respondents reported observing duty 5 (Figure 5.2B). Duty 1 was the most commonly observed by students at 91%, while duties 2 and 3 were also frequently observed at 79% and 75%, respectively. The most common duty performed by LAs was duty 2, in which 100% of LAs reported monitoring laboratory safety, and 95% of LAs reported performing duty 1 (Figure 5.2D). The largest differences between student and LA responses were that LAs reported performing duty 5 and duty 4 at higher rates than students reporting observing these activities, with discrepancies of 34% and 23%, respectively.

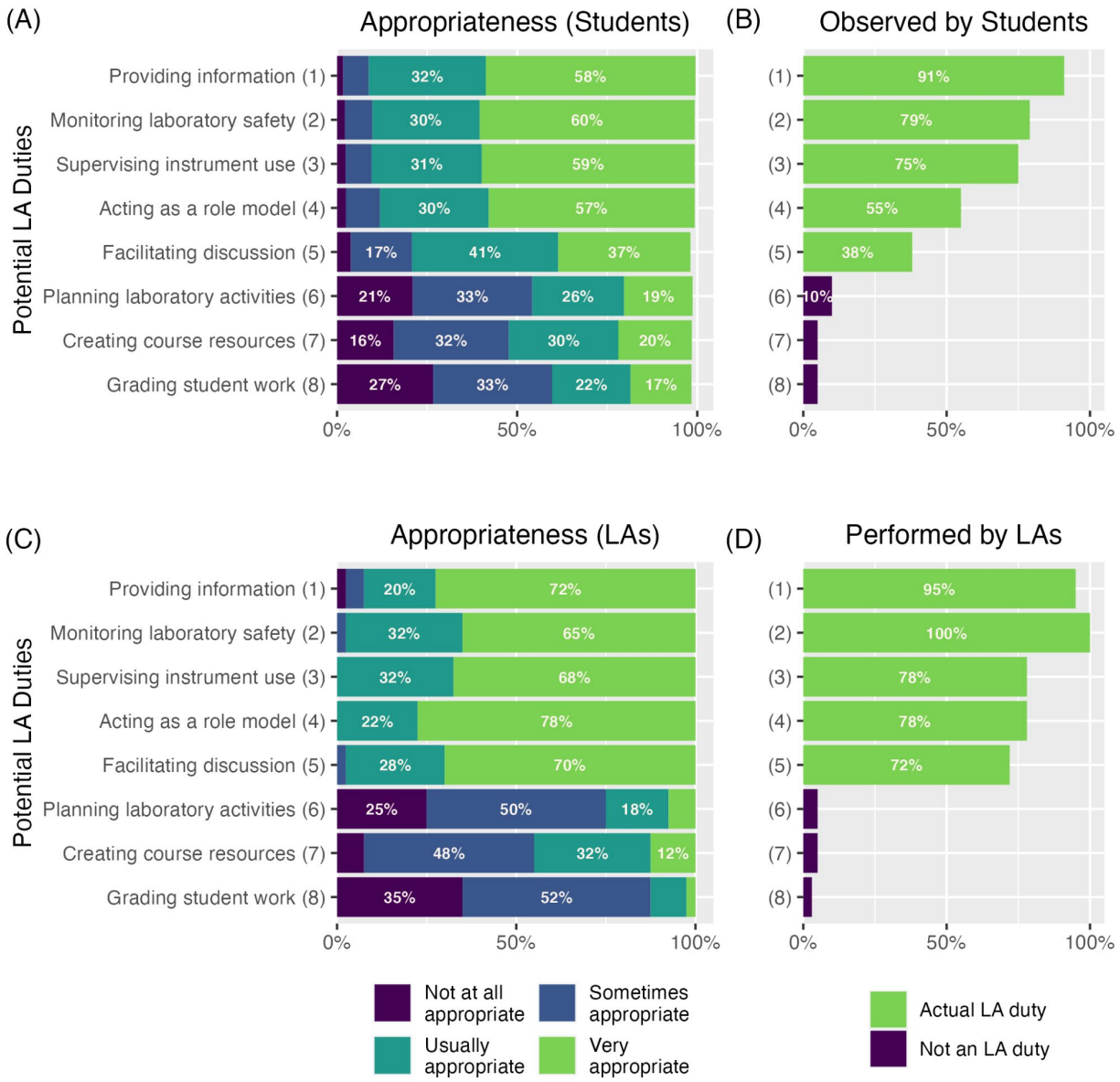

Figure 5.2. Student and LA responses to survey questions about the appropriateness and observation of LA duties. (A) Appropriateness of potential LA duties as determined by students. (B) Observation of LAs performing these duties as reported by students. (C) Appropriateness of potential LA duties as determined by LAs themselves. (D) Self-reporting of LAs performing these duties.

In addition to the actual LA duties, responsibilities that are instead assigned to other instructional staff were also included in this question. These non-LA duties included (6) planning laboratory activities, (7) creating course resources, and (8) grading student work. While students

tended to underrate the appropriateness of duties 1–5 lower compared to LAs, the opposite trend was observed for duties 6–8. Student responses to the appropriateness of duty 6 were not as straightforward as for duties 1–5, with a broad range spanning “sometimes appropriate” (33%), “usually appropriate” (26%), and “very appropriate" (19%). LA responses skewed towards “sometimes appropriate” (50%), with 18% indicating “usually appropriate” and 8% indicating “very appropriate.” Similarly, a small majority of students stated that duty 7 is “sometimes appropriate” at 32%; however, the majority of LA responses (48%) indicated it was “sometimes appropriate.” Lastly, the majority of both students and LAs indicated that it would be “sometimes appropriate” for LAs to perform duty 8 (33% and 52%, respectively) with “not at all appropriate” being the second most common response (27% of students and 35% of LAs). Despite the fact that these duties were not assigned to LAs, a minority of both students and LAs (≤10%) observed or self-reported LAs performing duties 6–8.

Student Learning from LAs and GTAs

Following the work of Bourne et al., we investigated the order in which students preferred to ask GTAs, LAs, and peers certain types of questions (Figure 5.3). For content, equipment, and procedure questions, the majority of students indicated that they would approach a GTA first (51–64%). A smaller proportion of students indicated that they would approach a peer first (24–29%), and a small minority of students indicated that they would approach an LA first (6–20%). LAs were consistently the most popular second choice for asking these types of questions (52–56%), while students indicated that they would approach GTAs second 20–26% of the time and peers second 14–16% of the time. Grading did not follow the trend observed for content/equipment/procedure questions, as a larger majority of respondents (87%) indicated that they would approach GTAs first for questions about grading. Life questions were the only

category in which students did not indicate GTAs as their first priority, as 48% reported that they would first approach a peer. Across all question categories, LAs were consistently considered students' second priority (grading: 57%; life: 48%).

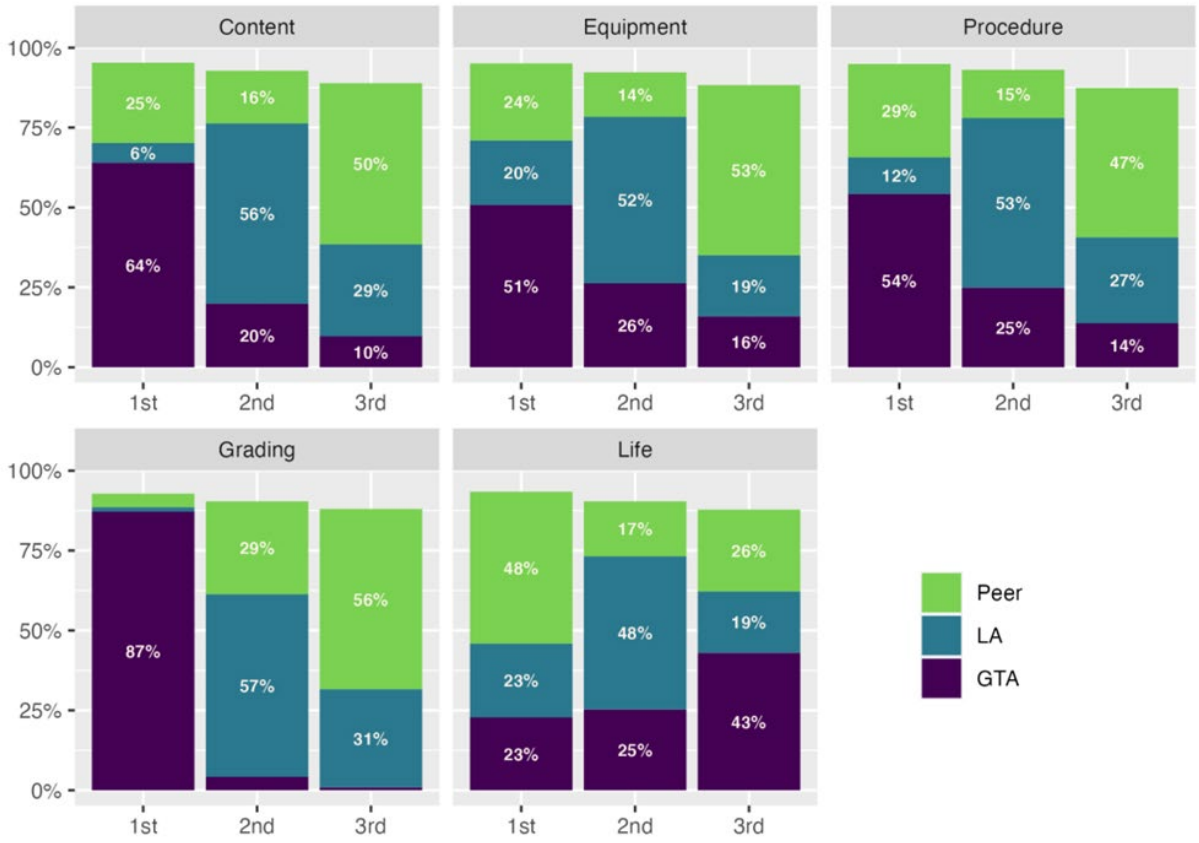

Figure 5.3. Student responses to the question "Please indicate the order in which you would approach the following people (GTA, LA, peer) to ask the following types of questions." Survey respondents were not required to give a 1st, 2nd, and 3rd priority for each category of question, so percentages may not add up to 100%.

Affective Domain

A primary research question in this study was "Do students with no prior in-person laboratory experience self-report increased feelings of comfort, confidence, and safety when a laboratory LA is present?" In Figure 5.4A, we have separated results from the Spring 2022 term compared to Fall 2022–Spring 2023 (Figures 5.4B, C). Spring 2022 was the first term at our

university since 2020 in which OCL courses were offered fully in person. For Spring 2022, a dramatic difference in students' self-assessment of their comfort, confidence, and safety was noted compared to later terms. Confidence appeared to be split fairly evenly between "agree" (no LA 48%, LA 54%) and "disagree" (no LA 52%, LA 46%) responses, while comfort and safety lean slightly towards "agree" responses (comfort: no LA 63%, LA 66%; safety: no LA 63%, LA 66%). For students with no LAs, comfort, confidence, and safety were strongly disagreed with 35%, 47%, and 34% of the time, respectively. With an LA, these results were 31%, 40%, and 31%, respectively.

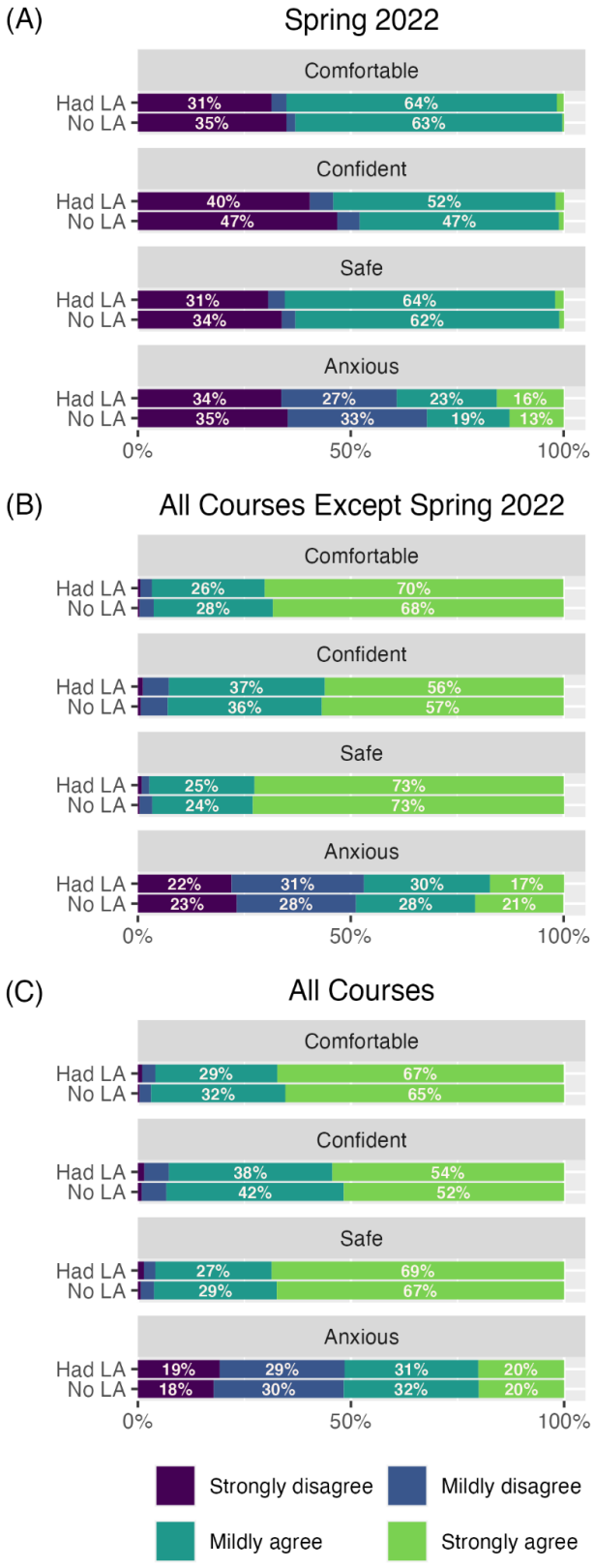
(A)
Spring 2022
Comfortable
Had LA
No LA
31%
64%
35%
63%
Confident
40%
52%
47%
47%
Safe
31%
64%
34%
62%
Anxious
34%
27%
23%
16%
35%
33%
19%
13%
0%
50%
100%
(B)
All Courses Except Spring 2022
26%
70%
28%
68%
37%
56%
36%
57%
25%
73%
24%
73%
22%
31%
30%
17%
23%
28%
28%
21%
(C)
All Courses
29%
67%
32%
65%
38%
54%
42%
52%
27%
69%
29%
67%
19%
29%
31%
20%
18%
30%
32%
20%
Strongly disagree
Mildly disagree
Mildly agree
Strongly agree

Figure 5.4. Student responses to the question "Please rate the degree to which you agree with the following statement: 'I felt [adjective] performing in-person laboratory experiments this quarter.'" (A) Student responses for Spring 2022 only, the first instructional period since the beginning of the COVID-19 pandemic in which the full 10-week laboratory course was offered in person with no interruption. (B) Student responses for each term during the study period other than Spring 2022. (C) Student responses for all terms included in the study period.

Expectedly, students reported feeling more comfortable, confident, and safe when they had prior laboratory experience compared to when they did not: For Fall 2022–Spring 2023, responses overwhelmingly skew towards "agree" for comfort (no LA 96%, LA 96%), confidence (no LA 93%, LA 93%), and safety (no LA 97%, LA 98%). Anxiety, a negative affect trait compared to the positive traits of comfort, confidence, and safety, was consistently more varied in student responses: Furthermore, students appeared to self-report higher anxiety in terms other than Spring 2022, as "agree" responses increased (no LA: 32% to 49%; LA: 39% to 47%).

Open-Ended Survey Question Responses

Responses from students and LAs to open-ended questions were used to identify major conceptual themes describing the benefits of the laboratory LA program (Table 1). As a result of LAs answering student questions, students identified improvements to experimental efficiency and LAs identified improvements to communication skills. Students described LAs as being effective near-peer instructors, highlighting previous experience in the course, approachability, and their similar institutional knowledge. Students described LAs as beneficial to the learning experience because LAs were able to support both GTAs and students with their experienced perspective. Additionally, students felt that LAs promoted a safer laboratory environment.

Table 5.1. Representative examples of common responses to open-ended survey questions. Responses are categorized by common themes and highlight the unique perspectives of students and LAs.

	Student Perspective	LA Perspective
LAs answer student questions. *Answering questions, laboratory efficiency, communication*	"Yes I think having multiple upper division role models will help when students have a lot of questions. It also makes labs go by much faster when there are more sets of hands to aid in conducting the lab. My LA was also very helpful when my TA was busy helping someone else. I could ask her for anything about the experiment or conceptually questions and she mostly has the answers to help." "Labs are usually very hectic and many students are constantly asking questions, so having a second option to refer to for questions greatly helped keep everyone moving efficiently." "Having the sense of mentorship is a nice touch. Having an extra set of eyes and supervisor helps cut down the time spent on waiting for the TA answer your questions after something goes wrong."	"I wanted to improve on my active learning skills during my time as an LA. I feel as though the lab course I chose to assist helped immensely with this because it challenged me to come up with certain tactics to use in assisting students rather than just giving them the answer. This helps both me and the student because it strengthens problem solving skills while also allowing the students to use their own knowledge to get to the answer themselves." "As far as I can recall, the most important professional skill I wanted to to refine was my communication/teaching skills because in the field of medicine it is required of people to be able to elaborate certain medical knowledge that can be difficult to explain without a particular level of education. I believe that so far this position has been great at helping me rethink how I explain things and I have been able to compartmentalize what knowledge is important to knowing the concept vs what knowledge is going overboard better than I have been able to do before." "It is a great experience if someone is trying to get exposed to more teaching positions. It also strengthens communication and problem-solving skills which is an important skill to have for the future and life in general."
Neer-peer instructors facilitate student learning. *Near-peer instructors, approachability, community*	"I see LAs as the middle ground between TA and peer. They are super helpful because sometimes students don't want to go straight [to] the TA for what they may	"I think having another student in the lab really helps both the TA and students. It makes it easier for students to approach other fellow students and can facilitate a more comfortable environment where discussion and

	think is a stupid question. If a peer doesn't know, LA is the next best. I find this to be pretty common in lab settings. Maybe someone messed up the experiment, but they are too embarrassed to ask for help. A kind and understanding LA would be awesome!" "LAs are more relatable for undergraduates, and just having them present is reassuring because they were in our shoes somewhat recently and they passed the class." "It's nice seeing someone relatively our age be passionate about chemistry. It encourages learning [in] the lab environment."	questions are encouraged. I think that the main thing [is] that I am only a year older than most of the students, it provides another person of 'authority' that the students can depend on while also being more comfortable with as there is a very tiny age gap…" "I think the lab in general can be pretty long and tiring which can exhaust students sometimes, but seeing someone who has taken the lab and come back to LA can make them feel like they're capable of getting through it. It also gives them the opportunity to ask questions about their current course content and future courses in a bit of a peer-to-peer way rather than [professionally]." "I feel like I succeeded since many students ended up enjoying ochem lab. It wasn't a stressful experience and it made people open their eyes to how great chemistry is."
GTAs and LAs form a cooperative teaching team. *GTA-LA teamwork, LAs supplement and support Tas, experienced student perspective*	"Yes Having the LA program is beneficial for both the student and the LA. In the case of the students, it allows a different perspective of the experiment and being an undergraduate student compared to the graduate student TAing." "If in-lab Learning Assistants are present in the lab, the TA will not be too busy tending to students' questions and will have time to go over crucial concepts more thoroughly with the lab section. The chances of safety and waste violations such as breaking equipment and items being placed into the wrong waste	"Quick rundown of what the experiment run should look like, potential issues, common questions we'll get, demonstrations and theory we need to go over before the lab, what can I do as the LA to help her and the lab run smoother." "Before each lab, we would talk about how 'tricky' students may find the experiment, or if I got a lot of the same question I would let them know so they could make an announcement or address it in some way" "With both TAs I worked with, I was able to converse with them freely. They both made me feel like we ran lab as a unit, a team. Both completing the same duty of answering the students questions. There were often

	containers might be lowered. Overall, having more eyes and hands to monitor the multiple reactions happening in lab will make things more efficient and safe" "I had an LA during Winter 2022. They were really helpful with answering questions about experiment procedure and safety when the TA was busy with other students. I was also able to clarify concepts with the LA during down time if the TA was busy."	times where I did not know how to answer a students question, so I asked my TA and got back to them. When there was down time, my TA and I would sometimes stand towards the front and talk about random stuff."

Discussion

Comparison to Previous Results

Despite differences in our implementation of laboratory LAs (the COVID-19 pandemic, our LA training process, 10-week course length, etc.), our results are consistent with Bourne et al. Students approached TAs first for all question categories other than life, where peers are instead ranked first (Figure 5.3). LAs were ranked as second for each question category. For grading specifically, TAs were overwhelmingly ranked first. Furthermore, we observed similar student observation and LA self-assessment of the various LA duties; for each of the actual LA duties, a majority of both student and LA respondents reported these duties (with the exception of "facilitating discussion;" see Limitations) (Figure 5.2). For each of the duties LAs were *not* intended to perform, the majority of students and LAs did not observe or report these duties, respectively.

Tandem LA Training/Experiment Testing

We find that LAs are useful for testing new or revised curricula. Because of their

previous experience in the course, LAs are motivated to improve the clarity and organization of course materials. Following a session of LA experiment testing, we propose organizing LA feedback into (1) identified problems and (2) proposed solutions. While students and LAs are effective at identifying problems, their proposed solutions are not always actionable; this necessitates the review of LA comments and suggestions by an experienced instructor before changes are made to course materials. We find that LAs feel prepared by their training (Table S5.2). Their familiarity with the tested experiments further equipped them to address student questions.

Student and LA Perspectives of Laboratory LA Benefits

LAs Answer Student Questions

Students report that LAs improve laboratory efficiency. Many students recalled a long line to ask the GTA a question; the presence of an additional instructor in the form of an LA increased the rate at which questions were answered. This is consistent with Figure 5.3, in which most students would approach the LA second for content, equipment, and procedure questions. Many students reported directing "minor" questions to LAs, while TAs addressed more in-depth questions about chemical principles or specific experimental troubleshooting. However, students indicated that, during periods of an experiment where they had few questions, LAs passively waited until there were questions to answer rather than approaching students to initiate discussion.

LAs consistently indicated the importance of observing, learning, and practicing teaching and communication skills in both their motivations for participating in the program and their primary outcomes from participating. To assess achievement of personal goals, LAs were asked to recall and reflect on their motivations for joining the program and the transferable skills

identified as part of their application to the program. Responses overwhelmingly reflected the desire to practice teaching and communication skills, both for career development and to help fellow undergraduate students. Some LAs expressed a desire for more direction and did not feel comfortable approaching students to initiate discussions when students were not asking questions, but overall, LAs felt more confident in their abilities to solve problems, clearly communicate information, and guide students in their learning process. These skills were specifically identified as being transferable to education, healthcare, and GTA positions in graduate programs.

Near-Peer Instructors Facilitate Student Learning

Students report experiencing emotional stress during laboratory experiments — which may be caused by time management issues, the desire to obtain perfect results, or concerns about their grade — that could inhibit learning in the course. Although student responses to Likert-scale questions about their comfort in the laboratory did not differ based on whether or not an LA was present (Figure 5.4), open-ended responses indicated an increased sense of comfort from LAs that made the laboratory sections more enjoyable. Students perceive LAs to be more relatable than GTAs or professors because they are closer in age and experience to the students and have recently been in their position. Students identified mentorship and role-modeling as additional benefits of the LA's presence in the laboratory, which is consistent with the majority of students identifying "acting as a role model" as being an appropriate LA duty (Figure 5.2). LAs can "empathize" and "understand the struggle" students are encountering and provide an experienced perspective on how to succeed in the course. A number of students shared that LAs gave them advice about navigating their undergraduate degree. LAs additionally brought camaraderie to the laboratory sections, making them more "fun" and "interactive" while still

ensuring that experiments were conducted safely.

Many students addressed the teaching hierarchy that vertical learning communities with near-peer instructors seek to mitigate. Students reported feeling intimidated to approach their GTA with certain questions if a mistake was made or for fear of being judged. LAs serve to assist both parties by answering student questions and reducing the burden on the GTA. Accordingly, students reported that LAs are generally more approachable than GTAs, citing that LAs had no power over grades and that LAs tended to explain concepts in a way more digestible to undergraduate students.

Many LAs were motivated by personal experience, joining the LA program out of a desire to reduce stress and increase confidence for students by being an approachable source of support and familiarity. LAs commented on their personal struggles when enrolled in the course and wanted to share their expertise. Throughout an instructional term, LAs described developing a rapport with students by discussing subjects outside of chemistry to help ease chemistry-related discussions. LAs emphasized the near-peer aspect of the program, in which students who were intimidated by their GTA could instead ask someone closer in age and experience. In "bridging the gap" between the GTA and students, LAs reported connecting professionally and personally with both the students and the GTA, fostering a sense of community in the laboratory.

GTAs and LAs Form a Cooperative Teaching Team

Students overwhelmingly recommended that the LA program be continued, with the most common reason being that LAs help to supplement GTAs in the laboratory. Students recognize that GTAs are often busy running the laboratory section and cannot help every student simultaneously. A common example was an experiment in which the GTA operated an instrument in an adjacent room while most students remained in the main laboratory space; LAs

assisted GTAs by being where the GTA could not. Students recognized that the ability for LAs to supervise students while the GTA was busy improved overall laboratory safety (Figure 5.2). Finally, students recognized that LAs provide a useful and complementary perspective to the GTA, as LAs are current undergraduate students and have already performed well in the OCL series. This perspective reaches beyond course content, as 85% of students indicate that "My LA helped me improve my understanding of how to navigate UCI as an undergraduate" (Figure S5.1).

LAs and GTAs were expected to work as a team, conferring at the beginning of a laboratory period to discuss how to optimize time management and students' general experience with the experiment at hand. Correspondingly, LAs were surveyed regarding interactions with their laboratory section's GTA. A small number of LAs mentioned consulting with the GTA before the laboratory period began to get a general sense of how the laboratory period should proceed. This type of response was less common than expected, which may indicate that our implementation of LAs would benefit from increased structure and clearer expectations of LAs. Based on survey responses, LAs understand their role as being supplemental to and supportive of GTAs; in other words, LAs recognize that their participation can benefit both the students and the GTA.

Limitations

The primary limitation of this study is the use of surveys that are not validated instruments. Specifically, we observe that certain words or phrases, such as "facilitate discussion," may be interpreted differently by students and LAs and that those interpretations may differ from our intent. In the case of "facilitate discussion," students may interpret this to refer to a recitation section of the course as opposed to the laboratory component (Figure 5.2).

LAs may instead interpret “facilitate discussion” to mean “facilitated discussions/conversations about concepts with students,” which is closer to our intent. Additionally, the results presented are in aggregate and may not represent the experiences of students who hold specific marginalized identities. Due to the scale of our OCL series and the complexity of undergraduate student scheduling, it is unlikely that we will ever be able to provide an LA for each laboratory section in a single term. This is a limitation of our implementation, as LAs are not assigned evenly throughout different section types (i.e., day of week and time of day).

Conclusion

We have described the process by which we implemented a laboratory LA program in non-chemistry major OCL for the first time at our institution. This was done in response to instructional discontinuity caused by the COVID-19 pandemic, which necessitated the development of remedial laboratory curricula. In order to (1) test these new curricula and (2) train LAs in hands-on laboratory techniques, LAs participated in the development of the new curricula. Following implementation of both LAs and the new experiments in the OCL series, survey results from students and LAs were compared to the previous study by Bourne et al., which took place prior to shutdowns caused by COVID-19. We find that students correctly identify LAs duties and prioritize LAs over peers when asking questions about experimental content, equipment, or procedure, which is consistent with the previous study. We identify three major categories of student and LA open-ended survey responses which describe the benefits that LAs bring to the teaching laboratory.

We plan to repeat this strategy of curricular development/LA training in the near future as we transition our OCL format to Argument-Driven Inquiry.[28–30] LA feedback indicated that the program could benefit from increased structure, such as additional prescribed leading and exit

questions to engage student groups during experiments. Qualitative GTA feedback (excluded from this work) indicated that LA-GTA teamwork could be improved if GTAs were provided with a specific list of LA responsibilities. We have created and compiled resources with which other instructors in a broad range of learning environments can recruit, train, and implement LAs while developing new laboratory curricula. The LA application form, associated rubric, and surveys for both students and LAs are included in the Supplementary Material. Tandem LA training/curricular design proved useful in responding to the instructional interruption caused by the COVID-19 pandemic, but we believe that this strategy is generalizable to any kind of curricular innovation/reform in a chemistry laboratory course series. Although the large-scale disruptions to in-person courses necessitated by the onset of the COVID-19 pandemic have passed, other events such as labor actions, natural disasters, or civil unrest could result in a cohort of students entering laboratory courses without in-person laboratory experience; these students may benefit from the presence of LAs in their laboratory courses.

Supplementary Material for Chapter V

IRB Statement

This study was approved by the University of California, Irvine, Institutional Review Board as exempt (IRB #741) including FERPA compliance.

Sample Learning Assistant Application Form

Chemistry 51LC Spring 2023 Learning Assistant application

Thank you for your interest in serving as a Learning Assistant for Chemistry 51LC! The laboratory Learning Assistant program for Chemistry 51L is still going strong, and we would be happy to have you join our team this coming quarter. Winter quarter last year was our first opportunity to have in-person Learning Assistants help teach the 51L series, and we are thankful to have additional help in making sure that our students feel confident and capable while performing these in-person experiments.

Prerequisites
In order to be eligible for this application, you must:

- Have already completed Chemistry 51LC (in-person or online).
- Have an interest in teaching, chemistry or otherwise!
- Already have in-person chemistry or biology laboratory experience. This can be from:

(1) A laboratory course at UC Irvine that held in-person laboratory experiments
(2) Undergraduate research in a research laboratory at UC Irvine
(3) Any other in-person laboratory experience (please elaborate on your training and responsibilities when completing the application)

Co-requisite

In order to serve as an LA, you must have either already taken the Certified Learning Assistants Program (CLAP, University Studies 176) or be enrolled in it the same quarter that you are an LA. If you have already taken CLAP, there is no further requirement. If you have not already taken CLAP, you will be given an enrollment code for the course upon being chosen as an LA. US 176 will be offered at the following times in Spring 2023:

Tuesdays 2:00pm-3:50pm
Wednesdays 10:30am-12:20pm
Wednesdays 3:00pm-4:50pm
Thursdays 2:00pm-3:50pm

If you have not yet taken US 176, please make sure that you can attend at least one section before submitting your application.

Responsibilities

As an in-person Learning Assistant for Chem 51LC in Spring 2023, LAs will:

- Attend a weekly LA meeting with a Head TA for Chem 51LC (30 min/week)
- Attend a weekly laboratory section led by a Chem 51LC TA (4 hours/week)

For one additional unit of course credit, LAs may choose to accept the following additional responsibilities:

- Attend one of three weekly in-person lab lecture sections (1 hour/week)
- Monitor the online course discussion board, Ed Discussion, to answer student questions (2–4 hours/week)

LAs will receive either 2 or 3 units of course credit by enrolling in University Studies 198. There is no coursework associated with enrollment; it is simply a way to receive credit for your work as an LA.

Prerequisites

1. In which quarter and year did you complete [relevant course]?
2. Do you have in-person laboratory experience?
    - Yes, a class at UCI (please specify the class)
    - Yes, a research group at UCI (please specify the group)
    - Yes, outside of UCI (please briefly detail your training and responsibilities)
3. Please elaborate on your answer to the previous question.
4. Have you completed the Certified Learning Assistants Program (CLAP, University Studies 176)?
    - Yes (Which quarter? Which classes have you previously been an LA for?)
    - No, but I can attend at least one section held in Winter 2023 (Which sections?)
5. Please elaborate on your answer to the previous question.

Motivation

6. What is your motivation for wanting to be a learning assistant? This can be related to why you want to help teach the 51L series and/or how being a learning assistant will help you achieve your own personal goals.
7. What is one specific professional skill that you hope to develop by participating as an in-person Learning Assistant for a laboratory course? Why do you want to develop this skill, and how will being a Learning Assistant help you develop this skill?

Teaching techniques

8. Think of an instructor that you have had in the past (UCI or otherwise) that you would describe as an "effective instructor." What did that instructor do that was effective? What strategy or approach did they use when teaching that made them effective?
9. Which hands-on technique from an organic chemistry laboratory course (or other in-person laboratory experience) did you find most challenging to understand?

10. What advice would you give to a student who is currently struggling with the same technique? Be specific.
11. Which concept or topic from an organic chemistry lecture course did you find most challenging to understand?
12. What advice would you give to a student who is currently struggling with the same concept or topic? Be specific.

Example questions

When students are having trouble understanding a concept, they sometimes articulate their questions about the concept in ways that are difficult to understand. One job of an instructor is to "understand the misunderstanding;" in other words, you must correctly interpret the question being asked in order to answer it helpfully.

However, an additional consideration when answering questions on a public forum such as Ed Discussion is not to give away too much information — students learn the most when they are able to come to their own conclusions, rather than copying answers to questions that someone else asked.

Choose ONE of the following three examples of a student question, then do the following:

(A) Rephrase the question. What does the student not understand, or what is their misconception about the concept?
(B) Completely answer the question, correcting any misunderstandings or misconceptions.
(C) Answer the question the way you might on Ed Discussion: Do not completely give away the answer to the question, but give the student enough information that they can continue working through the problem productively.

Example question #1
"When looking for impurities in spectra, is it okay to add the impurity to my NMR table if only some of the compound's peaks are on the NMR? For instance, if the NMR only has peaks that match hydrogens from CH2 and CH3 of ethanol, but not OH, is it still reasonable to hypothesize that ethanol is present?"

Example question #2
"I'm not sure what type of elimination 1-butanol undergoes. In the elimination handout it states that the reaction should proceed by E1, but in 51B I was taught that a primary carbocation is extremely unstable and cannot be formed, so that reaction would occur by an E2 mechanism. Which elimination really happened?"

Example question #3
"In lab lecture I learned that a 50/50 mixture of syn and anti addition products has to have a melting range below 202 - 204 degrees celsius, which is the melting range for the anti bromination product. However, the melting range of the mixture can be above the melting range (93.5 - 95.0) for the syn product. I'm looking for some clarification on this. Is it that for a 50/50 mixture, the melting range should be below 202 degrees? Would the end of the melting range for

a mixture be 201 degrees? Or can a 50/50 mixture have a melting range of 195-203 degrees celsius?"

13. Which example question are you choosing?
    - Example question #1: NMR
    - Example question #2: Elimination
    - Example question #3: Melting range
14. (A) Rephrase the question. What does the student not understand, or what is their misconception about the concept?
15. (B) Completely answer the question, correcting any misunderstandings or misconceptions.
16. (C) Answer the question the way you might on Ed Discussion: Do not completely give away the answer to the question, but give the student enough information that they can continue working through the problem productively.

Student Response Anonymization

Survey responses were not accessed until the course was complete and final letter grades were submitted. Student's university email addresses were collected as identifiers with survey responses. Each student email address was then replaced with a unique, randomly generated numerical code to preserve student anonymity. The key to this code (number to participant name) was stored in a separate electronic file that was only accessible to the corresponding author.

Open-Ended Response Analysis

Responses from students and LAs to open-ended survey questions were analyzed using the Taguette free, open-source qualitative research tool (https://www.taguette.org/). LA survey responses were evaluated by two independent coders using two separate Taguette documents. Codes were individually developed based on identified relations, similarities, and differences that were grouped conceptually. Coders then discussed and negotiated codes to determine which themes were most representative of the overall data. Student survey responses were evaluated by three independent coders. The coders independently reviewed the responses, noting any overarching themes, and met to compare notes and determine codes. Specific questions were

then evenly distributed between each reviewer, who then tagged responses based on the agreed upon codes.

Learning Assistant Application Rubric

1. In which quarter and year did you complete [relevant course]?
    - Applicants must have completed the course they are applying to LA for in order to be considered.
2. Do you have in-person laboratory experience?
3. Please elaborate on your answer to the previous question.
    - If the in-person laboratory experience is not from the relevant course, priority is given to laboratory experience in organic chemistry over laboratory experience in other disciplines (e.g., biology, hospital volunteering).
4. Have you completed the Certified Learning Assistants Program (CLAP, University Studies 176)?
5. Please elaborate on your answer to the previous question.
    - Students who have not yet completed CLAP but can co-enroll have no priority over students who have already completed CLAP.
    - Students who have not yet completed CLAP and cannot co-enroll are not eligible to be LAs.
6. What is your motivation for wanting to be a learning assistant?
    - (3/3) - This student has a specific and relevant professional or academic goal for wanting to be a learning assistant.
    - (2/3) - This student has a goal for wanting to be an LA, but it is not communicated clearly how it is specific or relevant to the student's professional or academic goals.
    - (1/3) - This student appears to only want to be an LA in order to fill a resume, without any specific applications to their own career path.
7. What is one specific professional skill that you hope to develop by participating as an in-person Learning Assistant for a laboratory course? Why do you want to develop this skill, and how will being a Learning Assistant help you develop this skill?
    - (3/3) - This student has a professional skill related to both STEM and their career goal (good examples include science communication and leadership) and describes how that skill is related to their career goal.
    - (2/3) - This student mentions a relevant skill, but does not describe how they would benefit from developing that skill or how being an LA will help them to develop that skill.
    - (1/3) - This student mentions a skill that would not be relevant to the LA environment.
8. Think of an instructor that you have had in the past (UCI or otherwise) that you would describe as an "effective instructor." What did that instructor do that was effective? What strategy or approach did they use when teaching that made them effective?
    - (3/3) - This student specifically identifies a trait/approach and an implementation strategy of that trait/approach from a previous instructor that they perceived to

help them with their learning. Examples would include instructors that prioritized flexibility, active learning, opportunities for feedback, etc. in their course design.
    - (2/3) - This student identifies a general trait/approach, but not a specific implementation, that would be considered effective (enthusiastic approach to class, kind in interactions with students, etc.).
    - (1/3) - This student identifies a previous instructor, but does not address a concrete trait/approach that made them "effective."
9. Which hands-on technique from an organic chemistry laboratory course (or other in-person laboratory experience) did you find most challenging to understand?
10. What advice would you give to a student who is currently struggling with the same technique? Be specific.
    - (3/3) - This student identifies an actual technique from an in-person laboratory experience. The advice they propose is actionable (meaning we believe an actual student would benefit from following the advice), clear, and correct.
    - (2/3) - This student identifies an actual technique from an in-person laboratory experience, but their proposed advice is not actionable or is unclear.
    - (1/3) - This student either identifies an irrelevant technique or their advice is incorrect.
11. Which concept or topic from an organic chemistry lecture course did you find most challenging to understand?
12. What advice would you give to a student who is currently struggling with the same concept or topic? Be specific.
    - (3/3) - This student identifies an actual concept from an organic chemistry course series. The advice they propose is actionable (meaning we believe an actual student would benefit from following the advice), clear, and correct.
    - (2/3) - This student identifies an organic chemistry concept, but their proposed advice is not actionable or is unclear.
    - (1/3) - This student either identifies an irrelevant topic or their advice is incorrect.
13. Which example question are you choosing?
    - A choice of any of the three example student questions to address is equally valid.
14. (A) Rephrase the question. What does the student not understand, or what is their misconception about the concept?
    - (3/3) - Applicant correctly identifies the misunderstanding in the example question and contrasts this to the correct interpretation/meaning of the concept/information.
    - (2/3) - Applicant partially identifies the misunderstanding, but not in a complete way.
    - (1/3) - Applicant incorrectly identifies the misunderstanding.
15. (B) Completely answer the question, correcting any misunderstandings or misconceptions.
    - (3/3) - Applicant's answer is clear and correct, including an actionable correction of the misconception (meaning a student could reasonably understand their mistake based on this explanation.

- (2/3) - Applicant's answer is correct, but not clear; we anticipate that an actual student may have trouble understanding the explanation or require additional clarification.
- (1/3) - Applicant's answer is incorrect.

16. (C) Answer the question the way you might on Ed Discussion: Do not completely give away the answer to the question, but give the student enough information that they can continue working through the problem productively.
    - (3/3) - Applicant provides correct, but leading, information, such that a student could reasonably continue working through the problem on their own.
    - (2/3) - Applicant correctly answers the question, but does not leave room for the student to do any of their own thinking.
    - (1/3) - Applicant incorrectly answers the question.

Student Survey Results

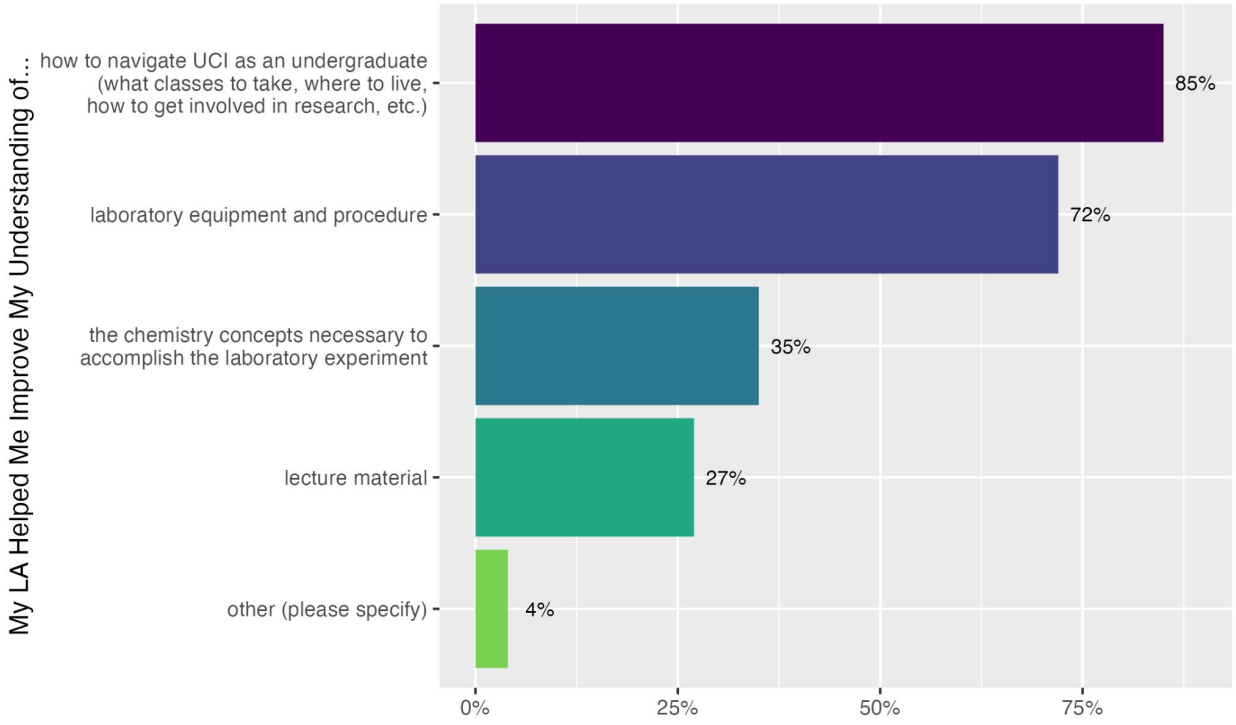

Figure S5.1. Student learning from LAs only. Student responses to the question "Choose all that apply: This quarter, my Learning Assistant helped me to improve my understanding of…"

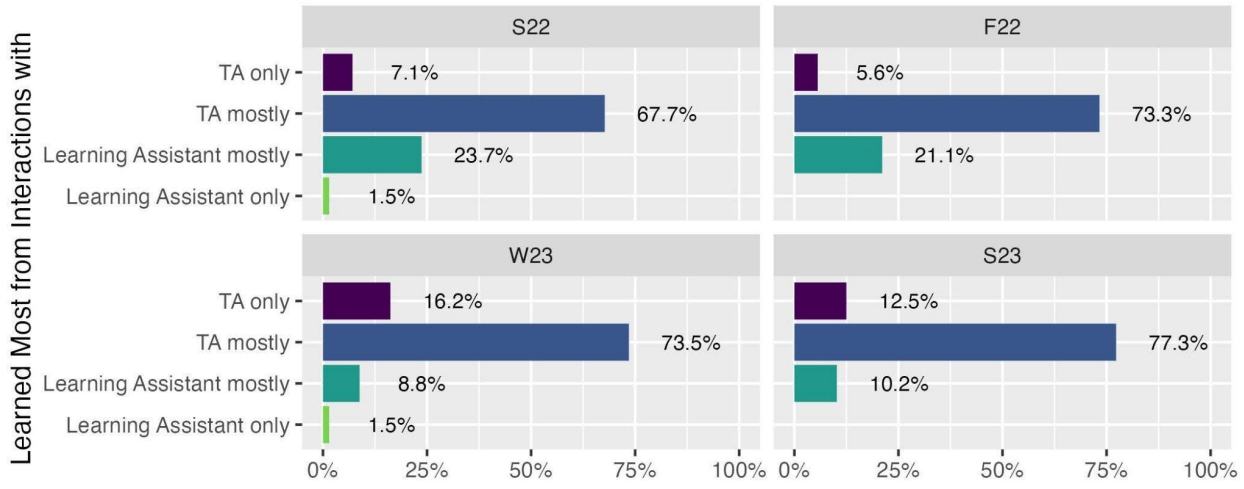

Figure S5.2. Student learning from LAs and GTAs. Student responses to the question "Think of your interactions with your Learning Assistant and TA in lab this quarter. Who do you feel you learned the most from interacting with?"

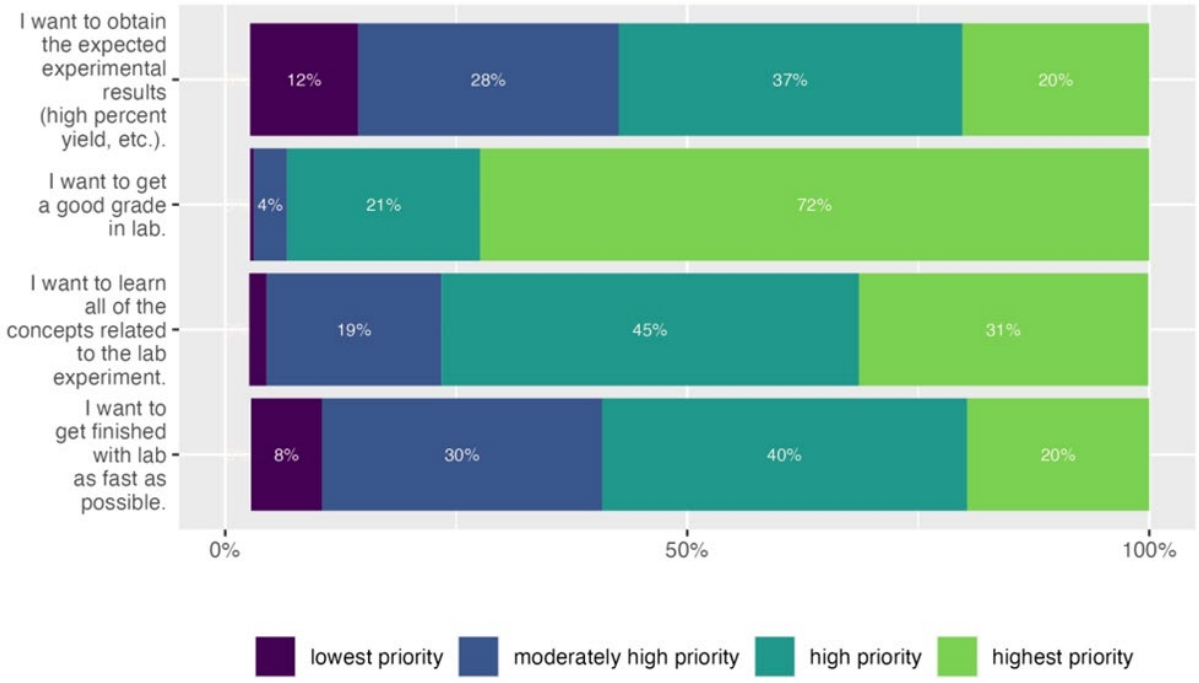

Figure S5.3. Student priorities in the laboratory. Student responses to the question "Please rate your own personal priorities in lab this quarter. There is no 'better' answer than another. We want to learn what laboratory students value. Please answer as honestly as possible."

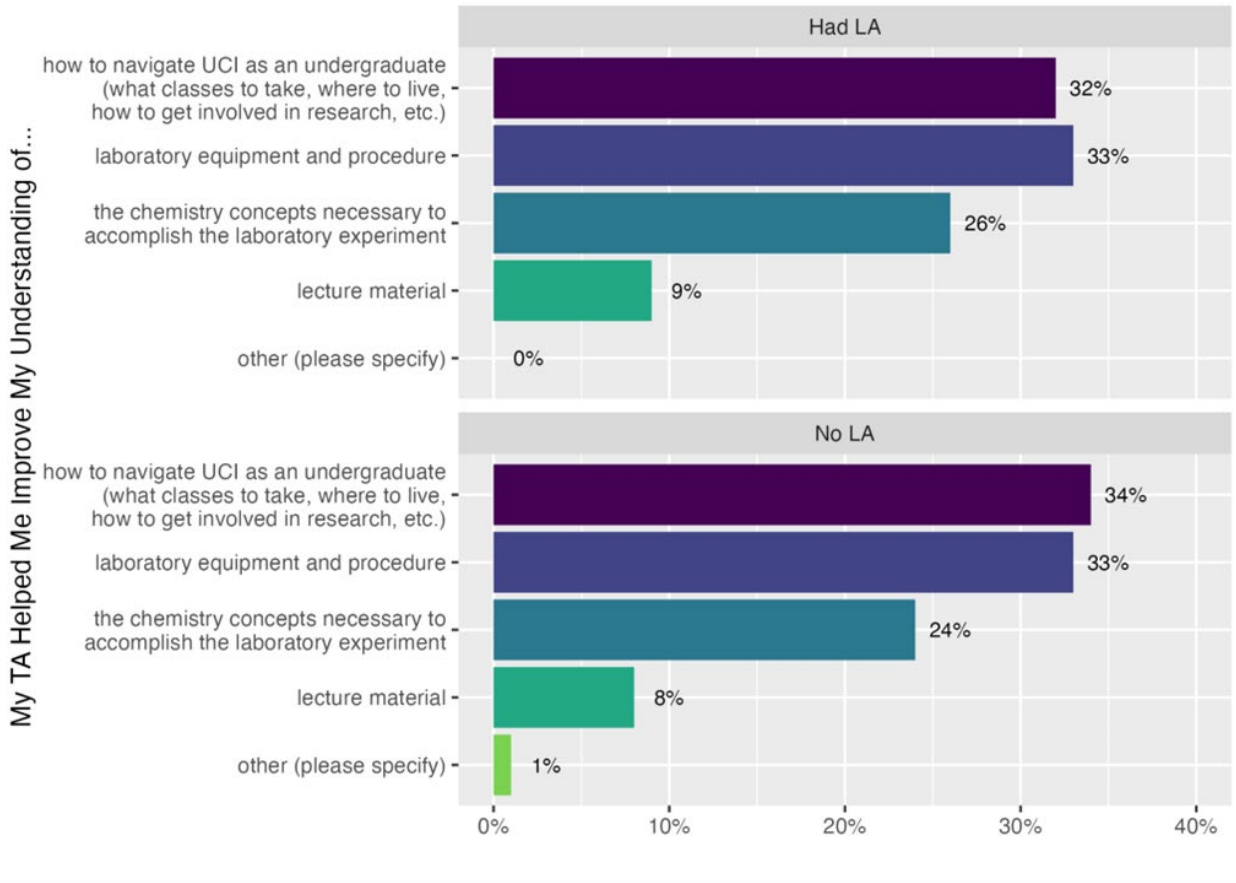

Figure S5.4. Student learning from GTAs only. Student responses to the question "Choose all that apply: This quarter, my TA helped me to improve my understanding of…"

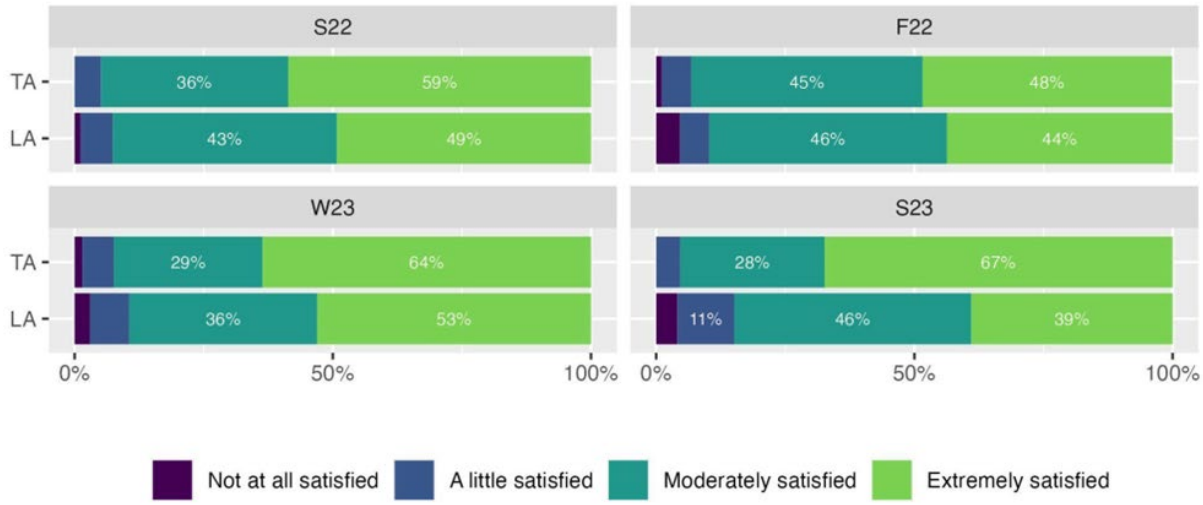

Figure S5.5. Student satisfaction with GTA and LA answers to questions. Student responses to the question "If you asked your TA/Learning Assistant a question in lab, how satisfied were you with the quality and accuracy of the answer you were given?"

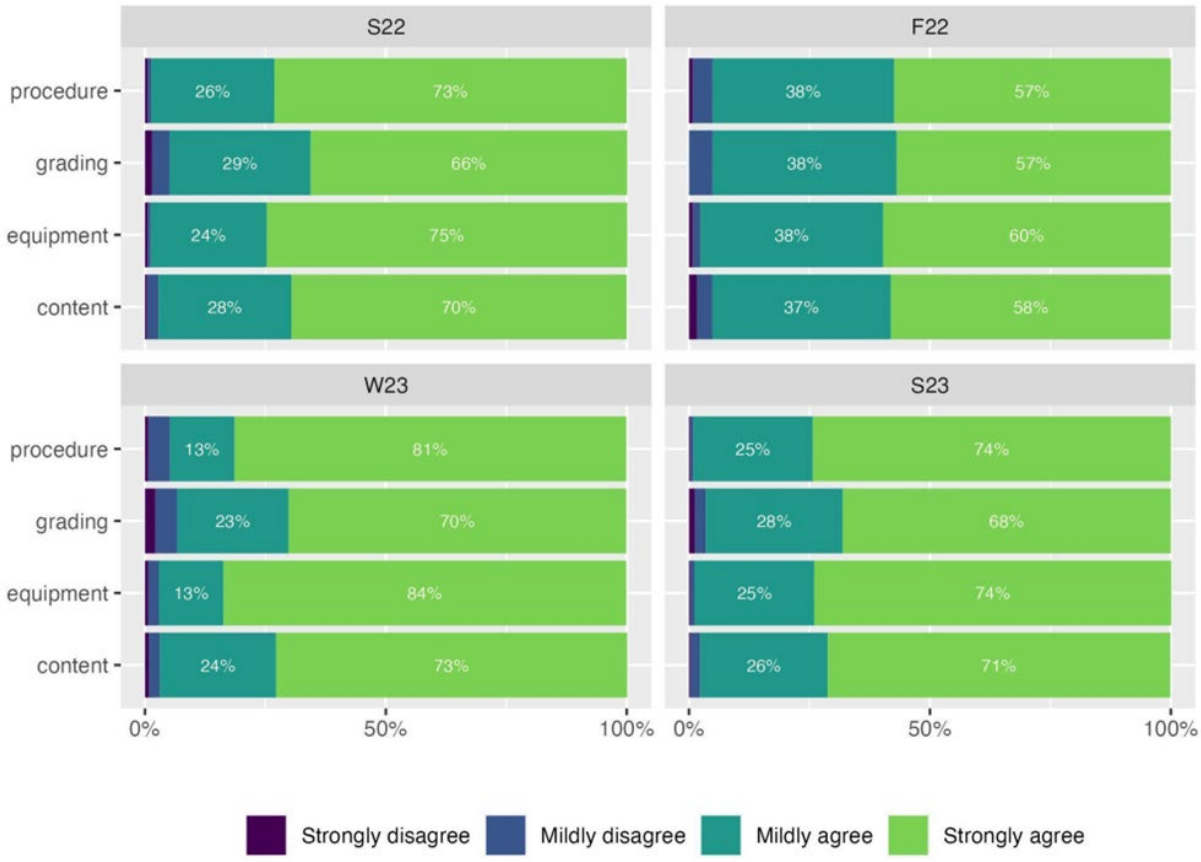

Figure S5.6. Student perception of timeliness of answers to questions. Student responses to the question "Please rate the degree to which you agree with the following statements. During lab, my questions about [topic] were answered in a timely fashion."

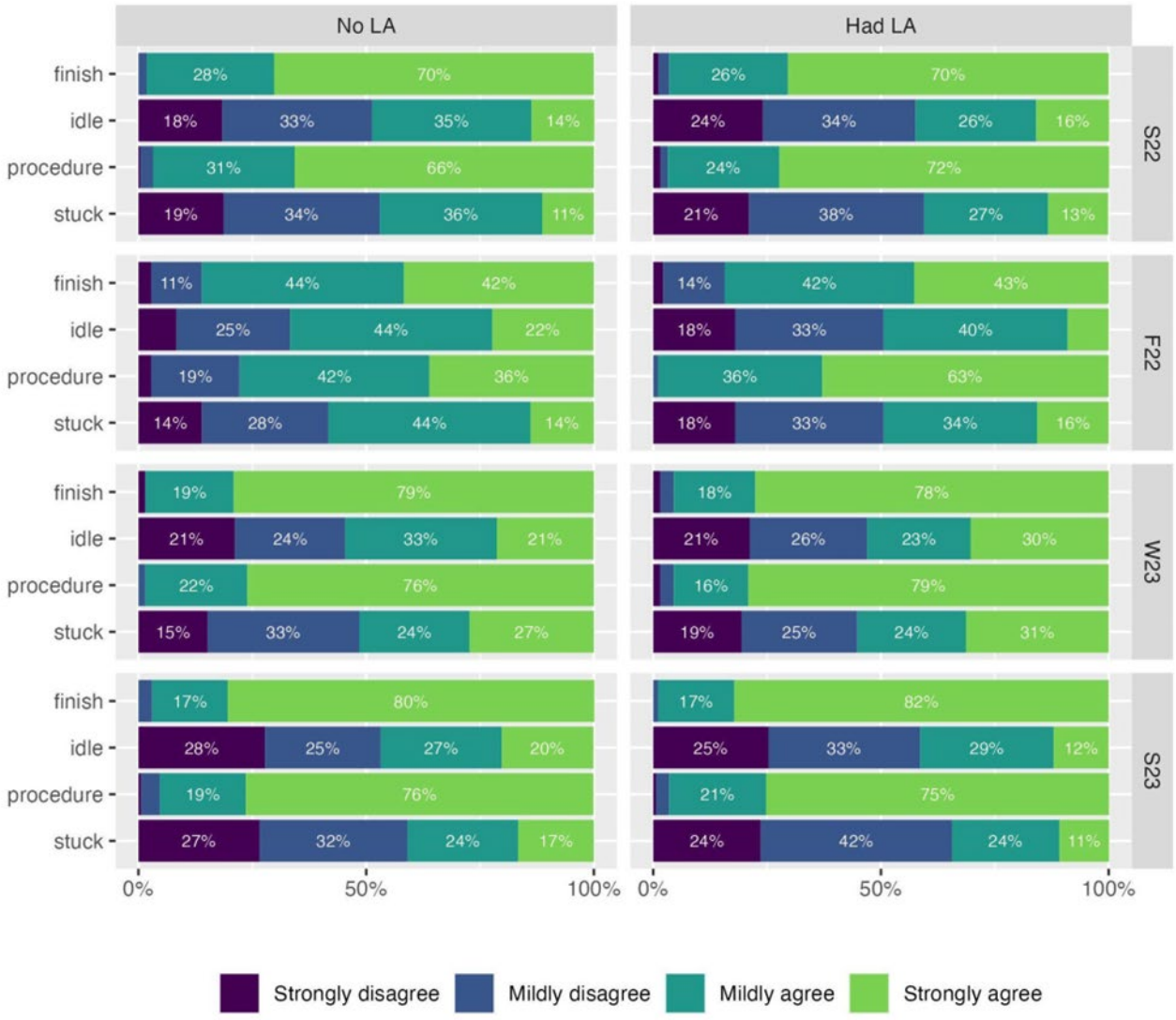

Figure S5.7. Student perception of time management during experiments. Student responses to the question "Please rate the degree to which you agree with the following statements." Statement 1: "My partner and I were able to finish laboratory experiments in the time provided." Statement 2: "All of my questions about the experimental procedure were answered during the lab period." Statement 3: "My partner and I often felt 'stuck' waiting to ask a question about experimental procedure before we could continue the experiment." Statement 4: "My partner and I spent idle time waiting to ask questions about experimental procedure before we could continue the experiment."

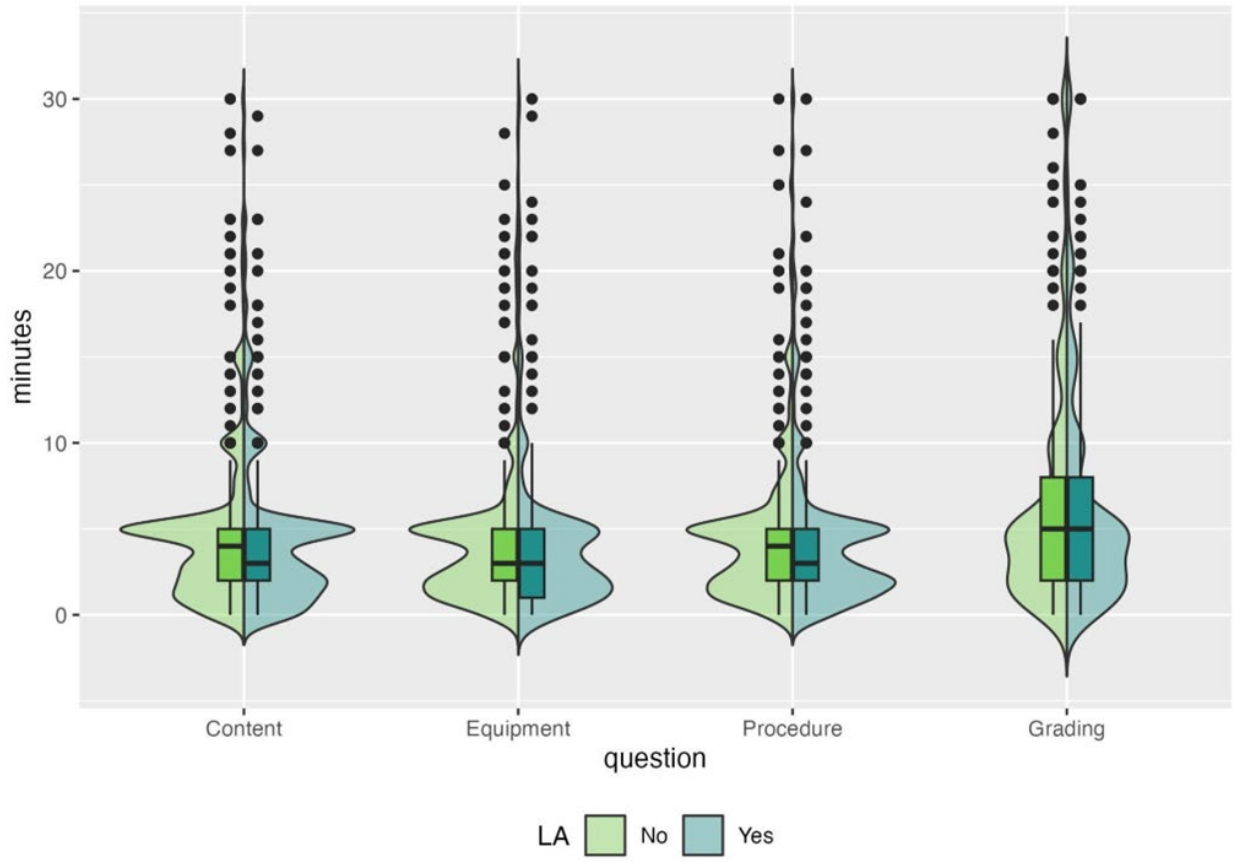

Figure S5.8. Student perception of time spent waiting for questions to be answered (overall). Student responses to the question "On average, how many minutes did you need to wait for the following types of questions to be answered during the lab period?" Students were allowed to choose an integer number of minutes between 0 and 30 minutes, or to select "Not Applicable."

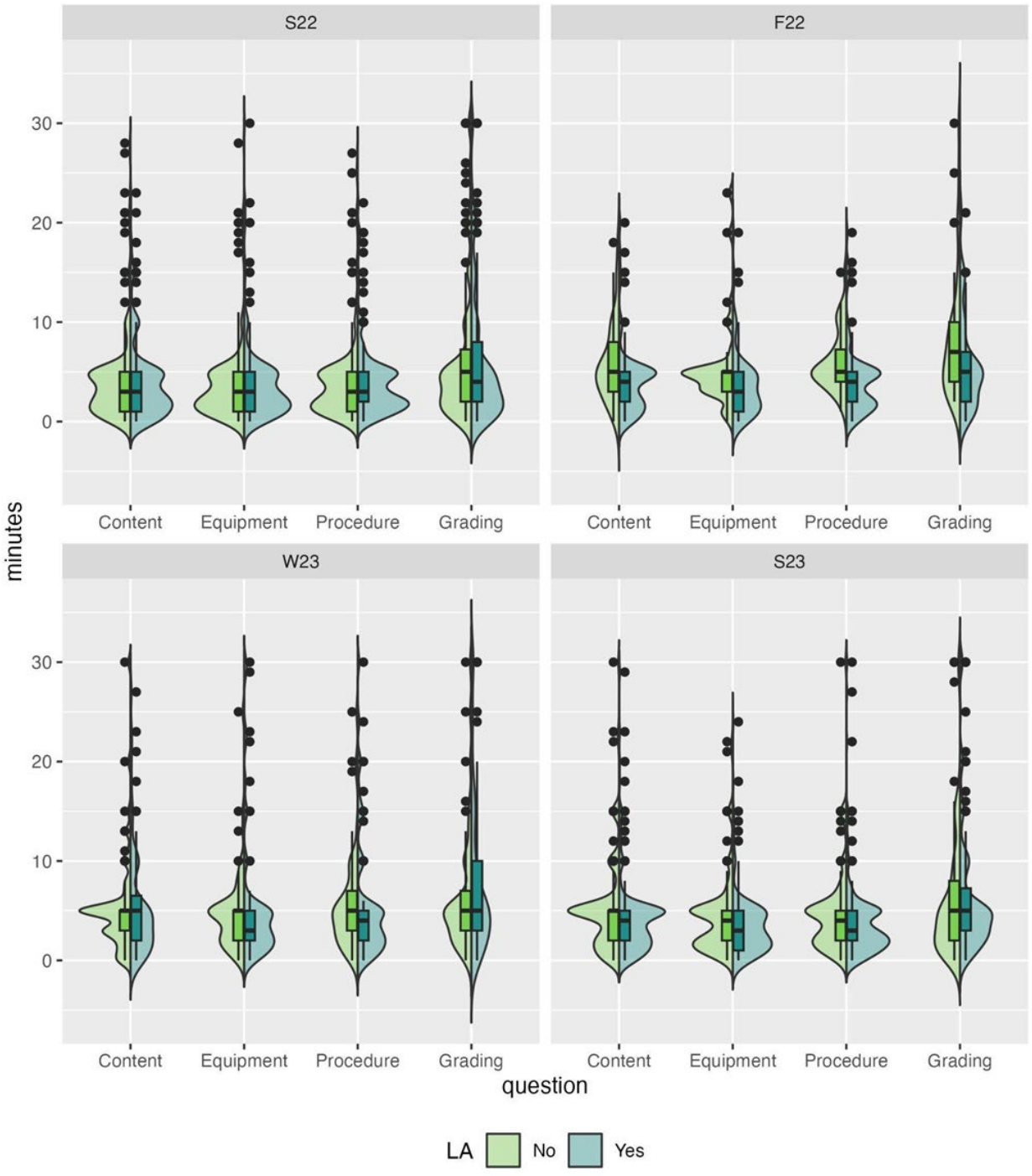

Figure S5.9. Student perception of time spent waiting for questions to be answered (by term). Student responses to the question "On average, how many minutes did you need to wait for the following types of questions to be answered during the lab period?" This figure contains the same data as Figure S8, but broken down by individual instructional terms.

Learning Assistant Survey Results

Table S5.1. LA characteristics.

	S22	F22	W23	S23
Number of LAs	23	12	26	27
Returning LAs	74%	83%	18%	85%
Participated in F21 Training	66%	33%	10%	13$
Had In-Person Lab Experience Prior to Survey Academic Year	78%	100%	100%	100%
LA Majors:				
Biological Sciences	39%	25%	56%	54%
Chemistry	35%	17%	15%	15%
Public Health Science	4%	16%	15%	12%
Pharmaceutical Science	13%	42%	11%	15%
Engineering	0%	0%	3%	4%
Multiple Majors	9%	0%	0%	0%

Table S5.2. Perceived benefits of LA training. Selected LA responses to the questions "Please explain whether you feel that the Fall 2021 LA training + beta testing prepared you to be an in-lab Learning Assistant" and "Please explain whether you feel that the Fall 2021 LA training + beta testing increased your confidence as an in-lab learning assistant."

LA training allowed LAs to anticipate conceptual and practical roadblocks	LA training allowed LAs to transition to in-person laboratory experience	LA training refreshed LAs on previously learned laboratory techniques
"...I felt like the training and testing helped me prepare [what] to expect, what was going to be done in-lab, as well as how to properly help students with questions!"	"It actually did prepare me a lot because this was after COVID and when UCI finally transitioned to in-person after two years of online learning. It allowed me to test my skills after watching so much lecture [material]. And it was great to be hands-on."	"The beta testing helped me prepare for being an in-lab assistant because it gave me a brief refresher on the experiments."
"I felt it gave me useful details for how to troubleshoot experiments."	"...the training helped me be hands on and actually test what I understood from me watching the videos and this was all coming out of COVID."	"The beta testing helped me re-familiarize myself with the lab setting and equipment."

Table S5.3. LA comments on professional development. Selected LA responses to questions such as "Recall your motivations for wanting to be a Learning Assistant. Please explain whether you feel that you succeeded in any of those motivations" and "Recall the professional skills that you wanted to develop by being a Learning Assistant. Please explain whether you feel that you succeeded in developing any of those professional skills."

LA program improved ability to explain complex concepts to less-experienced peers	LA program improved ability to ask guiding questions	LA program developed mentorship and leadership skills
"A big part of being in healthcare is teaching other people the material you already know. For a pharmacist, it is their responsibility to teach their customers how to properly use drugs for optimal efficacy. I think this position is helpful in the sense that it exposes you to being in a position of leadership and trust from the students which is something that should definitely be encouraged before entering pharmacy school."	"I wanted to improve on my active learning skills during my time as an LA. I feel as though the lab course I chose to assist helped immensely with this because it challenged me to come up with certain tactics to use in assisting students rather than just giving them the answer. This helps both me and the student because it strengthens problem solving skills while also allowing the students to use their own knowledge to get to the answer themselves."	"The reason why I chose to be a LA is because I wanted to expand my overall teaching skills and its been a while since I've done that, since high school senior year actually. Due to the pandemic I haven't been able to showcase my leadership and social skills. But with the opportunity of being a LA I was able to guide students through their experiments and make them understand better about the material."
"I think I was pretty good at explaining concepts and I learned how to use different modes to explain them. I'm able to verbally and visually explain concepts to students I wanted to be able to explain concepts and answer questions effectively. When I will be working with patients, I need to be able to explain different concepts to them in a way that they understand but I also need to be able to accept questions."	"I have definitely seen a lot of growth in my communication skills. Articulating in person has become a lot easier and with teaching in specific, the type of wording and angles to take in regards to each student has become more instinctive. However, I recognize that I still have room to grow because there were times where the only approach I knew how to take with a question was to give the answer."	"I have been a learning assistant for a little over two years. It was an integral part of my UCI experience, and made me realize I have a passion in teaching. Hopefully in the future, I can be a mentor!"

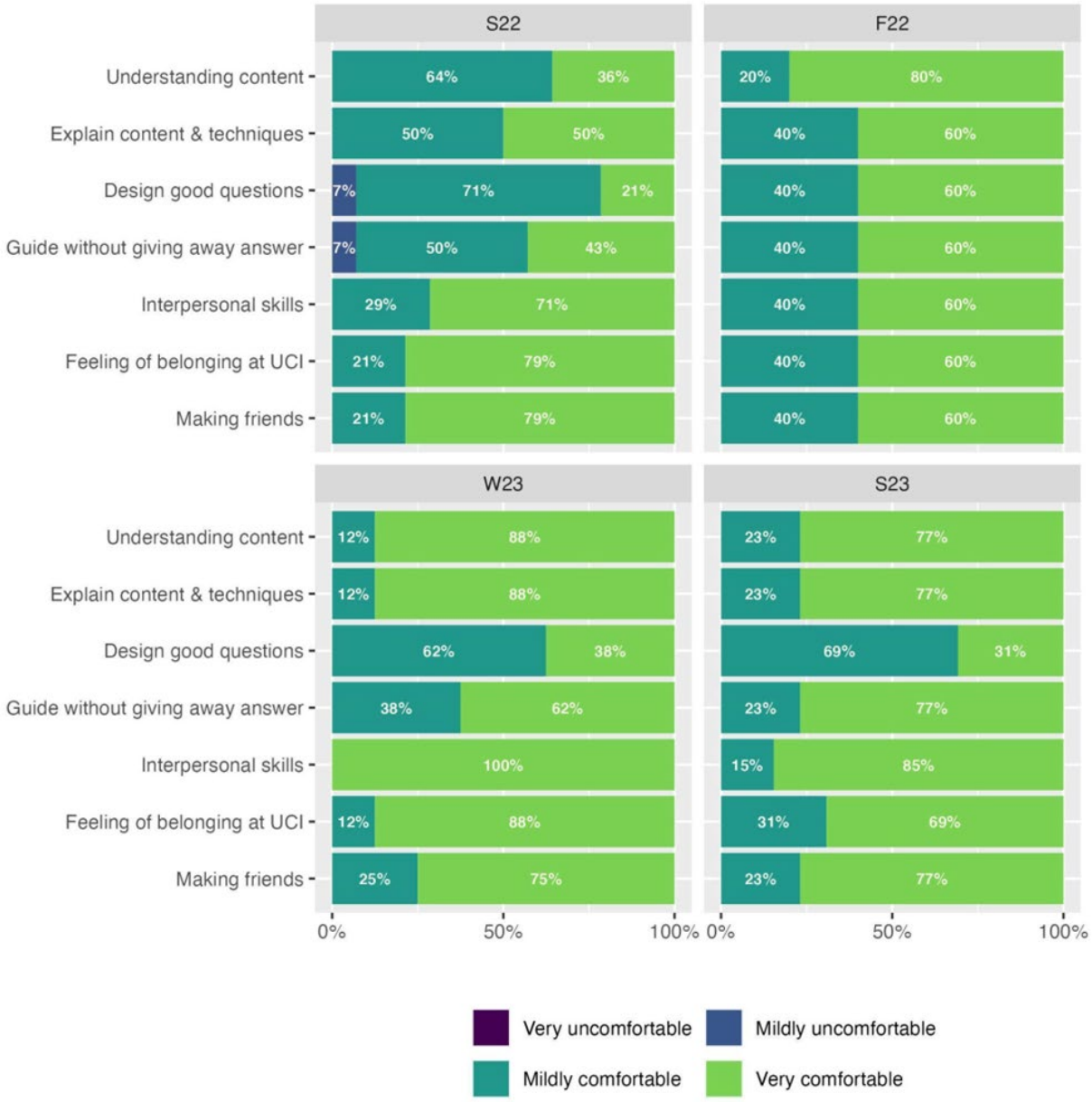

Figure S5.10. LA self-assessment of skills and abilities. LA responses to the question "Please rate your comfort level with each of the following factors now that you have completed this quarter as a Learning Assistant."

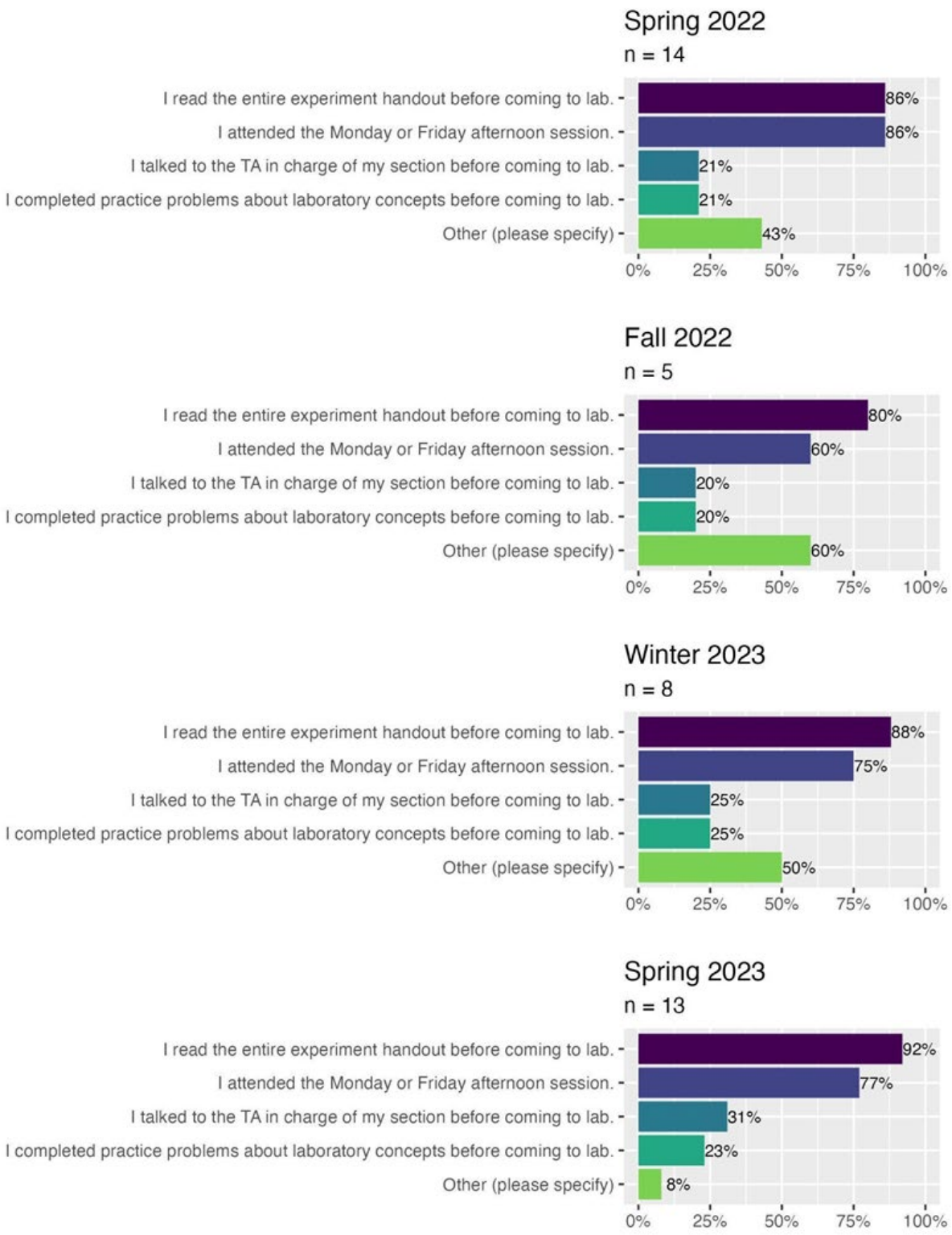
Spring 2022
n = 14
I read the entire experiment handout before coming to lab.
I attended the Monday or Friday afternoon session.
I talked to the TA in charge of my section before coming to lab.
I completed practice problems about laboratory concepts before coming to lab.
Other (please specify)
86%
86%
21%
21%
43%
0%
25%
50%
75%
100%
Fall 2022
n = 5
I read the entire experiment handout before coming to lab.
I attended the Monday or Friday afternoon session.
I talked to the TA in charge of my section before coming to lab.
I completed practice problems about laboratory concepts before coming to lab.
Other (please specify)
80%
60%
20%
20%
60%
0%
25%
50%
75%
100%
Winter 2023
n = 8
I read the entire experiment handout before coming to lab.
I attended the Monday or Friday afternoon session.
I talked to the TA in charge of my section before coming to lab.
I completed practice problems about laboratory concepts before coming to lab.
Other (please specify)
88%
75%
25%
25%
50%
0%
25%
50%
75%
100%
Spring 2023
n = 13
I read the entire experiment handout before coming to lab.
I attended the Monday or Friday afternoon session.
I talked to the TA in charge of my section before coming to lab.
I completed practice problems about laboratory concepts before coming to lab.
Other (please specify)
92%
77%
31%
23%
8%
0%
25%
50%
75%
100%

Figure S5.11. How LAs prepared for laboratory meetings. LA responses to the question "How did you prepare for each week's laboratory session? Choose all that apply." Common responses for "Other (please specify)" included reviewing pre-lab content or their own work/notes from when they took the course.

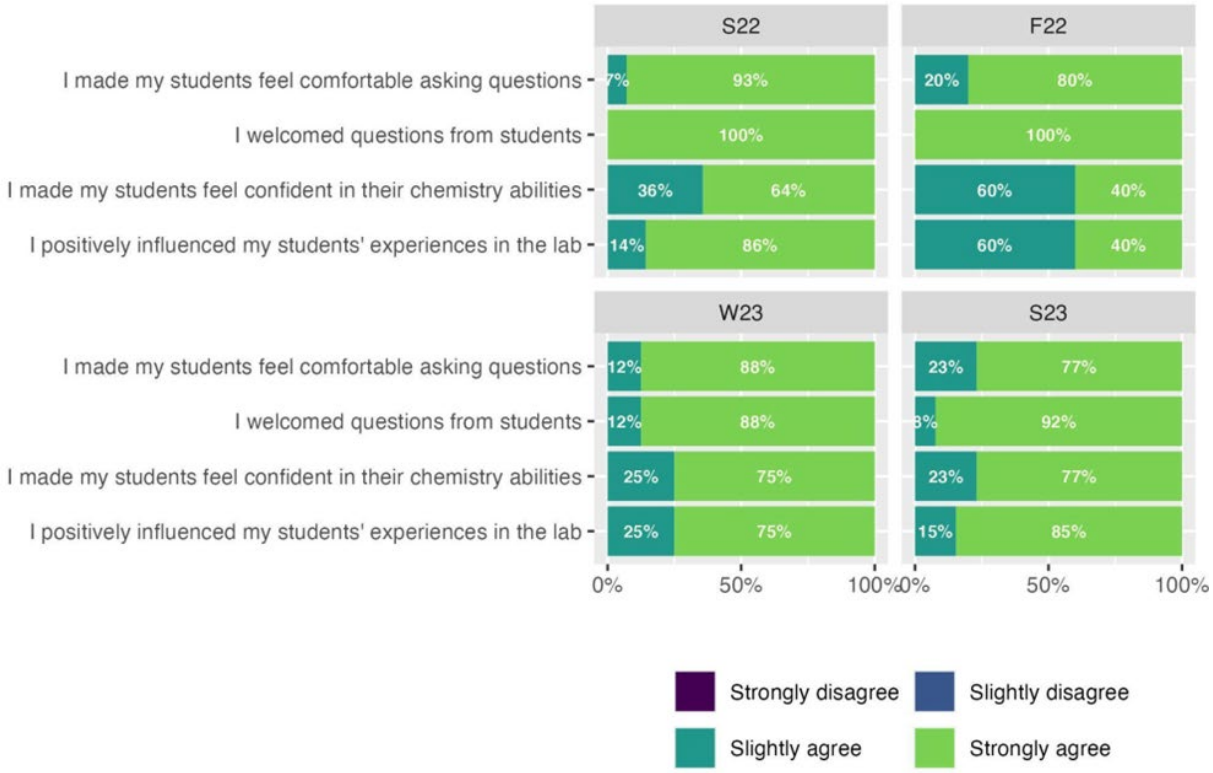

Figure S5.12. LA self-assessment of student interactions. LA responses to the question "Please rate the degree to which you agree with the following."

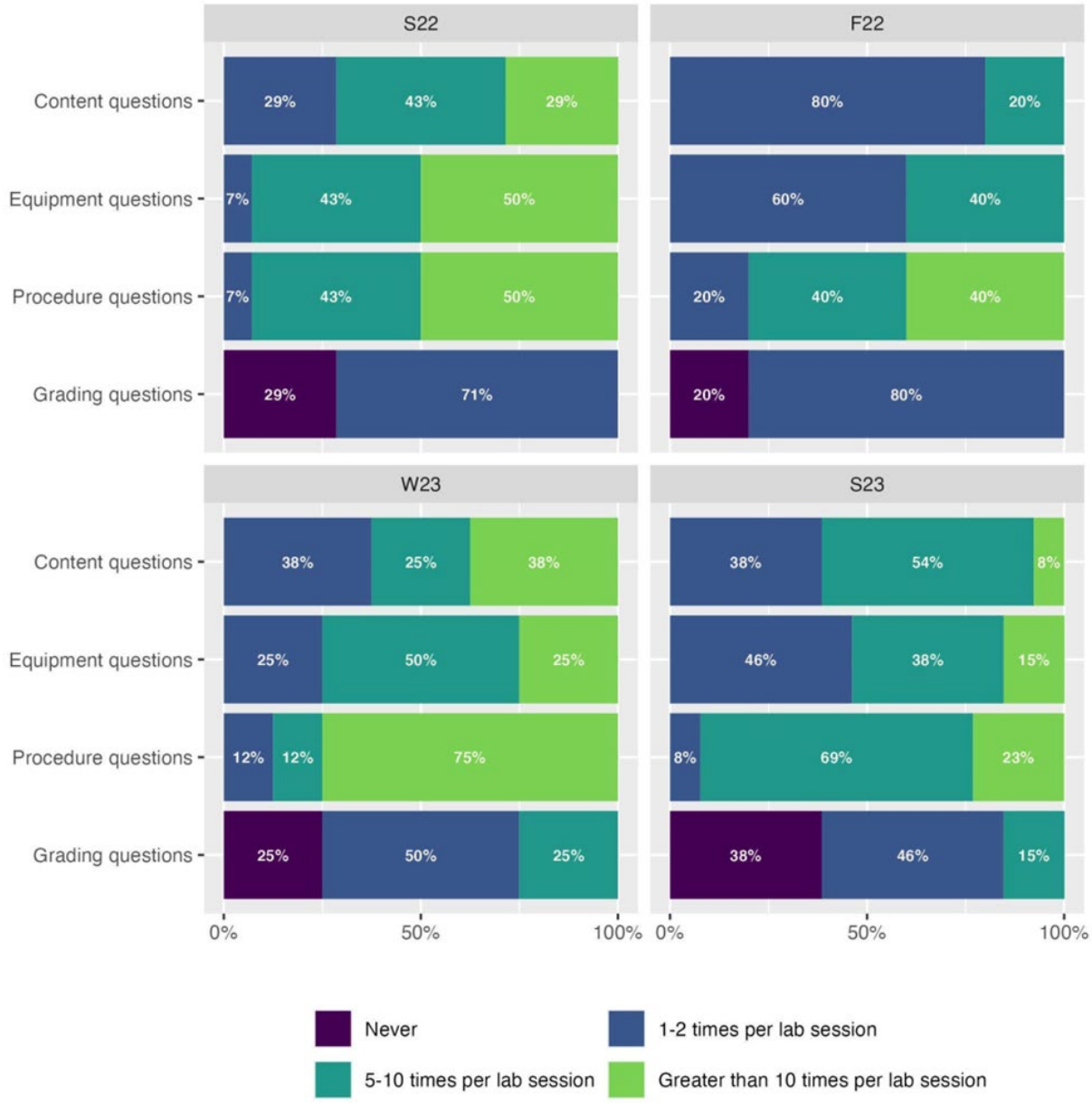

Figure S5.13. Frequency of questions received by LAs. LA responses to the question "Please indicate how frequently you were asked the following types of questions during your lab sessions."

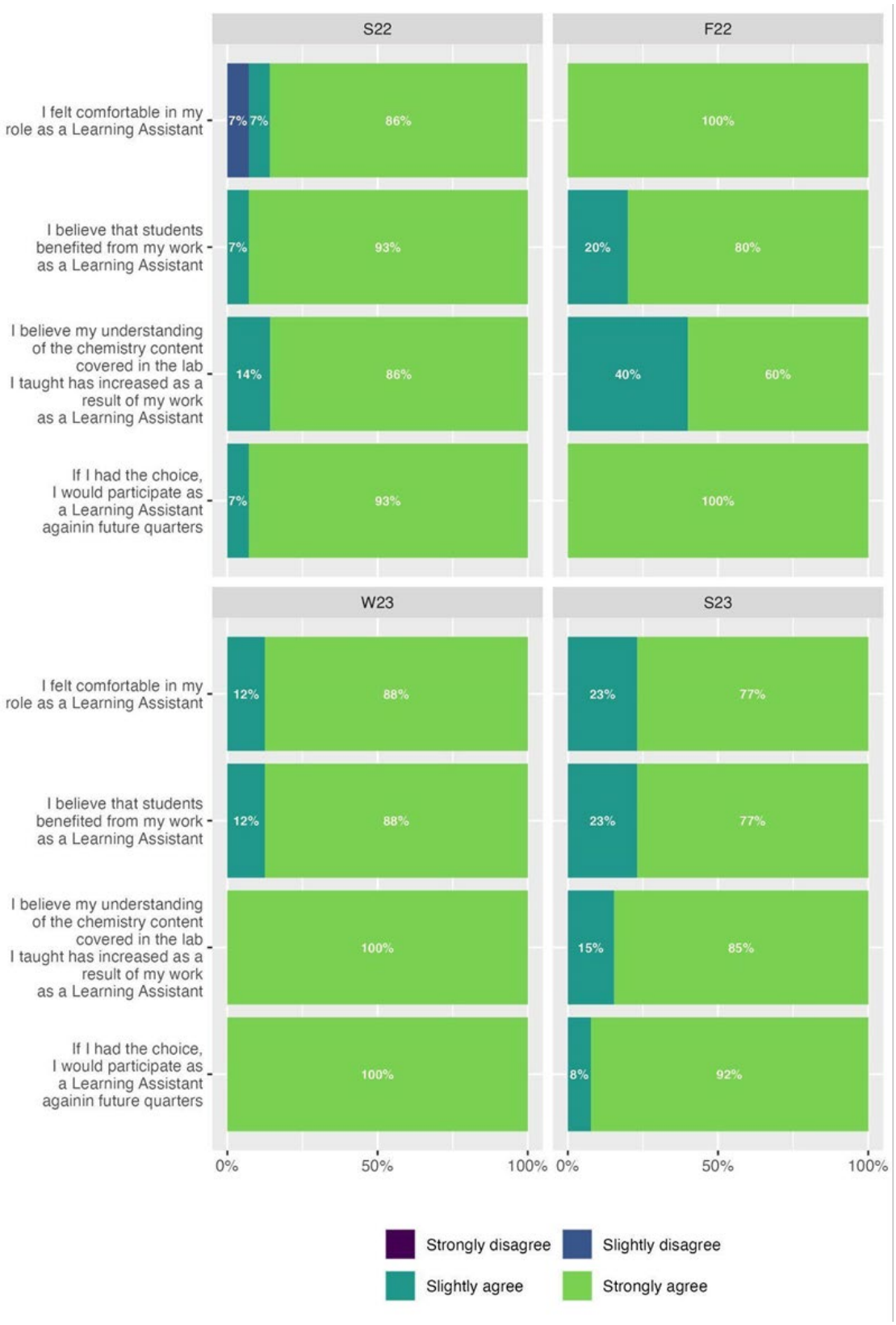
S22
F22
W23
S23
I felt comfortable in my role as a Learning Assistant
I believe that students benefited from my work as a Learning Assistant
I believe my understanding of the chemistry content covered in the lab I taught has increased as a result of my work as a Learning Assistant
If I had the choice, I would participate as a Learning Assistant againin future quarters
7%
7%
86%
100%
7%
93%
20%
80%
14%
86%
40%
60%
7%
93%
100%
12%
88%
23%
77%
12%
88%
23%
77%
100%
15%
85%
100%
8%
92%
0%
50%
100%
Strongly disagree
Slightly disagree
Slightly agree
Strongly agree

Figure S5.14. LA self-assessment of the value of the LA program. LA responses to the question "Please rate the degree to which you agree with the following."

References for Chapter V

[1] Emenike, M. E.; Schick, C. P.; Van Duzor, A. G.; Sabella, M. S.; Hendrickson, S. M.; Langdon, L. S. Leveraging Undergraduate Learning Assistants to Engage Students during Remote Instruction: Strategies and Lessons Learned from Four Institutions. *J. Chem. Educ.* **2020**, *97* (9), 2502–2511. https://doi.org/10.1021/acs.jchemed.0c00779.

[2] Barrasso, A. P.; Spilios, K. E. A Scoping Review of Literature Assessing the Impact of the Learning Assistant Model. *IJ STEM Ed* **2021**, *8* (1), 12. https://doi.org/10.1186/s40594-020-00267-8.

[3] Thompson, A. N.; Talbot, R. M.; Doughty, L.; Huvard, H.; Le, P.; Hartley, L.; Boyer, J. Development and Application of the Action Taxonomy for Learning Assistants (ATLAs). *IJ STEM Ed* **2020**, *7* (1), 1. https://doi.org/10.1186/s40594-019-0200-5.

[4] Bourne, S. M.; Limfat, S.; Dilip, S.; Han, S.; Robak, M. T.; Marsden, P.; Baranger, A. M. The Undergraduate Teacher-Scholar Program: Comparing Near-Peer and Non Near-Peer Instructors in Laboratory Courses. *Journal of College Science Teaching* **2021**, *50* (5), 10–17. https://doi.org/10.1080/0047231X.2021.12290521.

[5] Ten Cate, O.; Durning, S. Peer Teaching in Medical Education: Twelve Reasons to Move from Theory to Practice. *Medical Teacher* **2007**, *29* (6), 591–599. https://doi.org/10.1080/01421590701606799.

[6] Bretz, S. L. Novak's Theory of Education: Human Constructivism and Meaningful Learning. *J. Chem. Educ.* **2001**, *78* (8), 1107. https://doi.org/10.1021/ed078p1107.6.

[7] Galloway, K. R.; Malakpa, Z.; Bretz, S. L. Investigating Affective Experiences in the Undergraduate Chemistry Laboratory: Students' Perceptions of Control and Responsibility.

J. Chem. Educ. **2016**, *93* (2), 227–238. https://doi.org/10.1021/acs.jchemed.5b00737.

[8] Lawhon, C. *Answering the Call: The Story of How UCI Responded and Adapted to the Historic COVID-19 Pandemic*; University of California, Irvine, 2020. https://specialreports.news.uci.edu/uci-during-covid/index.php (accessed 2024-03-07).

[9] Hall, S.; Stephens, J.; Andrade, T.; Davids, J.; Powell, M.; Border, S. Perceptions of Junior Doctors and Undergraduate Medical Students as Anatomy Teachers: Investigating Distance along the Near-peer Teaching Spectrum. *Anatomical Sciences Ed* **2014**, *7* (3), 242–247. https://doi.org/10.1002/ase.1419.

[10] Micari, M.; Pazos, P. Connecting to the Professor: Impact of the Student–Faculty Relationship in a Highly Challenging Course. *College Teaching* **2012**, *60* (2), 41–47. https://doi.org/10.1080/87567555.2011.627576.

[11] Frosch, E.; Goldstein, M. Using a Learning Community Model for Virtual Medical Student Support during the COVID19 Pandemic. *Int J Med Educ* **2021**, *12*, 136–139. https://doi.org/10.5116/ijme.60e2.c777.

[12] Bulte, C.; Betts, A.; Garner, K.; Durning, S. Student Teaching: Views of Student near-Peer Teachers and Learners. *Medical Teacher* **2007**, *29* (6), 583–590. https://doi.org/10.1080/01421590701583824.

[13] Akinla, O.; Hagan, P.; Atiomo, W. A Systematic Review of the Literature Describing the Outcomes of Near-Peer Mentoring Programs for First Year Medical Students. *BMC Med Educ* **2018**, *18* (1), 98. https://doi.org/10.1186/s12909-018-1195-1.

[14] Price, S.; Wallace, K.; Verezub, E.; Sinchenko, E. Student Learning Assistants: The Journey from Learning Advice to Creating Community. *Journal of Further and Higher Education*

2019, *43* (7), 914–928. https://doi.org/10.1080/0309877X.2018.1425379.

[15] Otero, V.; Pollock, S.; Finkelstein, N. A Physics Department's Role in Preparing Physics Teachers: The Colorado Learning Assistant Model. *American Journal of Physics* **2010**, *78* (11), 1218–1224. https://doi.org/10.1119/1.3471291.

[16] Seery, M. K.; Agustian, H. Y.; Zhang, X. A Framework for Learning in the Chemistry Laboratory. *Israel Journal of Chemistry* **2019**, *59* (6–7), 546–553. https://doi.org/10.1002/ijch.201800093.

[17] Penn, M.; Ramnarain, U. South African University Students' Attitudes towards Chemistry Learning in a Virtually Simulated Learning Environment. *Chem. Educ. Res. Pract.* **2019**, *20* (4), 699–709. https://doi.org/10.1039/C9RP00014C.

[18] Flaherty, A. A. A Review of Affective Chemistry Education Research and Its Implications for Future Research. *Chem. Educ. Res. Pract.* **2020**, *21* (3), 698–713. https://doi.org/10.1039/C9RP00200F.

[19] Vishnumolakala, V. R.; Southam, D. C.; Treagust, D. F.; Mocerino, M.; Qureshi, S. Students' Attitudes, Self-Efficacy and Experiences in a Modified Process-Oriented Guided Inquiry Learning Undergraduate Chemistry Classroom. *Chem. Educ. Res. Pract.* **2017**, *18* (2), 340–352. https://doi.org/10.1039/C6RP00233A.

[20] Smith, T. Integrating Undergraduate Peer Mentors into Liberal Arts Courses: A Pilot Study. *Innov High Educ* **2008**, *33* (1), 49–63. https://doi.org/10.1007/s10755-007-9064-6.

[21] Kornreich-Leshem, H.; Benabentos, R.; Hazari, Z.; Potvin, G.; Kramer, L. The Cognitive and Affective Roles of Learning Assistants in Science, Technology, Engineering, and Mathematics College Classrooms: An Exploration of Classroom Experiences and Students'

Metacognitive Awareness and Disciplinary Identity. *Science Education* **2022**, *106* (3), 545–572. https://doi.org/10.1002/sce.21703.

[22] Wilson, S. B.; Varma-Nelson, P. Implementing Peer-Led Team Learning and Cyber Peer-Led Team Learning in an Organic Chemistry Course. *Journal of College Science Teaching* **2021**, *50* (3), 44–50. https://doi.org/10.1080/0047231X.2021.12290507.

[23] McKnelly, K. J.; Howitz, W. J.; Thane, T. A.; Link, R. D. Specifications Grading at Scale: Improved Letter Grades and Grading-Related Interactions in a Course with over 1,000 Students. *J. Chem. Educ.* **2023**, *100* (9), 3179–3193. https://doi.org/10.1021/acs.jchemed.2c00740.

[24] Garnier, S. (2018). viridis: Default Color Maps from "matplotlib." Available at: https://CRAN.R-project.org/package=viridis (accessed 2024-03-07).

[25] R Core Team (2019). R: A Language and Environment for Statistical Computing. Vienna, Austria: R Foundation for Statistical Computing Available at: https://www.R-project.org/.

[26] Wickham, H.; Averick, M.; Bryan, J.; Chang, W.; McGowan, L.; François, R.; Grolemund, G.; Hayes, A.; Henry, L.; Hester, J.; Kuhn, M.; Pedersen, T.; Miller, E.; Bache, S.; Müller, K.; Ooms, J.; Robinson, D.; Seidel, D.; Spinu, V.; Takahashi, K.; Vaughan, D.; Wilke, C.; Woo, K.; Yutani, H. Welcome to the Tidyverse. *JOSS* **2019**, *4* (43), 1686. https://doi.org/10.21105/joss.01686.

[27] Rampin, R.; Rampin, V. Taguette: Open-Source Qualitative Data Analysis. *JOSS* **2021**, *6* (68), 3522. https://doi.org/10.21105/joss.03522.

[28] Walker, J. P.; Sampson, V. Argument-Driven Inquiry: Using the Laboratory To Improve Undergraduates' Science Writing Skills through Meaningful Science Writing, Peer-Review,

and Revision. *J. Chem. Educ.* **2013**, *90* (10), 1269–1274. https://doi.org/10.1021/ed300656p.

[29] Howitz, W. J.; Frey, T.; Saluga, S. J.; Nguyen, M.; Denaro, K.; Edwards, K. D. A Specifications-Graded, Sports Drink-Themed General Chemistry Laboratory Course Using an Argument-Driven Inquiry Approach. *J. Chem. Educ.* **2023**, *100* (2), 672–680. https://doi.org/10.1021/acs.jchemed.2c00860.

[30] Saluga, S. J.; Burns, A. M.; Li, Y.; Nguyen, M. M.; Edwards, K. D. A Specifications-Graded, Spice-Themed, General Chemistry Laboratory Course Using an Argument-Driven Inquiry Approach. *J. Chem. Educ.* **2023**, *100* (10), 3903–3915. https://doi.org/10.1021/acs.jchemed.3c00433.